UNIVERSITY OF CALIFORNIA, SAN DIEGO

NF-κB RelB/p52 heterodimer: Biogenesis and DNA recognition

A dissertation submitted in partial satisfaction of the

requirements for the degree Doctor of Philosophy

in

Chemistry

by

Amanda J. Fusco

Committee in charge:

Professor Gourisankar Ghosh, Chair
Professor Christopher Glass
Professor Alexandar Hoffmann
Professor James Kadonaga
Professor Elizabeth Komives
Professor Amitabha Sinha

2007

The dissertation of Amanda J. Fusco is approved, and it is acceptable in quality and form for publication on microfilm:

_____

_____

_____

_____

_____

_____

Chair

University of California, San Diego

2007

TABLE OF CONTENTS

LIST OF FIGURES

LIST OF TABLES

ACKNOWLEDGMENTS

Chapter V, in part, is in preparation as Stabilization of RelB requires multi-domain interaction with p100/p52, Amanda J. Fusco, Olga V. Savinova, Rashmi Talwar, Jeffrey D. Kearns, Alexander Hoffmann & Gourisankar Ghosh. The dissertation author was the primary researcher and author of this publication.

I would like to thank my dissertation advisor Dr. Gourisankar Ghosh, for his encouragement and understanding. Working with him has been an enjoyable and memorable experience. I would like to thank our collaborator Dr. Alex Hoffmann and members of his lab for providing material and expertise. I would like to thank Debin Huang for his help in learning and solving my x-Ray crystal structure. His help and guidance was vital to finishing the RelB/p52:DNA x-Ray crystal structure.

I would like to thank the members in my lab. They have made the lab an enjoyable place to work and the last 6 years a lot of fun. I would first like to thank Sutapa for being a great friend and for all the advice and help that she has provided to me over the years in both science and life. She will always be like a sister to me. I would like to thank Jacky for being a good office mate and for his help in freezing all of my crystals. It meant a great deal to me. I would also like to thank Don Vu, for being a great bench and office mate and without his help I may have never got diffracting quality crystals. I would like to thank Erika for making lab a happy atmosphere with her good smile and joyful attitude. I would also like to thank her for her help and guidance in learning the retrovirus expression system. I want to thank Jessica for being such a sweet and thoughtful person and being so encouraging. I

would also like to thank her for all the help that she has given in proof reading my thesis and a number of other things. I would like to thank Anthony for always making me smile and for being such a fun and remarkable person. I would like to thank Olga for the trips to coffee and all of the insightful conversations we have had about science. I would like to thank Vivien, Kayla, Nhat, and Suhyung for making lab an enjoyable place to work. I would like to thank Thomas and Dustyn for their help in cloning. I would also like to thank past lab members, Anu Moorthy, Tom Huxford and Rashmi Talwar, Eileen Kennedy, Randall Lukasiewicz, Sebastian Vallee, Chris Phelps, Brad Nolen for their helpful suggestions and guidance. I would like to thank Leila for being a good friend, a lot of fun and a great running partner.

I would like to thank my family for all of their support and love. I would like to thank my husband Todd and son Michael for their love and support and understanding of the late nights and long hours in lab. I would like to thank my Dad for his constant encouragement and guidance throughout my life. I would like to thank my sister Jill and my brother Peter, for being such good friends and telling me that I can do anything, even though they both thought that I was crazy for getting my PhD. I would like to thank my sister-in-law Marnie for proof reading my whole thesis and for being my climbing partner (it kept me sane throughout the years).

I would like to dedicate this work in loving memory of my mother, Janet Lee Fusco. She has been an inspiration to me throughout my life. She has always believed in me no matter what endeavor I was pursuing. Her encouragement, good advice and understanding throughout my PhD and life kept me going when things became difficult and I was ready to give up. She was an amazing woman, mother, and

friend and her strength, unconditional love and talent made me lucky to have her as a role model in my life.

VITA

1999	B.S, State University of New York College of Environmental Science and Forestry
2003	M.S, University of California, San Diego
2007	Ph.D., University of California, San Diego

PUBLICATIONS

Fusco, A. J., Savinova, O., Kearns, J. D., Hoffmann, A. and Ghosh, G. (2007) Stabilization of RelB requires multi-domain interaction with p100/ p52. (In preparation)

Fusco, A. J., Haung, D., and Ghosh, G. 2007. RelB reveals versatile κB DNA binding modes only as the RelB/p50 heterodimer. (In preparation)

Fusco, A. J., Savinova, O., Basak, S., Hoffmann, A., and Ghosh, G. 2007. RelB both induces and inhibits p100 processing. (In preparation)

Huang, D., Phelps, C. B., Fusco, A. J., and Ghosh, G., (2005). Crystal Structure of a Free κB DNA: Insights into DNA Recognition by Transcription Factor NF-κB. J. Mol. Biol. *346*, 147-160.

ABSTRACT OF THE DISSERTATION

NF-κB RelB/p52 heterodimer: Biogenesis and DNA recognition

by

Amanda J. Fusco

Doctor of Philosophy in Chemistry

University of California, San Diego, 2007

Professor Gourisankar Ghosh, Chair

NF-κB is a family of dimeric transcription factors made up of five family members, p50 (NF-κB1), RelA (p65), p52 (NF-κB2), c-Rel and RelB, that regulate the expression of a large number of genes involved in innate and adaptive immunity. The NF-κB dimers regulate gene expression by binding to a class of decameric DNA duplexes known as κB sites. RelB is the most poorly understood and unique member of the NF-κB family. Unlike other members, RelB does not form a stable detectable homodimer *in vivo*. In uninduced cells, RelB preferentially associates with p100 and to a lesser extent with p50. Gene knockout studies demonstrated that RelB and p52 are involved in common biological functions such as secondary lymphoid organ development and B-cell maturation. It was subsequently found that these two proteins act together as a heterodimeric transcription factor that activates a set of genes in the developmental programs. The promoters of several of these genes have shown to

contain κB sites that somewhat deviate from the classical κB sites. There are two important questions that remain to be answered. These questions are 1) how is the RelB/p52 heterodimer generated and 2) how does this heterodimer bind to κB sites? The purpose of this dissertation was to provide answers to these questions.

The RelB/p52 heterodimer is the product of NF-κB signaling pathways, referred to as the non-canonical pathways, which involve processing of the precursor protein p100 into p52. However, whether the RelB/p52 heterodimer is generated from the p100/RelB complex observed in uninduced cells was unclear. Results shown in this dissertation demonstrate that NF-κB RelB is an unstable protein that is stabilized by forming complexes with both p100 and p52. The p100/RelB complex involves all functional domains of each protein and is not processing competent. A large body of experimental results shown here clearly suggests that p52 is primarily generated from newly synthesized p100 and not from the pre-existing p100/RelB complex. Processing of the newly synthesized p100 is facilitated when bound to a newly synthesized NF-κB subunit, including RelB. However, the binding of newly synthesized p100 with RelB can also lead to the formation of an inactive p100/RelB complex. Therefore a dynamic binding mode between p100 and RelB, where one is processing competent and the other is not, is proposed.

To understand the κB DNA recognition by the RelB/p52 heterodimer, the complex between the heterodimer and κB DNA has been crystallized and the 3.05 Å crystal structure is reported in this dissertation. The structure has revealed a new mode of DNA interaction by an NF-κB dimer that has never been observed

previously. In addition to the conserved DNA contacts made by all NF-κB family members, a conserved arginine of RelB contacts the outermost G:C base pair of the RelB DNA half site. At the same time RelB loses one contact with the innermost A:T base pair of the half site normally mediated by a conserved tyrosine residue. Binding affinity measurements demonstrate that the RelB/p52 heterodimer binds to the κB DNA tested, including the newly identified ones indicated above, with similar affinities. We propose that the RelB/p52 heterodimer binds to different κB sites with high affinity by altering the DNA contact. The RelB subunit allows for different binding modes by binding to some κB sequences using the tyrosine contacts and to other κB sequences by utilizing the arginine contact. Specific DNA sequences at the center and flanking region dictate the RelB binding modes.

I. Introduction

A. NF-κB Transcription Factors

NF-κB is a family of eukaryotic transcription factors originally described in 1986 as a nuclear factor necessary for immunoglobulin kappa light chain transcription in B cells (Sen and Baltimore, 1986). NF-κB is found in most cells, and in mammals is made up of five evolutionarily conserved family members: p50 (NF-κB1), RelA (p65), p52 (NF-κB2), c-Rel, and RelB. There are three gene products that have been found in Drosophila that are homologous to NF-κB, *relish*, *dorsal*, and *dif* (Silverman and Maniatis, 2001). NF-κB proteins are an important component in the inducible expression of many genes, including genes involved in growth, development, apoptosis, stress responses, and innate and adaptive immunity (Baeuerle and Baltimore, 1996; Baeuerle and Henkel, 1994; Baldwin, 1996; Ghosh et al., 1998). A large number of stimuli, such as UV-radiation, bacterial and viral products (lipopolysaccharide (LPS)), cytokines, growth factors, and inter-cellular contact (TCR-MHC-antigen) activate NF-κB (Figure 1-1) (Pahl, 1999).

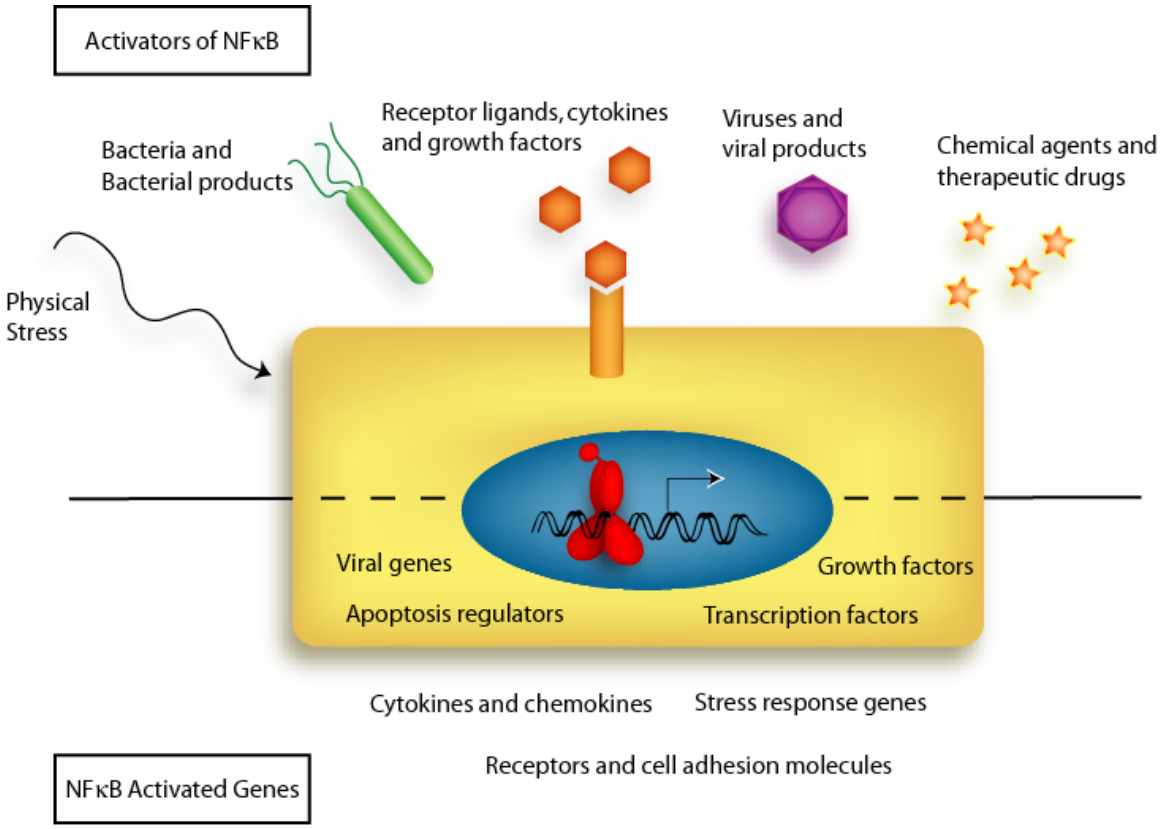

Figure 1-1. *Activators and responses of NF-κB mediated transcription.* Schematic representation of a cell. The general classes of NF-κB activators are shown in the top half of the figure, and the gene products whose production is activated by NF-κB dimers are shown in the lower half (separated by dashed line).

B. NF-κB activation pathway

In unstimulated cells, NF-κB dimers are maintained inactive through stable protein-protein association with a class of inhibitor proteins known as Inhibitor of κB (IκB) (Baldwin, 1996; Ghosh et al., 1998). A large variety of extracellular signals activate NF-κB by relieving inhibition from IκB. One of the key events in the NF-κB activation pathway is the phosphorylation of two serines of IκB proteins in a region known as the destruction box by a kinase complex, referred to as IκB kinase (IKK). Phosphorylation of IκB leads to ubiquitination by the E3 ubiquitin ligase complex consisting of Cul1, Skp1, Roc1, an E2 ubiquitin ligase, and the β-Transducin repeat containing protein (βTrCP) (Karin and Ben-Neriah, 2000). Poly-ubiquitination of IκB leads to its rapid degradation through the 26S proteasome. Once released from IκB, NF-κB translocates to the nucleus and participates in transcriptional activation of target genes by binding to specific DNA sequences (Figure 1-2) (Ghosh and Karin, 2002).

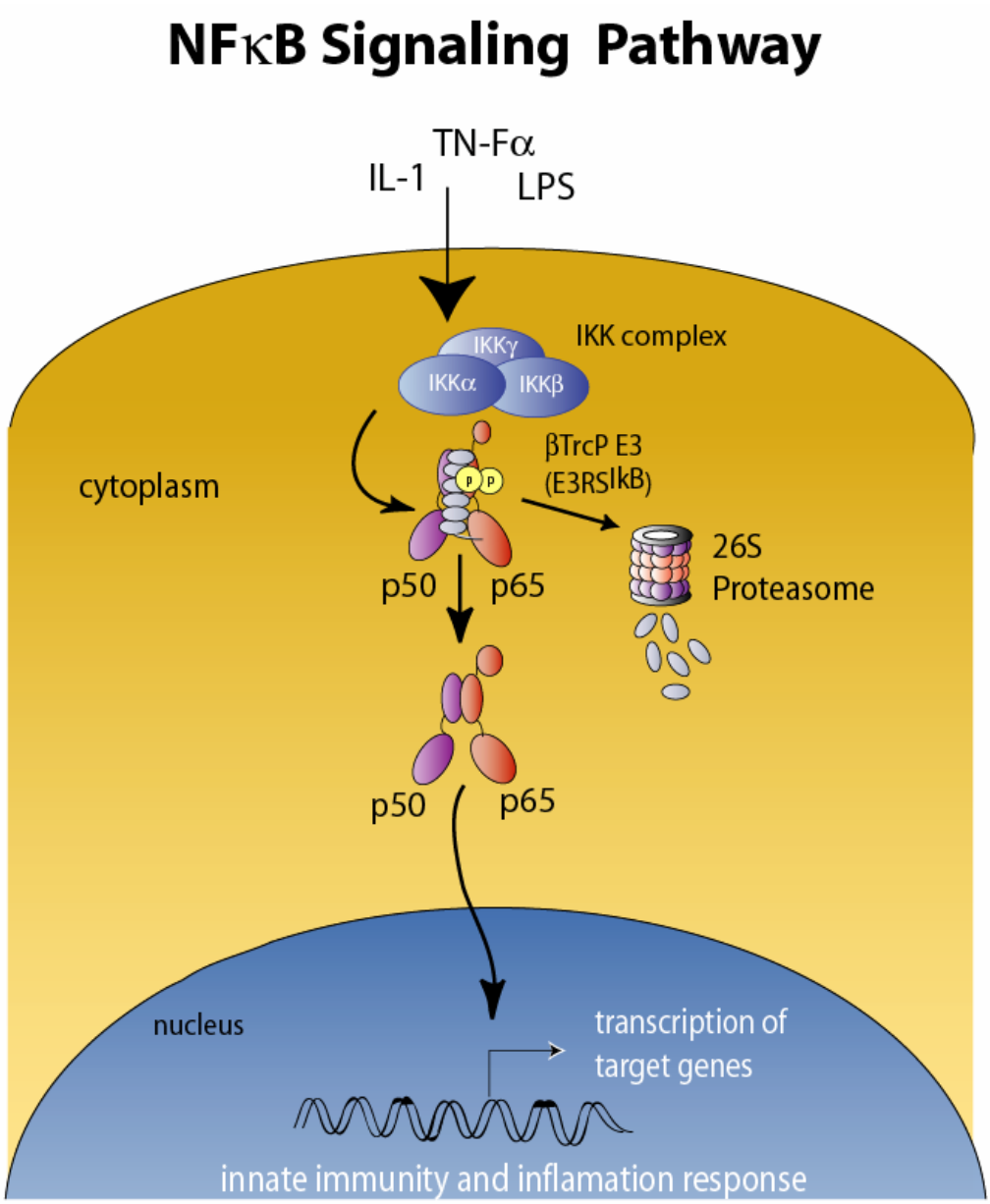

Figure 1-2. *The NF-κB activation pathway.* Signals that ultimately activate NF-κB are received at the cell's surface and converge at and activate the IKK complex (blue). IKK phosphorylates IκB (grey) on serines in IκB's N-terminus. Phospho-IκB is then ubiquitinated by a ubiquitin ligase complex which marks it for degradation by the 26S proteosome (purple and pink). Removal of IκB unmasks the NF-κB NLSs allowing it to translocate into the nucleus, where it binds to κB DNA sites and activates its target genes.

C. NF-κB family

The NF-κB family members are active as both homo- and heterodimers. All family members share a highly conserved region of approximately 300 amino acids in length, referred to as the Rel Homology Region (RHR) (Figure 1-3) (Baeuerle and Baltimore, 1996; Baldwin, 1996). The RHR is responsible for dimerization, DNA-binding, inhibitor binding and nuclear localization. The RHR consists of two domains with an immunoglobin-like fold; an N-terminal domain (NTD) that contains the amino acids responsible for base-specific contacts, and a C-terminal dimerization domain (DD). These two domains are connected by a short, flexible linker. A nuclear localization sequence (NLS) is located just C-terminal to the DD.

NF-κB subunits can be divided into two classes. The p50 and p52 subunits belong to class I by virtue of not having an activation domain, thus categorizing them as transcriptional repressors. The p50 and p52 subunits are synthesized from the precursor proteins p105 and p100, respectively (Bours et al., 1990; Ghosh and Baltimore, 1990; Kieran et al., 1990). The other three subunits (RelA, cRel and RelB) constitute class II due to the presence of a transcriptional activation domain (TAD). Homo- and heterodimers with at least one class II subunit have transcription activation potential. (Figure 1-4) (Baldwin, 1996; Ghosh et al., 1998).

Each NF-κB family member has a non-conserved N-terminus varying in length from 6 amino acids in cRel to 123 amino acids in RelB. RelBs extended N-terminus conatins a leucine zipper (LZ) domain, identified by the presence of a leucine-rich heptad repeat. The function of the LZ domain is still unknown, although it has been shown to be important for the transcriptional activation of RelB (Dobrzanski et al.,

1995; Ryseck et al., 1992). p50 and p52 have the highest homology in their RHRs. Both share a helical insert in their N-terminal domain that is absent in the other three. cRel and p65 are also closely related while RelB's sequence is intermediate. RelB's N-terminal domain is more similar to p65 and cRel, while its dimerization domain is closer to p50 and p52 (Figure 1-3).

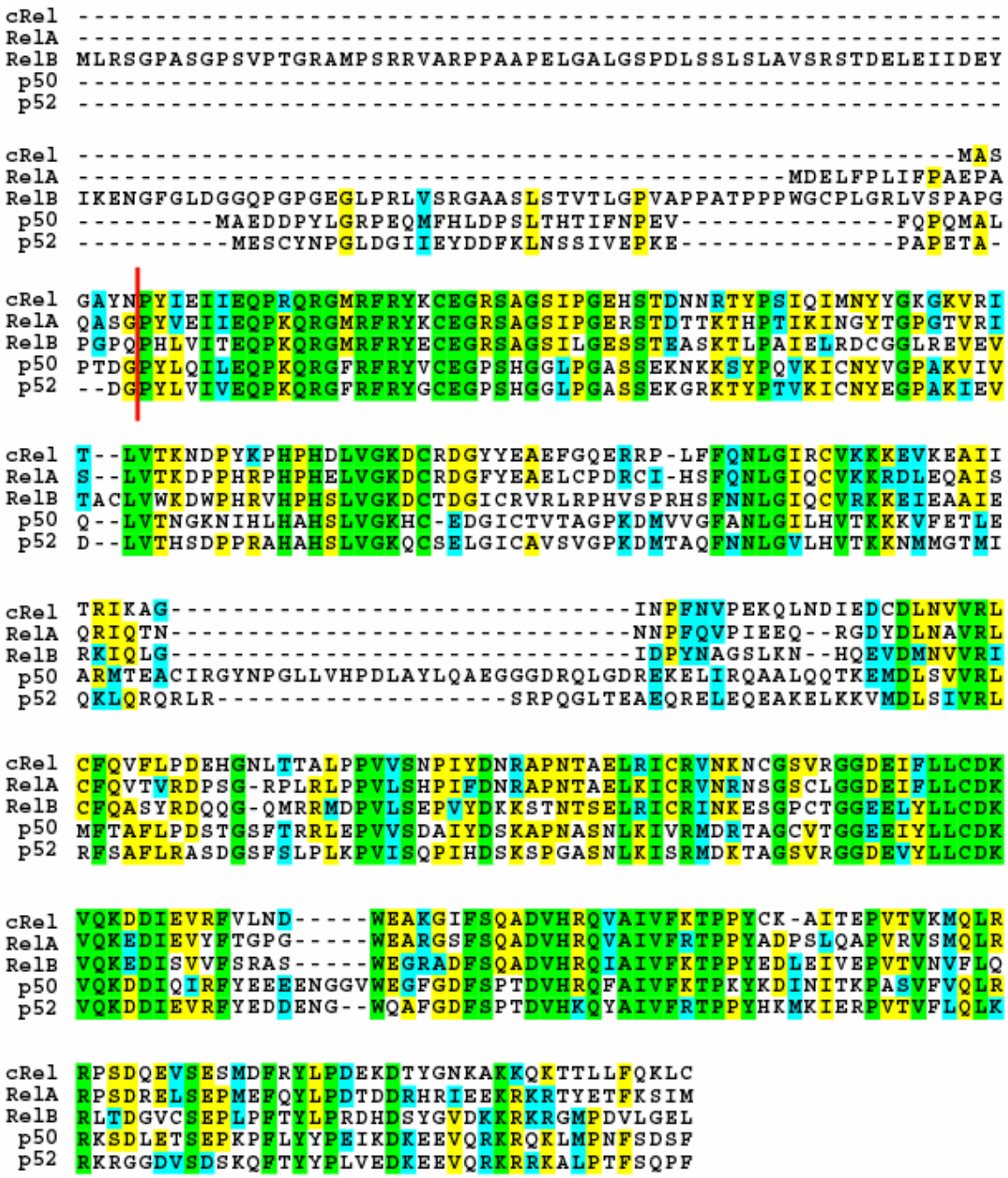

Figure 1-3. *Sequence alignment of the RHRs of the human Rel/NF-κB family members.* The N-terminal extensions of the different family members are shown before the red line. The red line indicates the beginning of the RHR. Identical residues are indicated in green and the locations of conservative substitutions in cyan. Portions of the sequence that are identical in three or four of the family members are in yellow.

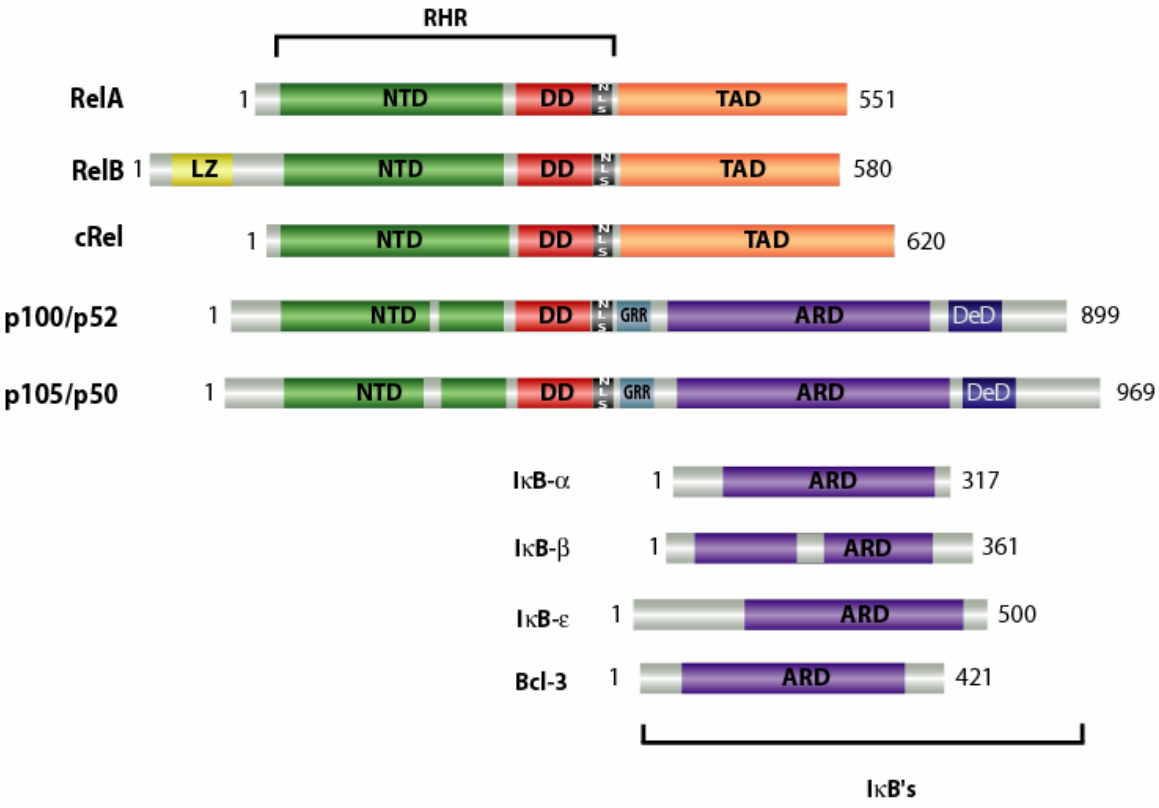

Figure 1-4. *The NF-κB and IκB family of proteins.* p105 and p100 share features in common with members of both families. The RHR of NF-κB are shown in green (N-terminal domain) and red (dimerization domain), the transactivation domains in orange, the GRR in blue, and leucine zipper in yellow. The location of the NLS is also labeled. For the IκB proteins the ARDs are shown in purple.

D. IκB family

In unstimulated cells, NF-κB dimers are maintained inactive by binding to the inhibitor protein, IκB. The IκB family is made up of 7 members in higher vertebrate cells (IκBα, IκBβ, IκBε, IκBζ, IκBγ, IκBδ, and Bcl3) and one protein (*cactus*) in Drosophila. The central region of IκB proteins contain multiple regions of homology known as the ankyrin repeats (AR), which are protein-protein interaction domains that fold into a single domain, referred to as the AR domain (ARD) (Figure 1-4) (Baldwin, 1996; Ghosh et al., 1998). The ARD of IκB and the RHR (primarily the DD) of NF-κB dimers are primarily responsible for the IκB/NF-κB complex formation which is responsible for the masking of the NLS (Huxford et al., 1998; Jacobs and Harrison, 1998; Malek et al., 1998).

There are two distinct classes of IκB proteins in cells. IκBα, IκBβ and IκBε constitute the first class. These inhibitors bind primarily to p65- and cRel-containing NF-κB dimers. The NF-κB precursor proteins p100 and p105, which also function as non-specific inhibitors of NF-κB, comprise the second class of IκB proteins. The IκB-like C-termini of these two molecules use their ARD to inhibit NF-κB (Figure 1-4) (Dobrzanski et al., 1995; Liou et al., 1992).

IκBα is the best characterized member of this family. It is a 37 kDa protein made up of three independent regions: an N-terminal signal response region (SRR), which contains the destruction box and the lysines that are poly-ubiquitinated, a central ankyrin repeat domain (ARD) and a C-terminal acidic PEST region that is rich in proline, glutamic acid, serine, and threonine residues. The PEST region is involved

in the basal turnover of the protein (Verma et al., 1995). This tripartite organization is also seen in IκBβ and IκBε.

IκBα also plays a role in the termination of p50/p65 activated transcription. The promoter of the *iκbα* gene contains binding sites for NF-κB, which activates the upregulation of the transcription of IκB. Newly synthesized IκBα then binds to active p50/p65 dimers and dissociates them from DNA. The IκBα/NF-κB complex is then exported from the nucleus via a nuclear export signal (NES) in IκBα, returning the complex to its pre-induction, inactive, cytoplasmic state(Arenzana-Seisdedos et al., 1995; Arenzana-Seisdedos et al., 1997; Brown et al., 1993; Chiao et al., 1994; Sun et al., 1993).

Bcl-3 is the most unusual member of the IκB family. Bcl-3 has binding specificity for p50 and p52 homodimers, and is found in the nucleus (Franzoso et al., 1992; Nolan et al., 1993; Wulczyn et al., 1992). Bcl-3/p52 complexes can also bind to DNA and activate transcription (Bours et al., 1993). Bcl-3 is the only family member that is able to activate transcription when bound to NF-κB dimers.

E. IKK complex

IκB's degradation is initiated through signal-induced phosphorylation by IκB kinase (IKK). IKK is a high molecular weight complex (700-900 kDa) composed of a minimum of three subunits; IKKα (IKK1), IKKβ (IKK2) and IKKγ (NEMO) (Karin and Ben-Neriah, 2000). IKKα and IKKβ are the catalytic subunits of the complex while IKKγ is the regulatory subunit (Rothwarf and Karin, 1999). IKKα and IKKβ

are serine/threonine kinases characterized by the presence of an N-terminal kinase domain, a C-terminal helix–loop–helix domain and a leucine zipper domain that exhibit similar substrate specificities *in vitro* for two serines at the N-terminus of IκB (Zandi et al., 1997). IKKγ contains a C-terminal zinc finger-like domain, N- and C-terminal coiled-coil domains, two α-helices and a leucine zipper. It interacts with IKKα and IKKβ through their NEMO binding domain (NBD), which is composed of a C-terminal hexapeptide sequence (Leu-Asp-Trp-Ser-Trp-Leu) (May et al., 2002). Other proteins are constitutively associated with the IKK complex, such as Cdc37, HSP70 and Hsp90. Disruption of these proteins from the IKK complex inhibits TNFα induced NF-κB activation (Chen et al., 2002; Ran et al., 2004).

Genetic studies have demonstrated that IKKβ is the major kinase phosphorylating IκBα upon proinflammatory cytokines stimulation, and that IKKγ also plays a key role in IKK complex activity (Gloire et al., 2006). It has been demonstrated that IKKα kinase activity is crucial in the cytoplasm for activating the alternative NF-κB activation pathway which will be discussed below (Cao et al., 2001; Senftleben et al., 2001). IKKα has also been shown to translocate into the nucleus to regulate NF-κB-dependent and -independent gene expression. For a review see (Gloire et al., 2006).

F. p100 and p105 are precursor proteins of p52 and p50, respectively

As mentioned above, p50 and p52 belong to class I of the NF-κB family due to the lack of a TAD and therefore can act as transcriptional repressors as homodimers.

p50 and p52 are expressed as precursor proteins p105 and p100, respectively. p105 and p100 contain an IκB-like domain at their C-terminus, which is made up of an ankyrin repeat domain (ARD) and a death domain (DeD). The dimerization domain (DD) and ARD are connected by a largely unstructured region, which contains the site of processing and critical elements regulating processing, such as the glycine-rich region (GRR) (Heusch et al., 1999; Perkins, 1997; Siebenlist et al., 1994). One major difference observed between p105 and p100 is that p105 undergoes constitutive (non-regulated) processing while p100 processing is tightly regulated (Xiao et al., 2001b). The mechanisms by which p100 is processed is the subject of study in this thesis.

G. NF-κB and Transcription

The NF-κB family members bind to DNA as dimers. These dimers show distinct specificity and affinity for a class of DNA sequences known as κB-sites found in the promoter/enhancer region of NF-κB target genes. The x-ray structures of different NF-κB dimers bound to DNA reveal that the DNA contacts are all made by residues on loops emanating from cores of the N-terminus and DD. The κB DNA targets are composed of two 4- to 5-base pair (bp) half sites, to which each monomer binds, separated by a central A/T base pair. The binding half site has a preferred 5'-GGRN-3' sequence. The 5 bp half site has an additional guanine at the 5' end that is recognized by p50 and p52. This is due to a histidine residue in p50 and p52 that is an alanine (which is incapable of hydrogen bonding) in p65, cRel and RelB. Therefore, the κB DNA sequences can be divided into three main classes (Table 1-1) (Berkowitz

et al., 2002; Chen et al., 1998a; Cramer et al., 1997; Ghosh et al., 1995; Huang et al., 2001; Muller et al., 1995).

Table 1-1. *Classes of κB sites.* The three classes of κB DNA targets are listed along with the rules that define them, as well as the specific dimers that bind them and their consensus sequence. For the consensus DNA sequences R = a purine nucleotide, Y = a pyrimidine nucleotide, W = either A or T, and N = any nucleotide.

Class	11 bp	10 bp	9 bp
Rule	5 + 1 + 5	5 + 1 + 4	4 + 1 + 4
NFκB dimers	p50/p50	p50/p65, p50/cRel	p65/p65, cRel/cRel, p65/cRel
Consensus	GGGRN W NYCCC	GGGRN W NTCC	GGAN W NTCC
Example	MHC I GGGGA A TCCCC	Ig/HIV κB GGGAC T TTCC	IL8 GGAA T TTCC

Active NF-κB dimers, bound to their target κB DNA sites, do not activate transcription alone. Genes regulated by NF-κB require additional factors for initiation of transcription. Eukaryotic gene enhancers contain binding sites for multiple, different transcription factors which work in concert to synergistically activate gene transcription (Carey, 1998). The multi-protein/enhancer DNA complexes are referred to as enhanceosomes. It is thought that the assembly of protein factors on DNA is cooperative and involves coactivators, such as CBP (CREB binding protein)/p300). The enhanceosome was thought to be a stable surface capable of interacting with and stabilizing the basal transcriptional machinery (such as TBP, TFIIs, and the RNA PolII complex), thus allowing transcriptional activation. One such example is the well studied IFNβ enhancer (Figure 1-5) (Thanos and Maniatis, 1995).

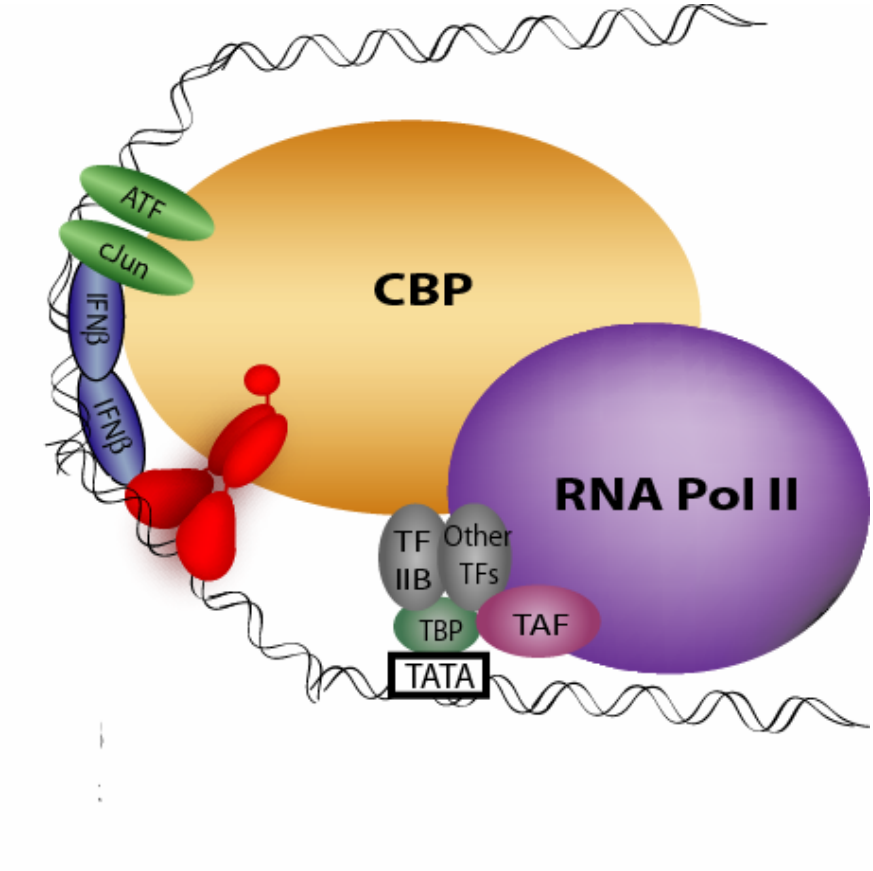

Figure 1-5. *Model of enhanceosome assembly based on the IFNβ enhancer.* First, specific transcription activators (green), such as NF-κB, and DNA-binding architectural proteins (blue) bind cooperatively to specific sites in the gene's enhancer. These factors in conjunction with coactivators (cyan) provide a surface that stabilizes the formation of the basal transcriptional machinery, which includes TBP (TATA-binding protein, purple), TAFs (TBP associated factors, magenta), general transcription factors (TFIIs, violet), and the RNA pol II complex (grey).

H. p100 processing (The Non-canonical activation pathway)

As mentioned above, p100, the precursor protein of p52, acts as an inhibitor protein (IκBδ). The pathway responsible for the processing of p100 to p52 is commonly referred to as the non-canonical pathway. It has been shown that the non-canonical pathway is important for B-cell maturation, lymphoid organogenesis, cell proliferation and survival (Caamano et al., 1998; Franzoso et al., 1998; Gross et al., 2001; Ishikawa et al., 1997; Khare et al., 2000; Mackay et al., 1999; Senftleben et al., 2001). This pathway is tightly regulated and is activated by a set of inducers, such as lymphotoxin β (LTβ), B-cell activating factor (BAFF), RANKL and CD40 ligand (Bonizzi et al., 2004; Cao et al., 2001; Claudio et al., 2002; Coope et al., 2002; Dejardin et al., 2002; Novack et al., 2003; Senftleben et al., 2001; Xiao et al., 2001b). Recently a lot of light has been shed on the mechanism of p100 processing; however there are many questions that remain unanswered.

It has been shown that the key mediators of p100 processing are NF-κB inducing Kinase (NIK), IkappaB kinase1 (IKK1) and the 26S proteasome.(Fong and Sun, 2002; Senftleben et al., 2001; Xiao et al., 2004; Xiao et al., 2001b). NIK was originally identified as a MAP kinase kinase kinase (MAP3K) that interacted with the TNF receptor–associated factor 2 (TRAF2) and activated NF-κB when expressed in mammalian cells (Malinin et al., 1997). Unlike the canonical pathway, described above, which depends on IKKγ and IKKβ as the two central regulators, the non-canonical pathway only depends on IKKα. NIK, activated by upstream receptors, activates IKKα, recruiting it to the p100 complex via a phosphorylation dependent

(the phosphorylation of two C-terminal serines 866 and 870 of p100) and independent manners (Senftleben et al., 2001; Xiao et al., 2004). p100 is then phosphorylated by IKKα at both N- and C-terminal serines (99, 108, 115, 123 and 872). The phosphorylation of these specific serines is a prerequisite for ubiquitination by the β-TrCP ubiquitin ligase and subsequent processing of p100 by the 26 S proteasome (Figure 1-6) (Fong and Sun, 2002; Xiao et al., 2001a). The serine residues that are phosphorylated by NIK and IKKα are unique to p100, absent in p105, and are conserved amongst different species (Figure 1-7). It is also important to note that new protein synthesis is required for p100 processing, however it is still unclear which synthesis is required (Liang et al., 2006; Mordmuller et al., 2003). One possibility is the requirement of newly synthesized NIK. It has recently been shown that the main mechanism for regulating NIK is by controlling its stability. The level of NIK is very low in resting cells, whereas upon stimulation with non-canonical inducers NIK level is increased (Qing et al., 2005b). It is thought that NIK degradation is due to its interaction and subsequent ubiquitination by TRAF3 (He et al., 2007; Liao et al., 2004). However, the requirement for newly synthesized RelB and/or p100 cannot be ruled out.

The activation of the RelB/p52 heterodimer is a significant outcome of the non-canonical pathway. Biochemical experiments demonstrate that in unstimulated cells, RelB primarily associates with p100, forming an inactive complex, and to a lesser extent with p50 (Solan et al., 2002). In induced cells the predominant RelB dimer is the RelB/p52 heterodimer. However, p100 is found to be associated with both RelB and non RelB containing NF-κB dimers (Basak et al., 2006). The

specificity of RelB for both p100 and its processed product p52 is unique amongst NF-κB family members. It is not understood why RelB and not other family members have this unique specificity.

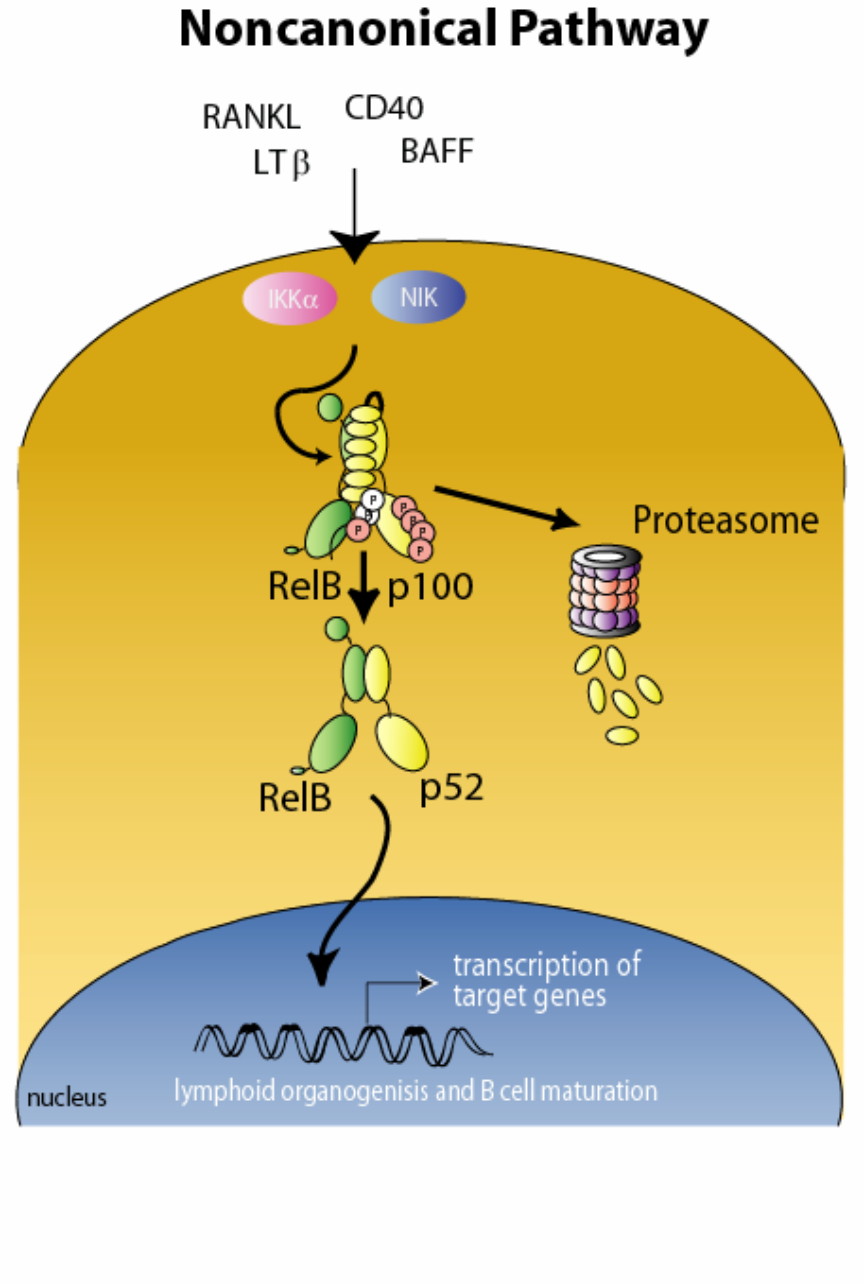

Figure 1-6. *The non-canonical activation pathway.* Signals that activate the non-canonical pathway are received at the cell surface and activate NIK (blue). NIK then activates and recruits IKKα (Pink) to p100 (yellow). P100 is phosphorylated by NIK (white) and IKKα (pink) at its N- and C-terminus. Phospho-p100 is then ubiquitinated and processed by the 26S proteosome (purple and pink). Processed p52 then translocates to the nucleus and activates transcription of genes important in lymphoid organogenesis and B cell maturation.

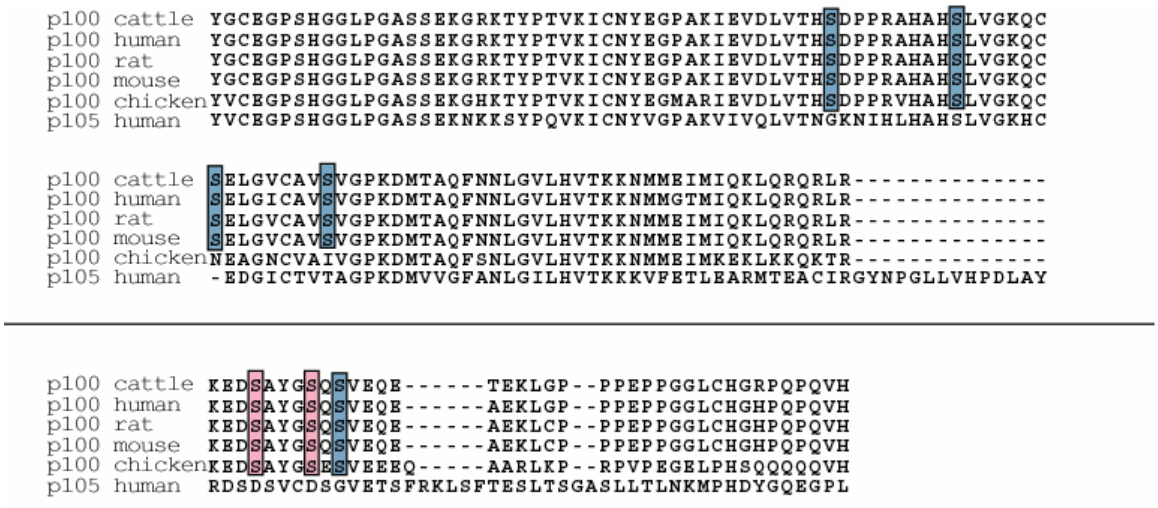

Figure 1-7. *Sequence alignment of p100.* Both the N- and C-terminal (above and below the black line respectively) phosphorylation sites of p100 are conserved amongst different species. The NIK phosphorylation sites are shown in pink and the IKKα phosphorylation sites are shown in blue. The serine residues are unique to p100 and they are not conserved in p105.

I. Biological functions of p100, p52 and RelB

The biological functions of different NF-κB, IKK and IκB family members have been widely studied by different groups. Table 1-2 summarizes the biological roles of different family members. Here, I will discuss the biological significance of different members of the non-canonical pathway, p100, p52 and RelB. Rearrangements in the *nfkb2* gene result in constitutively processed p100 due to the loss of its C-terminal processing inhibitory domain (PID) (Xiao et al., 2001a). The constitutively processed p100 has been associated with development of various lymphomas/leukemias such as T-cell lymphoma and chronic lymphocytic leukemia (Neri et al., 1991; Sun and Xiao, 2003; Xiao et al., 2001a). A recent report has given insight into the mechanism of constitutive processing of the C-terminally truncated p100 (p100ΔC) (Qing et al., 2007). They demonstrate that p100ΔCs bind to the κB promoter region and subsequently recruit the proteasome. The stable proteasome/p100ΔC/DNA complex mediates the processing of p100ΔCs to p52. The processing is initiated by a proteasome-mediated endoproteolytic cleavage at amino acid D415. This demonstrates that p52 and not p100ΔCs themselves cause oncogenic potential by upregulating a subset of tumor associated genes. Abnormal persistent processing of p100 is also found to be associated with T-cell transformation by HTLV-I (human T-cell leukemia virus type I) (Jeang, 2001). The processing of p100 is caused by the virus encoded oncoprotein Tax. Tax specifically recruits IKKα to p100, triggering its processing (Xiao et al., 2001a).

Overproduction of p52 has also been observed in other tumors such as breast cancer and pancreatic cancer (Chandler et al., 2004; Cogswell et al., 2000). The p52 protein also associates with the IκB-like Bcl-3 oncoprotein, leading to the formation of a functional transcription factor complex (Bours et al., 1993). In human breast cancer this may be due to the over expression of p52 and Bcl-3.

relb knockout mice have T-cell inflammatory infiltrates of multiple organs, T-cell-dependent myeloid hyperplasia, splenomegaly resulting from extramedullary hemopoiesis and inflammatory dermatitis. Although the underlying basis of the inflammatory phenotype remains to be determined, it is thought to involve impaired regulatory T-cell function resulting from a combination of stromal and hemopoietic defects (Thomas, 2005).

It has also been shown that p52 and RelB play an important role in devolopment. RelB and p52 are important for secondary lymphoid organ development, such as Peyer's patches, spleen and lymph nodes (Beinke and Ley, 2004; Weih et al., 2001; Weih and Caamano, 2003; Yilmaz et al., 2003). RelB and p52 are also important for B-lymphocyte maturation, germinal center formation and the generation of marginal zones in B cells (Beinke and Ley, 2004; Senftleben et al., 2001; Weih et al., 2001; Weih and Caamano, 2003). It has also been shown that RelB is required for the normal devolpment and function of T-lineage cells (Elewaut et al., 2003; Sivakumar et al., 2003).

Table 1-2. *Summary of mouse knockout studies.* Abbreviations used: Con A, concanavalin A; LPS, lipopolysaccharide; NF-κB, nuclear factor-κB; TLR, toll-like receptor; TNF-α, tumor necrosis factor-α; DC, dendritic cells; ERK, extracellular signal-regulated kinase; GM-CSF, granulocyte–macrophage colony-stimulating factor; IFNγ, interferon*γ*; IL, interleukin; NK cells, natural killer cells; pDC, plasmacytoid DCs; TLR, toll-like receptor(Gerondakis et al., 2006).

Knock out mice for NFκB's

Genotype	***Lethality***	***Defect/phenotype***
nfkb1 $^{-/-}$	No	B cells: marginal zone and $CD5^+$ peritoneal B cells reduced; response to LPS diminished, turn over rapidly *in viv*o; defective isotype switching and impaired humoral immune response Th2 differentiation is impaired NK cells display enhanced proliferation and increased IFNγ production Macrophages: ERK mitogen-activated protein kinase pathway activation in response to TLR signals is impaired leading to reduced expression of IL-6, IL-10 and Cox-2
nfkb2 $^{-/-}$	No	Defective secondary lymphoid organ development, impaired B-cell development; enhanced DC function
c-rel $^{-/-}$	No	B cells: cell-cycle and survival defects; impaired isotype switching T cells: defects in CD4 and CD8 T-cell responses, Th1 development and cytokine production (IL-2 and GM-CSF) in $CD4^+$ T-cell responses Reduced number of pDC, impaired IL-12 production and DC priming of CTL Neuronal survival defects
rela $^{-/-}$	Yes (~ E15)	TNF-α-induced cell death: hepatocytes, macrophages and fibroblasts Impaired secondary lymphoid organ development Defects in leukocyte recruitment, T-cell-dependent responses, isotype switching to IgG3 Spatial learning responses Epidermal homeostasis
relb $^{-/-}$	No	Complex inflammatory phenotype and hematopoietic abnormalities Defects in secondary lymphoid organ structure and germinal center formation Lack certain DC populations, DC functional defects

Table 1-2. *Summary of mouse knockout studies continued.*

Knock out mice for IKK's

Genotype	*Lethality*	*Defect*
ikka $^{-/-}$	Die at birth	Skeletal and epidermal defects Reduced number of mature B cells
ikkb $^{-/-}$	Yes (~E13)	Macrophages exhibit enhanced NF-κB activation TNFα-induced hepatocyte apoptosis
nemo $^{+/-}$	Females are viable	Female mice develop an inflammatory skin disease following birth very similar to humans with incontinentia pigmenti
nemo $^{-/-}$	Die at ~E10–11	Hepatocyte apoptosis. B and T cells fail to develop in radiation chimeras. IgM^+ B cells develop in an *in vitro* differentiation assay. These immature B cells exhibit enhanced apoptosis

Knock out mice for IκB's

Genotype	*Lethality*	*Defect/phenotype*
ikbα $^{-/-}$	7–10 days after birth	Severe inflammatory dermatitis and amplified granulocytic compartment Proliferation of B cells is enhanced and that of T cells is reduced
ikbε $^{-/-}$	No	Increased expression of certain Ig isotypes and cytokines
ikba $^{-/-}$ *ikbe* $^{-/-}$	Neonatal	Severe disruption of lymphopoiesis; almost complete absence of B and T cells, reduced NK cell numbers
bcl3 $^{-/-}$	No	Splenic architecture disrupted Defective Th1 and Th2 differentiation

J. Focus of Study

The primary focus of this study is centred around the RelB/p52 heterodimer. Though discovered around the same time as the other members, the mode of actions of this heterodimer is coming to light only recently. RelB is primarly bound to p100 or its processed product p52. The mechansim of this selective association is unknown. The fact that the RelB/p52 heterodimer is important for developmental programs, understanding the mechansims of p100 processing and the formation of the RelB/p52 heterodimer are important.

This heterodimer is a trancriptional activator which enhances gene transcription by binding to κB DNA. A report by Bonizzi (Bonizzi et al., 2004) showed that the RelB/p52 heterodimer prefers a subset of κB DNA which vary significantly at the 3' half-site. Therefore, another focus of my research is the 3-D strucure of RelB/p52 bound to DNA. Although we do not expect any major difference in this strucutre as compared to other known complexes, one cannot rule out the possibility that the 3-D structure may reveal new insights into the specificity of the RelB/p52/DNA complex.

In addition to structural studies, it is important to investigate how RelB/p52 heterodimers bind to different κB DNA as compared to other NFκB dimers. With the knowledge of structures, *in vitro* binding affinity, and *in vivo* dimer specificity for different target genes, one may be able to estabilsh the rule of how different dimers recognize a specific subset of target κB DNA sequences. *In vivo* specificity may in

part arise from the interaction between multiple activators bound to DNA sequences arranged in tandem. Therefore, one of my research focuses is determining how NF-κB interacts with other activators such as CREB and C/EBPβ.

The focus of this study, therefore, is to i) investigate the mechanism of generation of the RelB/p52 heterodimer, ii) elucidate the three dimentional x-ray crystal structure of a κB DNA bound to the RelB/p52 heterodimer, iii) understand the mechanism of differential DNA binding by various NF-κB dimers and iv) investigate if NF-κB dimers cooperate with other activators bound to the neighboring site of specific promoters.

II. Materials and Methods

A. Protein Expression and Purification

1. Purification of the RelB/p52 heterodimer

The vector pET29b RBS p52(1-344) and pET11a p52(1-408) was provided by Joane Wu. pET29b RBS p52(35-328), and pET11a p52(35-341): The inserts for these expression plasmids were generated by PCR amplification of the relevant cDNA segment from pET15b RBS p52(1-344). The 5' primer for these constructs carried a BamHI restriction site.

p52(35)NTBamHI: 5' AGGACGGGATCCATGGCTGATGGCCCCTAC3'

The 3' primers for these constructs had a NotI restriction site. Stop codon (underlined) was encoded to stop expression of the C-terminal tag in pET11a:

p52(344)CTNotI: 5'TTTTCCTTTTGCGGCCGCCTAGGGCAAGGCCTTCCT3'

p52(329)CTNotI: 5'TTTTCCTTTTGCGGCCGCCTACACCAGAGGGTAATA3'

The resulting DNA fragment was gel purified, double digested with the restriction enzymes BamHI and NotI (New England Biolabs) and then gel purified again. The fragment was then ligated into either the vector pET11a or pET29b RBS (Novagen) which was previously double digested by the same restriction enzymes. The ligated products were transformed into *E. coli* JM109 cells and colonies obtained were screened for the presence of p52 cDNAs by restriction analysis and sequencing. The vector pET15b RelB(1-400) was a gift from Don Vu.

Recombinant human p52 RHR constructs and mouse RelB RHR protein were overexpressed separately in BL21[DE3] *E. coli* cells. Large scale cultures (usually 2 L) of LB/Ampicillin (200 μg/mL) or LB/Kanamycin (10 μg/mL) were grown to an

$O.D._{600}$ of 0.3 at 37°C and induced for 16 hours at room temperature (approximately 25°C) with 0.1 mM IPTG. Cells were harvested by centrifugation and the proteins were purified independently.

Cells overexpressing p52 protein were lysed by sonication in 20mM Tris HCl pH 7.5, 50 mM NaCl, 1mM DTT, 10% glycerol, 0.5mM EDTA, 0.1mM PMSF and 0.1X Sigma Protease Inhibitor Cocktail (Sigma/Aldrich). Insoluble material was removed from the lysate by centrifugation in a SS-34 rotor (Sorvall) at 14,000 r.p.m. for 35 minutes. The soluble lysate was loaded onto a gravity Q-sepharose Fast Flow column (resin from Amersham/Pharmacia) followed at 4°C. Presence of the protein in the flow through was determined by SDS-PAGE analysis. The flow through was then loaded onto a Fast Flow SP-sepharose cation exchange gravity column (Amersham/Pharmacia). The column was washed with 50 mL of the same buffer. The column was then eluted using a linear NaCl gradient (200 ml) from 50 to 400 mM NaCl in a Tris HCl pH 7.5, 1mM DTT, 10% glycerol, 0.5mM EDTA. Peak fractions were identified through Bradford Assays (Biorad) and confirmed by 10% SDS-PAGE prior to pooling.

Cells overexpressing RelB protein were lysed by sonication in 20mM Tris pH 7.5, 1 M NaCl, 10% glycerol, 0.1mM PMSF and Sigma Protease Inhibitor Cocktail (Sigma/Aldrich). Insoluble material was removed from the lysate by centrifugation at 14,000 r.p.m. for 35 minutes. The soluble lysate was loaded onto an Invitrogen ProBond Ni-affinity resin column. The column was washed with 30 mL of 30 mM Imidazole, 20mM Tris pH 7.5, 1 M NaCl, 10% glycerol. The protein was eluted with 15 mL of 300 mM Imidazole, 20mM Tris pH 7.5, 1 M NaCl, 10% glycerol. Peak

fractions were identified through Bradford Assays (Biorad) and confirmed by 10% SDS-PAGE prior to pooling.

p52 and RelB proteins were unfolded with a 1.2 molar excess of RelB and a final total protein concentration of 0.8 mg/mL in 8 M Urea, 20mM Tris pH 7.5 and 250 mM NaCl. The proteins were then refolded by dialysis using MWCO 3,500 dialysis tubing (Spectrum Laboratories, Inc.) for 3 hours at 4°C in two liters of 20mM Tris pH 7.5 and 250 mM NaCl, 7 mM BME, 10% glycerol and 0.5 mM PMSF. The buffer was then changed two more times for three hours and once for 12 hours. The refolded protein was then dialyzed with two liters of 20mM Tris pH 7.5 and 50 mM NaCl, 1 mM DTT, 10% glycerol and 0.5 mM PMSF for three hours at 4°C to lower the salt concentration.

Thrombin (Sigma) was then added (1 reaction unit/µl)to the dialysate and mixed at 25°C for 2 hours and 15 minutes to remove the hexa-histidine tag. The lysate was then filtered using a 0.8 MIC filter (Nalgene) to remove any insoluble protein. The soluble lysate was then loaded onto a cation exchange HiTrap-SP column (Amersham/Pharmacia) and eluted with a linear, 20 column-volume gradient from 50 to 500 mM NaCl to remove any remaining homodimer contamination. This method works because RelB has no affinity for the SP-column and the RelB/p52 heterodimer elutes from the column at a lower salt concentration (250 mM NaCl) compared to the p52 homodimer (400 mM NaCl). The heterodimer peak fractions (confirmed by 10% SDS-PAGE) were pooled and concentrated using a centriprep -30 (Amicon) and then diluted to 3.5 mL with 20 mM Tris-HCl pH 7.5 and 1 mM DTT and re-concentrated (to decrease the salt concentration to approximately 50 mM NaCl)

to 7mg/mL and flash froze in small aliquots. 0.1mg of the complex was loaded onto an analytical size exclusion column using Superdex 200 resin (Amersham/Pharmacia) in a buffer of 20 mM Tris-HCl pH 7.5, 75 mM NaCl and 1 mM DTT to confirm that the p52/RelB was a single dimeric species. The protein concentration was determined by molar extinction coefficient (determined by Prot Param tool at Expasy.org).

All p52/RelB heterodimer complexes were purified with this method. The only variation was whether the complex was treated with thrombin.

2. Purification of p52/RelB/IκBδ complex

RelB (1-400) was cloned into 21dHT His tag/TEV site expression vector based on pET21d (gift from Greg Van Duyne). The insert for this plasmid was generated by PCR amplification using pET15b RelB(1-400) as a template. The primers used are listed below:

RelB(1)NTBamHI: 5'AGGACGGGATCCATGCCGAGTCGCCGC 3'

RelB(400)NotI: 5'TTTTCCTTTTGCGGCCGCCTAGCTCAACTCTCCAAGGAC 3'

IκBδ (406-899) was cloned into pGV67 GST/TEV expression vector, based on pET21a (gift from Greg Van Duyne). The insert for this plasmid was generated by PCR by amplification using pHis8 p100 (1-899) a gift from Rashmi Talwar. Primers used are listed below:

IκBδ(406)NTBamHI: 5' AGGACGGGATCCATGGCCGCCACGGTGCCC 3'

IκBδ(899)CTNotI: 5'TTTTCCTTTTGCGGCCGCCTA3'

pET29b RBS p52 (1-344) plasmid was a gift from Joane Wu.

RelB/p52 heterodimer was purified the same way as described above without thrombin cleavage. IκBδ was overexpressed in BL21[DE3] E. coli cells. Large scale cultures (2 L) of LB/Ampicillin (200 μg/mL) were grown to an $O.D._{600}$ of 0.3 at 37°C and induced for 16 hours at room temperature (approximately 25°C) with 0.1 mM IPTG. Cells were harvested by centrifugation and lysed by sonication in 20mM Tris pH 7.5, 150 mM NaCl, 1mM DTT, 10% glycerol, 0.5mM EDTA, 0.1mM PMSF and 0.1X Sigma Protease Inhibitor Cocktail. Insoluble material was removed by centrifugation at 14,000 rpm for 40 minutes. The soluble lysate was loaded onto a glutathione-sepharose gravity column (GST-column). Following loading, the GST-column was washed with 30 mL of the same buffer. The column was then eluted in 1 mL fractions using the same buffer as mentioned above plus 10 mM reduced glutathione pH 7.5. Peak fractions were analyzed by 10% SDS-PAGE to confirm the purity of the protein then pooled.

The p52/RelB/IκBδ complex was formed by mixing p52/RelB (14 ml of 56 μM) and IκBδ (6.1 ml of 54 μM) at 25μ°C for 30 minutes. The complex was concentrated using Amicon (30,000 MWCO) to approximately 10 mg/mL. TEVPM4 protease (gift from Shutapa Chakrabarti) was then added and mixed at 25°C for 2.5 hours to remove the histidine and GST tag from RelB and IκBδ, respectively. The amount of TEV protease added was determined by:

$$x\ \mu M\ TEV = \mu M \times volume/(50/number\ of\ cut\ sites)$$

The complex was further purified on a Superdex 200 gel filtration column in 20 mM Tris-HCl pH 7.5, 150 mM NaCl and 1 mM DTT. The peak fractions (determined by

SDS-PAGE) were concentrated using a centriprep-30 to 8 mg/ml and then flash frozen.

3. Purification of p52/p52/IκBδ complex

p52 (residues 1-344) homodimer was expressed and purified as described above. The p52/52/IκBδ complex was formed and purified the same way as described for the p52/RelB/IκBδ complex. The only difference was p52/p52 homodimer was added to IκBδ at 1.5 molar excess versus 1.1 molar excess of p52/RelB heterodimer.

4. Purification of GST tagged proteins

The vectors pHis8 p100 (1-899), pET15b p105(1-969) and pcDNA of p65(1-549) were gifts from Rashmi Talwar, Anu Krishnimorty and Tom Huxford, respectively. The following inserts were subcloned into the vector pGEX 4T2 (Amersham) using the identical procedure described above: IκBδ(344-899), IκBδ(406-899), IκBδ(764-899), IκBδ(764-851), IκBδ(406-765), IκBδ(406-851)), IκBδ(482-899), p52(225-344), p52(1-222), p50(241-354), p50(1-245), p65(186-296): The inserts for these expression plasmids were generated by PCR amplification of the relevant DNA segments from pHis8 p100(1-899), pET15b p105(1-969) or pcDNA p65(1-549). The majority of the 5' primers for these constructs carried a BamHI restriction site.

IκBδ(344)NTBamHI: 5' AGGACGGGATCCATGCCCACCTTCTCCCAG 3'

IκBδ(406)NTBamHI: 5' AGGACGGGATCCATGGCCGCCACGGTGCCC 3'

IκBδ(482)NTBamHI: 5’ AGGACGGGATCCATGACGGCGCAGGACGAG 3’

IκBδ(764)NTBamHI: 5’AGGACGGGATCCATGGCAGGGCCGGGACTG 3’

p52(1)NTBamHI: 5’ AGGACGGGATCCATGGAGAGTTGCTAC 3’

p52(225)NTBamHI: 5’ AGGACGGGATCCATGGCATCAAACCTG 3’

p50(1)NTBamHI: 5’ AGGACGGGATCCATGGCAGACGATGATCCC 3’

p50(241)NTBamHI: 5’ AGGACGGGATCCATGAAAGCCCCGAATGCA 3’

p65(186)NTBamHI: 5’ AGGACGGGATCCATGAACCGGGCCCCCAAC 3’

The 5’ primer for pGEX 4T2 p65(1-325) and pGEX 4T2 p65(1-191) constructs carried a EcoRI restriction site.

p65(1)NTEcoRI: 5’ AGGACGGGATCCATGGACGATCTGTTTCCC 3’

The 3’ primers for these constructs had a NotI restriction site.

IκBδ(899)CTNotI: 5’TTTTCCTTTTGCGGCCGCCTA3’

IκBδ(851)CTNotI: 5’TTTTCCTTTTGCGGCCGCCTATTCTGGACCCCTCAG 3’

IκBδ(765)CTNotI: 5’TTTTCCTTTTGCGGCCGCCTACCCTGCTGGGCTGGG 3’

p52(222)CTNotI: 5’TTTTCCTTTTGCGGCCGCCTAAGATTTGCTGTCATG 3’

p52(344)CTNotI: 5’TTTTCCTTTTGCGGCCGCCTAGGGCAAGGCCTTCCT3’

p50(354)CTNotI: 5’TTTTCCTTTTGCGGCCGCCTATTTGTCTTTGATTTC 3’

p50(245)CTNotI: 5’TTTTCCTTTTGCGGCCGCCTA3’

p65(325)CTNotI: 5’TTTTCCTTTTGCGGCCGCCTACCGGGGTTCAGT 3’

p65(296)CTNotI: 5’TTTTCCTTTTGCGGCCGCCTAGTGGCGATCATCTGT 3’

p65(191)CTNotI: 5’TTTTCCTTTTGCGGCCGCCTAAGTGTTGGGGGC 3’

GST tagged proteins were cloned as described above into pGEX 4T-2 which contains a thrombin cleavage. Recombinant proteins were overexpressed in

BL21[DE3] E. coli cells. Large scale cultures (usually 2 L) of LB/Ampicillin (200 μg/mL) were grown to an $O.D._{600}$ of 0.3 at 37°C and induced for 16 hours at room temperature (approximately 25°C) with 0.1 mM IPTG. Cells were harvested by centrifugation and lysed by sonication in 20mM Tris pH 7.5, 150 mM NaCl, 1mM DTT, 5% glycerol, 0.5mM EDTA, 0.1mM PMSF and Sigma Protease Inhibitor Cocktail (Sigma/Aldrich). Insoluble material was removed by centrifugation at 14,000 rpm for 35 minutes. The soluble lysate was loaded onto GST-column (resin from Amersham/Pharmacia). Following loading, the GST-column was washed with 50 mL of the same buffer. The column was then eluted in 1 mL fractions using the same buffer with 10 mM reduced glutathione pH 7.5.

The final step of purification was size exclusion using Superdex 75 or 200 resin (Amersham/Pharmacia) in a buffer of 20 mM Tris-HCl pH 7.5, 150 mM NaCl, and 1 mM DTT. Peak fractions were analyzed by 10% SDS-PAGE to confirm the purity of the protein then pooled and concentrated in a centriprep-30 (Amicon).

5. Purification of Histidine tagged proteins

The plasmid pBABE RelB V314R, F358Q, V366E (1-558) puro, was a gift from Rashmi Talwar. Mutagenesis of mouse RelB was carried out according to manufacturer's protocol for the Stratagene Quikchange Mutagenesis Kit. The RelB M5 mutant (RelB V314R, F358Q, V366E, A324G and L362K) was made sequentially using pBABE RelB V314R, F358Q, V366E (1-558) puro as a template for PCR. The presence of each mutation was verified by sequencing. The primers used for mutagenesis were:

RelB(A324G)F: 5’ CCTGGGAAGGCCGTGGCGACTTCTCTCAAGC 3’

RelB(A324G)R: 5’ GCTTGAGAGAAGTCGCCACGGCCTTCCCAGG 3’

RelB(L362K)F and RelB(L362K)R were kind gifts from Don Vu.

The following inserts were subcloned into the vector pET21d (TEV cleavage site) using the identical procedure described above: RelB M5(1-400), RelB(1-400) and RelB(401-558). The inserts for these expression plasmids were generated by PCR amplification of the relevant cDNA segment from pBABE RelB M5(1-558) puro or pBABE RelB(1-558) puro. The 5’ primers for these constructs carried a BamHI restriction site.

RelB(401)NTBamHI: 5’ AGGACGGGATCCATGAGCTCTGATCCACAT 3’

RelB(1)NTBamHI: 5’ AGGACGGGATCCATGCCGAGTCGCCGC 3’

The 3’ primers for these constructs had a NotI restriction site.

RelB(558)NotI: 5’TTTTCCTTTTGCGGCCGCCTACGTGGCTTC 3’

RelB(400)NotI: 5’TTTTCCTTTTGCGGCCGCCTAGCTCAACTCTCCAAGGAC3’

Histidine tagged proteins were cloned as described above into pET21d. Recombinant proteins were overexpressed in BL21[DE3] E. coli cells. Large scale cultures (usually 2 L) of LB/Ampicillin (200 μg/mL) were grown to an $O.D._{600}$ of 0.3 at 37°C and induced for 16 hours at room temperature (approximately 25°C) with 0.1 mM IPTG. Insoluble material was removed from the lysate by centrifugation at 14,000 r.p.m. for 35 minutes. The soluble lysate was loaded onto an Invitrogen ProBond Ni-affinity resin column. The column was washed with 30 mL of 30 mM Imidazole, 20mM Tris-HCl pH 7.5, 150-500 mM NaCl, 10% glycerol. The protein was eluted in 5 mL fractions with 300 mM Imidazole, 20mM Tris pH 7.5, 150-500

mM NaCl, 10% glycerol. Peak fractions were identified through Bradford Assays (Biorad) and confirmed by 10% SDS-PAGE prior to pooling. Protein was concentrated (centriprep-30 or centriprep-3) then flash frozen.

6. Purification of CREB

The DNA binding domain of $CREB_{341}$ subcloned into pET15B (Novagen) was a gift from Dr. R. Goodman's lab. $CREB_{341}$ was overexpressed in BL21[DE3] E. coli cells. Large scale cultures (4 L) of LB/Ampicillin (200 μg/mL) were grown to an $O.D._{600}$ of 0.7 at 37°C and induced for 16 hours at room temperature (approximately 25°C) with 0.2 mM IPTG. Cells were harvested by centrifugation and lysed by sonication in 20mM Tris-HCl pH 8.0, 100 mM NaCl, 1mM DTT, 0.5mM EDTA, 0.5mM PMSF and 0.1X Sigma Protease Inhibitor Cocktail. Insoluble material was removed by centrifugation at 14,000 rpm for 40 minutes. Lysate was loaded onto a Fast Flow SP-sepharose cation exchange gravity column. Following loading, the SP-column was washed with 50 mL of the same buffer. The protein was eluted with a salt gradient from 100 mM to 1M NaCl in 20 mM Tris-HCl pH 8.0, 1mM DTT and 0.5mM PMSF. The peak fractions were pooled and concentrated based on Bradford assay and SDS-PAGE. The final step of purification was size exclusion using Superdex 75 resin (Amersham/Pharmacia) in a buffer of 20 mM Tris-HCl pH 8.0, 150 mM NaCl, and 1 mM DTT. Peak fractions were analyzed by 10% SDS-PAGE to confirm the purity of the protein then pooled and concentrated in a centriprep-3 (Amicon) and flash frozen. Protein was concentrated to 2.2 mg/ml determined by Bradford assay.

7. Purification of C/EBPβ

The DNA binding domain of C/EBPβ was a gift from Steve Smelt. C/EBPβ was overexpressed in BL21[DE3] E. coli cells. Large scale cultures (3 L) of LB/Ampicillin (200 μg/mL) were grown to an $O.D._{600}$ of 0.7 at 37°C and induced for 16 hours at room temperature (approximately 25°C) with 0.2 mM IPTG. Cells were harvested by centrifugation and lysed by sonication in 20mM Tris-HCl pH 8.0, 100 mM NaCl, 0.5mM PMSF and 0.1X Sigma Protease Inhibitor Cocktail. Insoluble material was collected by centrifugation at 14,000 rpm for 40 minutes. To the insoluble fraction, 20mM Tris-HCl pH 8.0,100 mM NaCl and 6M Urea was added and mixed at 25°C for 1.5 hours. The sample was then centrifuged for 20 minutes at 14,000 rpm. Lysate was loaded onto a Fast Flow SP-sepharose cation exchange gravity column. Following loading, the SP-column was washed with 50 mL of the same buffer. A second wash was done with 20 mM Tris-HCl pH 8.0 and 100 mM NaCl. The protein was eluted with a salt gradient from 100 mM to 1M NaCl in 20 mM Tris-HCl pH 8.0. The peak fractions, determined by Bradford assay, were concentrated and loaded onto a Superdex 75 size exclusion column (Amersham/Pharmacia) in a buffer of 20 mM Tris-HCl pH 8.0 and 150 mM NaCl. Peak fractions were analyzed by 10% SDS-PAGE to confirm the purity of the protein then pooled and flash frozen. Protein was concentrated to 3.0 mg/ml determined by Bradford assay.

B. Mammalian Expression

1. Transient Transfections

Human p100 and a series of p100 and p52 deletion mutants (p100(1-899), p100(221-899), p52(1-344), p52(221-344)), were generated by PCR and cloned into pEYFP-C1 vector (Clontech) which was modified by deleting YFP and adding both a N-terminal Flag tag and C-terminal HA tag. Human p100 and a series of p100 and p52 deletion mutants p52(1-222), IκBδ(342-899), IκBδ(408-899), IκBδ(408-765), IκBδ(482-899) were generated by PCR and cloned into pEYFP-C1 vector (Clontech) which was modified by deleting YFP and adding a C-terminal Flag tag. The 5' primers for these constructs carried a HindIII restriction site.

p100(1)NTHindIII: 5' GACGAAGCTTCGATGGAGAGTTGCTAC 3'

p100(221)NTHindIII: 5' GACGAAGCTTCGATGAAATCTCCGGGG 3'

IκBδ(408)NTHindIII: 5' GACGAAGCTTCGATGGCCGCCACGGTG 3'

IκBδ(342)NTHindIII: 5' GACGAAGCTTCGATGGCCTTGCCCACC 3'

IκBδ(482)NTHindIII: 5' GACGAAGCTTCGATGACGGCGCAGGACGAG 3'

The 3' primers for these constructs had a EcoRV restriction site.

p100(899)EcoRV: 5'CCGGATATCGTGCACCTGAGG 3'

p100(765)EcoRV: 5'CCGGATATCCCCTGCTGGGCTGGG 3'

p52(344)EcoRV: 5'CCGGATATCGGGCAAGGCCTT 3'

p52(222)EcoRV: 5'CCGGATATCAGATTTGCTGTC 3'

Mouse RelB and RelB deletion mutants (RelB(1-558), RelB M5(1-558), RelB(1-400), RelB M5(1-400), RelB(278-400), RelB M5(278-400), RelB(1-276),

RelB(403-558)) were generated by PCR using pBABE RelB(1-558) and pBABE RelB M5(1-558)(gift from Rashmi Talwar) as templates. The constructs were subcloned into pEGFP-N1 vector (Clontech) to express C-terminal GFP fusion proteins in mammalian cells. The 5' primers for these constructs carried an EcoRI restriction site.

RelB(1)EcoRI: 5' CCGGAATTCTGATGCCGAGTCGCCGC 3'

RelB(278)EcoRI: 5' CCGGAATTCTGATGACATCGGAGCTG 3'

RelB(403)EcoRI: 5' CCGGAATTCTGATGAGCTCTGATCCACAT 3'

The 3' primers for these constructs had a BamHI restriction site.

RelB(558)BamHI: 5'AGGACGGGATCCCGCGTGGCTTCAGGCCC 3'

RelB(400)BamHI: 5'AGGACGGGATCCCGGCTCAACTCTCCAAG 3'

RelB(276)BamHI: 5'AGGACGGGATCCCGGGTGGACTT 3'

Mutagenesis of mouse RelB and human p100 were carried out according to manufacturer's protocol for the Stratagene Quikchange Mutagenesis Kit. The pEYFP-YFP+N-terminal Flag+C-terminal HA p100 Y247A(1-899), pEGFP-N1 RelB Y300A(1-400) and pEGFP-N1 RelB Y300A(1-558) mutants was made using pEYFP-YFP+N-terminal Flag+C-terminal HA p100 (1-899), pEGFP-N1 RelB(1-400) and pEGFP-N1(1-558) as templates for PCR, respectively. The presence of each mutation was verified by sequencing. The primers used for mutagenesis were:

p100(Y247A)F: 5' GGTGGAGATGAAGTTGCCCTGCTTTGTGACAAG 3'

p100(Y247A)R: 5' CCACCTCTACTTCAACGGGACGAAACACTGTTC 3'

RelB(Y300A)F and RelB(y300A)R were a kind gift from Vivian Wong

Mouse p65 deletion mutants (p65(1-325), p65(305-549)) were generated by PCR using pcDNA p65(1-549) as a template (gift from Tom Huxford). The constructs

were subcloned into pEGFP-N1 vector (Clontech) to express C-terminal GFP fusion proteins in mammalian cells. The 5' primers for these constructs carried an EcoRI or XhoI restriction site (sequence listed below).

p65(1)XhoI: 5' GATCTCGAGATGGACGATCTGTTT 3'

p65(305)EcoRI: 5' CCGGAATTCTGATGACCTATGAGACCTTC 3'

The 3' primers for these constructs had a EcoRI or BamHI restriction site.

p65(549)BamHI: 5' AGGACGGGATCCCGGGAGCTGATCTGACT 3'

p65(325)EcoRI: 5' CAGAATTCGCCGGGGTTCAGTTGG 3'

HA-tagged human NIK expression vector was a gift from Dr. Shao-Cong Sun.

Human embryonic kidney (HEK) 293 cells were cultured with Dulbecco's modified Eagle's medium supplemented with 10% fetal bovine serum, 2 mM glutamine and antibiotics. The cells were seeded 24 hours prior to transfection in 12 well plates (for direct IB) and 6 well plates (for IP) and transfected using Lipofectamine^{TM} 2000 reagent (Invitrogen) following manufacturer's protocol. Cells were harvested 48 hours post transfection in 25-100 uL of lysis buffer (20 mM Tris-HCl ph 7.5, 200 mM NaCl, 1% Triton X-100, 2 mM DTT, 5 mM p-nitrophenyl phosphate, 2 mM Na2VO4, 1X Protease Inhibitor Cocktail, 1 mM PMSF). An empty vector was transfected when needed to ensure equal amounts of DNA were used.

2. Retrovirus Mediated Gene Transduction

Wild type and knock-out Mouse Embryonic Fibroblast (MEF) cells (kind gift from Alex Hoffmann) were grown in Dulbecco's modified Eagle's medium supplemented with 10% calf serum, 2 mM glutamine and antibiotics. Mouse p100 and

p52 expressing retroviral constructs were kind gifts from A. Hoffmann. p100 Y300A and p52 Y300A mutants were generated by PCR as described above using pBABE p100 puro and pBABE p52 puro as templates, respectively. Mouse RelB (1-558) expressing retroviral construct was a kind gift from Rashmi Talawar. RelB M5 (1-558) was generated by PCR as described above. RelB deletion mutant (RelB(1-395)) was subcloned into pBABE-puro as described above using restriction sites SalI and EcoRI. The primer sequences are given below:

RelB(1)NEcorI: 5'-CCGGAATTCATGCCGAGTCGCCGCGCT-3'

RelB(395)CSalI: 5'-ACGCGTCGACCTAATCCCGAGGCAG-3'

Retroviral constructs (7 μg) were cotransfected with 3 μg of pCL.Eco (Novagen) into HEK 293 cells as described above. 42 hours post-transfection the supernatant was filtered using a 0.45 uM filter (Millipore) and used to infect MEF cells with 8 ug/mL of polybrene. 42 hours post-infectionion the transduced cells were selected with 10 ug/mL puromycin hydrochloride (Sigma).

Cell extracts were prepared by harvesting cells followed by lysis with buffer containing 20 mM Tris-HCl pH 7.5, 0.2 M NaCl, 1% Triton-X-100, 1 mM EDTA, 2 mM DTT, 0.1 mM phenyl-methylsulfonyl fluoride (PMSF), and protease inhibitor cocktail (Sigma). 15-30 μg protein from the total cell extracts was separated by 10% SDS-PAGE followed by transfer to nitrocellulose membrane. Immunodetection was performed using specific antibodies.

Stimulation was done 42 hours post seeding of MEF cells using 0.8 μg of anti-mouse LTβR (kind gift from A. Hoffmann and Carl F. Ware) either in the presence or absence of cyclohexamide (CHX) Cell extracts were prepared by harvesting and

lysing cells at different time points after stimulation as described above. Westerns were quantitated by scanning the blots then using ImageQuant version 1.2 from Molecular Dynamics.

3. Antibodies

The RelB (C-19), RelB (N-17), β-actin (C-11), and GST (sc-138), and all secondary HRP-conjugated antibodies were purchased from Santa Cruz. Flag (M2), GFP (A6-455), HA-antibody (16B12) and penta-His antibodies were from Sigma, Invitrogen, Covance and Qiagen, respectively. p52 (1495) antibody was a gift from Dr. Nancy Rice.

C. DNA Purification

All oligonucelotides used for biochemical studies and crystallization were purchased from GenBase, INC. or Alele Biotechnologies. Oligonucleotides were resuspended in 10 mM NaOH, 100 mM NaCl and any insoluble material was removed via centrifugation. Oligonucletides were then purified by anion exchange chromatography (Source Q resin, Amersham/Pharmacia) in a 10 mM NaOH buffer, eluted with a 0.1 to 1 M NaCl gradient. Peak fractions were pooled and immediately buffered to 50 mM MES pH 5.8, desalted and concentrated with a 1 ml Q-Sepharose column. The oligonucleotides were then desalted and concentrated in Centriprep-3 (Amicon) in a final buffer of 20 mM Tris-HCl pH 7.5 and their concentration determined by A_{260}, using the following equation to calculate their molar extinction coefficient :

$\varepsilon = G(13.7\ mM^{-1}cm^{-1})+C(9.3\ mM^{-1}cm^{-1})+A(15.4\ mM^{-1}cm^{-1})+T(9.7\ mM^{-1}cm^{-1})$

Equal-molar amounts of complimentary oligos were combined, heated to 100^{o}C, and slowly cooled to room temperature to allow them to anneal.

D. Assays and Data Analysis

1. Co-Immunoprecipitation Assay

HEK 293T cells were harvested 48 post co-transfection in 25-100 uL of lysis buffer (20 mM Tris-HCl ph 7.5, 200 mM NaCl, 1% Triton X-100, 2 mM DTT, 5 mM p-nitrophenyl phosphate, 2 mM Na2VO4, 1X Protease Inhibitor Cocktail, 1 mM PMSF). 200-1200 µg of cell extract was diluted to 300 µl with lysis buffer. 0.1 µg of α-Flag (Sigma) antibody was added and incubated at 4°C for one hour before 15 µl of protein G sepharose (Upstate Biotechnology) was added and the mixture incubated overnight at 4°C. Bound complex was washed three times with 20 mM Tris-HCl pH 7.5, 150 mM NaCl, 1% Triton X-100 and separated by SDS-PAGE followed by Immuno Blot (IB).

Wild type and knock-out MEF cells were grown in Dulbecco's modified Eagle's medium supplemented with 10% calf serum, 2 mM glutamine and antibiotics. The extracts were prepared by harvesting cells followed by lysis with lysis buffer. Coimmunoprecipitation was done with 600 µg of identical cell extracts and 100 ng of anti-RelB (Santa Cruz) antibody by incubating the mixture in the lysis buffer overnight in the presence of 15 µl protein G sepharose (Upstate Biotechnology). Bound complex was washed three times and separated by SDS-PAGE followed by IB.

2. Fluorescence Anisotropy Assay (FAA)

Eight 5′ fluorescein labeled oligonucleotides were used for these assays:

A 39-mer, containing the Ig-κB target site from the HIV-LTR (underlined):

5′-GATCGCTGGGGACTTTCCAGGGAGGCGTGGCCTGAGTCC-3′

A 17-mer containing the IFNβ-κB site (underlined):

5′-AGTGGGAAATTCCTCGG-3′

A 33-mer containing the IL2-CD28RE (underlined):

5’-TGGGGGTTTAAAGAAATTCCAGAGAGTCATCAG-3’

A 33-mer containing the IL8-κB site (underlined):

5’-GTTGCAAATCGTGGAATTTCCTCTGACATAATG-3’

A 21-mer containing the ELC-κB site (underlined):

5’-ATCGAGGGGGAATTTTGGGAA-3’

A 21-mer containing the BLC-κB site (underlined):

5’-TATTTTGGGAGATTTGAAAAC-3’

A 21-mer containing the SDF1-κB site (underlined):

5’-TGGGCGGGTCTCATTGAATCT-3’

All oligonucleotides were annealed to unlabeled complimentary strands prior to use. NF-κB dimers were then serially diluted into 0.5 mL binding reactions (20 mM Tris-HCl pH 8.0, 50 mM NaCl). After dilutions, the labeled oligonucleotides were added at constant concentration of 0.2 nM. Reactions were incubated at 25°C for 30 minutes to 1 hour. The anisotropy value of each reaction tube was then measured using a Beacon 2000 Fluorescence Polarization Analyzer (Panvera, WI). Buffers used in

determining salt dependence were 20 mM Tris-HCl pH 8.0, and 0.5, 1.4, 4.1, 12, 37, 111, 333 and 1000 uM of $MgCl_2$. $CaCl_2$ NH_4Cl.

3. DNA-binding Data Analysis

First, the fraction of DNA bound in each reaction was determined. This was calculated by subtracting the experimentally determined polarization value for free DNA from the observed polarization value for each data point, then dividing each by the polarization value for NF-κB saturated DNA.

Fraction DNA bound = $(A_{sample} - A_{min})/(A_{max} - A_{min})$

The apparent dissociation constant (K_{app}) was determined graphically as the point where fraction bound equals 0.5. Data from all homodimer experiments were globally fit to a cooperative binding model using the following equation:

Fraction DNA Bound (FB) = ([NF-κB]/K)/(([NF-κB]/K) + 1)

Where K is the equilibrium dissociation constant of a dimer interacting with its DNA binding site.

4. Fluorescence Anisotropy Competition Assay

We used pure recombinant N-terminal GST tagged IκBδ(342-899), IκBδ(406–899) , IκBδ(406–851), IκBδ(406–765), IκBδ(482–899) to test their ability to inhibit DNA binding of RelB(1-400)/p52(1-344) complex. This was done using fluorescence anisotropy competition assay. Increasing concentration of IκBδ was

used to dissociate preformed complexes of p52/RelB and 5' fluorescently labeled DNA (IgκB sequence listed below).

5′-GATCGCTGGGGACTTTCCAGGGAGGCGTGGCCTGAGTCC-3′

0.5 ml reactions of 200 pM DNA saturated with 34 nM p52/RelB(1-400) or 15.4 nM p52/RelB(67-400) were set up in 20 mM Tris-HCl (pH 7.5) and 100 mM NaCl with increasing concentrations of IκBδ (starting at approximately 1 nM and increasing to 15 μM). The anisotropy value for each sample was measured using a Beacon 2000 Fluorescence Polarization Analyzer (Panvera) along with controls of free and p52/RelB saturated DNA. All experiments were carried out at 25^{o}C and repeated at least three times. Milli-Polarization (mP) values were graphed against the concentration of IκBδ using Excel.

5. Fluorescence Anisotropy Co-operativity Assay

We used pure recombinant CREB DBD and C/EBPβ DBD to test their ability to have co-operative DNA binding with cRel homodimer, p50/cRel (kind gifts from Chris Phelps), p50 homodimer (kind gift from Anu Krishnamorthy) and p50/p65 (kind gift from Lili) on physiologically relevant DNA. DNA was synthesized off site (Alele Biotechnologies) with a 5′ fluorescein label and purified and annealed to unlabeled complimentary strand as described above (IL2 CD28RE and CRP whose sequences are listed below):

IL2-CD28RE: 5'TGGGGGTTTAAAGAAATTCCAGAGAGTCATCAG 3'

CRP: 5'ACATAGTGGCGCAAACTCCCTTACTGC 3'

Binding reactions were performed using constant IL2-CD28RE (concentration 200 pM) and CREB DBD (800 nM) concentrations with serially diluted cRel homodimer (1.3 μM to .02 nM) in 500 μl binding buffer (25 mM Tris-HCl pH 7.5, 100 mM NaCl, 0.5 mg/ml bovine serum albumin, 5 mM BME and 10% glycerol) at 25°C for 45 minutes. The anisotropy value for each was measured with a Beacon 2000 Fluorescence Polarization Analyzer (Panvera) along with controls of free and protein saturated DNA. The same method was used for setting up the binding reaction using constant cRel (200 nM) concentration with serially diluted CREB DBD (15 μM to 0.08 nM). Binding reactions were done as described above using constant CRP (200 pM) and C/EBPβ DBD (370 nM) or p50 homodimer (42 nM) concentration with serially diluted p50 homodimer or C/EBPβ DBD (10 μM to 0.5 nM), respectively, in 20 mM Tris-HCl pH 7.5, 50 mM NaCl. The assay was repeated with p50/p65 heterodimer (serial dilution of 5μM to 0.25 nM or a constant concentration of 100 nM) using IL2 CD28RE DNA (200 pM) and CREB DBD(500 nM) in 20 mM Tris-HCl pH 7.5 and 50 mM NaCl. p50/p65 heterodimer (serial dilution of 5μM to 0.25 nM or a constant concentration of 200 nM) and p50/cRel (serial dilution of 5μM to 0.25) were also used to test their co-operativity with C/EBPβ(370 nM) using IL2 CD28RE DNA (200 pM). All experiments were carried out at 25^{o}C and repeated at least three times. Fraction bound was graphed against the concentration using Excel.

6. Protein/DNA Electrophoretic Mobility Shift Assay (EMSA)

DNA was synthesized off site (Alele Biotechnologies) with the following sense strand sequences and their corresponding antisense strands:

IL2-CD28RE: 5'TGGGGGTTTAAAGAAATTCCAGAGAGTCATCAG 3'

CRP: 5'ACATAGTGGCGCAAACTCCCTTACTGC 3'

The oligonucleotides contain a high affinity NF-κB dimer and either CREB DBD or C/EBPβ DBD target site (underlined). These oligonucleotides were annealed to their complimentary strand and radiolabeled with γ^{32}P-dATP using T4 polynucleotide kinase (New England Biolabs). The labeled DNA was then purified with a nucleotide removal kit (Qiagen).

Binding reactions were performed using constant IL2-CD28RE (concentration 16 nM) and CREB DBD (728 nM) concentrations with serially diluted cRel homodimer (10 μM to 14 nM) in 20 μl binding buffer (25 mM Tris-HCl pH 7.5, 100 mM NaCl, 0.5 mg/ml bovine serum albumin, 5 mM BME and 10% glycerol, 0.1% Triton X-100) at 20°C for 30 minutes. The reaction mixes were then loaded onto a 6% 0.25X TBE polyacrylamide gel and run for 3 hrs at 120 V. The gels were then dried and exposed to a phosphor image storage plate for a Molecular Dynamics Storm 860 scanner, which was used to visualize the gels. The same method was used for setting up the binding reaction using constant cRel (180 nM) concentration with serially diluted CREB DBD (10 μM to 14 nM). Binding reactions were done as described above using constant CRP (7.5 nM) and C/EBPβ DBD (850 nM) or p50 (188 nM) homodimer concentration with serially diluted p50 homodimer or C/EBPβ DBD (10 μM to 14 nM), respectively.

7. GST Pulldowns

Equal amounts of GST tagged protein and putative binding partner were mixed in a buffered solution (20 mMTris-HCl pH 7.5, 150 mM NaCl, 1mM DTT and 0.5%

TritonX-100) and incubated for 30 minutes at room temperature before adding a 15 µl slurry of Glutathione Sepharose 4B. The samples were then incubated for another 30 minutes at room temperature. The supernatant was removed after centrifugation followed by washing twice with dilution buffer. Samples were boiled with 1X SDS buffer and bound proteins were separated by SDS-PAGE and visualized by IB or coomassie.

GST pulldowns were done under both denaturing and renaturing conditions. Equal amounts of GST tagged protein and putative binding partner were mixed in 50 µl of denaturing buffer (3 M Urea, 20 mM Tris-HCl pH 7.5, 200 mM NaCl) at 25°C for 1 hour then added 1.5 ml of refolding buffer (20 mMTris-HCl pH 7.5, 200 mM NaCl, 1mM DTT, 5% glycerol and 0.5% TritonX-100). Samples mixed for 10 minutes at 25°C before adding 15 µl slurry of Glutathionine Sepharose 4B. The samples were then incubated for another 30 minutes at 4°C. The supernatant was removed after centrifugation followed by washing twice with refolding buffer. Samples were boiled with 1X SDS buffer and bound proteins were separated by SDS-PAGE and visualized by Coomassie staining.

E. Crystallization and Data Collection

Different p52/RelB heterodimer constructs (p52(35-344)/RelB(1-400), p52(35-329)/RelB(1-400), p52(1-344)/RelB(1-400) with and without the Histidine tag removed by thrombin cleavage) were tested against a range of different DNA to obtain a diffracting p52/RelB/DNA crystal. The DNA ranged in length, in blunt ended

versus base pair overhangs, and in different NF-κB DNA binding sequences (DNA sequences listed below).

p65-11n	TCGGCTGGAAATTTCCAGCCG
p65-11o	CCTGGAAATTTCCAG
p65-12n	CGGCTAGGAATTCCTAGCCG
p6513n	TCGGCTAGGAATTCCTAGCCG
p65-13o	TCGGAAATTTCCCGA
p65-14n	GGCTAGGAATTCCTAGCC
p65-17B	TTCTGGAAATTTCCAGA
p65-17A	CGCTGGAAATTTCCAGC
p65-18n	CTAGGAATTCCTAG
p50-1	AGGGAATTCCC
p50-2:	CGGGAATTCCC
p50-3	TGGGAATTCCC
P52-12	TGGGAGATTTGA
P52-13	TTGGGAGATTTGA
p52-14	TTGGGAGATTTGAA
p52-15	CTTGGGAGATTTGAA
p52-16	CTTGGGAGATTTGAAC
p52-17	CCTTGGGAGATTTGAAC
p52-18	CCTTGGGAGATTTGAACC
MR4	GCACTGGAAATTCCTAGTA

RelB conatins a cryptic thrombin cleavage site around residue 64; therefore the thrombin cleaved refolded heterodimer p52(35-341)/RelB(1-400) is actually p52(35-341)/RelB(~64-400). The p52/RelB heterodimer at 91 μM was complexed to 50-2 DNA at a 1:7 molar ratio of protein to DNA. Crystals grew after 1-14 days at 18ºC from 2 μl hanging drop containing 1 μl of the p52/RelB/DNA complex and 1 μl of the reservoir solution (50 mM NaCl, 6% polyethylene glycol 4000, 10 mM DTT, 2 mM Spermidine, 10 mM Sodium Citrate and 0.1% β-octyl-glucopyranoside. To confirm the presence of the protein-DNA complex in the crystal, crystals were removed from the mother drop, washed three times in 30 μl of reservoir solution and then dissolved in SDS dye. The samples were run on a 10% SDS-PAGE and visualized with Coomassie stain.

Cryosolvent consisted of the same components as the reservoir solution plus 25 % Ethylene glycol. Before data collection, crystals were mounted in nylon loops and flash frozen. X-ray diffraction data was collected at APS ID19 synchrotron source. The diffraction pattern revealed that the crystals belong to the orthorhombic space group C222(1) with unit cell dimensions are: a=77.64, b=124.130, c=189.593, $\alpha=\beta=\gamma=90.0°$. There is one RelB/p52/DNA complex plus one additional strand of DNA in the asymmetric unit. X-ray diffraction data was integrated and scaled using HKL2000 (Otwinowski and Minor, 1997).

F. Structure Solution and Refinement

The structure of the complex was solved by molecular replacement using AMoRE (Navaza, 2001). The search model consisted of RelB from the

p50/RelB/DNA complex (Moorthy, A. in preparation) and the monomer of human p52/DNA complex (Cramer et al., 1997). Molecular replacement results showed that C222(1) is the correct space group. The solution of the dimer/DNA complex was refined by rigid-body refinement, followed by minimization, simulated annealing, and temperature factors refinements using the CNS system. Except for rigid-body refinement, all refinement procedures included NCS restraints for main-chain atoms of one RelB monomer, one p52 monomer and three chains of DNA. The model rebuilding was performed with XtalView (McRee, 1999) based on 2Fo-Fc difference map. Water molecules were deduced from Fo-Fc difference electron density maps and accepted on the basis of hydrogen bond geometry and temperature factor criteria. The final results of the refinement are included in Table 2-1.

Table 2-1. *Summary of crystallographic analysis*

Data collection	
Space group	C2221
Unit cell (Å)	
a	77.64
b	124.13
c	189.59
Resolution (Å)	3.05(3.16-3.05)
I/σ	14.4 (3.0)
Completeness (%)	01.7 (60.0)
Rsymm* (%)	6.4 (4.8)
Refinement	
Resolution (Å)	35-3.05
No of reflections	14507
No of protein atoms	4595
No of DNA atoms	644
No of waters	49
R crystal† (%)	23.88
R free‡ (%)	27.5
Rms deviations	
bond length (Å)	.004
bond angle (°)	1.02

* $R_{symm} = \sum|I_{obs}-I_{avg}| / \sum I_{avg}$

† $R_{cryst} = \sum||F_{obs}|-|F_{calc}|| / \sum F_{obs}$

‡ R_{free} was calculated with 5% of data.

III. X-ray structure of the RelB/p52 heterodimer bound to κB DNA

A. Introduction

The NF-κB family of proteins are important transcription factors that regulate the expression of genes primarily involved in immune and inflammatory responses and programmed cell death. NF-κB is retained in the cytoplasm in an inactive form bound to an inhibitory protein known as IκB (Baeuerle and Henkel, 1994; Baldwin, 1996; Ghosh et al., 1998). Signal dependent degradation of IκBs lead to NF-κB activation (Baeuerle and Henkel, 1994; Ghosh et al., 1998). Active NF-κB binds to target DNA sequences in gene enhancers (called κB DNA sites) to activate transcription. The contacts made by the NF-κB family members with DNA were first discovered by structural analysis of the p50 homodimer complexed to DNA (Ghosh et al., 1995; Muller et al., 1995). This structure revealed that all contacts with DNA are made by residues on loops emanating from cores of the N-terminal and dimerization domains of NF-κB. The base-specific contacts are made by residues on the L1-loop of the N-terminal domain (Figure 3-1). The loops from the C-terminal domain (loops L4 and L5) make non-specific sugar-phosphate backbone contacts, as do the residues on the loops L2 and L3 of the N-terminal domain (Figure 3-1). Multiple structures of NF-κB dimers bound to DNA have been solved. This includes all NF-κB homodimers (Chen et al., 1998b; Chen et al., 2000; Cramer et al., 1997; Ghosh et al., 1995; Huang et al., 2001; Muller et al., 1995), except RelB, and the p50/p65 (Berkowitz et al., 2002; Chen et al., 1998a) and RelB/p50 (Moorthy et al, 2007) heterodimers. The κB-DNA sequences bound by NF-κB dimers all share a core sequence of 5'-GGRNNNYCC-3' (R = purine, Y= pyrimidine, and N = any

nucleotide). The structures revealed that the NF-κB family members bind to a 5 base pair (bp) half site (p50 and p52) and a 4 bp half site (cRel, RelB and RelA).

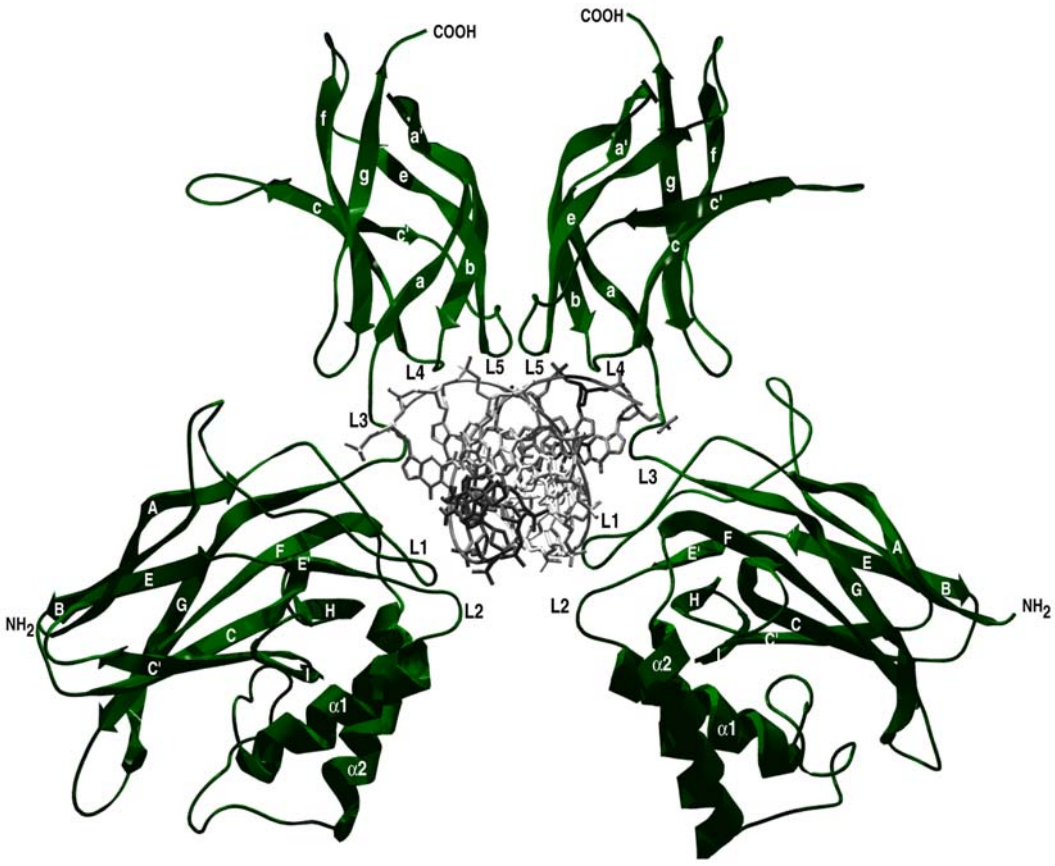

Figure 3-1. *Structure of the p50 RHR bound to DNA.* p50 is represented in ribbon form (green), the DNA backbone is traced and the DNA bases are shown as sticks (grey). The secondary structure is labeled (Ghosh et al., 1995).

RelB and p52 are activated by the non-canonical pathway and bind to and activate a class of genes that contain unique κB sites (Table 3-1) (Bonizzi et al., 2004). However, the mechanism by which the RelB/p52 heterodimer is able to bind κB sequences, divergent from the consensus κB sequence, present in the promoters of stromal cell-derived factor-1 (SDF-1), B lymphocyte chemoattractant (BLC) and Epstein-Barr virus-induced molecule 1 ligand chemokine (ELC) genes is unknown. Therefore, the focus of this study was to investigate the mechanism of DNA recognition by the RelB/p52 heterodimer.

We report the 3.05 Å crystal structure of RelB/p52 heterodimer bound to a κB DNA sequence of 5'-CGGGAATTCCC-3'. This is a palindromic κB sequence with an overhanging C at the 5'-end. In the crystal, DNA duplexes stack end to end forming a long duplex with one κB site being recognized by the protein and another site is mostly free of protein contacts. The primary sequence and corresponding secondary structure of the RelB/p52 heterodimer is shown if figure 3-2. Although the global mode of DNA recognition by the RelB/p52 heterodimer is similar to all known NF-κB/DNA complexes, the structure reveals that the RelB subunit of the heterodimer makes direct contact with an additional base pair at the 3'-end of the κB site. This causes RelB to bind to a 5 bp subsite. The amino acid that contacts this extra base pair is conserved in NF-κB family members RelA, cRel and RelB; yet the RelA and cRel amino acid fails to make a DNA interaction. Even more surprisingly, the same RelB residue in the p50/RelB heterodimer does not recognize DNA. We further show that RelB/p52 heterodimer binds to a diverse sub-class of κB sequences with a high

affinity. Recognition of an additional base pair by this heterodimer may, in part, explain this *in vitro* binding phenomenon.

Table 3-1. *Unique class of κB sites recognized by RelB/p52.* The names of the genes are highlighted in red. The sequences highlighted in blue are conserved bases compared to the consensus sequence. For the consensus DNA sequences R = a purine, Y = a pyrimidine, W = A or T, and N = any nucleotide.

κB site	Sequence
Consensus	GGRN W NTCC
ELC	GGGAA T TTTG
BLC	GGGAG A TTTG
SDF-1	GGGTC T CATTG
New Consensus for RelB/p52	GGGWR W WTTG

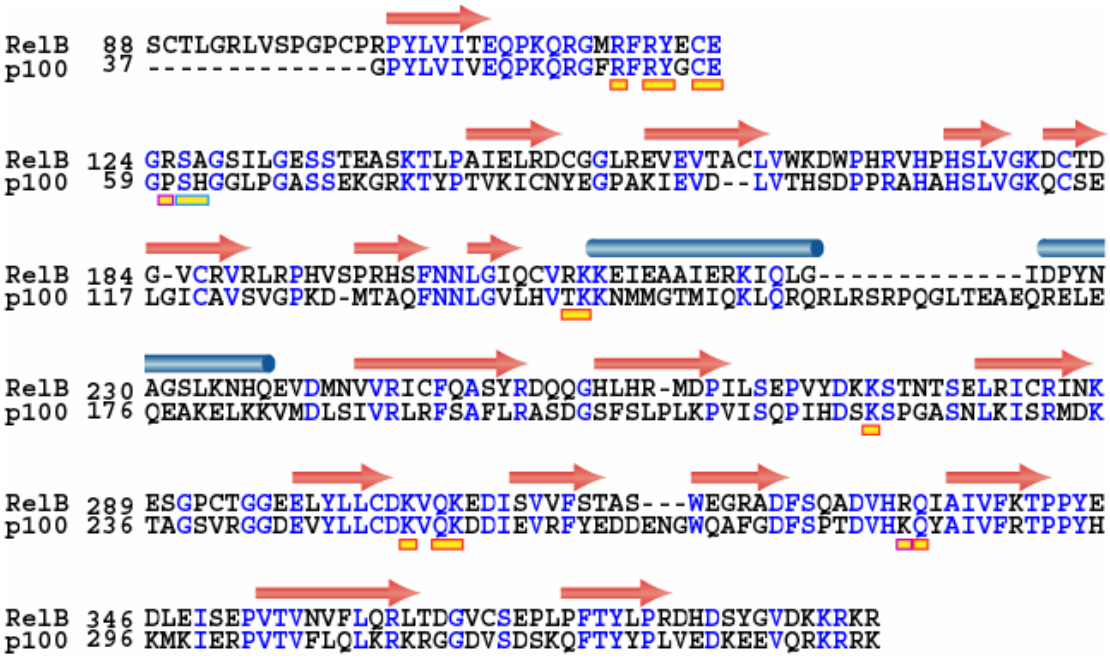

Figure 3-2. *Primary sequence and secondary structure of the RelB/p52 heterodimer.* The primary sequences and secondary structures of human p52 and mouse RelB. β-strands are represented by red arrows and α-helices are represented by blue cylinders. Identical residues between RelB and p52 are shown in blue. Residues that contact DNA (yellow boxes) are indicated. DNA contacts that are unique to p52 are yellow boxes outlined in blue and contacts that are unique to RelB are yellow boxes outlined with purple.

B. Results

1. Purification and crystallization of RelB/p52 heterodimer bound to DNA

Four different deletion mutants of p52 were used to form complexes with a construct of RelB containing the RHR, nuclear localization signal (NLS) and the N-terminal extension (Figure 3-3). Deletion mutants were generated to remove flexible portions present in the N and/or C-terminus of the protein. Figure 3-3 shows the cartoon representation of the deletion constructs. The first p52 deletion mutant (1-341) contained the N-terminal extension (35 amino acids) and the NLS. The second p52 deletion mutant (35-341) had the N-terminal extension removed however it contains the NLS. The third p52 deletion mutant (35-329) had both the N-terminal extension and the NLS removed. The last deletion mutant (1-408) contained the N-terminal extension, the NLS and the glycine rich region (GRR).

These deletion mutants were expressed without a tag and purified by a cation exchange column (Figure 3-4). The RelB construct was expressed with an N-terminal histidine tag. It was purified by Ni-affinity resin chromatography (Figure 3-4). The pure recombinant RelB and p52 proteins were then chemically denaturated and refolded to form the RelB/p52 heterodimer. RelB was added in slight excess (1.1-fold molar excess) to the RelB/p52 mixture to drive the equilibrium of dimer formation toward the heterodimer. Purification by cation exchange was used to carefully separate the residual homodimers from the heterodimer (Figure 3-4C). Since RelB RHR has no affinity for a cation exchange column and the pI of p52 (35-341) RHR is slightly higher (pI = 9.41) than that of RelB (65-400)/p52 (35-341) RHR (pI = 8.82),

the heterodimer binds less tightly to the cation exchange column and elutes before the p52 RHR homodimer in an increasing salt gradient (Figure 3-4C).

The complex was then subjected to thrombin cleavage to remove the histidine tag from the N-terminus of RelB. SDS-PAGE analysis revealed a lower molecular weight of RelB than expected. 64 N-terminal residues were removed during thrombin cleavage due to the presence of a cryptic cleavage site (Figure 3-4B). The presence and purity of the protein during purification was determined by Bradford colorimetric assay and SDS-PAGE (Figure 3-4D). All four heterodimers were purified in this manner. Figure 3-4 illustrates the purification of p52 (35-341)/RelB (65-400) heterodimer. The refolded RelB/p52 heterodimers were screened for crystallization using a number of different DNAs (listed in chapter II-E).

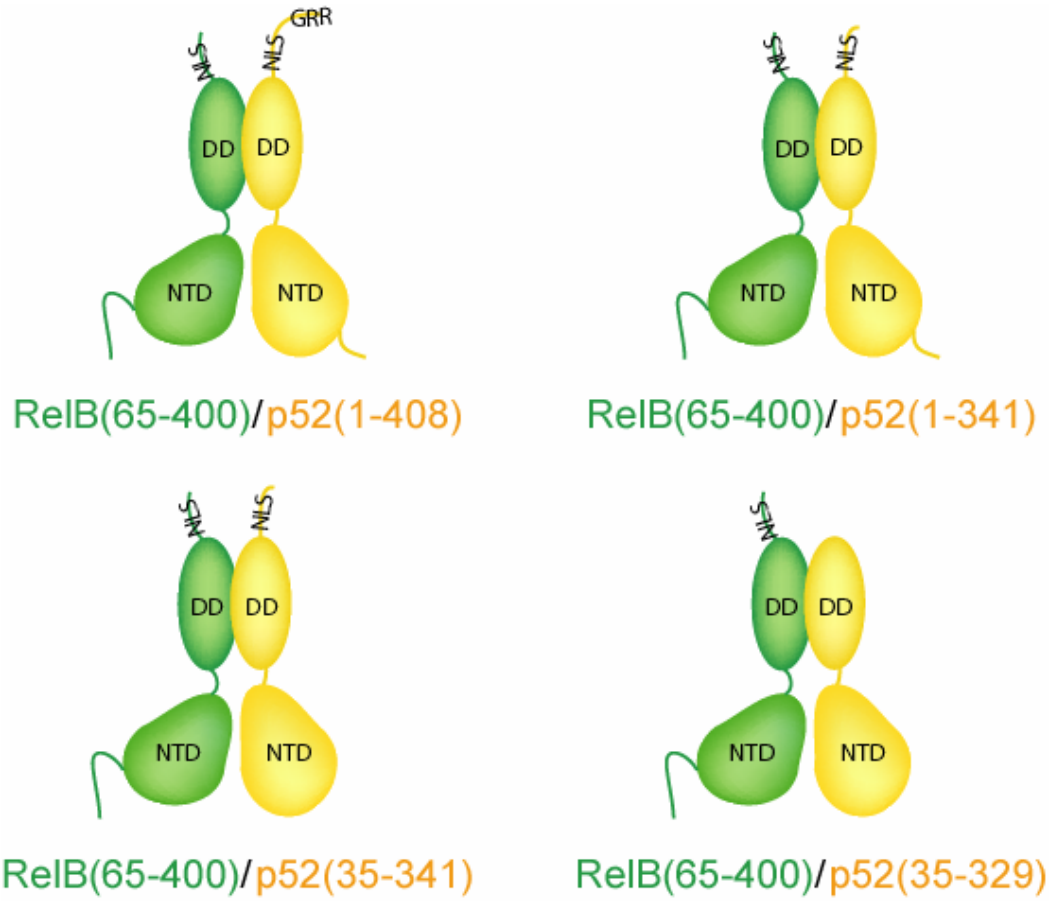

Figure 3-3. *RelB/p52 heterodimer complexes purified for crystallization.* Various N- and C- terminal deltion constructs of p52 were generated and used to form a heterodimer with RelB RHR.

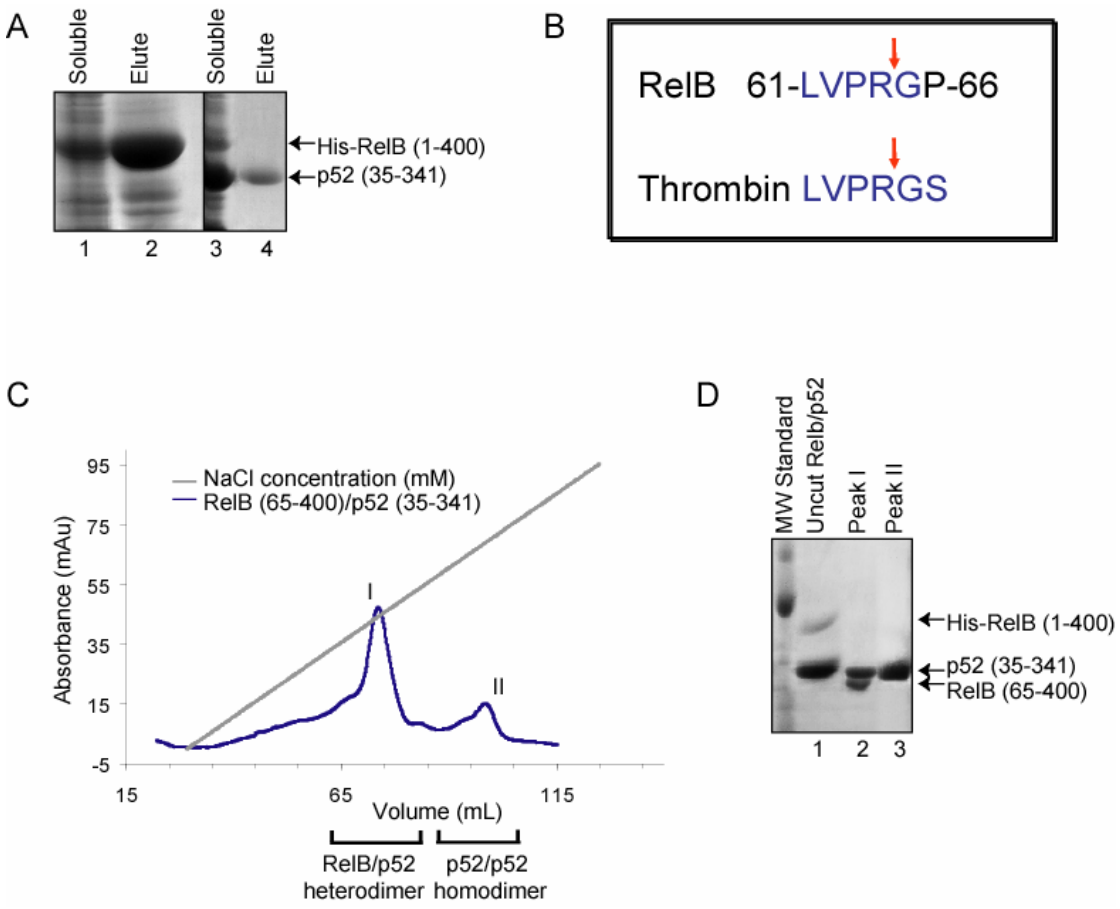

Figure 3-4. *Purification of refolded RelB/p52 heterodimer.* A.) Coomassie stained SDS-PAGE of the purified RelB (1-400) by (lane 2) and the purified p52 (35-341) (lane 4). B.) Figure depicting the cryptic thrombin cleavage site of RelB versus the native thrombin cleavage site. The red arrow indicates the cut site. C.) Co-refolded mixture of RelB/p52 RHR (blue) was separated by cation exchange (S-sepharose) chromatography. D.) Coomassie stained SDS-PAGE of co-refolded RelB/p52 samples before thrombin cleavage (lane 1) and after thrombin cleavage and S-column chromatography and (lane 2).

A knowledge-based crystal screen as well as unbiased sparse matrix crystal screen from Hampton Research were applied to obtain diffraction quality crystals. Crystals were obtained from all four RelB/p52 heterodimers complexed to a range of DNAs under many conditions. However, diffraction quality crystals were only obtained from RelB(65-400)/p52(35-341) complexed to a κB DNA of sequence 5'-CGGGAATTCCC-3' (referred to as p50-2 DNA) (Figure 3-5A). Interestingly, crystals were obtained only in the presence of ~ 7-fold molar excess of DNA from hanging drops and grew in 6-7% PEG 4000, 50 mM NaCl, 0.1% BOG, 10 mM DTT, 10 mM NaCitrate and 2 mM Spermidine. All other NF-κB/DNA crystals were grown from mixtures of protein-DNA complexes with only slight excess of DNA (1.1 to 1.2 molar excess). A crystal was dissolved and analyzed by SDS-PAGE, confirming the presence of both subunits in the crystal (Figure 3-5C). Diffraction data from a single frozen crystal was collected at the synchrotron source (ALS) (Figure 3-5B). The phases were obtained by molecular replacement using coordinates of RelB from the p50/RelB:DNA complex and coordinates of p52 from the p52/p52:DNA complex as search models. The model was refined to a resolution of 3.05Å (Summarized in Table 3-2).

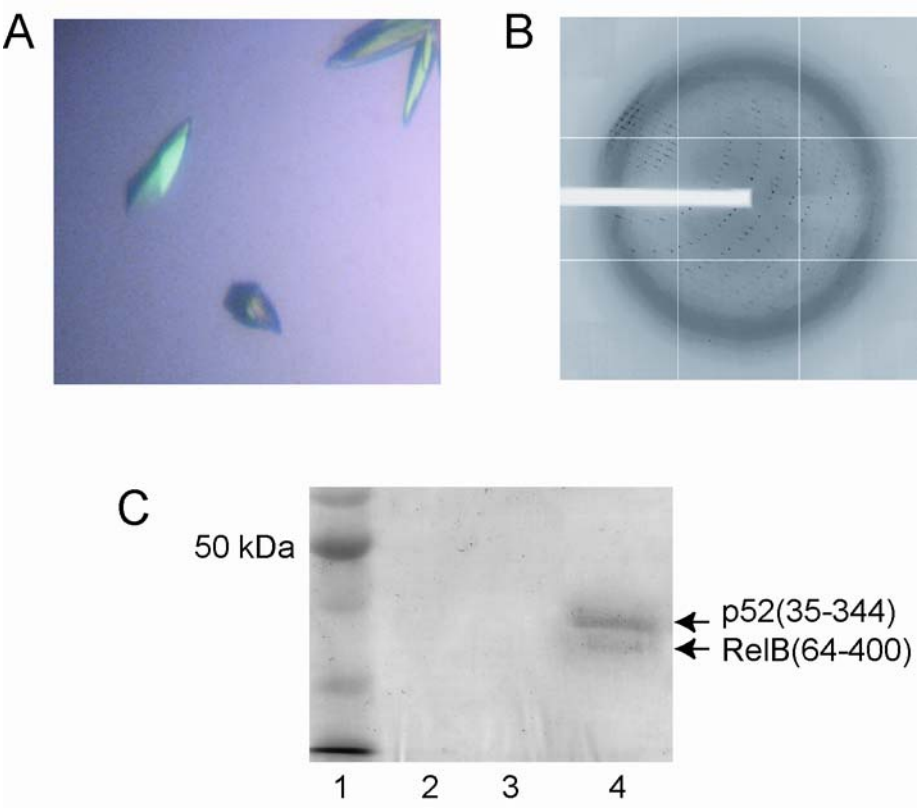

Figure 3-5. *Crystals of RelB/p52/DNA complex.* A.) Crystals of RelB/p52 heterodimer complex with DNA. Crystals were obtained from 6% PEG 4000, 50 mM NaCl, 0.1% BOG, 10 mM DTT, 10 mM NaCitrate and 2 mM Spermidine by the hanging drop method. B.) Diffraction pattern of RelB/p52/DNA complex. C.) SDS-PAGE analysis of the Dissolved crystal of the RelB/p52/DNA complex. Lane 1: Molecular Weight Standard; lane 2: wash 1; lane 3: wash 2; lane 4: dissolved crystal.

Table 3-2. *Summary of crystallographic analysis.*

Data collection	
Space group	C2221
Unit cell (Å)	
a	77.64
b	124.13
c	189.59
Resolution (Å)	3.05(3.16-3.05)
I/σ	14.4 (3.0)
Completeness (%)	01.7 (60.0)
Rsymm* (%)	6.4 (4.8)
Refinement	
Resolution (Å)	35-3.05
No of reflections	14507
No of protein atoms	4595
No of DNA atoms	644
No of waters	49
R crystal† (%)	23.88
R free‡ (%)	27.5
Rms deviations	
bond length (Å)	.004
bond angle (°)	1.02

* $R_{symm} = \sum|I_{obs}-I_{avg}| / \sum I_{avg}$

† $R_{cryst} = \sum||F_{obs}|-|F_{calc}|| / \sum F_{obs}$

‡ R_{free} was calculated with 5% of data.

2. Overall RelB/p52:DNA Complex Structure

The overall structure of the RelB (65-400)/p52 (35-341) heterodimer is similar to other NF-κB dimers; each subunit consists of two immunoglobulin-like domains connected by a flexible linker. The N-terminal domain binds DNA whereas the C-terminal is primarily responsible for dimer formation (Figure 3-6 and 3-1). Although, RelB contained 37 residues N-terminal to its RHR, the electron density only accounted for 15 residues immediately N-terminal to the RHR. This N-terminal extension of RelB makes homomeric contacts in the crystal which implies a possible role for protein-protein interaction of this segment.

The strucure of the RelB/p52/DNA complex is unlike other NF-κB/DNA complex structures in that there are three strands of DNA in an asymmetric unit compared to two strands for all other structures (Figure 3-6). The first two strands are based paired together with the first strand (shown in yellow) containing a 5' C base overhang. The 3' C of the first strand (shown in yellow) is not involved in a base contact with the second strand (shown in green) as expected, instead the 5' CG of a symmetry related second strand forms two base pairs with the 3' GC bases of the second strand (Figure 3-7B). The third strand (shown in grey) lies on the two fold axis therefore it is base-paired with a symmetry-related third strand of DNA to form a complementary double-stranded helix, with a 5' C base overhang (Figure 3-7). This causes two κB sites per asymmetric unit in which one site is recognized by the RelB/p52 heterodimer and the other site remains free of protein contact. Therefore this structure contains both bound and unbound κB DNA sites. This allows for

comparison of the DNA conformations in its free and protein bound states. Results of such comparison will be discussed in more detail later.

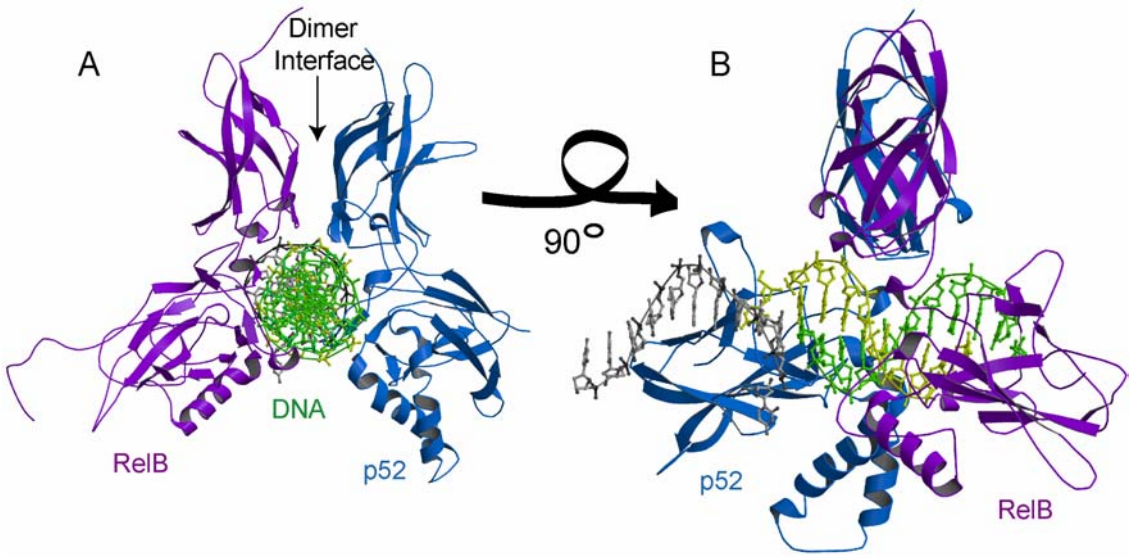

Figure 3-6. *The structure of the RelB/p52 heterodimer bound to DNA.* A.) Ribbon drawing of the entire complex viewed down the DNA helical axis. The RelB subunit is in purple, the p52 subunit is in teal, and the three DNA strands in yellow, green and gray. The colors will remain the same for RelB and p52 throughout the chapter. B.) The ribbon drawing in figure "A" rotated 90°along a vertical axis.

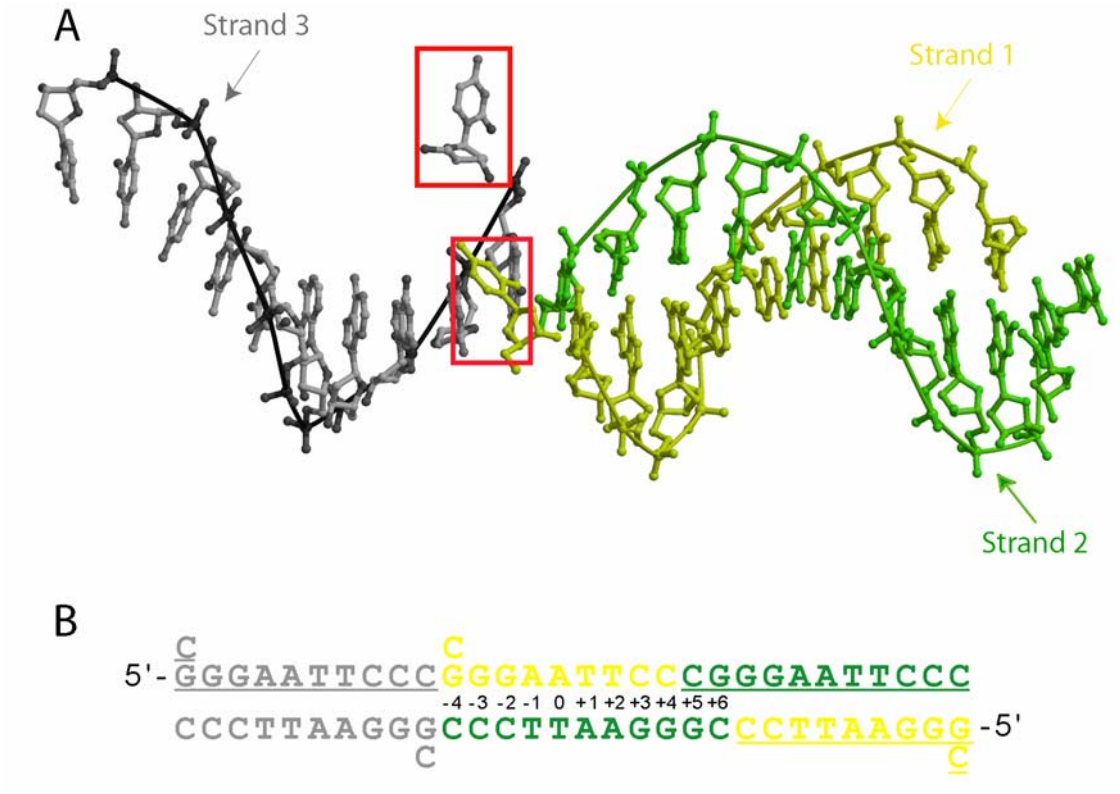

Figure 3-7. *Schematic diagram and overall structure of DNA*. A.) The overall structure of the DNA with the backbone traced and the DNA bases shown as sticks (bound DNA in green and yellow and unbound DNA in grey). The overhanging 5' C bases are highlighted by red boxes. B.) Schematic representation of the DNA sequence in the RelB/p52/DNA complex structure. Shown in grey is the DNA sequence that is not bound by a NF-κB dimer. The yellow and green represent the DNA sequence bound by RelB/p52 heterodimer. The underlined sequences represent symmetry related DNA sequences.

3. Dimerization Interface

Overall the dimer interface of the RelB/p52 heterodimer is similar to all known NF-κB dimers except for that of the RelB homodimer, which forms an intertwined homodimer (Huang et al., 2005b). The surface area buried upon dimerization is 1467 $Å^2$ which is in the same range as the other NF-κB dimers. Superposition of the DDs of the RelB/p52 heterodimer with the DDs of the RelB/p50 heterodimer and p52 homodimer reveals a root mean square deviation of only 1.076 and 1.125, respectively indicating their similarities (Figure 3-8).

The dimer interface consists of a hydrophobic core stapled together by various polar interactions (Figure 3-6, Figure 3-9A). The interface can be split into two regions, an upper and lower region (Figure 3-9B and C). The residues Tyr247 of p52 and *Tyr300* of RelB (hereafter all RelB residues will be shown in italics) are located at the center of the dimer interface and are essential for dimer formation. These tyrosine residues are responsible for both hydrogen bonds and van der Waals contacts. Mutation of either tyrosine residues results in a lack of dimer formation (shown in chapter V). The two tyrosine residues (*Tyr 300* and Tyr 247) are shifted towards each other and away from the side chain functional groups of Arg 232 and *Arg 285*. Therefore, the two tyrosine residues only make contacts with the backbone carbonyl (Figure 3-9B). This mode of interaction is conserved in the RelB/p50 heterodimer but not in other dimers. The homologous tyrosines in other NF-κB dimers make hydrogen bonds with both the backbone and the side chain functional groups of the Arg residue. A hydrogen bond between p52 Asp234 and RelB *Asn287* is observed; this contact is also observed in the p50/p65 and the RelB/p50 heterodimer. It is thought that this

hydrogen bond in the p50/p65 heterodimer contributes to the enhanced stability of the heterodimer versus the homodimers. In the p52 homodimer, an interaction between homologous Asp234 is energetically unfavorable, since this juxtaposes two like charges. Therefore, this hydrogen bond may be important for the increased stability of the RelB/p52 heterodimer versus the homodimers.

The lower region of the dimer interface is made up of a hydrophobic core that is stapled by various polar interactions (Figure 3-9C). Of particular interest are the hydrophobic residue *Ile335* of RelB and polar residue Tyr285 of p52. The two residues are closely packed together, and RelB is the only NF-κB subunit that contains an isoleucine at this position. The p52 Tyr285 and the equivalent p50 Phe307 are able to pack next to the isoleucine residue. It is possible that *Ile335* of RelB causes steric hindrance in the RelB homodimer. This may also give an explanation for why RelB forms preferential dimers with p50 or p52 as the corresponding residue in p65 and cRel is a valine (Figure 3-10).

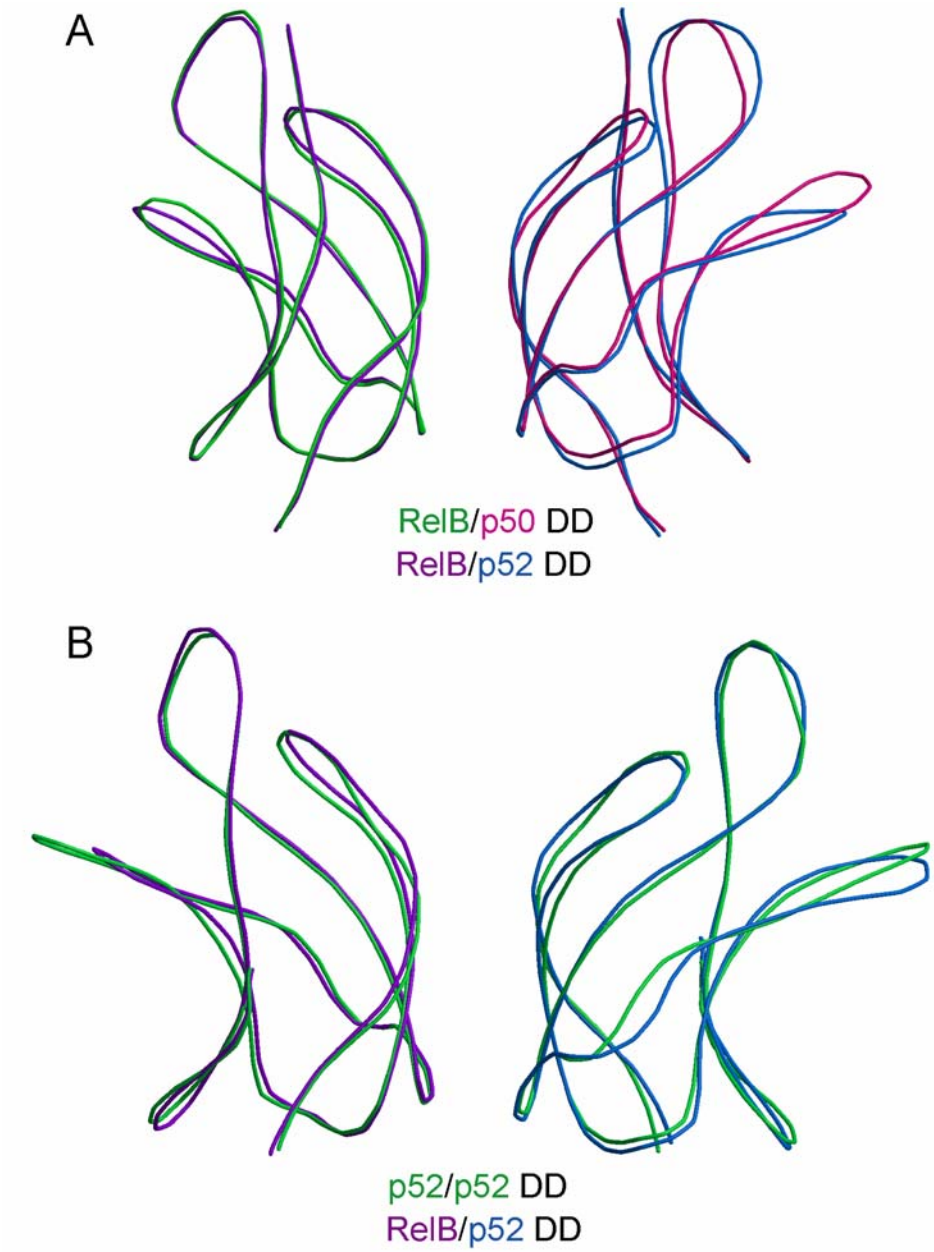

Figure 3-8. *Comparison of the dimerization domain conformations*. A.) Overlay of the dimerization domains of RelB/p52 heterodimer (purple and teal, respectively) and ReB/p50 heterodimer (green and magenta, respectively). B). Overlay of the dimerization domains of RelB/p52 heterodimer (purple and teal, respectively) and p52/p52 homodimer (green).

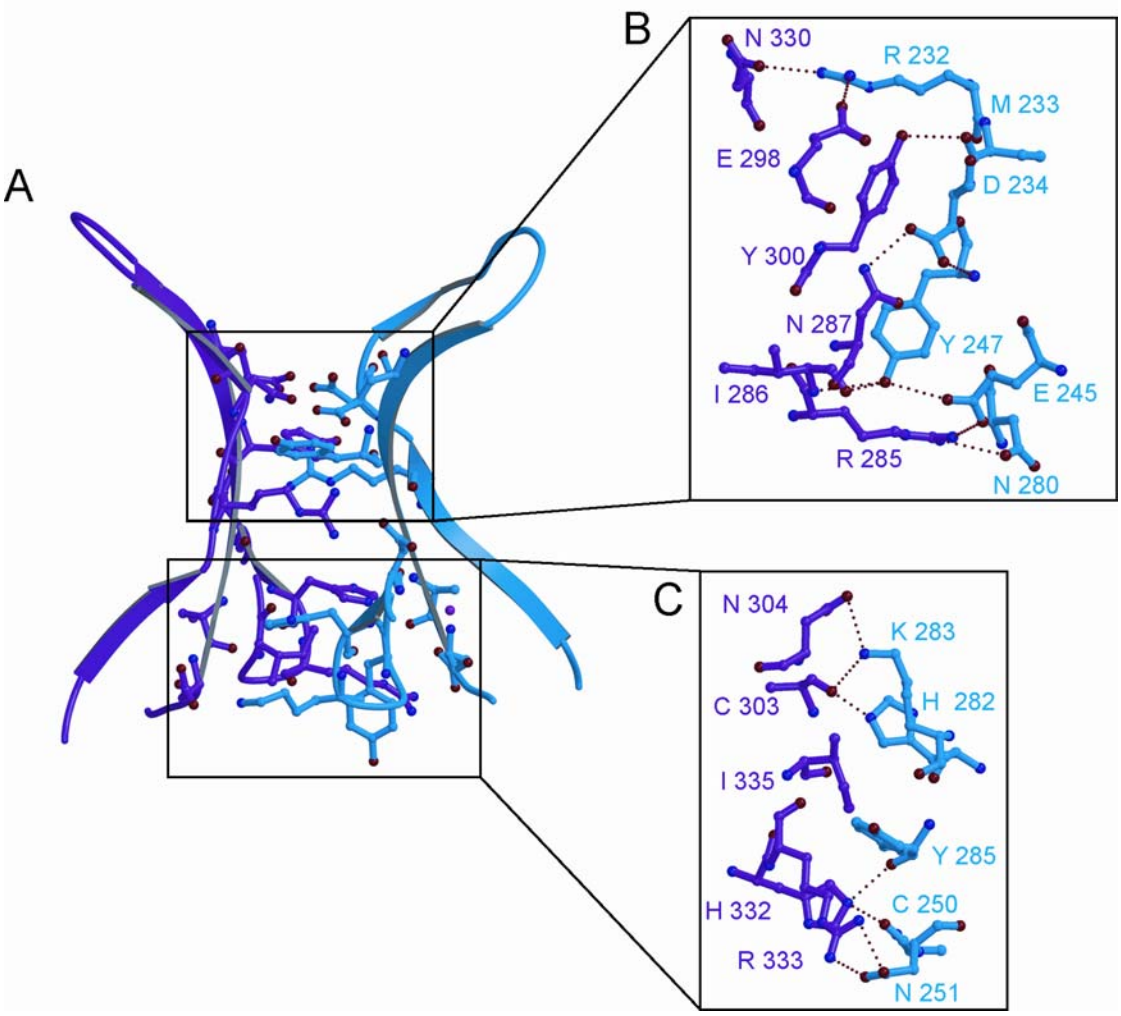

Figure 3-9. *Dimerization interface of RelB/p52.* A.) Detailed view of the core of the dimerization interface. The RelB subunit is shown in purple and the p52 subunit in shown in teal. B.) Close up view of the upper half of the dimerization interface. Hydrogen bonds are depicted by red dashed lines. C.) Close up view of the lower half of the dimerization interface. Hydrogen bonds are depicted by red dashed lines. Oxygen atoms are in red, nitrogen atoms in blue and red dashed lines represent hydrogen bonds.

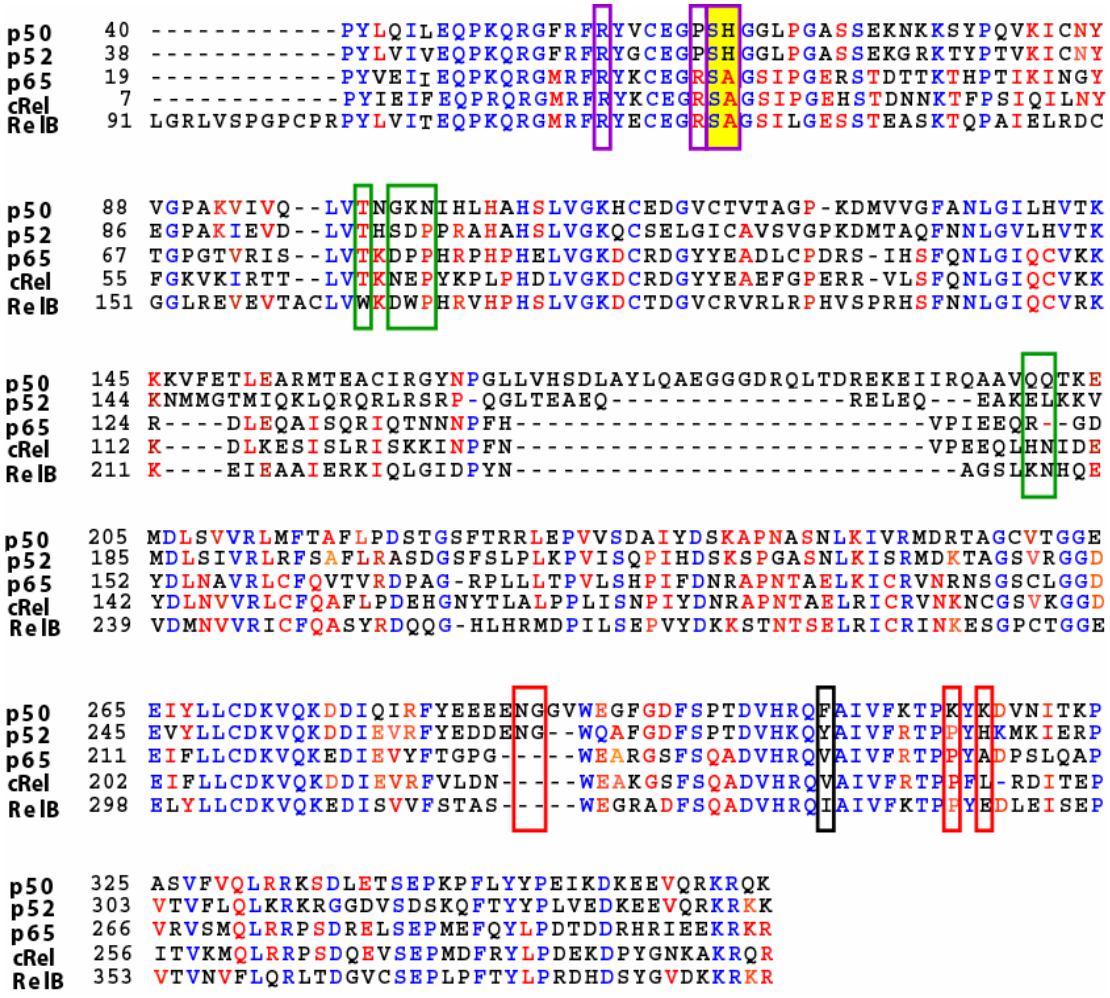

Figure 3-10. *Sequence alignment of NF-κB family members.* Primary Sequence alignment of the RHR of NF-κB family members. Identical residues are colored in blue and conserved residues are in red. The crystal contact residues are highlighted by a green box for the RelB subunit and a red box for the p52 subunit. The unique DNA interactions observed for RelB (purple box) and p52 (yellow box outlined in purple) are shown. The unique residue found in the DD of RelB is highlighted with a black box.

4. Protein DNA Interaction

As expected, the overall mode of DNA recognition by the RelB/p52:DNA complex is similar to all other known NF-κB:DNA complexes. Similar to other complexes, this complex buries approximately 3200 $Å^2$ solvent accessible surface area. The base-specific and non-specific contacts are summarized in figure 3-11. As mentioned earlier the DNA is packed in such a way that it forms a linear pseudo-continuous double helix containing two κB sites in an asymmetric unit. The packing arrangement causes the 5' unpaired C of the right hand κB site to be rotated away from the helix (figure 3-7A and 3-12B). The p52 subunit recognizes a half site made up of 4 bp and the extrahelical 5' C overhang. This extra helical C is contacted by His62 and Ser61. In a smooth duplex DNA if the 5^{th} base pair were a G:C then the bp would have been contacted by the histidine residue in the same manner as seen in the p52 homodimer:DNA complex. Therefore, the p52 subunit is destined to recognize a 5'-half site as observed in the p52 homodimer:DNA complex if the proper half-site sequence is present. However, the involvement of Ser61 in contacting such DNA is uncertain as this interaction would not be possible in a smooth DNA with the 5^{th} base pair being G:C. Another reason is the residue in p52 and the corresponding residue in p50 have never been observed to make sequence-specific contacts before (Figure 3-13). All other base-specific hydrogen bonding contacts between p52 and DNA are preserved in this complex. Invariant residues Arg52, Arg54 and Glu58 from loop 1 and Lys221 from the linker between the N- and the C-terminal domains are responsible for base specific interactions (Figure 3-12B). In addition, Tyr55 makes van der Waals contacts with the methyl group of T-2 and C^5 of C-3.

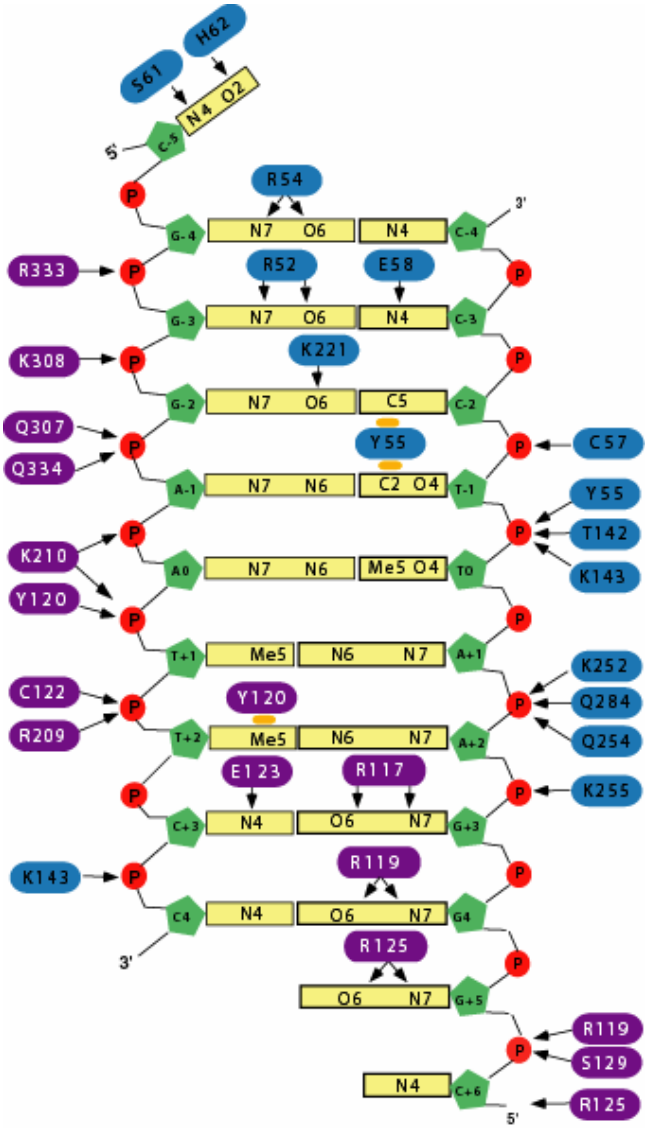

Figure 3-11. *DNA contacts made by the RelB/p52 heterodimer.* Schematic representation of the DNA contacts made by the RelB/p52 heterodimer. Purple and blue distinguish RelB and p52 subunits, respectively. Arrows denote hydrogen bonds while orange circles indicate van der Waals contacts. The RelB subunit binds to four base pair subsites while the p52 subunit binds to five base pair subsites.

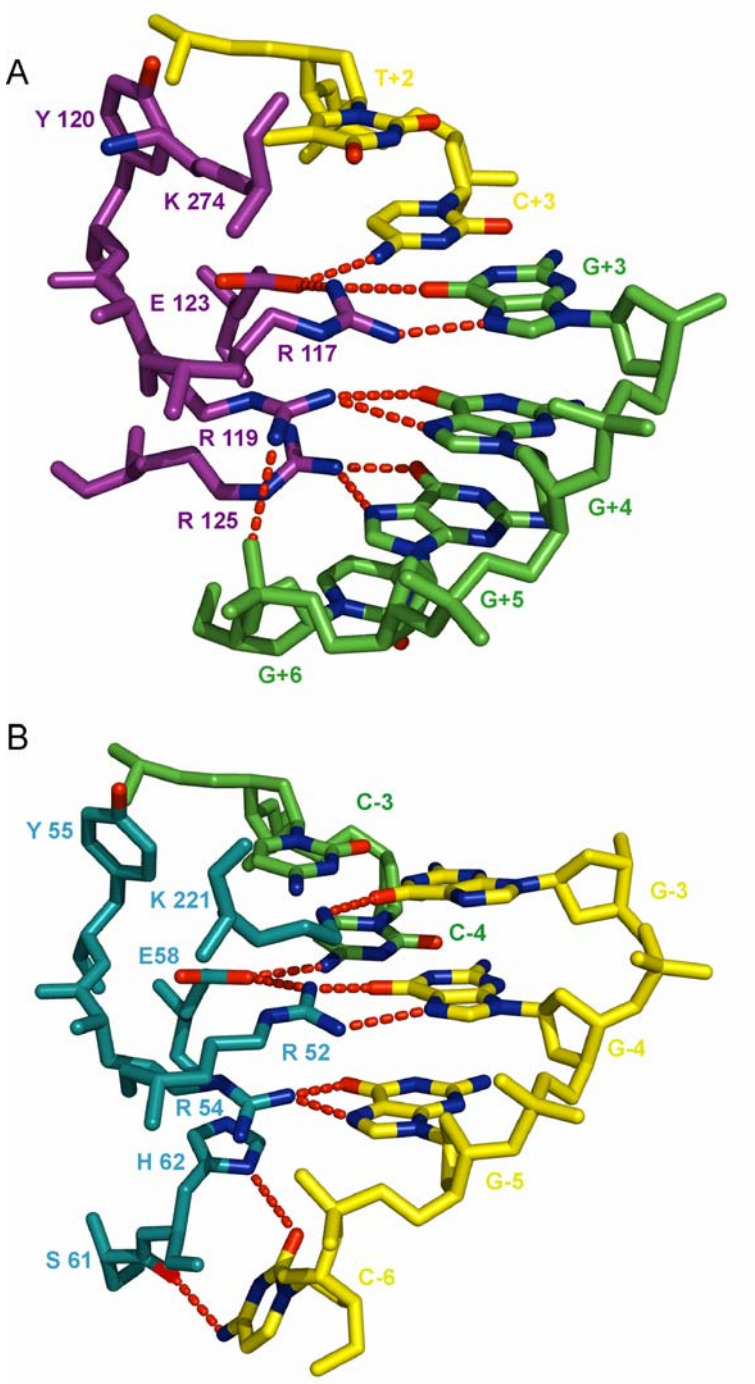

Figure 3-12. *Base specific DNA contacts made by RelB/p52 heterodimer.* A.) Base specific interactions mediated by Arg117, Arg119, Arg125 and Glu123 of the RelB subunit (purple). B.) Base specific interactions mediated by Arg54, Arg52, His62, Ser61, Glu58 and Lys221 of the p52 subunit (teal). Basic and acidic atoms are depicted by blue and red, respectively. Oxygen atoms are in red, nitrogen atoms in blue and red dashed lines represent hydrogen bonds.

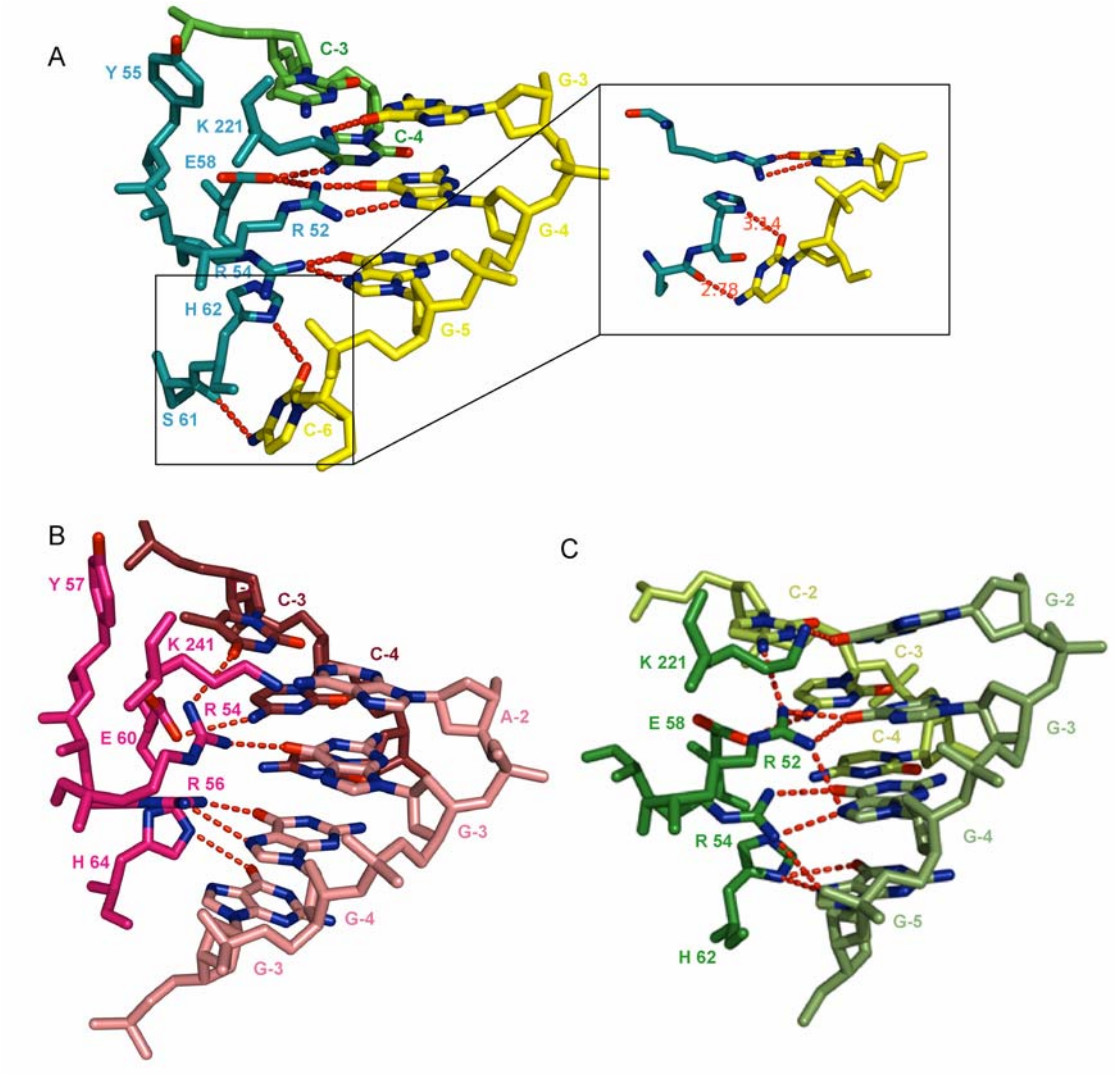

Figure 3-13. *Comparison of p52 base specific contact with other NFκB family members.* A.) Base specific contacts observed by the p52 subunit (teal), highlighting Ser61 and His62 (shown in close up). B.) Base specific contacts observed by the p50 subunit (magenta) from the RelB/p50/DNA complex structure highlighting the difference observed for His64, compared to p52's His62. C.) Base specific contacts observed by the p52 subunit (green) from the p52/p52/DNA complex structure highlighting the differences observed. Oxygen atoms are in red, nitrogen atoms in blue and red dashed lines represent hydrogen bonds.

Surprisingly, the RelB subunit also recognizes a 5 bp half site. Base-specific contacts are mediated through residues *Arg125, Arg117, Arg119, Glu123* and *Tyr120* (Figure 3-11 and 3-12A). All residues involved in base specific contacts involve hydrogen bonds except *Tyr120* which makes van der Waals contacts with T+2. The corresponding tyrosine in other complexes makes sequence-specific van der Waals contacts with two adjacent base pairs. However, in this complex a shift in the *Tyr120* residue prevents the interaction between this tyrosine and methyl group of T-1.

Another unique feature of RelB is the lack of a base specific contact for *Lys274* (Figure 3-14). This lysine residue is located in the linker region, between the N- and C-terminal domains, and the corresponding lysines (or arginines) Lys221 of p52, Lys241 of p50, Arg187 of RelA and Arg192 of c-Rel are all involved in contacting an A:T bp at the center. However, due to a change in conformation of loop 3, the flexible linker that connects the N-terminal domain and the C-terminal dimerization domain, *Lys274* is not in a position to make DNA contacts. As noted earlier in the RelB/p50 complex, loop3 of RelB adopts an helix-like structure, perhaps due to a proline to threonine substitution, which renders *Lys274* to position inwardly making an intramolecular hydrogen bond with residue *Thr276* (Figure 3-14C). Another unique feature is the binding of *Arg119* with the DNA backbone in addition to its base-specific contacts. The corresponding arginines in all NF-κB complexes, including that in the RelB/p50 complex, are involved only in base specific contacts (Figure 3-10 and 3-14). The backbone interaction made by *Arg119* is due to a rotation in the G+4 base. The base G+4 is involved in base pairing interactions with a

symmetry related DNA (depicted in Figure 3-7B), causing a rotation in the phosphate backbone toward RelB.

The most striking feature of the RelB base specific contacts is the base specific contact involving *Arg125*. The conserved Arg in RelA (Arg41) and cRel (Arg29) are not involved in any DNA interactions (Figure 3-10). In the RelB/p50 complex, Arg125 is involved in a hydrogen bond with the protein backbone and not involved in DNA interaction (Figure 3-14, compare A and C). The difference is due to the conformational change of loop-1. The DNA in the RelB/p52 complex occupies the area in which loop-1 of the RelB/p50 complex is located. Loop-1 of the RelB/p52 complex is rotated away from the DNA surface, resulting in the movement of *Arg125* side chain toward the DNA (Figure 3-14D). It is unclear at this stage if alternate binding interactions seen in this complex results from the crystal packing or the inherent property of the complex. In all, the RelB/p52 appears to interact through the flanking GGG:CCC core elements with very little contacts at the central four base pairs.

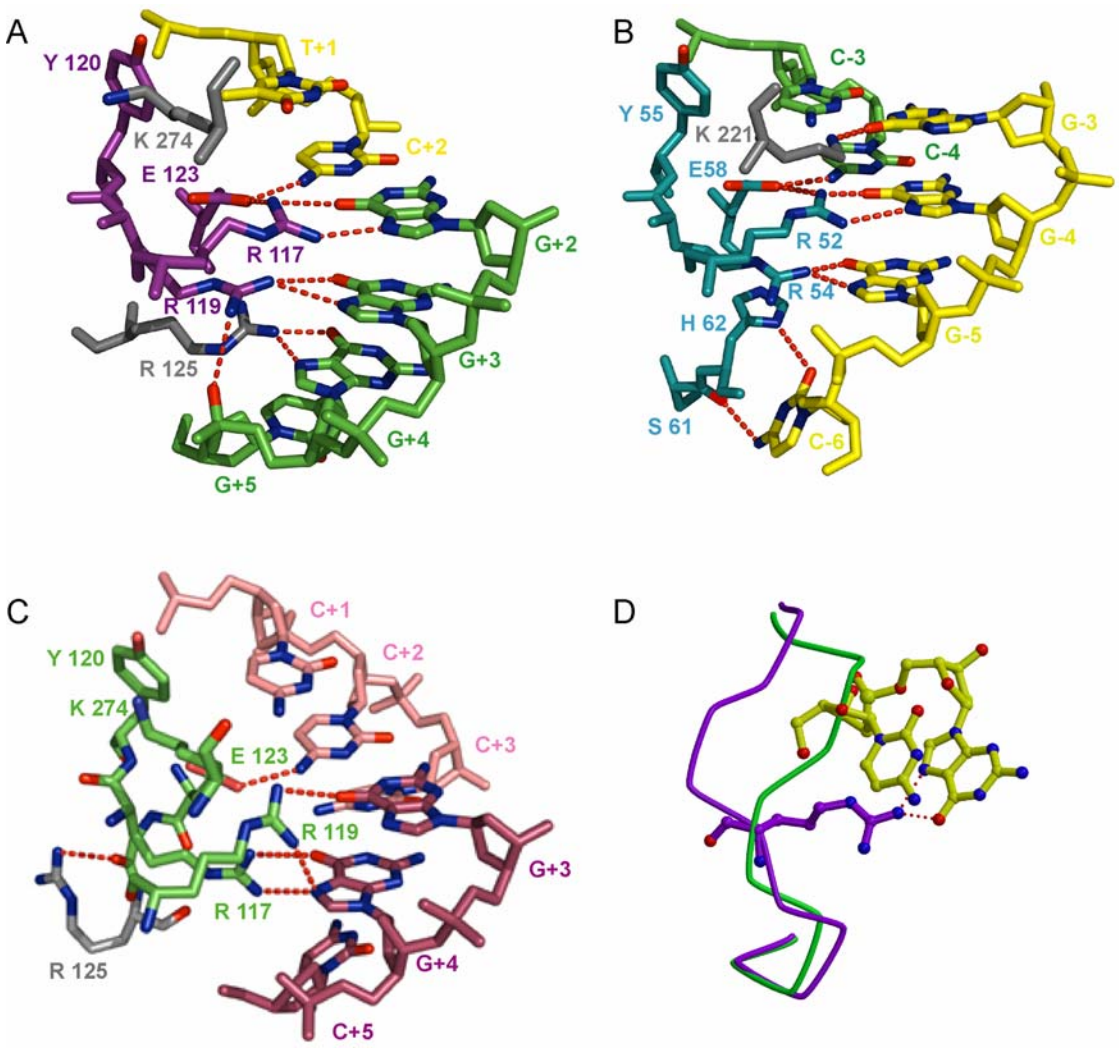

Figure 3-14. *Comparison of RelB base specific contact with other NFκB family members.* A.) Base specific contacts observed by the RelB subunit (purple), highlighting the differences observed for Arg125 and Lys274(shown in grey). B.) Base specific contacts observed by the p52 subunit (teal) highlighting the difference observed for Lys221 (shown in grey), compare to RelB's Lys274. C.) Base specific contacts observed by the RelB subunit (green) from the RelB/p50/DNA complex structure highlighting the difference observed for Arg125 (shown in grey). Oxygen atoms are in red, nitrogen atoms in blue and red dashed lines represent hydrogen bonds. D.) Overlay of loop 1 of RelB from the RelB/p50 complex (green) and the RelB/p52 complex (purple). The shift in loop 1 in the RelB/p52 complex allows for Arg125 to contact DNA.

5. N-terminal domains and crystal packing

Although the RelB/p50 heterodimer was complexed to the identical DNA as the RelB/p52 heterodimer, a superposition of the C-terminal dimerization domain of RelB/p52 heterodimer onto the C-terminal dimerization domain of RelB/p50 heterodimer requires 9.216º rotation and a 2.856 Å translation of the N-terminal domain of RelB from the RelB/p50 complex for superposition. A similar rotation (7.737º) and translation (3.084 Å) of the N-terminal domain of p50 are needed for superposition onto the p52 NTD (Figure 3-15). This *en bloc* domain movements observed are due in part to a shift in the half-sites recognized by both RelB and p52, which may results from very different crystal packing arrangements in the two complexes.

In addition to the domain movements, the backbone conformations of RelB NTDs present in the RelB/p52 and RelB/p50 heterodimers are different; an rms deviation of 1.705 Å is observed (Figure 3-16A). Two major regions of differences in the two RelB NTDs are highlighted by arrows in figure 3-16A. The first region (labeled 1) is the loop-1 region, discussed above. The second region (labeled 2) is centered around residue *Trp167* which is involved in contacting a crystallographically related p52 (Figure 3-17). *Trp167* of RelB lies in a groove formed by multiple hydrophobic residues from both RelB (*Trp164* and *Pro168*) and p52 (Pro163 and Pro293) subunits (Figure 3-17B). The polar interactions involve residues *Asn235* and *Lys234* from RelB, and Gly269 and Asn268 from p52. These residues are involved in multiple hydrogen bonds (Figure 3-17C). The RelB *Trp* residues and residues

involved in hydrogen bonds are unique amongst NF-κB family members and the p52 residues involved in hydrogen bonds are shared only by p50 (Figure 3-10).

When the N-terminal domains of p52 and p50 from the RelB/p52 and RelB/p50 heterodimers are superimposed, a root mean square deviation of 1.275 $Å^2$ is observed (Figure 3-16B). The overall features of p50 and p52 are conserved, with the exception of the insert region (highlighted with an arrow).

Another note worthy crystal contact observed is between two heterodimers bound to neighboring κB sites, not separated by an unbound κB site. This interaction involves contacts between the N-terminal domain of RelB and p52 subunits. This crystal contact is comprised of multiple polar interactions (Figure 3-18). The crystal contact observed between two RelB/p52:DNA complexes is also noteworthy. This contact involves the N-terminal domains of two p52 subunits different heterodimer complexes bound two two κB sites that are separated by the unbound κB site (Figure 3-19). However, the significane of these cyrstall contacts is unkown.

An intriguing possibility of these crystal contacts is that they might occur in solution and perhaps play a role in biological regulation. The role of a RelB surface that is involved in crystal contact in the RelB/p50:DNA complex has been examined. Mutational studies revealed that protein-protein interaction involving the crystal packing surface was critical in the formation of a stable ternary complex between two molecules of RelB/p50 heterodimer bound to DNA containing two adjacent κB sites (Moorthy et al 2007, JMB in press).

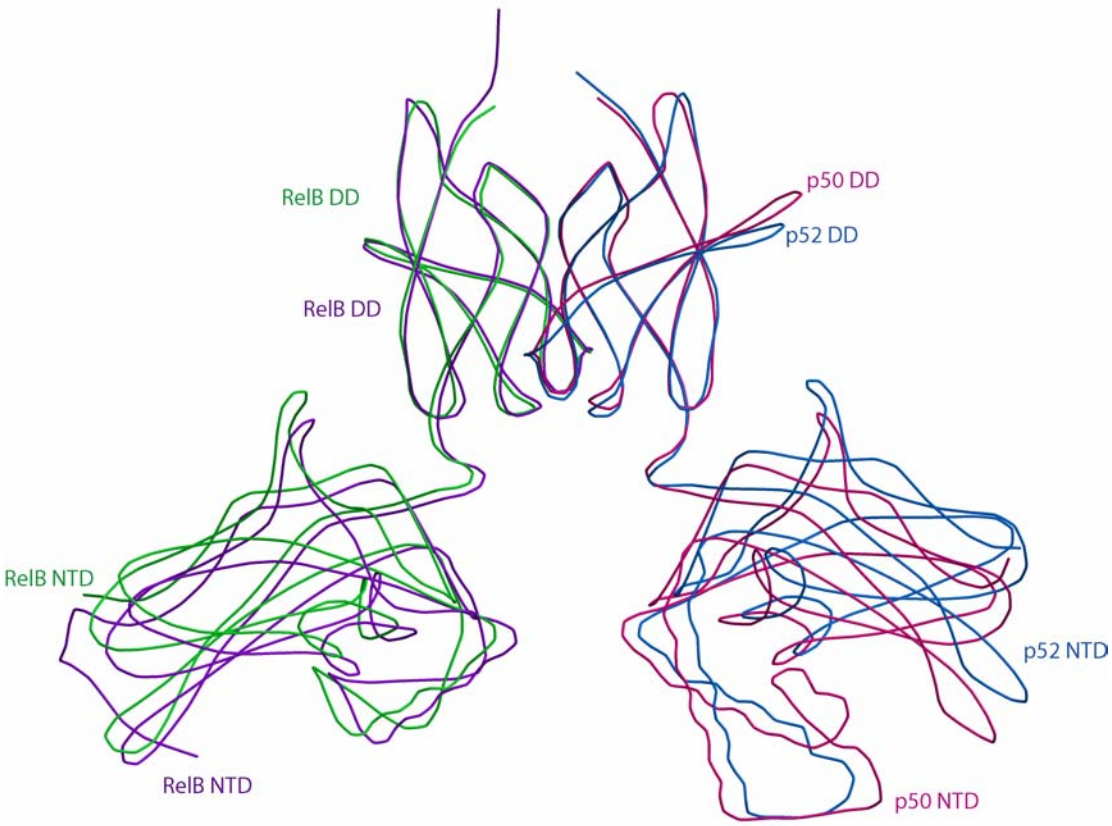

Figure 3-15. *Overlay of the RelB/p52 heterodimer and the RelB/p50 heterodimer.* Superposition of the C-terminal dimerization domains of the RelB/p52 heterodimer (purple and teal, respectively) and the RelB/p50 heterodimer (green and magenta, respectively).

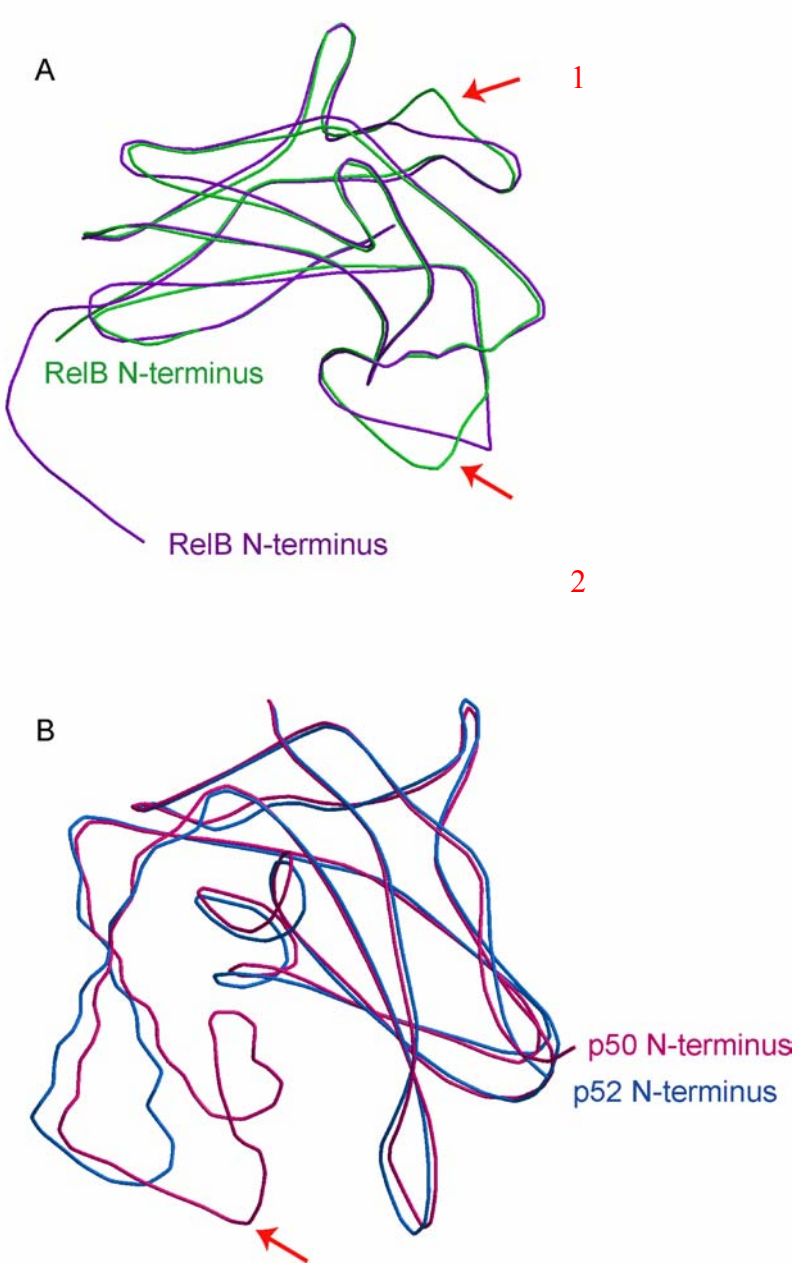

Figure 3-16. *Comparison of the N-terminal domain conformations*. A.) Overlay of the N-terminal domain of RelB subunit (purple) from the RelB/p52 heterodimer structure and the ReB subunit (green) from the RelB/p50 heterodimer structure. Root mean square deviation of 1.705 $Å^2$ is observed. Red arrows highlight two areas with different conformations. B). Overlay of the N-terminal domain of p52 subunit (teal) from the RelB/p52 heterodimer structure and the p50 subunit (magenta) from the RelB/p50 heterodimer structure. Root mean square deviation of 1.275 $Å^2$ is observed. Red arrow highlights the insert areas found in both p52 and p50.

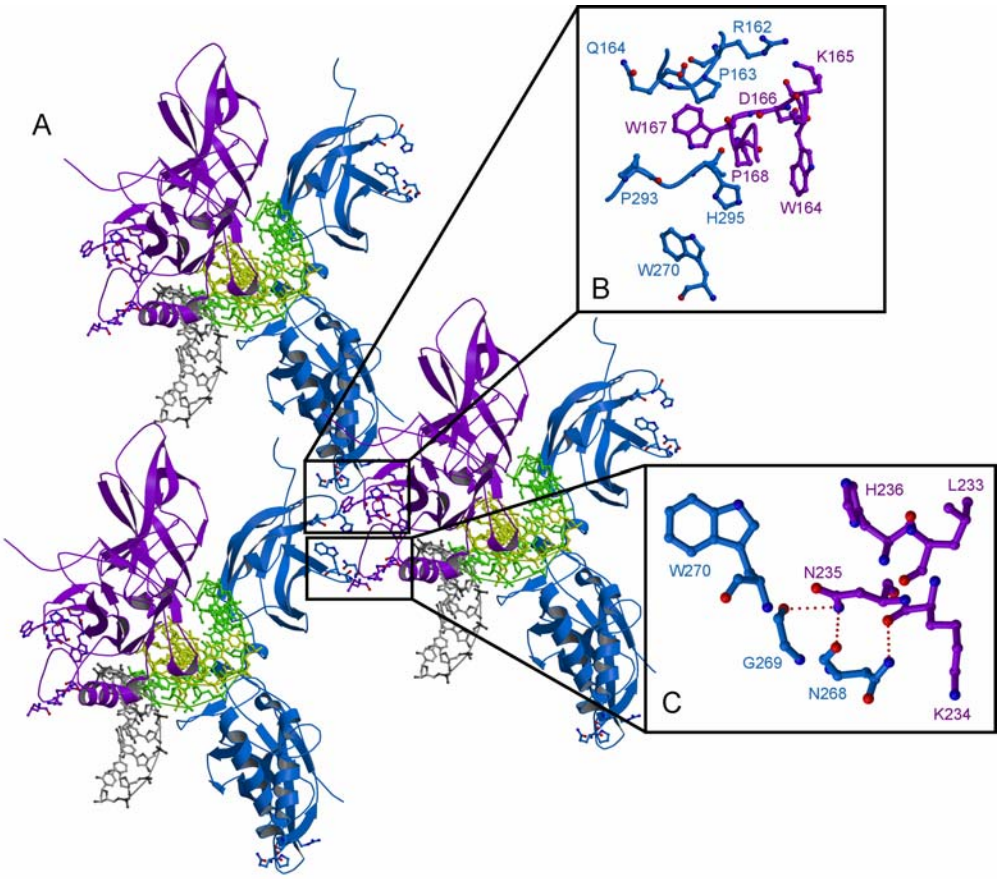

Figure 3-17. *Crystal packing contactsmade between multiple complexes.* A.) Overall view of the packing between different RelB/p52 heterodimers (purple and teal, respectively) from three different complexes. B.) A close up view of the same contact surface. C.) A close up view of the same contact surface. Oxygen atoms are in red, nitrogen atoms in blue and red dashed lines represent hydrogen bonds.

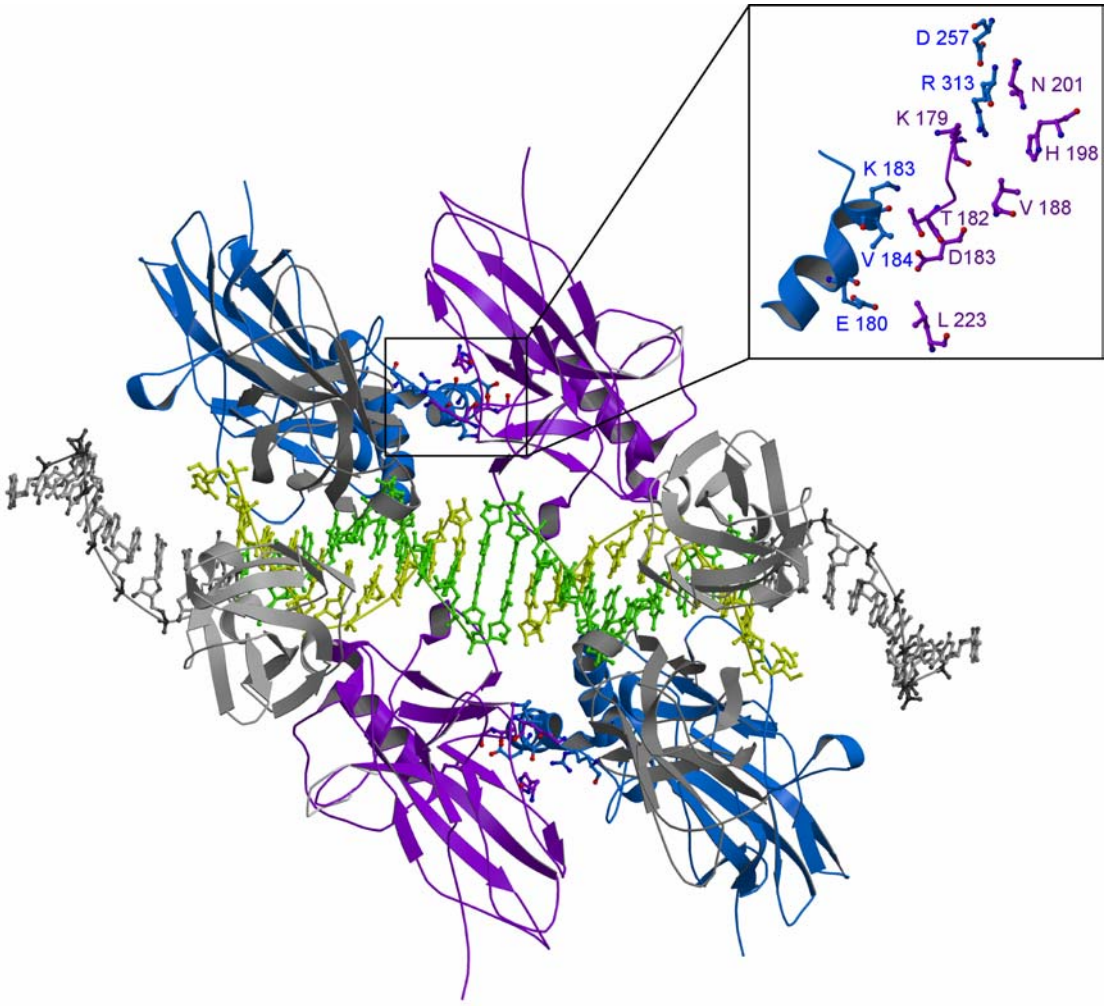

Figure 3-18. *Crystal packing contacts made between multiple complexes.* A.) Overall view of the packing between RelB and p52 from two different complexes binding to adjacent κB sequences. The dimerization domains are shown in grey (RelB DD) and dark grey (p52 DD). B.) A close up view of the same contact surface. Oxygen atoms are in red, nitrogen atoms in blue and red dashed lines represent hydrogen bonds.

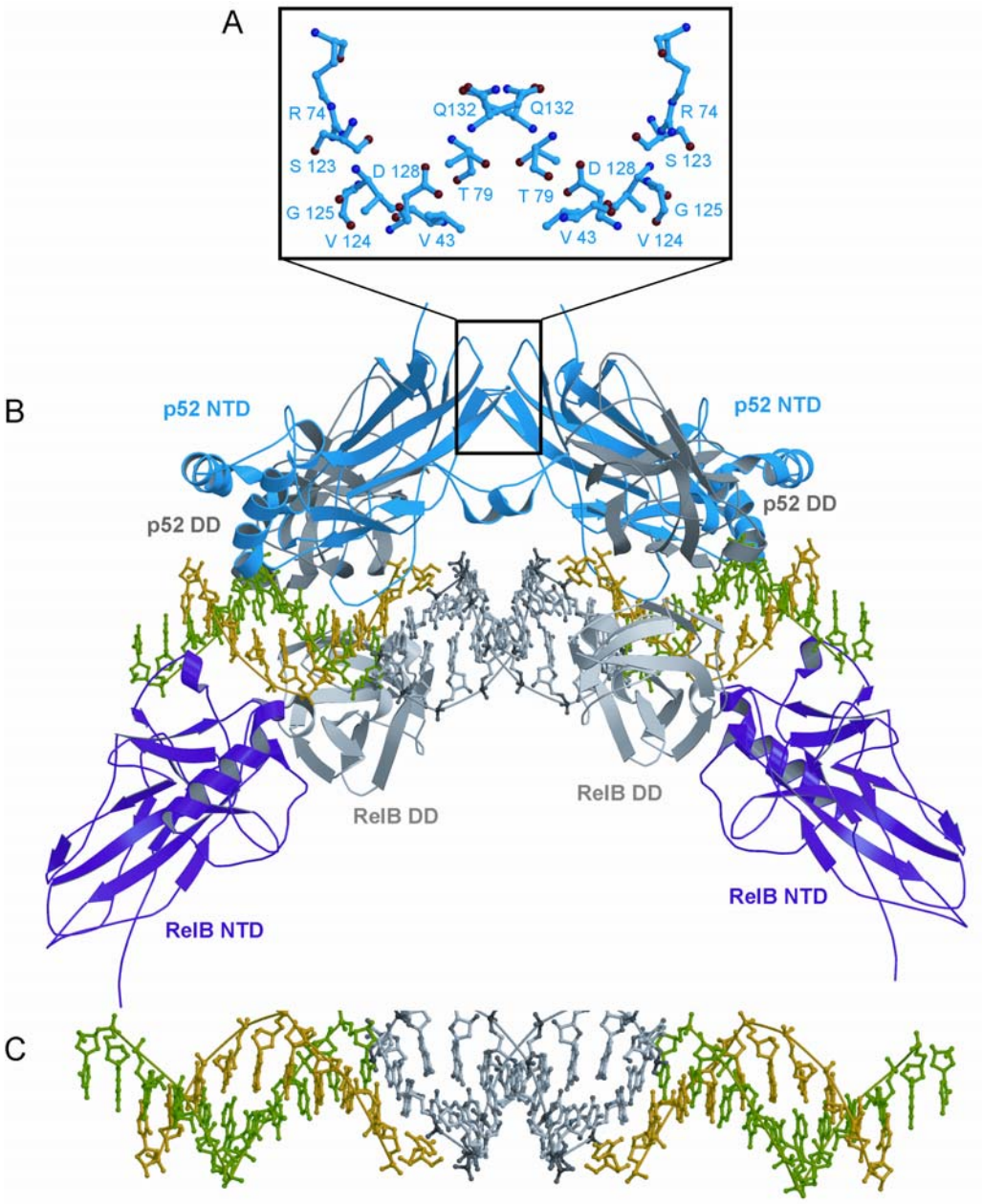

Figure 3-19. *Crystal packing contacts made between multiple complexes.* A.) A close up view of the contact surface shown in p52. B.) Overall view of the packing between two RelB/p52 heterodimers (purple and teal, respectively) bound to neighboring κB sites. The dimerization domains are shown in grey (RelB DD) and dark grey (p52 DD). C.) Overall view of the DNA packing. The grey DNA represents DNA that is not bound by any NFκB subunit. Oxygen atoms are in red, nitrogen atoms in blue.

6. Bound versus Unbound DNA

As mentioned above the two κB DNAs form a long linear helix through end to end packing where one DNA is bound to the RelB/p52 heterodimer and the other remains mostly unbound. The only contact observed for the unbound DNA is a hydrogen bond (3.93 Å) observed between Lys75 of the p52 subunit with the phosphate backbone of the 5' C of the symmetry related CCC:GGG base pairs (Figure 4-7B). This structure thus gives us an opportunity to test the conformational changes that the DNA undergoes when bound to the RelB/p52 heterodimer as compared to its unbound state (Figure 4-19C). Overlay of the free κB site (grey) and the RelB/p52 bound κB site (cyan) reveal several notable features. Although both DNAs are relatively straight, there is a sharp kink observed only at the G-3/A-4 base step in the bound DNA. The unbound DNA is more open compared to the bound DNA and the minor groove is only slightly compressed upon protein binding (Figure 4-20). These observations are vastly different than our previous observations where most DNAs exhibited significant minor groove compression upon NF-κB binding (Huang et al., 2005a). It is likely that few protein:DNA contacts at the center of the DNA observed in this complex might be responsible for lack of structural changes at the center of DNA. These observation further reinforces the idea that the RelB/p52 heteordimer employs a somewhat different mechanisms to recognize the κB DNA compared to the other dimers.

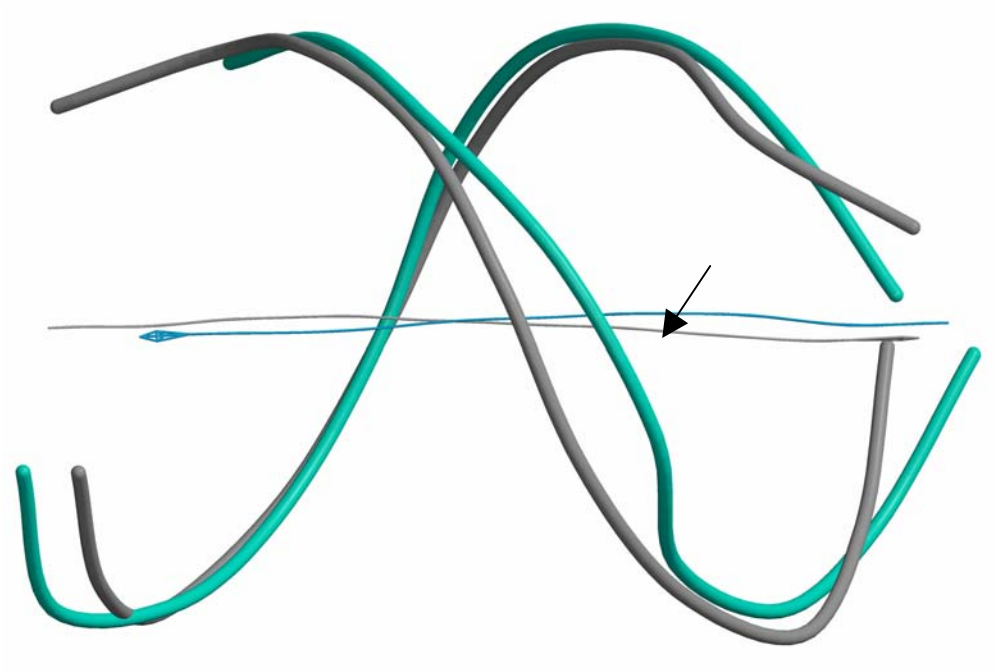

Figure 4-20. *Comparison of RelB/p52 Bound and Free κB DNA.* Overlay of bound versus free DNA illustrates that there is a compression in the minor groove of the DNA upon NFκB binding (highlighted by arrow). Colored in cyan is the backbone of the bound DNA. Colored in grey is the backbone of the unbound DNA.

7. DNA binding affinities

The ability of the RelB/p52 heterodimer to bind and activate a large number of genes by binding to their promoters led us to measure the affinities of different DNA molecules for the RelB/p52 heterodimer and compare it to that of other NF-κB family dimers. Solution based fluorescence polarization (FP) assays was used to determine the DNA binding affinities of the RelB (1-400)/p52 (1-341), p50 (35-363)/p65 (1-325) heterodimers and p50 (35-363) and p52 (1-341) homodimers. The pure recombinant proteins, p50 homodimer and p50/p65 heterodimer, were kind gifts from Anu Moorthy and Chris Phelps, respectively. The fluorecein labeled oligonucleotides used contained a single κB site (sequence listed in figure 3-21) from the CD39, BLC, ELC and SDF-1 promoters (Figure 3-21). RelB/p52 bound to this unique set of κB sites with high affinity, an average K_D of 44 nM (for CD39 and ELC) and 19.5 nM (for BLC and SDF-1). These κB sequences diverge from the consensus κB sequence. Interestingly, the p50/p65 heterodimer also bound to these sequences with a high affinity (average K_D = 37.9 for BLC, ELC and SDF-1) with the exception of CD39 κB site. A three fold decrease in binding was observed for the p50/p65 heterodimer to the CD39 κB site. The p50 and p52 homodimers also bound to this set of κB sites with a high affinity (average K_D =27 nM and 21 nM for p52 and p50 homodimers, respectively). Summary of the binding affinities are given in figure 3-21.

We further tested the binding affinities of RelB/p52 heterodimer for other well characterized κB DNA sites such as IL-2 CD28RE, IFN-β, IgκB, and IL-8 (Figure 3-21). The RelB/p52 heterodimer bound to all the κB sites tested with a high affinity

(an average K_D = 16.6 nM) with the exception of the IFN-β κB site which had an 8 fold decrease in binding affinity. In all, these results demonstrate that the RelB/p52 heterodimer was the only NF-κB family member tested that bound to most κB sites with a high affinity. Other dimers were more selective to the DNA κB sites tested (bound to two or more κB sites with low affinity).

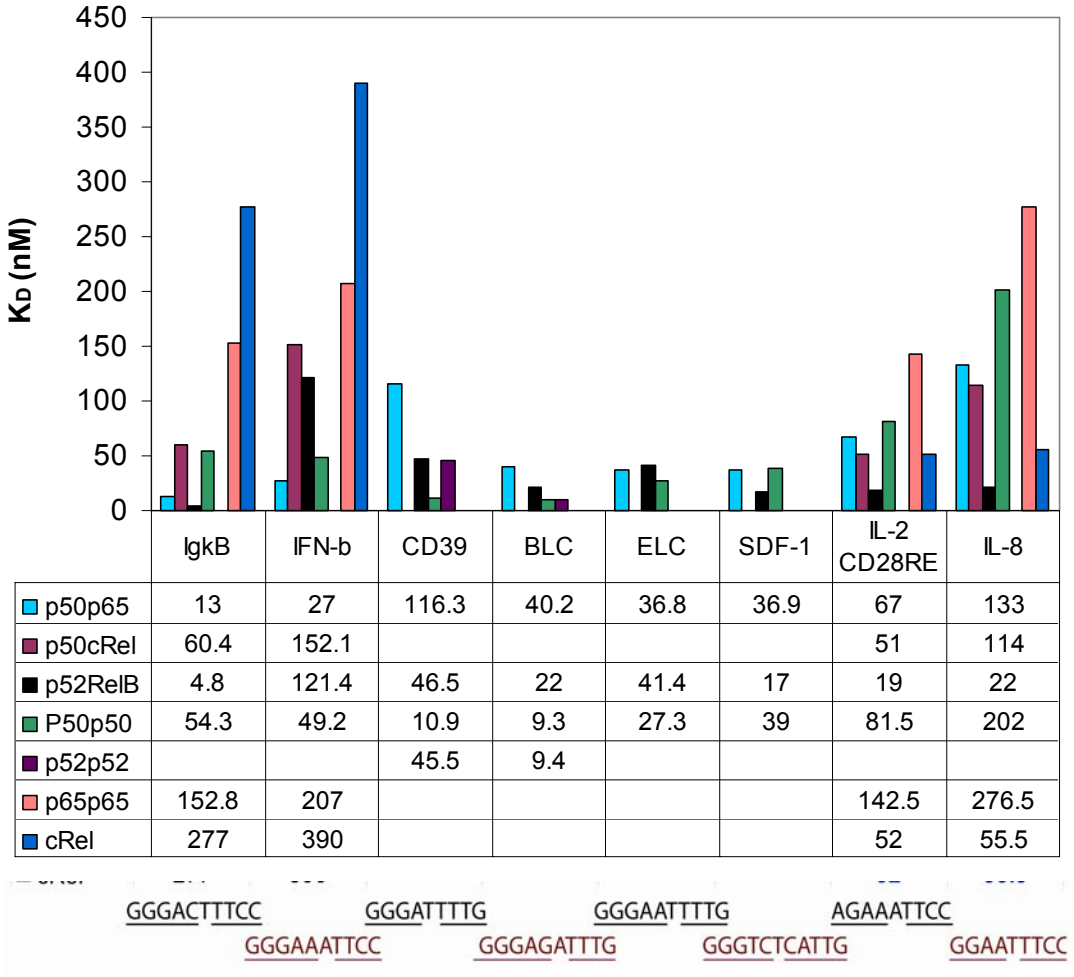

	IgkB	IFN-b	CD39	BLC	ELC	SDF-1	IL-2 CD28RE	IL-8
p50p65	13	27	116.3	40.2	36.8	36.9	67	133
p50cRel	60.4	152.1					51	114
p52RelB	4.8	121.4	46.5	22	41.4	17	19	22
P50p50	54.3	49.2	10.9	9.3	27.3	39	81.5	202
p52p52			45.5	9.4				
p65p65	152.8	207					142.5	276.5
cRel	277	390					52	55.5

Figure 3-21. *Binding affinities of NF-κB family members to κB sites.* Binding affinities (nM) are plotted for each κB DNA and NFκB family member. The table gives a summary of the K_D observed in each case. Underneath the table is the κB sequence for the gene listed above it. The K_D values highlighted in blue represent the NF-κB dimer that is thought to be important for the activation of the listed gene.

C. Discussion

The RelB/p52 heterodimer is a unique dimer amongst the NF-κB family of transcription factors. It is the only heterodimer that is activated through the non-canonical pathway. This heterodimer binds to and activates a large number of genes including ones that contain a distinct class of κB sites that do not follow the consensus 5'-GGRNNNYCC-3' sequence. The structure of the RelB/p52 heterodimer complexed to DNA provides some explanation as to why this heterodimer functions differently compared to others.

1. Dimerization by the RelB/p52 heterodimer

The RelB/p52 heterodimer is more stable than the corresponding homodimers both *in vitro* and in cells. Complex formation of the RelB/p52 heterodimer supports this idea as little, if any, RelB or p52 homodimer is formed. Although the overall structure of the dimerization domain of the RelB/p52 complex is conserved amongst NF-κB dimers, the structure reveals some hints as to why this heterodimer is more stable than the corresponding homodimers. This heterodimer mediates a unique set of contacts that are not possible in the respective homodimers. In addition, the homodimers also encounter destabilizing interactions at the interface; contacts between two aspartates (Asp234) in p52 homodimer or two isoleucines (*Ile335*) in RelB. In the heterodimer, these destabilizing interactions are converted into contacts that stabilize the complex. In addition, to these favorable interactions within the dimerization domain, additional unique interactions have been observed between the

two subunits which further stabilizes the heterodimer (discussed in greater detail in Chapter V).

2. DNA binding by the RelB/p52 subunit

Because of the distortion of the DNA some unusual DNA contacts are seen by the p52 subunit of the heterodimer. However, in a regular DNA the p52 subunit is expected to make contacts as observed in the monomer of the p52 homodimer/DNA complex. The most surprising result that emerged from our study is the involvement of *Arg125* of RelB in making base-specific contacts with a flanking G:C bp (G+5). Although equivalent arginine residues are present in p65 (Arg29) and cRel (Arg41), these residues are not involved in sequence specific DNA binding. This suggest small sequence variations elsewhere in the p52 and/or RelB subunits modulate the positioning of this arginine residue such that it enables DNA binding only in the case of RelB and not in other subunits. It is also possible that the differential mode of binding observed for this arginine is propagated through the DNA. Another interesting feature of this complex is the stacking interaction of *Tyr120* with only one thymine. In other subunits the equivalent tyrosine reisude packs against two successive tyrosines resulting in the compression of the DNA minor groove at the center and smooth bending of the DNA towards the major groove. This bending of DNA causes a shift of the flanking DNA residues such that Arg29 of p65 or Arg41 of cRel are unable to contact DNA. The end result of these differential contacts is that the RelB/p52 heterodimer prefers κB sites of 11 bp long with a GGG/CCC sequence at

the ends. Both proteins recognize this core sequences at both ends. In all, our structure reveals a distinct mode of DNA recognition by the RelB/p52 heterodimer.

3. DNA binding specificity

Gene experiments have suggested that NF-κB dimers preferentially and selectively activate a distinct but overlapping set of genes (Gerondakis et al., 1999; Sanjabi et al., 2000). The RelB/p52 heterodimer has been demonstrated to recognize a class of chemokine genes that contain a subset of κB sequence that differ from the classical κB sites (Bonizzi et al., 2004). However, the *in vitro* DNA binding affinities did not reveal any selectivity of κB DNA recognition by RelB/p52 heterodimer. Our structure can explain why this heterodimer binds κB sequences present in ELC, SDF-1 and BLC gene promoters. The last G:C base pair in these sequences can be optimally recognized by the RelB subunit. Further studies are required to test if alterations of this base pair or mutations of the *Arg125* residue reduce the affinity of the RelB/p52 complex to these DNA. However, we cannot explain why these sequences are also bound with high affinity by the other dimers. One cannot rule out the important role that the DNA conformation plays in the form of 'indirect readout' by the protein. It is likely that these sequences are flexible in a way that is complementary to binding by the NF-κB dimers.

IV. Transcriptional Synergy

A. Introduction

The ability of the body to generate a fully functional immune response is dependent on the integration of dual signals. A large part of the receptor mediated responses are governed at the level of transcription and are mediated by many transcription factors. The synergistic assembly of these transcription factors on the enhancer region of genes to form enhanceosomes (multimolecular protein-DNA complexes) is a key regulatory event in the activation and maintenance of transcription (Giese et al., 1995; Grosschedl, 1995; Thanos and Maniatis, 1995). It has been shown that the interaction of NF-κB dimers with enhancer-binding proteins in the enhancer regions of genes is important for stimulus dependent transcription of genes. Two transcription factors that have been shown to have transcriptional synergy with NF-κB are CREB (cAMP response element binding protein) and C/EBPβ (CCAAT/enhancer-binding protein).

CREB is a 43 kDa transcription factor that is ubiquitously expressed and is critical for a variety of cellular processes, such as proliferation, differentiation, hormonal control of metabolic processes and adaptive responses (Mayr and Montminy, 2001). It was initially identified as a mediator of the cAMP pathway and binds to the prototypical palindromic target sequence cAMP response element, CRE (5'-TGACGTCA-3') (Montminy et al., 1986; Sheng et al., 1990). CREB belongs to the CREB/CREM/ATF family of transcription factors. The CREB/CREM/ATF family share several similarities, including a highly homologous basic leucine zipper (bZIP) DNA binding domain, the ability to homo- and heterodimerize in specific combinations, and the presence of conserved activator regions and phosphorylation

sites (Lee and Masson, 1993; Meyer and Habener, 1993). CREB's activation domain contains two glutamine-rich regions (Q1 and Q2), the kinase-inducible domain (KID) which contains several phosphorylation sites (i.e.-Ser 133 by PKA or calcium-calmodulin kinase II and IV), and the adjacent basic and leucine zipper domains which are responsible for DNA binding and dimerization, respectively (Figure 4-1)((Dash et al., 1991; Gonzalez et al., 1991; Kerppola and Curran, 1995; Lee et al., 1990; Sheng et al., 1990; Sheng et al., 1991; Van Nguyen et al., 1990). Phosphorylation at serine 133 recruits binding of the transcriptional co-activator CBP (CREB binding protein) and confers phosphorylation induced activity (Lu et al., 2003).

Both CREB and NF-κB have been shown to be important for the expression of interleukin-2. The T cell growth factor interleukin-2 (IL-2) promoter contains an enhancer region, located between positions -164 and -154, that is induced by CD28 costimulation (Fraser et al., 1991; Verweij et al., 1991). NF-κB has been shown to bind to this region and be important for its transcriptional activation, in particular cRel and RelA (Figure 3-3A) (Bryan et al., 1994; Ghosh et al., 1993; Lai et al., 1995). Reports have shown that other transcription factors such as NFAT and CREB play a role in regulating CD28 responsiveness. It has been shown that CREB and cRel have synergy in the transcription of IL-2 CD28RE (Butscher et al., 1998).

A

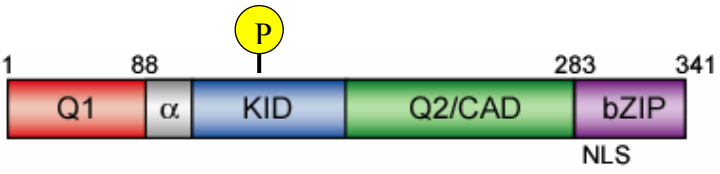

B

MTMDSGADNQQSGDAAVTEAESQQMTVQAQPQIATLAQVSMPAAHATS

SAPTVTLVQLPNGQTVQVHGVIQAAQPSVIQSPQVQTVQSSCKDLKRLFSGTQIS

TIAESEDSQESVDSVTDSQKRREILSRRPSYRKILNDLSSDAPGVPRIEEEKSEE

ETSAPAITTVTVPTPIYQTSSGQYIAITQGGAIQLANNGTDGVQGLQTLTMTNAA

ATQPGTTILQYAQTTDGQQILVPSNQVVVQAASGDVQTYQIRTAPTSTIAPGVVM

ASSPALPTQPAEEAARKREVRLMKNREAARESRRKKKEYVKSLENRVAVLENQNK

TLIEELKALKDLYSHKSD

C

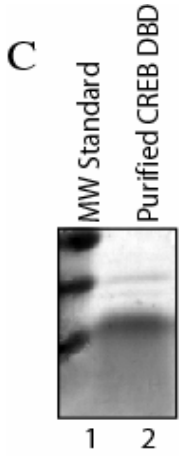

Figure 4-1. *Primary structure and sequence of CREB.* A.) Domain Organization of CREB. The domains of CREB are labeled and colored by their domains. Q1 and Q2 represent glutamine-rich regions. Q2 is also called constitutive activation domain (CAD). KID represents kinase inducible domain and contains serine 133, the phosphorylation of which is required for the activation of CREB. bZIP contains the basic region and the leucine zipper important for DNA binding and dimerization, respectively. NLS indicates nuclear localization signal. B.) Sequence of CREB. The domains are colored as in A. The KID domain shown in blue has Ser 133 highlighted in yellow. The bZIP domain (DBD), colored in purple, is the domain that was expressed and purified. C.) Commassie stain of human CREB DBD purified from cation exchange followed by gel filtration.

The second transcription factor that has been shown to have transcriptional synergy with NF-κB is C/EBPβ. C/EBPβ is a 32-kDa protein that is found in nearly all cells and was originally identified as a mediator of IL-6 signaling (Akira et al., 1990; Poli et al., 1990). It is a member of the C/EBP family of βZIP transcription factors that play an important role in controlling cell proliferation and differentiation (Darlington et al., 1998; Diehl, 1998; Lekstrom-Himes and Xanthopoulos, 1998). This family of six proteins (C/EBPα, C/EBPβ, C/EBPγ, C/EBPδ, C/EBPε, and C/EBPζ) share sequence homology and function. C/EBPα was the first identified and is the founding member. Each protein contains a similar basic region and leucine zipper domain at its C-terminus which mediates DNA binding and homo- and heterodimerization, respectively (except for C/EBPζ which lacks DNA binding activity). They also share effector domains at their N-termini that mediate transcriptional activation, repression and autoregulatory functions (except C/EBPγ) (Figure 4-2) (Agre et al., 1989; Landschulz et al., 1988; Vinson et al., 1993). C/EBP dimerization is a prerequisite to DNA binding; however, the binding specificity is determined by the DNA contact surface within the basic region (Landschulz et al., 1989).

A truncated isoform of C/EBPβ, termed liver inhibitory protein (LIP), possesses only the DNA-binding and leucine zipper domains. Heterodimerization of the truncated isoform with full-length C/EBPβ attenuates transcriptional activity (Descombes and Schibler, 1991; Poli et al., 1990).

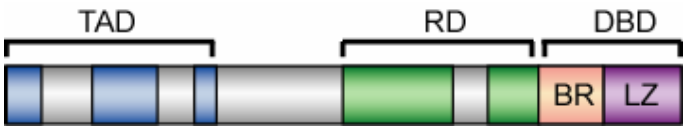

mhrllawdaaclpppaafrpmevanfyyepdclaygakaaraaprapaaepaigeh

eraidfspyleplapaadfaapapahhdflsdlfaddygakpskkpadygyvslgra

gakaappacfpppppaalkaepgfepadckraddapamaagfpfalraylgyqatps

gssgslstsssssppgtpspadakaapaacfagppaapakakakktvdklsd**eykmr**

rernniavrksrdkakmrnletqhkvleltaenerlqkkveqlsrelstlrnlfkql

pepllasaghc

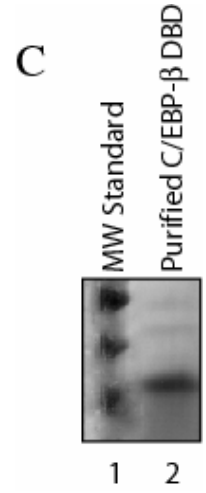

Figure 4-2. *Primary structure and sequence of C/EBP.* A.) Domain Organization of C/EBPβ. The leucine zipper dimerization domain (LZ) at the C-terminus is colored in purple. An adjacent highly conserved basic region (BR) that mediates sequence-specific DNA binding is shown in pink. A tripartite transactivation domain (TAD) at the N-terminus is shown in blue. The regulatory domain (RD) is shown in green. B.) Sequence of mouse C/EBPβ. The DNA binding domain is colored purple. The C/EBPb construct, made of the DBD, that was expressed and purified is underlined. C.) Commassie stain of mouse C/EBPβ DBD purified from cation exchange followed by gel filtration.

Two examples of transcriptional synergism between C/EBPβ and NF-κB are the expression of C-reactive protein (CRP) and serum amyloid A (SAA) (Agrawal et al., 2001; Agrawal et al., 2003; Betts et al., 1993; Cha-Molstad et al., 2000; Kleemann et al., 2003; LeClair et al., 1992; Vales and Friedl, 2002). Physical interactions have been observed between C/EBPβ and p50, p65 and cRel containing NF-κB's (Agrawal et al., 2003; Betts et al., 1993; Kleemann et al., 2003; LeClair et al., 1992). There is also evidence that p50 and cRel enhance and stabilize the binding of C/EBPβ to the CRP promoter (Agrwawal JI2001, Agrawal MI).

In spite of a wealth of information regarding transcriptional synergy between NF-κB and other transcriptional activators, no *in vitro* experiments have been done to test if synergism is due to cooperative interactions between either NF-κB and CREB or NF-κB and C/EBPβ. Consequently, I have worked to investigate the cooperative interactions between these proteins *in vitro.* Assays were done using pure recombinant proteins to observe cooperative interactions between C/EBPβ and NF-κB to a CRP promoter oligonucleotide, or CREB and NF-κB to a IL2 CD28RE promoter oligonucleotide (Figure 4-3C). Results of these experiments clearly demonstrate a lack of cooperativity through the DNA-binding domain of NF-κB and CREB or C/EBPβ.

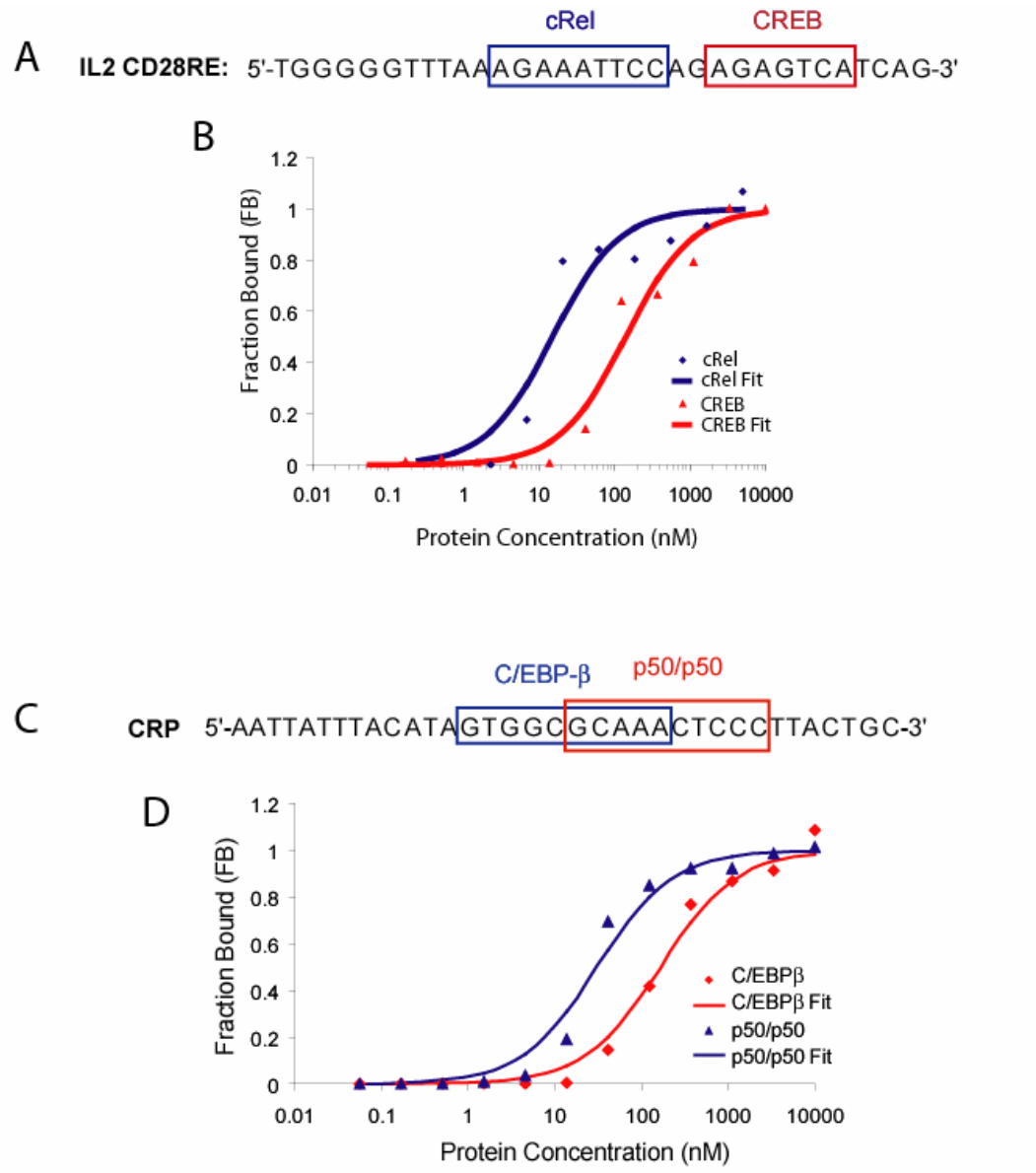

Figure 4-3. *Fluorescence anisotropy assays of DNA binding of CREB DBD, cRel/cRel, p50/p50 and C/EBPβ.* Semi logarithmic plot of concentration (nM) of protein vs. Fraction Bound. A.) Sequence of the probe used in the FAAs with CREB and cRel. The κB site is highlighted by a blue box and CRE site is highlighted by a red box. B.) IL-2 CD28RE (200 pM) was titrated with either CREB DBD (red line) or c-Rel homodimer (blue line). C.) Sequence of the probe used in the FAAs with C/EBPβ and p50. The κB site is highlighted by a red box and C/EBP site highlighted by a blue box. D.) CRE (200 pM) was titrated with either C/EBPβ DBD (red line) or p50 homodimer (blue line).

B. Results

1. Experimental Strategy

To test cooperativity, the DNA binding domains of NF-κB, CREB and C/EBPβ were expressed and purified to homogeneity. The pure recombinant NF-κB proteins cRel RHR (1-311) homodimer, p50 homodimer (35-363), p50 (35-363)/p65 (1-325) heterodimer and p50(35-363)/cRel (1-311) were kind gifts from Chris Phelps, Anu Krishnamoorty, Tom Huxford and Chris Phelps ,respectively. The CREB DBD was purified by cation exchange followed by size exclusion chromatography (Figure 4-1). C/EBPβ DBD was also purified by cation exchange followed by size exclusion chromatography (Figure 4-2C).

A 32 base pair DNA fragment of IL-2 CD28RE was used to examine the interaction between NF-κB and CREB. The fluorecienated oligonucleotide used contained the κB and CREB sites (Figure 4-3A). The NF-κB dimers used were: cRel homodimer and p50/p65 heterodimer.

To test the interaction between NF-κB and C/EBPβ a 35 base pair DNA fragment of the CRP promoter was used. The fluorecienated oligonucleotide used contained the κB and C/EBP sites (Figure 4-3C). Three different NF-κB dimers were used: p50 homodimer, p50/p65 and p50/cRel heterodimers.

A solution based fluorescence polarization assay was used to determine if the transcriptional synergism observed previously between CREB or C/EBPβ and NF-κB is due to cooperativity through DNA binding to the IL-2 CD28RE promoter or CRP

promoter, respectively. First each protein was tested for their DNA binding affinity independently. Next the binding of one protein was observed in the presence of a constant amount of the other protein. The constant amount of protein used was such that 50% to 90% of the DNA was occupied. If the binding interaction between NF-κB and the second activator was cooperative then the saturation of binding would occur at a lower concentration in the presence of constant amount of the activator as compared to its absence. This can be observed by FAA when there is an increase in total Milli-Polarization (indicating co-occupancy) and an improvement in the K_D value (indicating co-operative DNA binding) (Figure 4-4).

Similar experiments were carried out using Electrophoresis Mobility Shift Assay (EMSA). The basic premise of the systems is the same except FAA is purely solution based where EMSA is not. Cooperativity in an EMSA is observed through an increase in molecular weight (indicated by a higher migrating species) and an improvement in the K_D value.

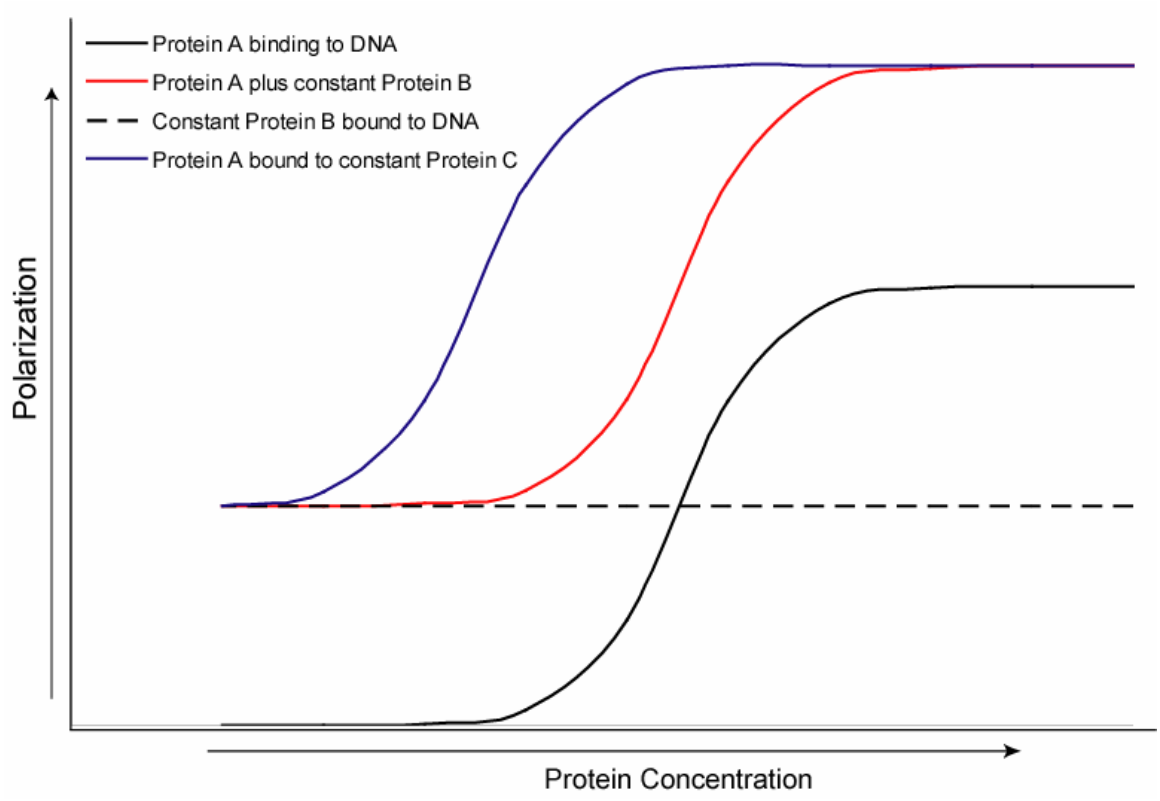

Figure 4-4. *Example of Co-operativity observed by FAA.* Example of DNA binding curve of Protein "A" (black line). Constant amounts of Protein "B" bound to DNA (black dashed line). When Protein "A" is added to constant amounts of Protein "B" co-occupation occurs (red line) which is observed by an increase in polarization (red arrow). When Protein "B" is added to constant amounts of Protein "C" co-operativity occurs (blue line) which is observed by an increase in polarization and an improvement in DNA binding occurs (blue arrow).

2. Interactions between CREB and NFκB on the IL-2 CD28RE promoter

FP assay showed that the cRel homodimer (RHR) bound to the DNA with an approximate K_D of 15 nM in a solution containing 50 mM NaCl at pH 7.5. The CREB DBD bound the same probe with a K_D of approximately 140 nM. The concentration required for 80% of CREB and cRel to be bound to DNA is 500 nM and 200 nM, respectively (Figure 4-3B).

CREB DBD and cRel homodimer were then assayed together to determine if their binding to the IL-2 CD28RE is cooperative. In the presence of near saturating concentration of CREB (200 nM) cRel homodimer was added, no improvement in CREB DBD binding was observed (Figure 4-5A). Interestingly, not only was no cooperativity observed between cRel homodimer and CREB binding, no increase in total Milli-Polarization (mP) was observed. This indicated that CREB and cRel were unable to cooccupy the DNA at the same time, which suggested that the binding was mutually exclusive. In the reverse experiment, constant amounts of near saturating CREB DBD (800 nM) was added to the titrated cRel homodimer prior to the addition of DNA. Again, there was no change in cRel's binding pattern as compared to titration in the absence of CREB. Binding appeared to be mutually exclusive (Figure 4-5B). This experiment was repeated using concentrations of CREB DBD at 140 nM, which is similar to the K_D value. This was done to observe if co-occupation could occur when the DNA is only 50% occupied. The decrease in the amount of constant CREB did not have a significant effect on the mutually exclusive DNA binding. However, at low concentrations of cRel (0.25 nM-6.9 nM) it appears that both cRel and CREB are able to co-occupy the DNA (shown by an increase in total mP).

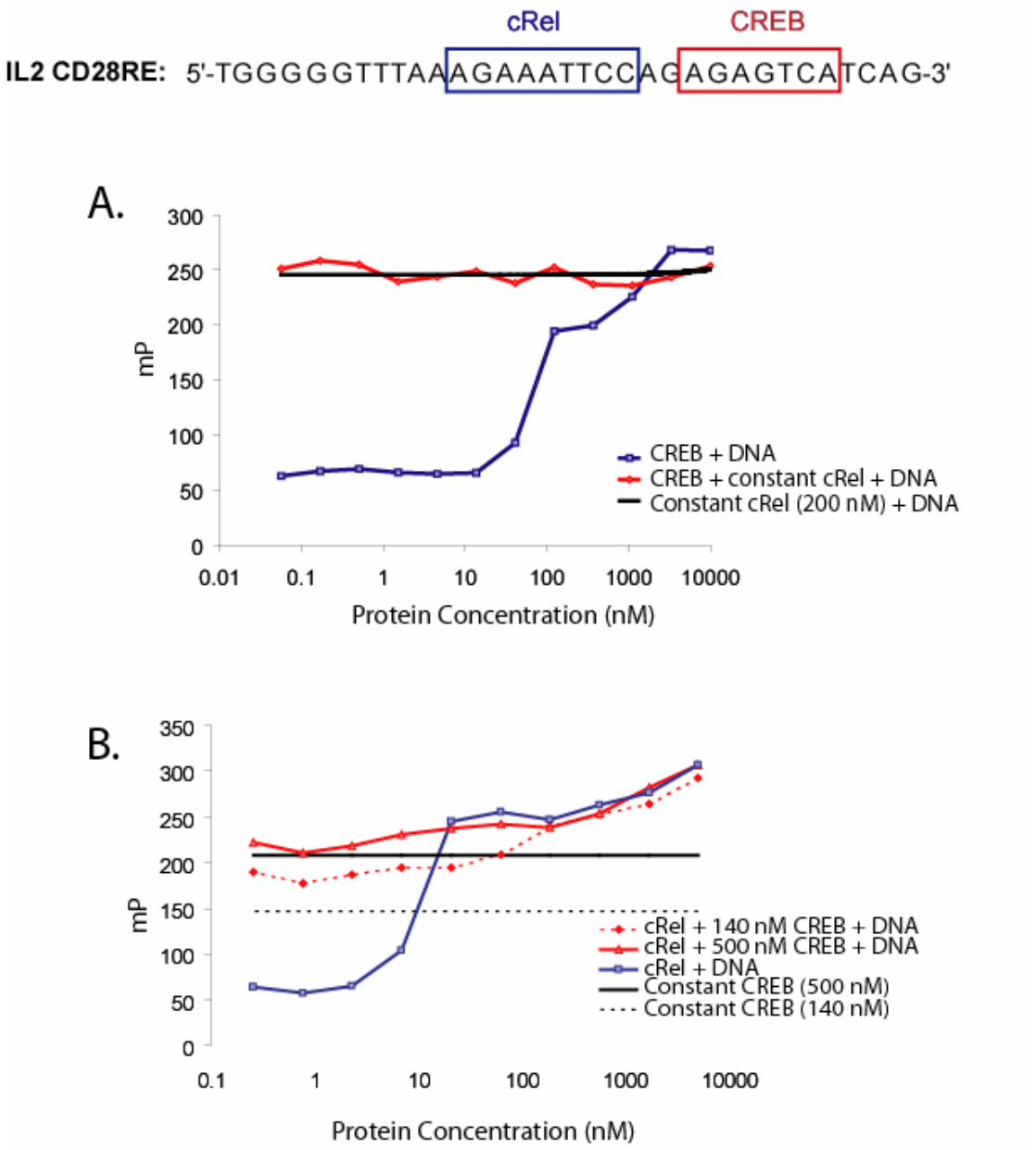

Figure 4-5. *Fluorescence anisotropy assays of non-cooperative binding of CREB DBD and cRel homodimer.* Milli-Polarization units are plotted against concentration of protein A.) cRel concentration was held constant (black line), titrated amounts of CREB DBD and DNA (blue line), constant amount of IL-2 CD28RE DNA (200 pM) was added to constant CREB DBD and titrated cRel (red line). B.) The reciprocal experiment as in "A" (constant 500 nM CREB DBD (black line) with titrated amounts of cRel (blue line) and IL-2 CD28RE (red line) or with constant 140 nM CREB DBD (broken black line) with titrated amounts of cRel (blue line) and IL-2 CD28RE (broken red line).

To observe if the order of addition has an affect on cooperativity, the order of addition to the DNA was reversed (i.e., protein was titrated with DNA prior to the addition of constant amounts of the second protein). This had been shown to have an affect previously in our lab for the interaction between NF-κB and Sp1 (Chris Phelps). However, the same pattern of mutually exclusive binding was observed when the titrated protein had the DNA added prior to or after the addition of the constant amount of the second protein (Figure 4-6). In all other FAA complex formation experiments, the constant protein was added to the titrated second protein prior to the addition of DNA.

EMSA was used to validate our observations made by FAA. The same DNA duplexes were used as probes, and the DNA binding by the cRel homodimer and CREB DBD were measured by EMSA. (Figure 4-7). Similar to what was observed previously using FAA, no improvement in cRel binding was observed in the presence of saturating CREB as compared to its absence, and the binding for IL-2 CD28RE was mutually exclusive (Figure 4-8A). However, it is possible that the aggregation of cRel at high concentrations masked co-occupancy of the DNA. In the reverse experiment, where saturating amounts of cRel (180 nM) was added to the CREB DBD DNA reactions, there was no change in CREB's binding. At high concentrations of CREB it appears that there is an increase in the amount of cRel bound to the DNA and at the same time a decrease in the level of CREB/DNA complex. It is possible that co-occupancy can occur under these conditions (Figure 4-8B). It is clear that the addition of cRel (or CREB) does not improve the DNA binding of CREB (or cRel).

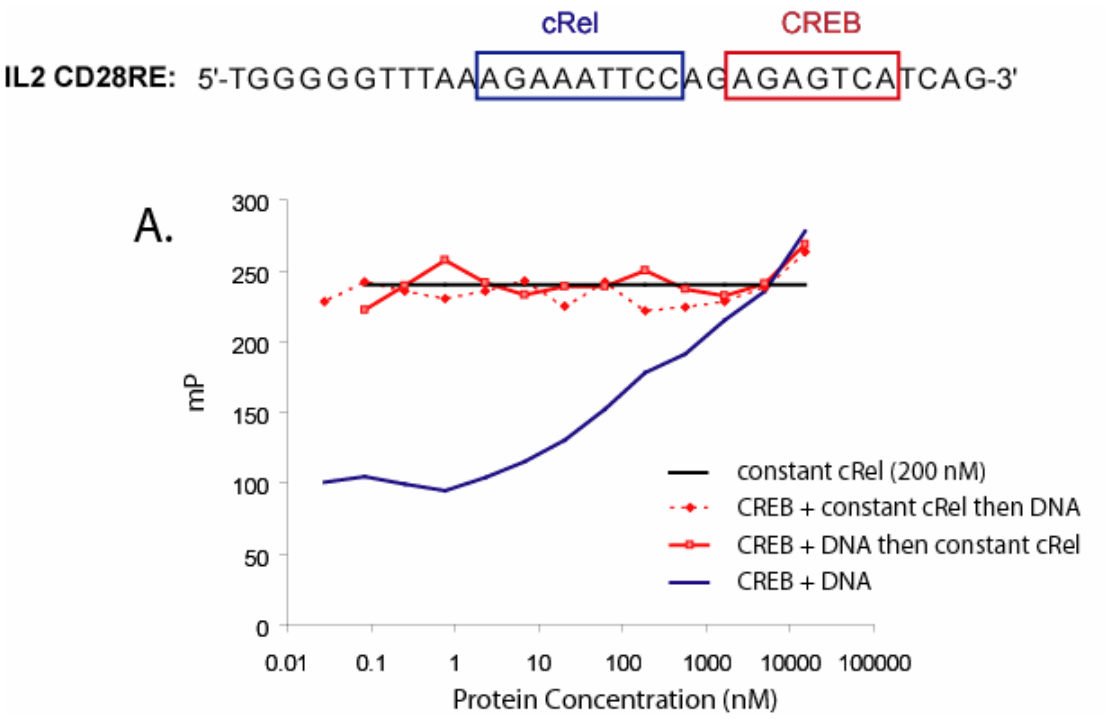

Figure 4-6. *Fluorescence anisotropy assays of non-cooperative binding of CREB DBD and p50/p65 heterodimer.* Milli-Polarization units are plotted against concentration of protein. A.) The blue line represents CREB DBD titrated into Il-2 CD28RE DNA (200 pM). The black line represents the Milli-Polarization value for the constant amount of cRel used. Constant amounts of cRel were added to titrated CREB DBD prior to the addition of DNA (red broken line). Constant amounts of DNA were added to titrated CREB DBD prior to the addition of constant cRel (red line).

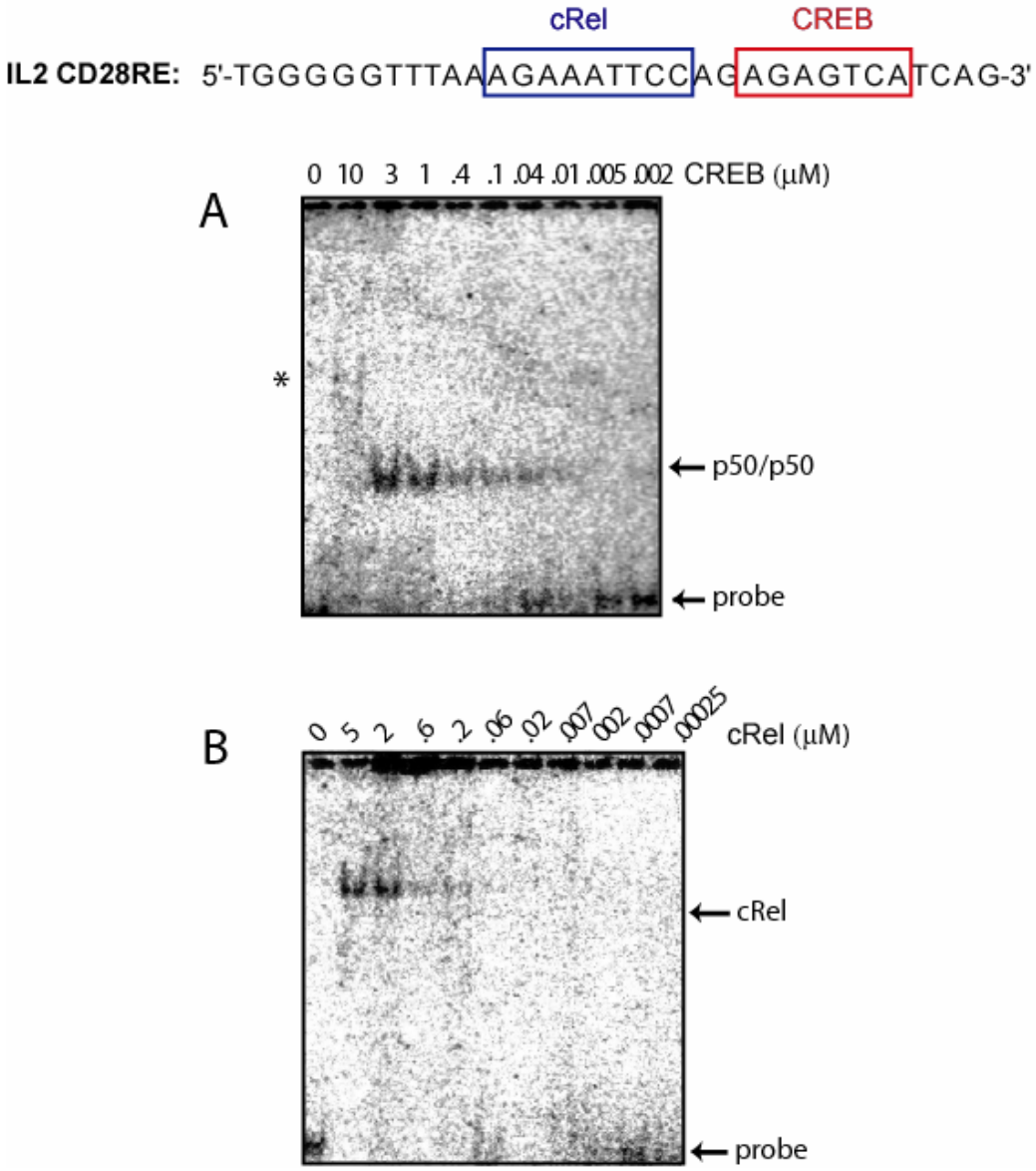

Figure 4-7. *Electrophoretic mobility shift assays of CREB DBD and cRel homodimer binding to IL-2 CD28RE probe.* A.) CREB DBD was titrated with constant amounts of IL-2 CD28RE probe. B.) cRel homodimer was titrated with constant amounts of IL-2 CD28RE probe. Arrows indicate the location of the c-Rel dimer/DNA complex, CREB/DNA complex and free CRP probe. "*" indicates aggregated protein bound to DNA.

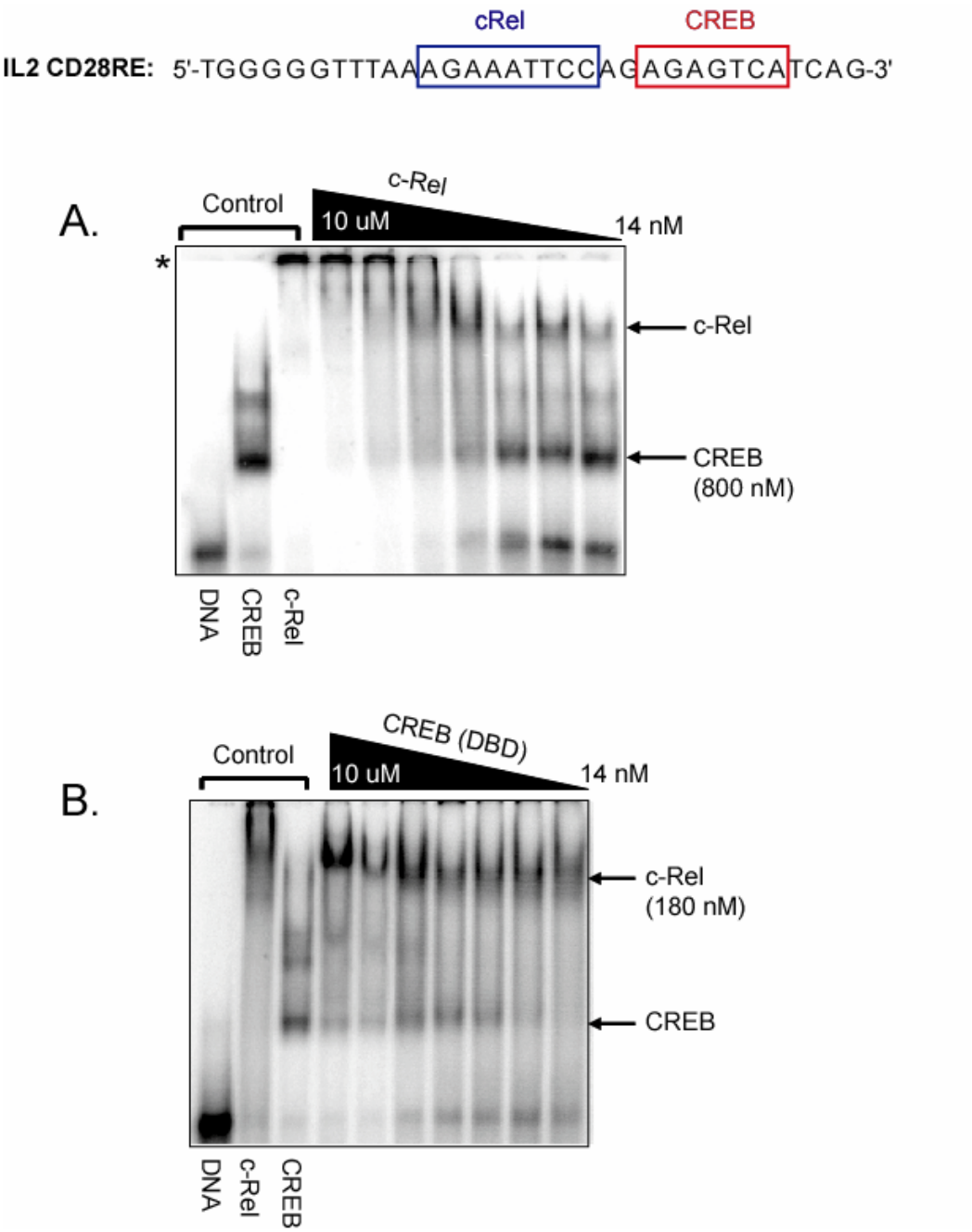

Figure 4-8. *Electrophoretic mobility shift assays of non-cooperative binding of CREB DBD and c-Rel homodimer.* A.) DNA and CREB DBD concentrations were held constant in each lane and titrated with decreasing c-Rel concentrations. B.) DNA and c-Rel homodimer concentrations were held constant in each lane and titrated with decreasing CREB DBD concentrations. Arrows indicate the location of the c-Rel dimer/DNA complex, CREB/DNA complex and free probe (IL-2 CD28RE). The * indicates DNA bound to aggregates of NFκB which occur at high protein concentration.

To further test how other NF-kB dimers interact with CREB, we investigated p50/p65 heterodimer. The FAA was repeated with pure recombinant p50/p65 heterodimer instead of c-Rel (kind gift from Frances Chen) and CREB DBD. Again, mutually exclusive DNA binding was observed when constant amounts of p50/p65 was added to titrated CREB DBD with IL-2 CD28RE, and also when constant amounts of CREB DBD was added to titrated p50/p65 (Figure 4-9).

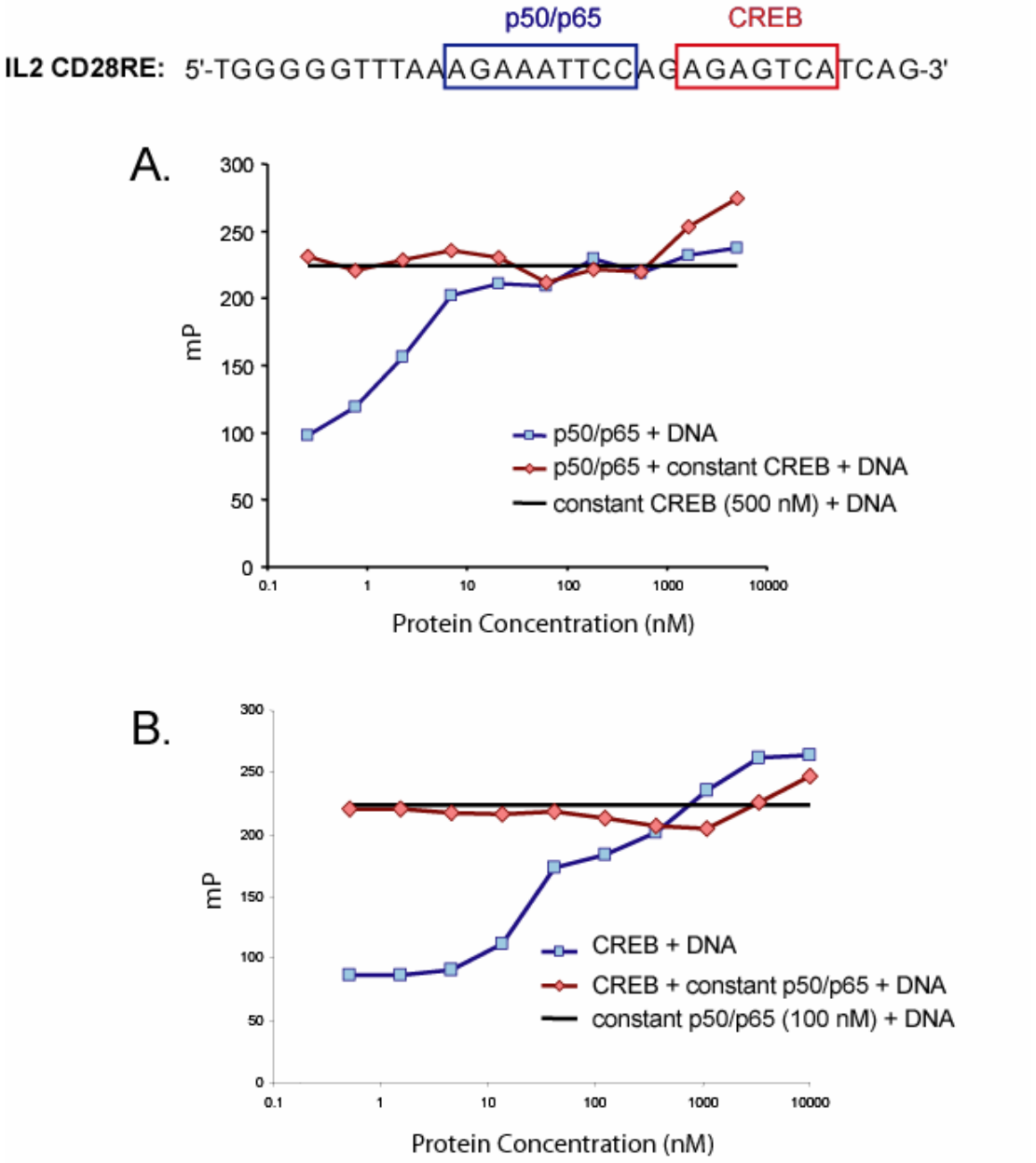

Figure 4-9. *Fluorescence anisotropy assays of non-cooperative binding of CREB DBD and p50/p65 heterodimer.* Milli-Polarization units are plotted against concentration of protein A.) CREB DBD concentration was held constant (black line) and titrated amounts of p50/p65 and DNA (blue line),constant CREB DBD plus titrated p50/p65 was added to constant amount of IL-2 CD28RE DNA (200 pM) (red line). B.) The reciprocal experiment as in "A" (constant p50/p65 (black line) with titrated amounts of CREB DBD (blue line) and IL-2 CD28RE (red line).

3. Interaction between C/EBPβ and NF-κB on the CRP promoter

To test the nature of the interaction between p50 and C/EBPβ on the CRP promoter, a similar series of experiments were carried out as described before. FAA was used to determine the binding affinities of the p50 homodimer:CRP DNA and C/EBPβ DBD:CRP DNA complexes. The p50 homodimer bound to the DNA with a K_D of approximately 31 nM whereas the C/EBPβ DBD bound with a K_D of approximately 167 nM. The concentration required for approximately 65% of C/EBPβ and p50 to be bound to DNA is 370 nM and 42 nM, respectively (Figure 4-3D). Due to the results observed for CREB and cRel the concentrations used in this case (65% of saturation) were less than the amount required for saturation.

When C/EBPβ DBD was added at a concentration of 370 nM no improvement in the p50 binding was observed by FAA (Figure 4-10A). Moreover, total mP remained constant which indicates that the DNA binding was mutually exclusive. In the reverse experiment, where constant amounts of saturating p50 (42 nM) was added to the increasing amounts of C/EBPβ DBD, there was no change in p50 binding. There was however, an increase in total mP at low concentrations (0.51 nM-41 nM) of C/EBPβ indicating DNA co-occupancy. At high concentrations of C/EBPβ the mP values follow the trend of C/EBPβ binding to DNA.

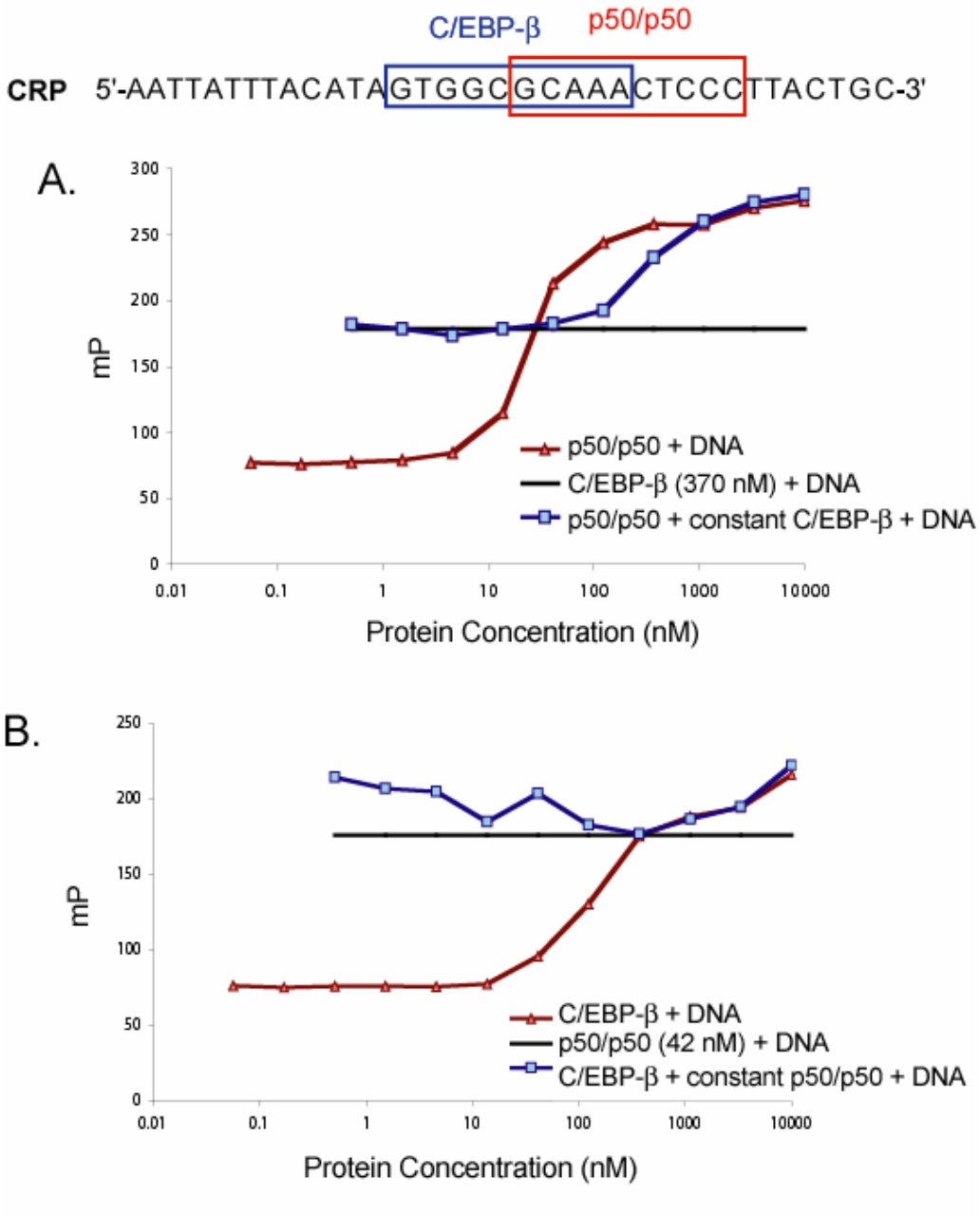

Figure 4-10. *Fluorescence anisotropy assays of non-cooperative binding of C/EBPβ DBD and p50 homodimer.* Milli-Polarization units are plotted against concentration of protein A.) C/EBP-β DBD concentration was held constant (black line), titrated amounts of p50/p50 and CRP DNA(blue line), constant amount of CRP DNA (200 pM) was added to constant C/EBPβ DBD and titrated p50/p50 (red line). B.) The reciprocal experiment as in "A" (constant p50/p50 (black line) with titrated amounts of C/EBPβ DBD (blue line) and DNA (red line).

Binding experiments were repeated using EMSA. First, the affinities of p50 homodimer and C/EBPβ DBD for CRP were measured independently and the results showed similar K_D values as determined with FAA. The complex was found to aggregate at high protein concentrations (Figure 4-11). Therefore, the concentration of C/EBPβ DBD and p50 homodimer used for DNA saturation was 850 nM and 188 nM, respectively. EMSA was then used to determine the interaction between C/EBPβ DBD and p50 homodimer. When a saturating amount of C/EBPβ DBD (850 nM) was added, no improvement in p50 binding to DNA was observed by EMSA (Figure 4-12). Similar to what was observed previously using FAA, the binding for CRP was mutually exclusive. In the reverse experiment, where constant amounts of saturating p50 was added to the C/EBPβ DBD DNA reactions, there was no change in C/EBPβ binding. At low concentrations of C/EBPβ, only p50 homodimer/DNA complex is observed. At higher concentrations of C/EBPβ the p50/DNA complex is replaced by the C/EBPβ/DNA complex. This supports that the DNA binding events are mutually exclusive.

There is evidence in the literature that suggests transcriptional synergy between C/EBPβ and p65 (Friedl JBC 2002) and C/EBPβ and cRel exists (Kushner MI 2003). Therefore, the FAA cooperativity assay was repeated with p50/p65 heterodimer (kind gift from Frances Chen) and cRel/p50 heterodimer (kind gift from Chris Phelps) with C/EBPβ DBD. As demonstrated in figure 4-13, these results clearly showed that in all cases binding of NF-κB and C/EBPβ to CRP was mutually exclusive.

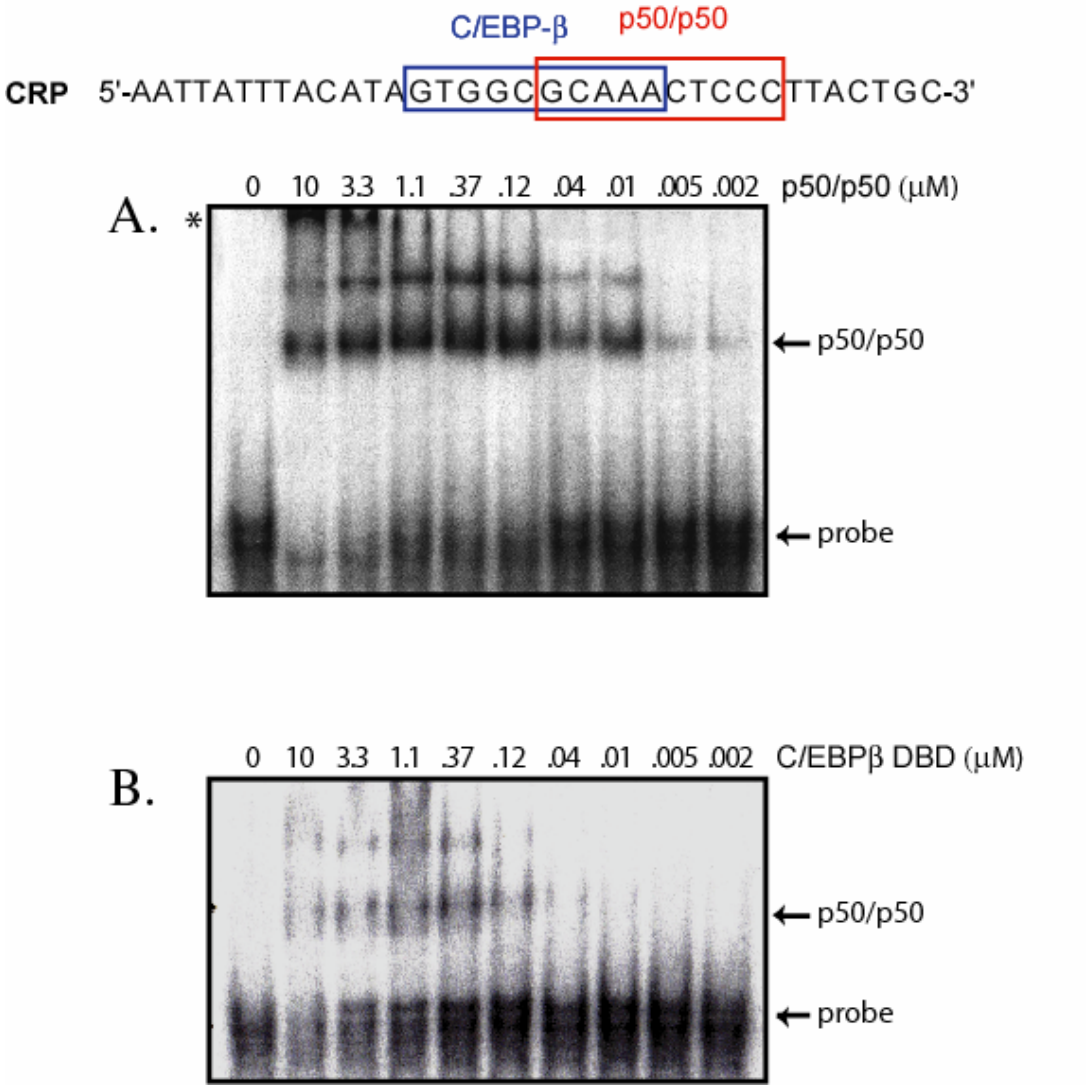

Figure 4-11. *Electrophoretic mobility shift assays of C/EBP-β DBD and p50 homodimer binding to CRP probe.* A.) p50 homodimer was titrated with constant amounts of CRP probe. B.) C/EBP-β DBD was titrated with constant amounts of CRP probe. Arrows indicate the location of the c-Rel dimer/DNA complex, CREB/DNA complex and free CRP probe. . "*" indicates aggregated protein bound to DNA.

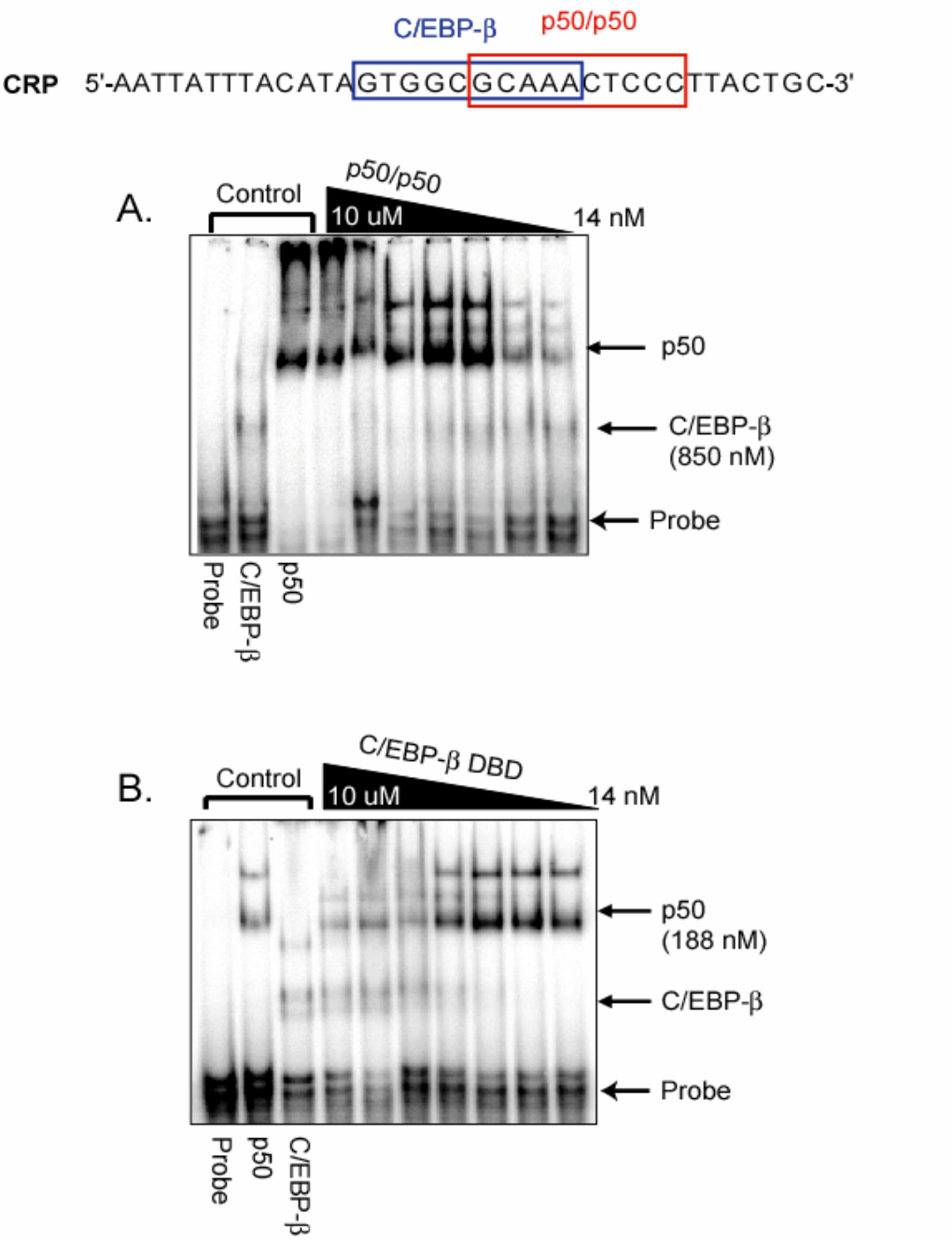

Figure 4-12. *Electrophoretic mobility shift assays of non-cooperative binding of C/EBPβ DBD and p50 homodimer.* A.) CRP and C/EBPβ DBD concentrations were held constant in each lane and titrated with decreasing p50 concentrations. B.) DNA and p50 homodimer concentrations were held constant in each lane and titrated with decreasing C/EBPβ DBD concentrations. Arrows indicate the location of the p50 homodimer/DNA complex, C/EBPβ/DNA complex and free probe (CRP promoter sequence). The * indicates DNA bound to aggregates of NFκB which occur at high protein concentration.

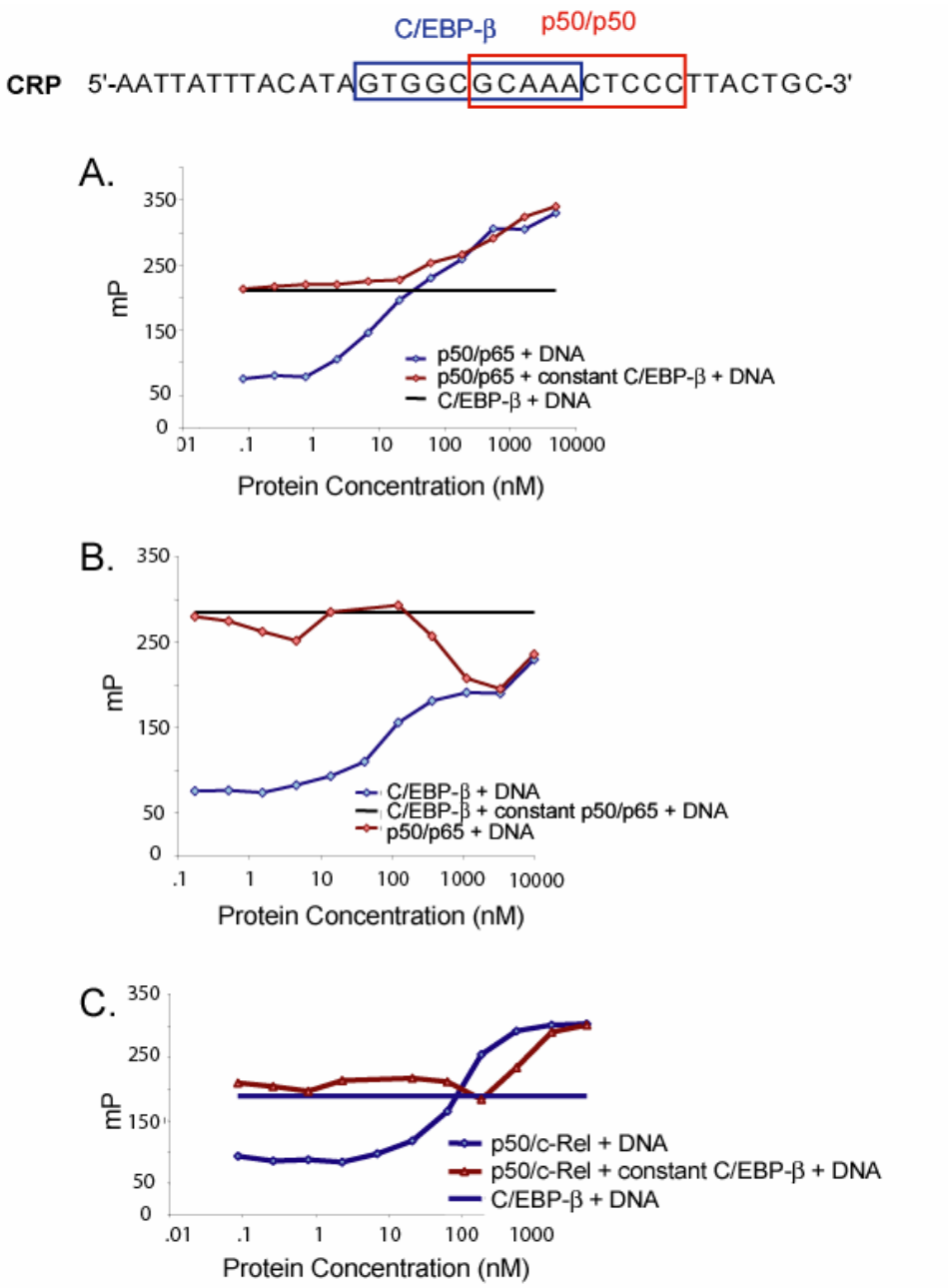

Figure 4-13. *Fluorescence anisotropy assays of non-cooperative binding of C/EBPβ DBD and p50/cRel or p50/p65.* Milli-Polarization units are plotted against concentration of protein A.) C/EBPβ DBD concentration was held constant (black line) and titrated amounts of p50/p65 and CRP DNA(blue line), constant amount of CRP DNA (200 pM) was added to constant C/EBPβ DBD and titrated p50/p65 (red line). B.) The reciprocal experiment as in "A" (constant p50/p65 (black line) with titrated amounts of C/EBPβ DBD (blue line) and DNA (red line). C.) C/EBPβ DBD concentration was held constant (black line) and titrated amounts of p50/cRel (blue line), constant amount of CRP DNA was added to constant C/EBPβ DBD and titrated p50/cRel (red line).

C. Discussion

In an effort to understand how NF-κB interacts with other activators on a promoter sequence where the binding sites are arranged tandemly, we have tested CREB and C/EBPβ. Synergistic transcriptional activation by NF-κB and C/EBPβ has been demonstrated for many target genes and most NF-κB subunits have been shown to act with C/EBPβ. There are only a few examples of such synergism between NF-κB and CREB, the most well studied of these genes is IL-2. It appears that CREB and cRel homodimer are able to co-occupy the DNA only under select conditions. When CREB (concentrations equal to the K_D) was added to increasing amounts of cRel, co-occupancy of the DNA occurred at low cRel concentrations. However, when cRel concentration is high, co-occupancy is abolished. In addition, even when the two factors co-occupy the DNA the binding is not cooperative. The EMSA and FAA experiments reveal that the binding of C/EBPβ and NF-κB to the CRP promoter is mutually exclusive under all conditions.

The apparent lack of cooperativity can be explained in several ways. One explanation is that these experiments were conducted with highly purified recombinant proteins purified from *E. coli* while all previous experiments were done with soluble cell extracts of endogenous or over expressed proteins. Therefore it is possible that the other putative components of the enhanceosome are required for stable assembly of the complex on the DNA which are present in cell extracts but absent in our experiments. It is also possible that the TAD of NF-κB or other regions

of CREB or C/EBPβ (other than their DBD) are required for the stable assembly of the enhanceasome complex.

However, none of the explanations mentioned above explain why the DNA binding domains of NF-κB and CREB or C/EBPβ should not co-occupy the DNA sites. Cooperativity precedes co-occupancy. That is, the two factors must first bind before they are engaged in supporting each other's binding. One possibility is that whereas one binds to DNA strongly, the other simply interacts with the DNA binding factor through protein-protein interaction. For example, p50 may bind to CRP strongly whereas C/EBPβ binds to p50. However, in that case too, a ternary complex must be formed. Perhaps, in that case the non-DBD portion of C/EBPβ is required for the protein-protein interaction. In other words, C/EBPβ might be functioning as a coactivator. Similarly, this may also be true for CREB and NF-κB.

V. RelB both Inhibits and Augments p100 Processing

A. Introduction

The dimeric NF-κB transcription factors are formed from five family members, p50 (NF-κB1), RelA (p65), p52 (NF-κB2), c-Rel, and RelB. These proteins share an approximately 300 residue long homologous region close to their N-termini. This element, referred to as the Rel Homology Region (RHR), is responsible for DNA binding, dimerization, inhibitor binding and nuclear localization. p50 and p52 are the processed products of precursor proteins, p105 and p100, respectively (Baldwin, 1996; Ghosh et al., 1998). NF-κB dimers that contain RelA, c-Rel and RelB have transcriptional activation potential. RelA and c-Rel homo- and heterodimers are tightly regulated by a class of inhibitor proteins, known as IκB, through the formation of stable IκB/NF-κB complexes that are unable to bind DNA. Activation of these dimers requires the degradation of IκB. A large number of stimuli, such as TNF-α and IL-1, activate IκB degradation through phosphorylation of IκB by IkappaB kinase (IKK) leading to ubiquitination and degradation of IκB by the 26S proteasome (Ghosh and Karin, 2002; Karin and Ben-Neriah, 2000). Signaling pathways leading to NF-κB activation through degradation of prototypical IκB proteins (IκBα, IκBβ and IκBε) are classified as the canonical pathways.

Many structures of the RHR have been solved and they reveal that the RHR forms two folded domains connected by a flexible linker, and contain a small unstructured segment containing the nuclear localization signal (NLS) at the C-terminus of the RHR (Chen et al., 1998a; Chen et al., 1998b; Cramer et al., 1997; Ghosh et al., 1995; Huang et al., 2003; Muller et al., 1995). Approximately 100 amino

acids of the C-terminal immunoglobulin (Ig) -like domain is wholly responsible for mediating dimer formation. As a consequence, this domain is commonly referred to as the dimerization domain (DD). All the NF-κB dimers activated through classical activation pathways exhibit a common mechanism of dimer formation where each monomer contributes symmetrical β-strand elements. These elements pack against each other to form a β-sheet dimer interface. The N-terminal domain of the RHR is primarily responsible for DNA binding. Each NF-κB subunit has a non-homologous extension at its N-terminus, ranging from 4 residues in c-Rel to 100 residues in RelB. The function of RelB's N-terminal extension, known as the leucine zipper (LZ) domain (due to the presence of a leucine-rich heptad repeat) is unknown (Ryseck et al., 1992). The LZ domain is not present in other NF-κB family members.

In many other respects, RelB is an unusual member of the NF-κB family. Prototypical IκB proteins do not regulate RelB-containing NF-κB dimers (Lernbecher et al., 1994; Solan et al., 2002). RelB homodimers do not have DNA binding activity, suggesting that unlike other members, RelB may not form a stable detectable homodimer *in vivo* (Ruben et al., 1992). The X-ray crystal structure of the RelB DD revealed an intertwined domain swapped arrangement of the two monomers, suggesting that this RelB domain-fold may be unstable and domain intertwining may be required for stabilization(Huang et al., 2005b). Biochemical experiments demonstrate that in unstimulated cells, RelB primarily associates with p100 and to a lesser extent with p50 (Solan et al., 2002). In induced cells the predominant RelB dimer is the RelB/p52 heterodimer. This stringent specificity for both the inhibited

complex (RelB/p100) and the transcriptionally active complex (RelB/p52 and RelB/p50) is unusual in the NF-κB family.

A distinct class of inducers such as LTβ, BAFF and CD40 activate the non-canonical pathways which result in the formation of the RelB/p52 heterodimer (Bonizzi et al., 2004; Claudio et al., 2002; Coope et al., 2002; Dejardin et al., 2002; Senftleben et al., 2001; Xiao et al., 2001b). The key event in the non-canonical pathways is the processing of p100 into p52 by the proteasome, which requires the activation of NF-κB inducing Kinase (NIK) and IKK1 (Figure 5-1)(Fong and Sun, 2002; Senftleben et al., 2001; Xiao et al., 2004; Xiao et al., 2001b). There is a close functional connection between components of the non-canonical pathway which are evident from shared phenotypes of mice strains deficient in several of the non-canonical pathway genes. Secondary lymphoid organ development and maintenance are defective in mice deficient in RelB, p52, LTβ, IKK1 or NIK (Franzoso et al., 1998; Fu and Chaplin, 1999; Weih et al., 2001; Yin et al., 2001). However, the precise mechanism of how the RelB/p52 heterodimer is formed is unknown. In particular, it is unclear if the RelB/p52 heterodimer arises directly from the pre-existing p100/RelB complex.

The present study aims to investigate the structural and functional relationship between RelB and p100/p52. Our genetic experiments reveal that the stability of the RelB protein stringently requires the presence of p100 or its processed product p52. Biochemical experiments demonstrate that the molecular basis for the stringent co-existence between RelB and p100 is due to a unique complex that involves all functional domains of each protein. These interactions are important for inhibition of

processing/degradation of p100 by RelB. The observations allow us to propose a model of how the non-canonical signaling pathways generate a transcriptionally active RelB/p52 heterodimer.

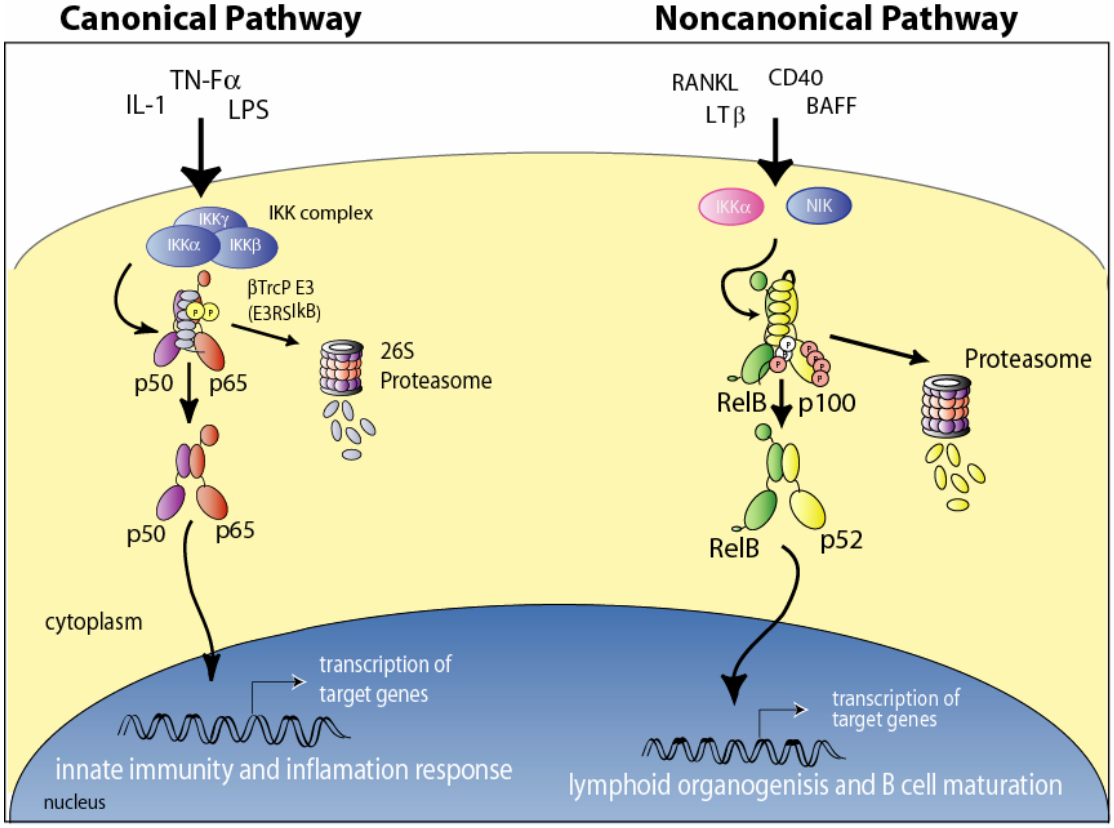

Figure 5-1. *Model of NF-κB activation.* The model depicts what is known about the canonical and non-canonical pathways, and their differences. The canonical pathway is activated by a number of inducers such as TNF, LPS and IL-1. This leads to the activation of the IKK complex and subsequent phosphorylation followed by ubiquitination and degradation of IκB. The NF-κB dimer then translocates to the nucleus. The non-canonical pathway is activated by a different set of inducers such at LTβ, BAFF and CD40. NIK and IKKα are activated and then phosphorylate p100 leading to its processing into p52 by the 26S proteasome.

B. Results

1. RelB is an unstable protein and is stabilized by p100/p52

To understand the biochemical relationship between RelB and p100 *in vivo*, we compared the steady state levels of RelB in wild type (wt), *nfkb1*$^{-/-}$, *nfkb2*$^{-/-}$ and *nfkb1*$^{-/-}$*/nfkb2*$^{-/-}$ mouse embryonic fibroblast (MEF) cells. Strikingly, RelB is almost absent in *nfkb1*$^{-/-}$*/nfkb2*$^{-/-}$ MEF cells (Fig. 5-2A, top panel, lane 2). To control for the integrity of the MEF cells, Immunoprecipitation (IP) experiments were done to demonstrate the association between RelB and p100 in MEF cells (Fig. 5-2B). We confirmed using RNase protection assay (RPA) that the level of RelB transcript in uninduced cells is not reduced in *nfkb1*$^{-/-}$*/nfkb2*$^{-/-}$ MEF cells compared to wt MEF cells. Therefore, p50 and p52 do not play an important role for the basal transcription of RelB. The mRNA level of RelB is increased in TNFα induced cells, which as described previously TNFa induces NFκB, therefore this confirms prior observations that RelB expression is induced by NFκB (Fig. 5-2C).

Although both *nfkb1*$^{-/-}$and *nfkb2*$^{-/-}$ MEF cells display a reduction in the levels of RelB, the level of p100 in *nfkb1*$^{-/-}$ is reduced compared to wild type. This indicates that basal p100 expression is regulated by p105/p50 (Figure 5-2A, middle panel, compare lanes 1 and 3). Thus the reduction of p100/p52 protein level appears to be the primary reason for reduced levels of RelB. Variation in RelB protein levels with p100 was further confirmed by stabily expressing transgenic RelB in *relb*$^{-/-}$ MEF cells. In these cells, levels of both RelB and p100 are higher than that in wt cells (Fig. 5-2A, compare lanes 1 and 6).

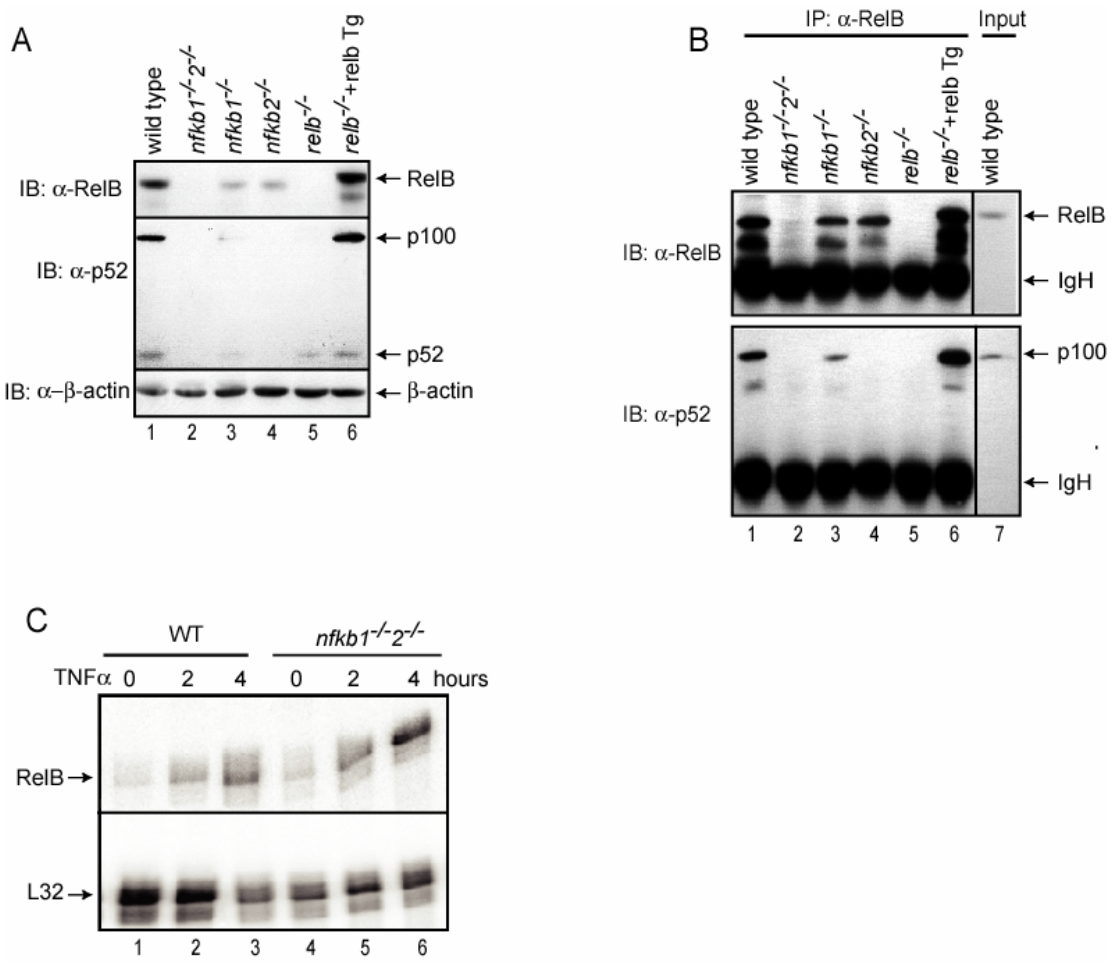

Figure 5-2. *Stability of RelB depends on the presence of p100 protein.* A.) Extracts of wild type, *nfkb1*$^{-/-}$, *nfkb2*$^{-/-}$, *nfkb1/nfkb2*$^{-/-/-/-}$, *relb*$^{-/-}$, and relb transgene (Tg) in *relb*$^{-/-}$ MEF cells were separated by SDS-PAGE followed by immunoblot with RelB antibody (Top panel), p52 antibody (middle panel) and β-actin antibody (Lower panel). B.) Cell extracts from the same cells as in 'A' were used to immunoprecipitate RelB-bound proteins using RelB antibody and the complexes were separated by SDS-PAGE followed by immunoblot with RelB antibody (Top panel) and p52 antibody (bottom panel). C.) RPA of RelB mRNA in wt and *nfkb1*$^{-/-}$*2*$^{-/-}$ MEF cells in resting and TNFα induced cells in the top panel and a control mRNA (ribosomal protein L32) in the bottom panel (Figure credit: Jeffrey Kearns and Alex Hoffmann).

These results suggest that in addition to other modes of regulation, RelB is also regulated at the protein level. RelB is an unstable protein whose stability requires the presence of p100/p52.

To understand why the p100/RelB complex is a preferred complex in the cytoplasm as compared to the p105/RelB complex we looked at the interaction between p105 and RelB. To test this, we qualitatively evaluated the affinity between the C-terminal domain (CTD) of p100 and RelB RHR/p52 complex. Pull down experiments revealed that the CTD (IκBδ) of p100 bound stably to the RelB RHR/p52 heterodimer (Fig. 5-3A). In addition, the CTD of p100 bound strongly to the p52 homodimer complex (Figure 5-3A, lane 9). To our surprise, the CTD (IκBγ) of p105 had no affinity for the RelB/p50 complex although it bound stoichiometrically to the p50 homodimer complex (Figure 5-3A, compare lanes 7 and 8). Although we do not know the relative affinities, these experiments suggest that the CTD of p100 binds both RelB/p52 heterodimer and p52 homodimer but RelB RHR repressed the ability of p50 to interact with the CTD of p105. To further test the lack of interaction of the CTD of p105 and RelB *in vivo,* we performed IP experiments using MEF cell extracts. RelB is unable to bind p105 (Figure 5-3B). These results give some understanding as to why p105 is unable to stabilize RelB and why p100/RelB is a preferred complex in the cytoplasm.

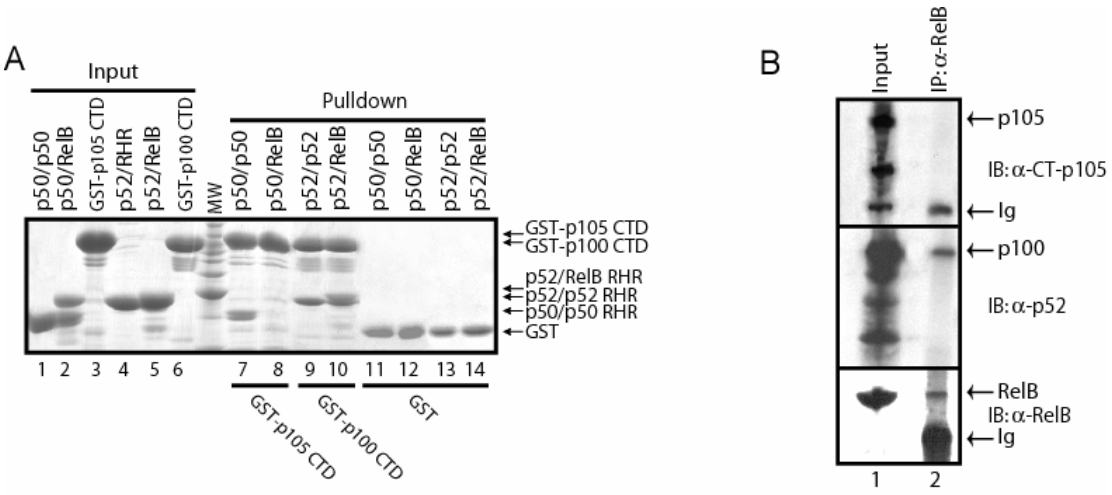

Figure 5-3. *p105 is unable to stabilize RelB due to its inability to interact with RelB.* A.) *In vitro* GST pull down experiments demonstrating the difference in the binding interaction between p100 CTD (IκBδ) and p105 CTD (IκBγ) with p52/RelB. Lane 8 demonstrates the lack of interaction of IκBγ with p50/RelB vs. the stable interaction between IκBδ and p52/RelB (lane 10). Lane 7 and 9 are positive controls of IκBγ interacting with p50 and IκBδ with p52, respectively. Lane 1-6 shows the inputs and lanes 11-14 show the controls. B.) Cell extract from MEF cells were used to immunoprecipitate RelB-bound proteins using RelB antibody and the complexes were separated by SDS-PAGE followed by immunoblot with RelB antibody (bottom panel) and p52 antibody (middle panel) and p50 (top panel).

2. RelB/p100 forms a unique complex in which all functional regions of p100 are involved

In stimulated cells, RelB associates with p52, the processed product of p100. This suggests that the stabilization of RelB in induced cells might also be conferred by p52. We wanted to investigate if and how p52 stabilizes RelB. We used a transient transfection system where a GFP-RelB RHR fusion protein was expressed alone, with Flag-p52 RHR or with Flag-p100 in HEK 293 cells. Western blot analysis revealed enhancement of RelB protein levels and a decrease in the amount of degradation products, when RelB is co-expressed with p52 or p100 compared to when RelB is expressed alone (Figure 5-4A, top panel, compare lanes 2, 3 and 4). In contrast, p52 RHR expresses as a stable protein irrespective of the presence or absence of RelB (Figure 5-4A, middle panel, compare lanes 4 and 9). This demonstrates that RelB instability is unique to NF-κB family members. We also tested the stability of RelB DD independently. As shown in figure 2A, GFP-RelB DD is also an unstable protein that gives rise to cleaved GFP. Similar to RelB RHR (in the presence of p100 or p52) the levels of RelB DD are enhanced. These observations led to the suggestion that RelB RHR is an unstable protein that can be stabilized by p52 RHR and p100.

Our qualitative *in vitro* experiments led to the same conclusion. In contrast to other NF-κB subunits, RelB RHR is difficult to purify from an *E. coli* expression system as it is continuously degraded during purification (Figure 5-4B, lane 3). The most likely explanation is that the folding stability of RelB RHR is weak, allowing *E. coli* proteases to cleave the unfolded regions of RelB RHR. However, when RelB RHR is co-folded with p52 RHR, a stable RelB/p52 RHR heterodimer is formed,

which is demonstrated by the fact that the complex can be further purified to homogeneity using an ion exchange chromatography step without any difficulty (Figure 5-4B and D). Intriguingly, our attempts to generate a heterodimer between RelB RHR and p52 DD were not successful; most of the RelB RHR remained free of p52 DD after refolding. This can be seen in the inability of RelB RHR to bind to the ion-exchange column and therefore comes out in the flow through of the column (Figure 5-4E, top panel, lane 3). Only a small amount of the complex could be generated, which remained susceptible to degradation (Figure 5-4E, top panel, lane 5). This suggests that the entire RHR of p52 is important for the stability of the RelB/p52 heterodimer and that the NTD (shown in figure 5-5) of p52 plays a role in stabilizing the RelB/p52 heterodimer. It was shown in our lab by Don Vu that the formation of the RelB/p50 heterodimer required the NTD of p50 (data not shown). In contrast, both the RelA/p50 RHR heterodimer and the RelA DD/p50 RHR heterodimer can be formed with equivalent efficiencies (Malek et al., 1998). Thus, the requirement of the NTD of p52 for stability of RelB appears to be unique to RelB. To further confirm the stabilization of RelB by p52, we reconstituted p52 in *nfkb2*$^{-/-}$ MEF cells. In these cells, RelB protein level is significantly higher than that in cells deficient in p100/p52 (Figure 5-4C, middle panel, compare lanes 2 and 3). These experiments demonstrate that RelB can be stabilized by p52 and p50, and that RelB has a unique interaction with p52 and p50 that requires their NTD.

Figure 5-4. *RelB RHR stability by p100 and p52.* A.) Western blot analysis of the steady state levels of RelB RHR and RelB DD proteins in HEK 293 cells transfected with Flag-p100, Flag-p52 and GFP-RelB in different combinations. In the presence of p100 and p52, RelB protein levels are enhanced. B.) Coomassie stained SDS-PAGE showing purity of p52/RelB heterodimer, p52 homodimer and RelB RHR homodimer. A lower concentration of p52/RelB heterodimer is shown in lane 4 to visualize the separation between the two proteins. RelB continuously degrades during purification and the degradation products are seen in the gel (lane 3). Aggregated species of RelB in lane 3 is marked by an "*". C.) Western blot analysis of the steady state levels of p100/p52 (top panel) and RelB (middle panel) in wt, *nfkb2*$^{-/-}$ MEF and p52-reconstituted *nfkb2*$^{-/-}$ cells. P52 Tg is larger than processed p52 because the construct used for p52 is larger than the processed product because the exact site of processing is unknown. D.) Co-refolded mixtures of RelB RHR and p52 RHR (red), and RelB RHR and p52 DD (blue) were separated by cation exchange (S-sepharose column) chromatography. E.) Coomassie stained SDS-PAGE samples from the S-column chromatography of the RelB RHR/p52 DD (top) and RelB RHR/p52 RHR (bottom). The load appears to contain excess p52, which masks the RelB RHR.

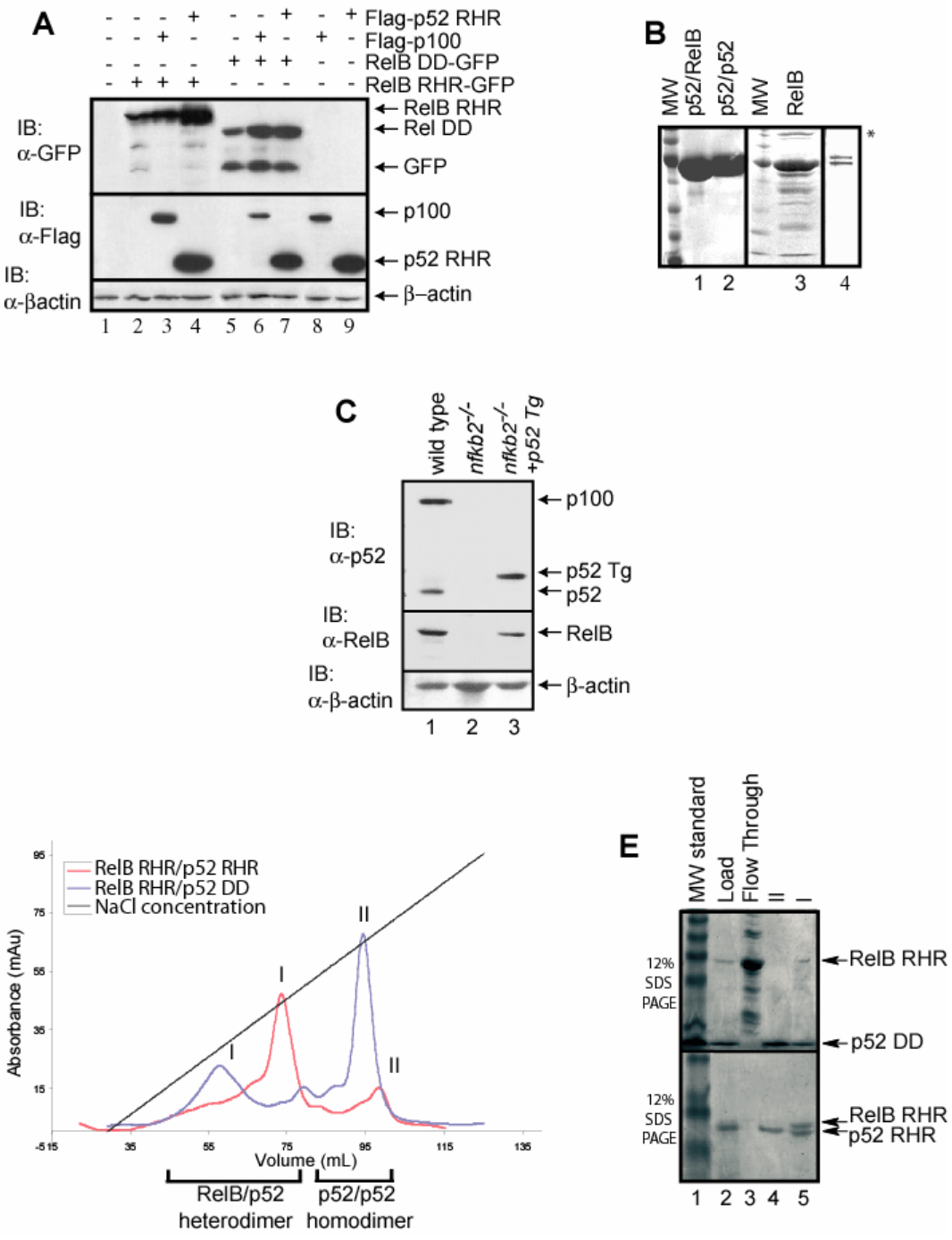
A
Flag-p52 RHR
Flag-p100
RelB DD-GFP
RelB RHR-GFP
IB: α-GFP
IB: α-Flag
IB: α-βactin
RelB RHR
Rel DD
GFP
p100
p52 RHR
β–actin
1 2 3 4 5 6 7 8 9
B
MW
p52/RelB
p52/p52
MW
RelB
*
1 2 3 4
C
wild type
nfkb2-/-
nfkb2-/- +p52 Tg
IB: α-p52
IB: α-RelB
IB: α-β-actin
p100
p52 Tg
p52
RelB
β-actin
1 2 3
D
RelB RHR/p52 RHR
RelB RHR/p52 DD
NaCl concentration
Absorbance (mAu)
Volume (mL)
I
II
RelB/p52 heterodimer
p52/p52 homodimer
E
MW standard
Load
Flow Through
II
I
12% SDS PAGE
RelB RHR
p52 DD
12% SDS PAGE
RelB RHR
p52 RHR
1 2 3 4 5

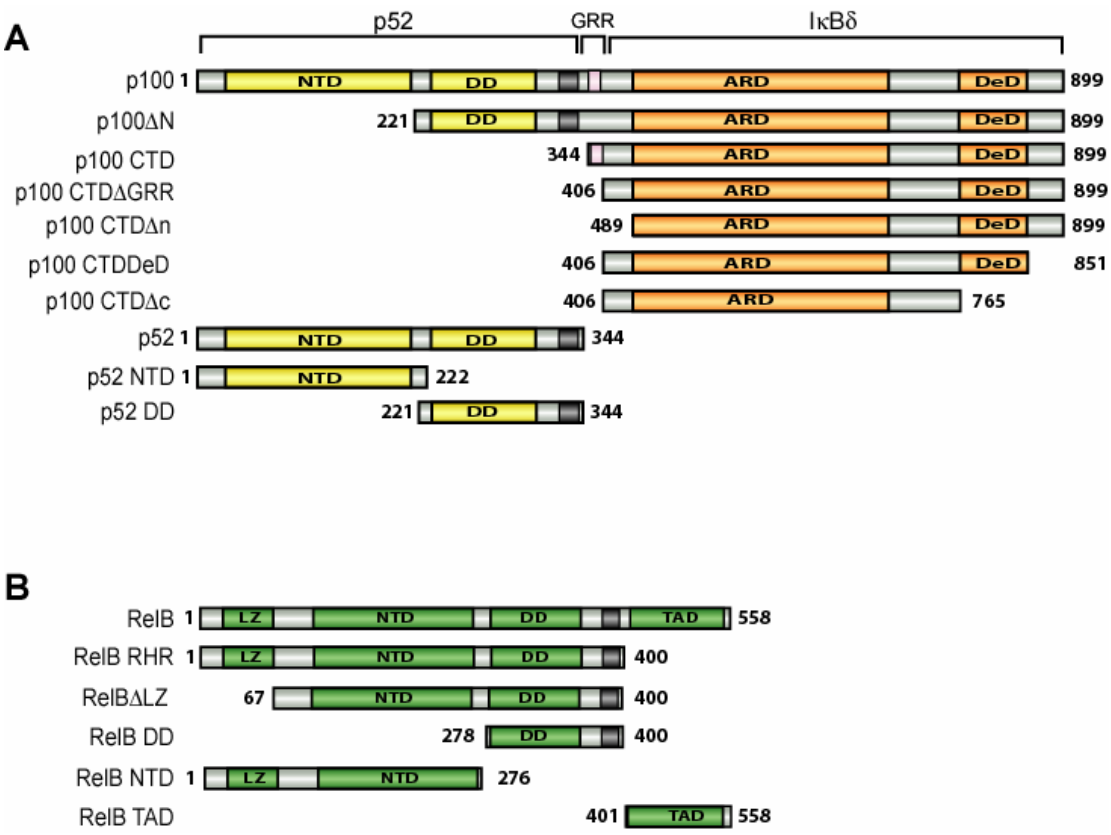

Figure 5-5. *Domain organization of p100 and RelB.* A.) Schematic representation of p100 and its deletion mutants. The dark grey and pink regions represent the nuclear localization signal and GRR region, respectively. B.) Schematic representation of RelB and its deletion mutants. The dark grey region represents the nuclear localization signal.

To understand the mechanism of the specific complex formation between RelB and p100, we investigated the role of each of the functional and structural domains of p100. p100 can be divided into five regions based on the known domain folds and/or functional importance; the NTD, DD and the flexible C-terminus (CTD, also known as IκBδ) which includes the glycine rich region (GRR), ankyrin repeat domain (ARD) and the death domain (DeD) (Figure 5-5A). To test if the NTD of p52 directly contacts RelB, GST pull down experiments were performed. *In vitro* pull down experiments revealed that GST-p52 NTD bound to RelB RHR (Figure 5-6A). Cell-based co-IP experiments from cell extracts expressing RelB as a GFP fusion protein and Flag tagged p52 also revealed that the NTD of p52 interacts with RelB RHR (Figure 5-6B). These results are consistent with earlier observations that the p52 NTD plays a role in stabilizing the RelB/p52 heterodimer. However, it should be noted that this interaction is weak, and the relevance of this weak contact perhaps is only appreciated in the context of the entire complex, where multiple weak contacts contribute to stabilize the native complex. Furthermore, this interaction appears to be specific to the RelB/p52 complex as no such interaction is observed in the p50/RelA complex (Figure 5-6C). To further confirm this we cotransfected p52 NTD-Flag and GFP-RelA into HEK 293 cells. As expected, RelA does not interact with the p52 NTD (Figure 5-6B, lane 4). In conclusion, our structural and biochemical experiments demonstrate that multiple segments/domains of p52, DD, and NTD, are involved in association with RelB. This is unique to the RelB/p52 complex as the RelA/p52 complex only engages the DD (Figure 5-6D).

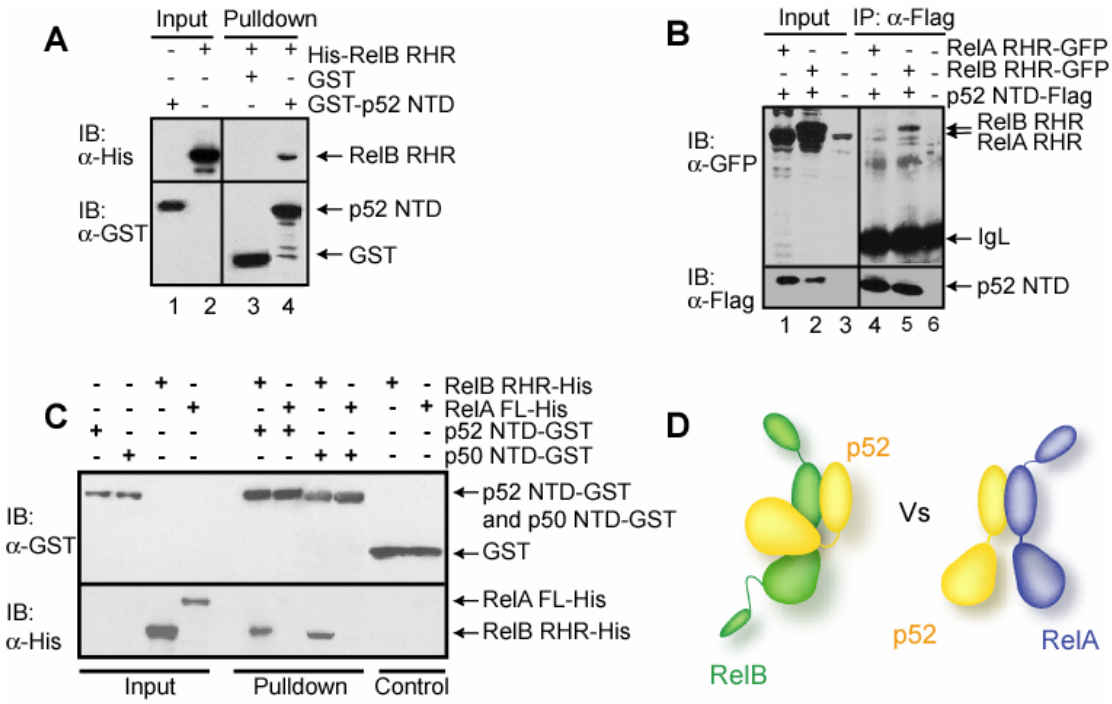

Figure 5-6. *Interaction of p52 NTD with RelB.* A.) Western blot analysis of *in vitro* GST pull down experiments demonstrating the binding interaction between the NTD of p52 and RelB RHR, followed by immunoblot with α-GST or α-His antibodies. B.) Co-IP experiments showing the interaction between p52 NTD-Flag and RelB RHR-GFP from the extracts of cotransfected HEK 293 cells. p52 NTD was isolated by IP and analyzed by IB (bottom panel) , and the co-precipitated RelB was analyzed by IB (top panel). C.) Western blot analysis of *in vitro* GST pull down experiments demonstrating no interaction between p50 NTD with p65. D.) Model of the interactions between RelB and p52 as compared to the interactions between p52 and RelA.

Previous studies have revealed a strong interaction between the CTD of p100 with the RelB/p52 heteordimer (Solan et al., 2002). However, the direct interaction of p100 CTD with RelB has not been studied. *In vitro* GST pulldown experiment were performed and demonstrate that the CTDΔGRR of p100 interacts with RelB RHR and RelB DD alone (Figure 5-7A). Their association has been further confirmed by co-IP using cell extracts where Flag-p100 CTD is expressed with either RelB RHR-GFP or RelB DD-GFP (Figure 5-7B). We next tested how the regions flanking the ARD of the CTD of p100 are involved in complex formation with RelB/p52 *in vitro*. Since the ARD portion of p100 apparently contributes to most of the binding affinity, we needed a more sensitive DNA binding inhibition assay to test this. Hence, we used pure recombinant p100 CTDΔGRR, p100 CTDΔn and p100 CTDΔc to test their ability to inhibit DNA binding of RelB/p52 complex in a solution based competition assay. Our results reveal that the removal of the N- and C-terminal regions reduced the inhibitory activity of the CTD, suggesting that in the context of p100 the entire CTD is involved in contacting the RelB/p52 sub-complex (Figure 5-7C). In all, our structural and biochemical experiments demonstrate that multiple segments/domains of p100 are involved in association with RelB (Figure 5-7D).

The observation that all functional regions of the CTD of p100 are involved in binding the p52/RelB heterodimer led us to investigate the difference between p100 CTD binding to p52 homodimer versus p100 CTD binding to the p52/RelB heterodimer. *E.coli* cell lysates expressing different GST tagged deletion mutants of p100 were used to pulldown either pure recombinant p52/p52 or p52/RelB RHR. These in vitro GST pull down experiments revealed that p100 CTD binds more

strongely to p52/RelB RHR than p52/p52 RHR (Figure 5-8A). It appears that the presence of the regions C-terminal to the ARD increase the difference between binding to p52 homodimer versus the p52/RelB heterodimer (Figure 5-8A, compare lanes 6 and 7 with 10 and 11). This suggests that the regions flanking the ARD are important for complex formation with p52/RelB. To further confirm that the p100 CTD binds more strongely to p52/RelB than p52 homodimer we used pure recombinant p100 CTDΔGRR to test its ability to inhibit DNA binding of RelB/p52 and p52/p52 complexes in a solution based competition assay. Our results reveal that p100 CTD does indeed bind more strongely to the p52/RelB complex (Figure 5-8B). In all, our experiments demonstrate that the multiple segments/domains of p100 involved in association with RelB render a strong interaction between the CTD of p100 with the RelB/p52 dimer.

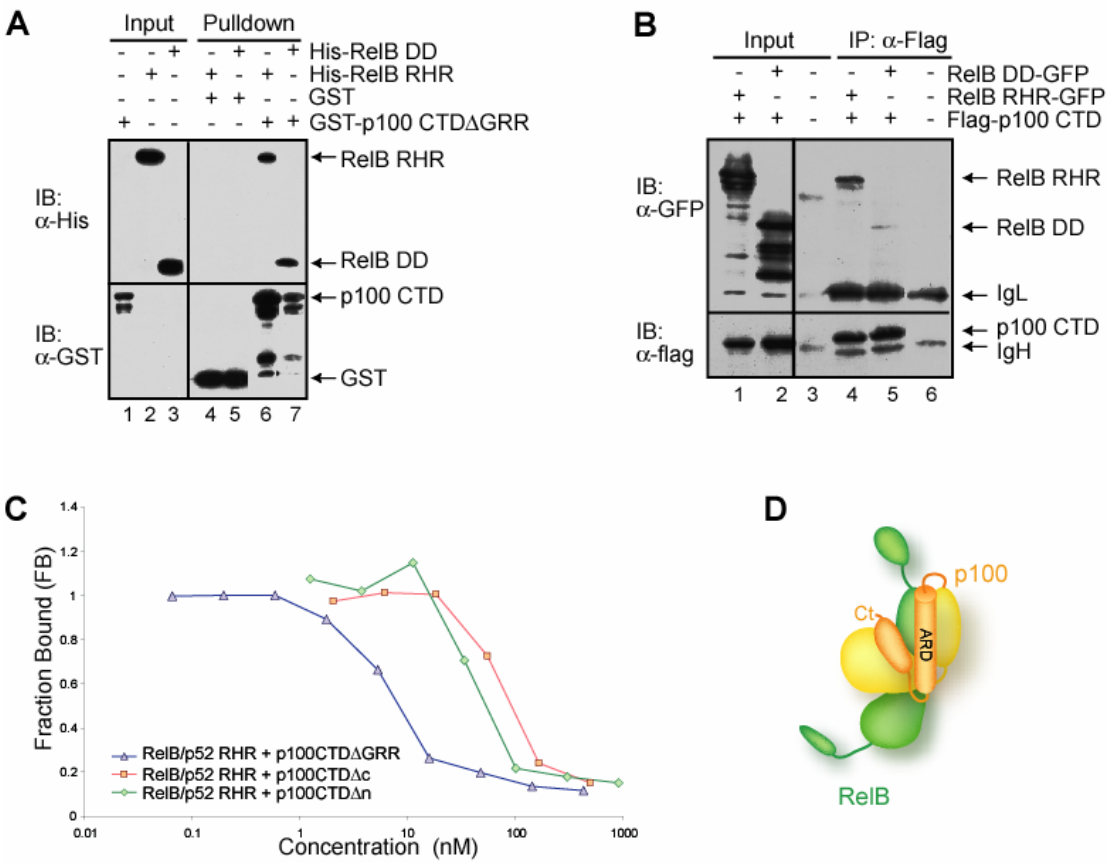

Figure 5-7. *Interactions of p100 CTD with RelB.* A.)Western blot analysis of *in vitro* GST-pull down experiments showing binding interaction between the GST tagged CTD of p100 and His-RelB RHR and His-RelB DD. B.) Co-IP experiments showing the binding interaction between the Flag tagged CTD of p100 and RelB RHR-GFP and RelB DD-GFP. These experiments were done similarly as described in figure 3-6. C.) Fluorescence polarization (FP) assays showing the effect of the regions flanking the ARD of p100 in inhibition of DNA binding by the RelB/p52 heterodimer. Constant amounts of RelB RHR/p52 bound to a fluorescently labeled DNA was titrated with increasing amounts of GST-p100 CTD proteins. Fraction protein bound is plotted against the concentration of p100 deletion mutants. D.) Model of the interactions observed for p100 in the RelB/p100 complex.

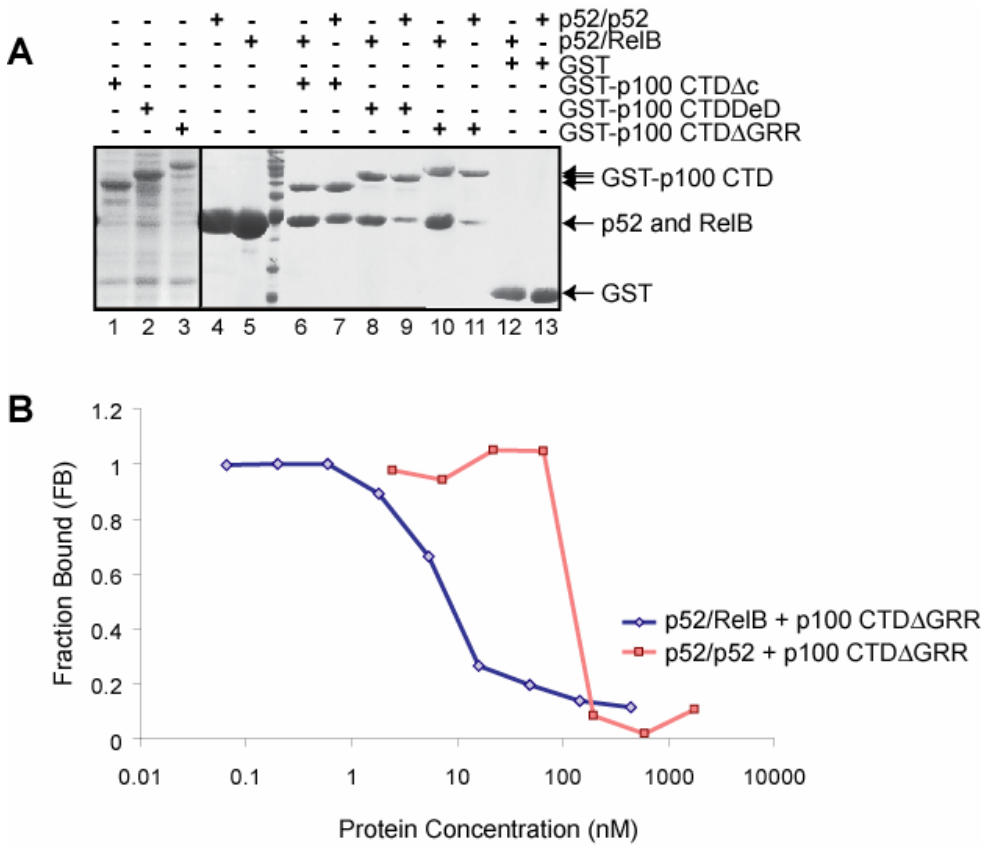

Figure 5-8. *p100 CTD interacts stronger with p52/RelB than p52/p52.* A.) Coomassie stain of *in vitro* GST pull down experiments demonstrating the difference in binding between p52 homodimer and p52/RelB heterodimer. Lanes 1-3 are cell lysate inputs of the *E. coli* expressed p100 deletion mutants. Lanes 4 and 5 are inputs of the pure recombinant p52/p52 and p52/RelB, respectively. B.) Fluorescence polarization (FP) assay showing the effect of p100 CTD in inhibition of DNA binding by the RelB/p52 heterodimer vs. p52/p52 homodimer. Constant amounts of RelB RHR/p52 or p52/p52 bound to a fluorescently labeled DNA was titrated with increasing amounts of GST-p100 CTDΔGRR.

3. RelB/p100 complex engages all domains of RelB

We next wished to examine how each of the RelB structural and functional domains is involved in the p100/RelB complex formation. RelB can be divided into three regions; NTD, DD and the transcriptional activation domain (TAD). The NTD of RelB is longer than other NF-κB proteins as it contains a 100 residue long LZ segment at the N-terminus (Figure 5-5B). As described above for p100, we have tested binding interactions by two ways; GST pulldowns using pure proteins *in vitro* and co-IP of proteins expressed in transiently transfected HEK 293 cells. RelB NTD was coexpressed with p100, p100ΔN and p52 in HEK 293 cells. IP confirmed that the RelB NTD associated with p100 but not with p52 or p100ΔN (Figure 5-9A). This indicates that the entire p100/RelB complex is important for this interaction.

As indicated earlier, the NTD of RelB has a 100 residue long LZ domain whose function has not yet been clarified. The presence of a cryptic thrombin cleavage site at residue 67 of RelB allowed us to remove the first 67 residues by thrombin treatment, then test the role of this region in p100 CTD binding. GST co-precipitation experiments using pure recombinant proteins revealed a drastic reduction in the binding interaction of the truncated RelB/p52 heterodimer for p100 CTD (Figure 5-9B, compare lanes 4 and 5). We further confirmed the role of the LZ domain using a fluorescence-based DNA binding inhibition assay. This assay revealed that the presence of the N-terminal 67 residues of RelB is essential for the CTD of p100 to efficiently inhibit the DNA binding of the heterodimer (Figure 5-9C).

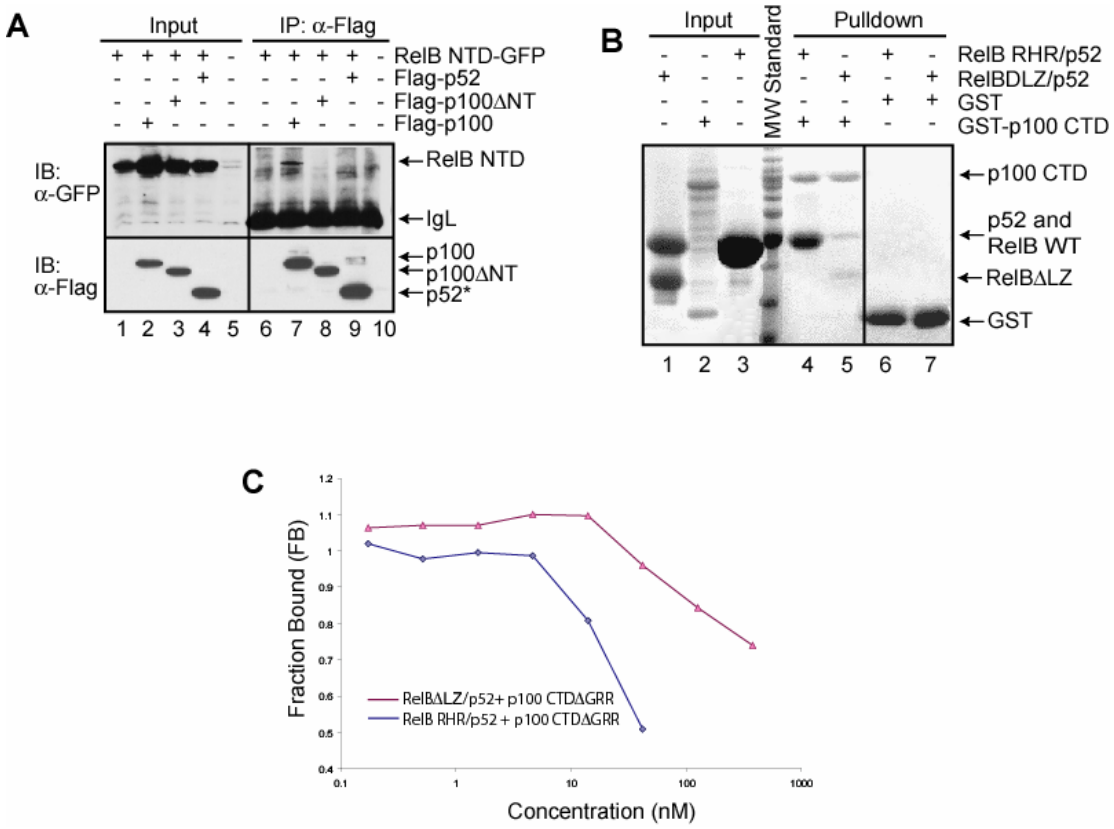

Figure 5-9. *Interactions of RelB NTD with p100.* A.) Co-IP experiments showing binding interaction between RelB NTD-GFP and wt or deletion mutants of p100 with the Flag peptide. Cells were cotransfected with GFP-RelB NTD and p100 mutants, extracts were IP-ed by α-Flag antibody and immunoblotted with Flag (bottom panel) and GFP (top panel). B.) *In vitro* GST pulldown experiments were done using equal amounts of pure recombinant proteins showing that the N-terminal LZ domain of RelB is involved in the binding interaction with the CTD of p100. Input and pull down samples were separated by SDS-PAGE followed by Coomassie staining. Please note that His-RelB RHR and p52 RHR co-migrate in the SDS-PAGE (lanes 3 & 4). At position 67 of RelB a cryptic thrombin cleavage site is located (lanes 1 & 5). C.) FP experiments showing the functional role of the LZ domain of RelB in binding the p100 CTDΔGRR. FP assay was done the same as in Figure 5-8.

We next tested the role of the RelB TAD in p100 binding. GST co-precipitation experiments showed that p100 CTD interacts specifically with the TAD of RelB. Interestingly, the C-terminal 134 residues of p100, which contain the death domain plus the sites of induced phosphorylation, are not important for stable interaction with the TAD (Figure 5-10A, lane 7). In contrast, deletion of the segment N-terminal to the ARD abolishes binding (Figure 5-10A, lane 6). Co-IP experiments further confirmed *in vitro* binding interactions. The TAD of RelB is involved in complex formation with both wt p100 and the CTD (Figure 5-10B). However, the RelB TAD binds more weakly to p100 CTD than p100 (Fig. 5-10B, compare lanes 8 to 9). Therefore, it is possible that the GRR in the isolated CTD negatively affects binding. This idea is supported by strong binding interactions observed between the TAD of RelB and p100 CTDΔGRR. When the CTD was further deleted to the beginning of the ARD, no binding to RelB TAD was observed (Figure 5-10B, compare lanes 10, 19 and 20). We conclude that the TAD of RelB directly interacts with the processing region (PR) of p100 (the segment bracketing the GRR and ARD). RelA TAD does not show any binding interaction with p100 suggesting that RelB interacts with p100 in a unique manner (Figure 5-10C). In all, these results clearly demonstrate that all known functional segments/domains of RelB participate in the complex formation with p100. The interaction between RelB TAD and the site of processing of p100 suggest that RelB may play a role in p100 processing.

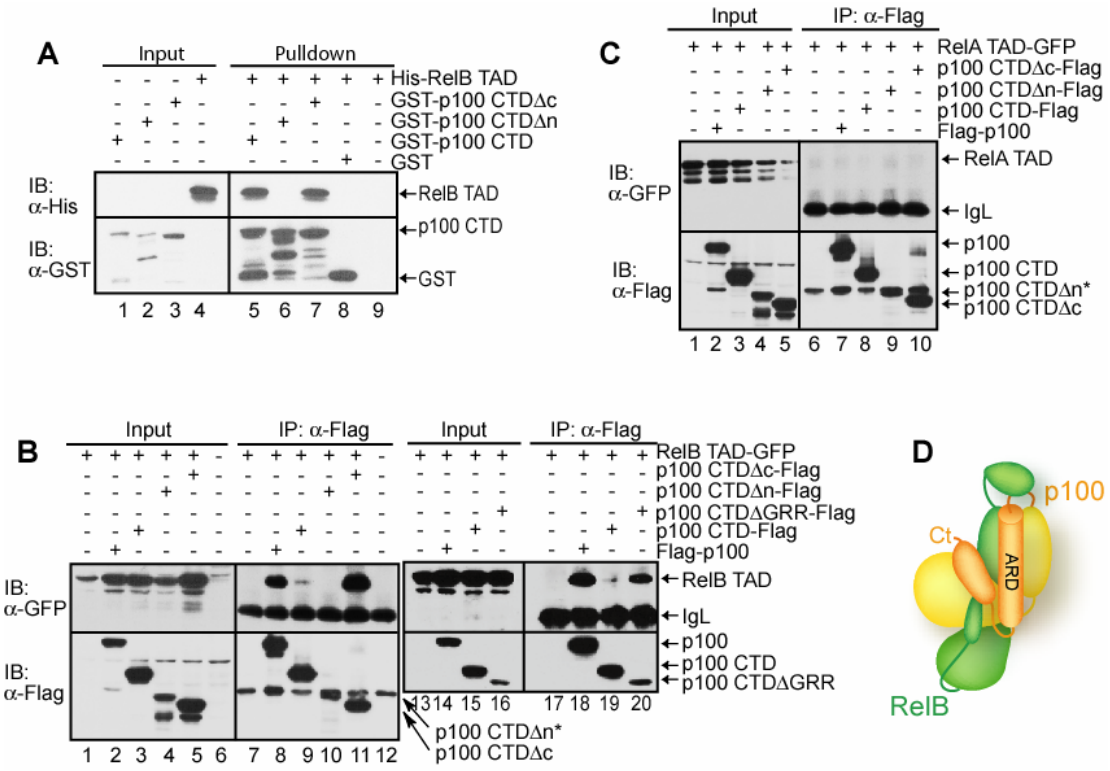

Figure 5-10. *Interactions of RelB TAD with p100.* A.) Western blot analysis of i*n vitro* GST pull down experiments showing the interaction between the TAD of RelB with the GST tagged CTD of p100. Input and pull down samples were separated by SDS-PAGE follwed by IB. B.) Co-IP showing the same interaction as in 'A' but in cotransfected HEK 293 cells. Flag-p100 or mutants were co-expressed with RelB TAD. IP-ed extracts were separated by SDS-PAGE and the presence of co-precipitated RelB was analyzed by IB (top panel). The levels of p100 and p100 CTD were analyzed by IB (bottom panel). RelB TAD interacts with p100 in the area between the GRR and ARD. D.) Model of the unique RelB/p100 complex engaging all functional domains and regions.

4. The dimerization domain of p52 induces reorganization of RelB/p52 heterodimer

The most important of all interactions required to stabilize both the RelB/p100 and RelB/p52 complexes presumably is the subunit association through the dimerization domains. Therefore, we looked at this interaction through structural analysis. The X-ray crystal structure of RelB DD revealed that it forms an intertwined dimer (Huang et al., 2005b). Domain swapping or intertwining occurs when a protein domain is relatively unstable. The intertwined nature of the RelB DD homodimer and stabilization of RelB in association with p52 prompted us to investigate whether the RelB/p52 heterodimer adopts any specialized conformation. The RelB DD/p52 DD heterodimer was crystallized by Don Vu and the X-ray structure was solved by Debin Huang in our lab. We observed that this heterodimer was not an intertwined dimer, and is similar to other NF-κB dimers where two β-sheets, one contributed by RelB DD and the other by p52 DD, stack onto each other (Figure 5-11A). It is interesting that the RelB DD subunit in the heterodimer is able to fold into an Ig-fold without requiring any intertwining. The key contacts across the subunit interface of RelB/p52 heterodimer are preserved compared to other NF-κB dimers. There are 10 residues from each subunit that make contacts across the subunit interface with Tyr300 of RelB and homologous Tyr247 of p52 placed at the center of the interface (Figure 5-11B).

The packing arrangement of dimers in the crystals revealed important features of the RelB DD surface. There are three dimers in the asymmetric unit and the packing is predominantly mediated by the close contacts of the RelB molecules (Fig 5-11C). A hydrophobic patch is present in RelB that is formed by residues V314, A324,

W320, F358, L362 and V366 and is involved in packing with the symmetrical face of another RelB molecule, which forms an apparently stable non-polar ring-like structure. These residues are RelB-specific, except for W320. Inside this non-polar ring there are three polar residues from each RelB molecule, E321, R323, and Q360, that form a total of six hydrogen bonds filling the center of the ring. In all, over 900 $Å^2$ exposed surface area is buried throughout this crystal packing. Residues in the hydrophobic patch are highly conserved among different species, implying a regulatory role for this unique surface (Figure 5-11D).

Figure 5-11. *Structure of the dimerization domains of p52/RelB.* A.) Ribbon diagram showing the structure of the RelB DD (red)/p52 DD (green) heterodimer. B.) The detailed interactions at the core of the RelB DD/p52 DD subunit interface. C.) The ribbon representation of the packing of RelB DD in the RelB DD/p52 DD heterodimer in crystals. The RelB DD subunit from two heterodimer molecules are packed closely together. Five hydrophobic residues of RelB DD are presented by space filling model. Polar residues and the hydrogen bonds are also shown. D). Sequence alignment of the DD of RelB from different species. Highlighted in blue are the conserved hydrophobic residues that are not found in p100, with the exception of W320. Highlighted in grey are the residues involved in dimerization.

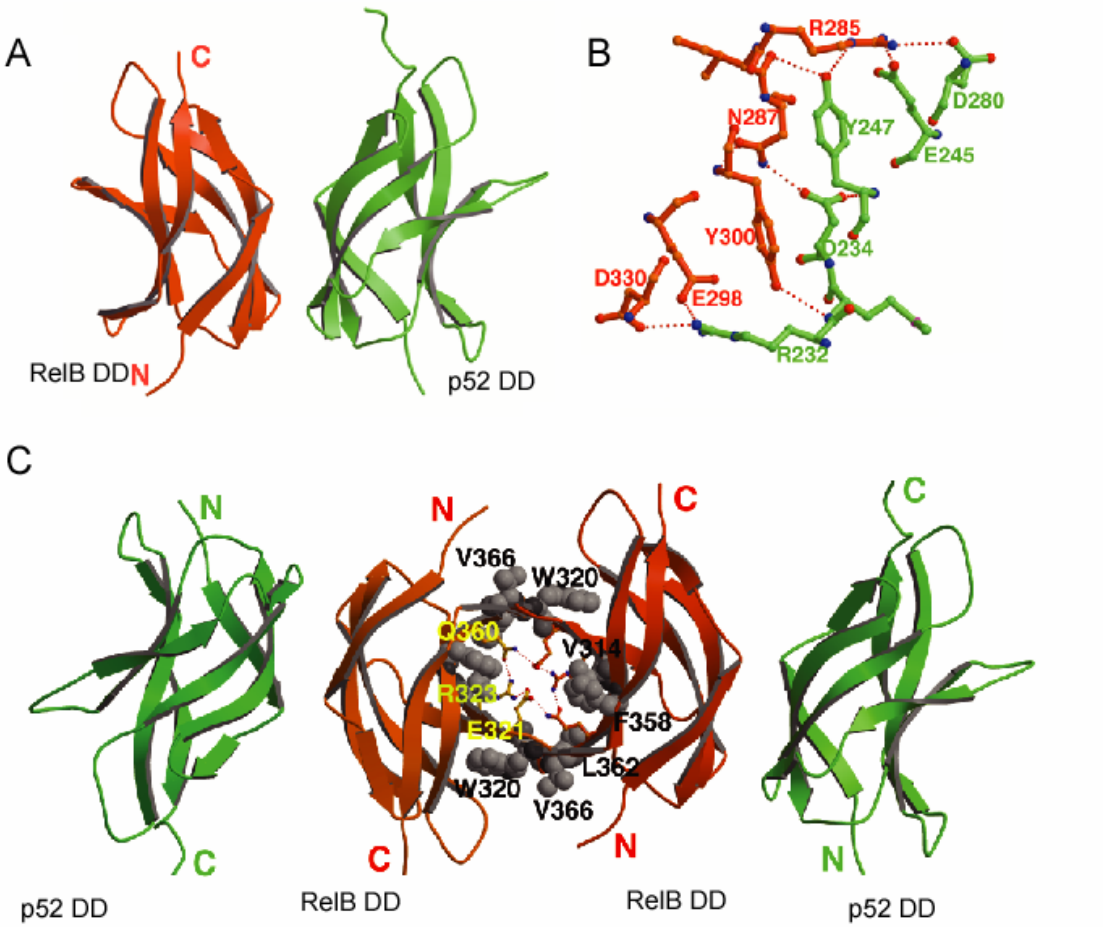

D

```
RelB mouse   TSELRICRINKESGPCTGGEELYLLCDKVQKEDISVVFSTAS---WEGRAD
  RelB cow   TSELRICRINKESGPCTGGEELYLLCDKVQKEDISVVFSRAS---WEGRAD
RelB human   TSELRICRINKESGPCTGGEELYLLCDKVQKEDISVVFSRAS---WEGRAD
RelB chicken TSELRICRMNKESGPCTGGEELYLLCDKVQKEDIAVVFRKEP---WEARAD
  RelB frog  TSELKISRMNKEYGRCEGGEEVYILCDKVQKEDILVIFGEDK---WEARAD
  p100 human ASNLKISRMDKTAGSVRGGDEVYLLCDKVQKDDIEVRFYEDDENGWQAFGD
```

```
RelB mouse   FSQADVHRQIAIVFKTPPYEDLEISEPVTVNVFLQRLTDGVCSEPLPFTYLPRD
  RelB cow   FSQADVHRQIAIVFKTPPYEDLEIVEPVTVNVFLQRLTDGVCSEPLPFTYLPRD
RelB human   FSQADVHRQIAIVFKTPPYEDLEIVEPVTVNVFLQRLTDGVCSEPLPFTYLPRD
RelB chicken FSQADVHRQGAIVLRTPPYRCVQLSEPVQVEVFLQRLTDRARSRGCPYTYLPRE
  RelB frog  FSQADVHRQIAIVLKTPPYHDLHITEPACVRVFLQRLTDGIRSEGMPFVYMPRV
  p100 human FSPTDVHKQYAIVFRTPPYHKMKIERPVTVFLQLKRKRGGDVSDSKQFTYYPLV
```

5. Mutations in RelB and p100 and their effect on the stabilization of the RelB/p100 complex

The unique relationship between p100 and RelB led us to test if destabilization of the p100/RelB complex affects p100 and/or RelB stability. I have generated two mutants of RelB and tested their ability to interact with p100 and p52. In one mutant we converted all five hydrophobic residues that make up the hydrophobic patch, observed in the RelB DD/p52 DD structure, into corresponding residues in p52 (RelB M5). The second mutant Y300 was mutated to alanine since the corresponding residue in p50 (Y267) significantly reduced p50 homodimer formation (Sengchanthalangsy et al., 1999). Before testing how the two mutants would affect stabilization, I used GST pulldown experiments to determine their effect on dimerization. As expected, GST pulldown experiments revealed that RelB Y300A DD was unable to form a dimer with p52 DD. The RelB M5 DD mutant also had a significant effect on dimerization, where very little, if any, RelB M5 DD/p52 DD complex was observed (Figure 5-12).

The M5 mutant was next tested to determine if it had an effect on the RelB/p52 complex. To test this, RelB RHR/p52 RHR heterodimers were allowed to form by refolding a mixture of purified denatured components followed by separation with cation exchange chromatography. Figure 5-13A shows the chromatographic behavior of the wt and M5 mutant heterodimers. Whereas the wt heterodimer eluted from the cation exchange column primarily in a single peak, the elution profile of refolded RelB M5/p52 RHR heterodimer was different; several peaks eluted, with the major peak being the p52 RHR homodimer. The components of the peaks were then

analyzed by SDS-PAGE, which revealed that in the case of RelB M5/p52 RHR heterodimer the majority of RelB was not involved in complex formation and was prone to aggregation. This was not the case for RelB/p52 RHR (Figure 5-13B). This suggests that the hydrophobic patch of RelB plays a role in forming the RelB/p52 RHR complex.

In addition to the RelB mutants, a p100 deletion mutant where the NTD was removed (p100ΔN), was also used to determine the effect on RelB stability. A transient transfection system was used to test the effect of the mutants on the stability of RelB and p100. GFP-RelB wt RHR and GFP-RelB M5 RHR fusion proteins were expressed alone, with Flag-p52 RHR, Flag-p100ΔN or with Flag-p100 in HEK 293 cells. Western blot analysis revealed enhancement of RelB protein levels and lesser amounts of degradation products for RelB wt than RelB M5 (Figure 5-13C, top panel, compare lanes 1 and 6 and 4 and 9). p100ΔN is able to be stabilized by and stabilize both wild type RelB and RelB M5 (Figure 5-13C, compare lanes 3, 8 and 17). We also tested the stability of RelB M5 DD independently to determine if the mutant affected the stability of the DD. As shown in figure 5-13C, RelB DD levels are enhanced and lesser amounts of degradation products are observed as compared to RelB M5 DD. It appeared that both RelB RHR M5 and DDM5 were still able to be stabilized by p100, as observed by the increased levels of RelB, however to a lesser extent than wild type RelB. It also appeared that p100 stability was affected by the presence of RelB (Figure 5-13C, compare lane 7 with 16). RelB M5 mutant also had an effect on the stability of p100 compared to wt. The RelB M5 mutant was not as efficient in stabilizing p100 (Figure 5-13C, compare lanes 7 with 2 and 14).

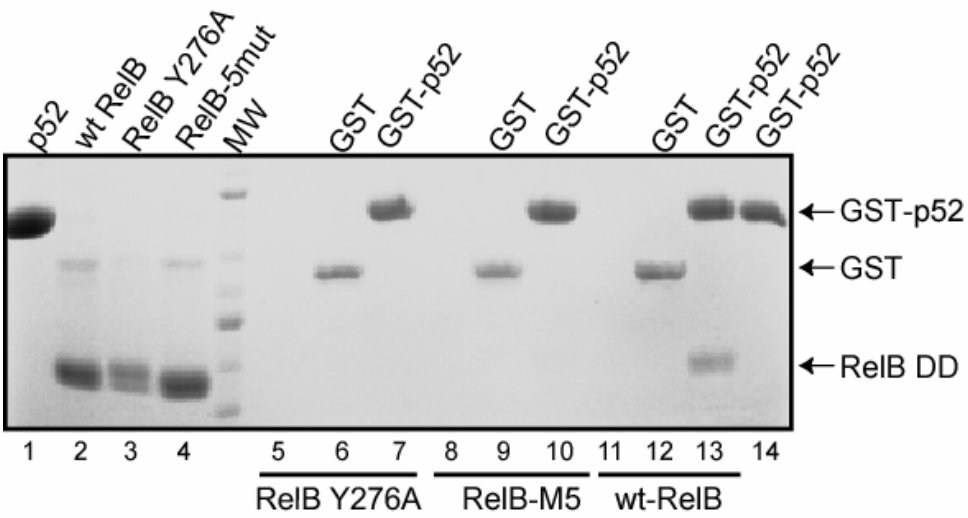

Figure 5-12. *Point mutations of RelB DD effect its dimerization with p52 DD. In vitro* GST pulldown experiments were done using equal amounts of pure recombinant proteins showing that the hydrophobic patch mutant (M5) has little if any dimerization with p52 DD. As expected, lB Y276A DD as expected does not form a dimer with p52 DD. Input and pull down samples were separated by SDS-PAGE followed by commassie staining.

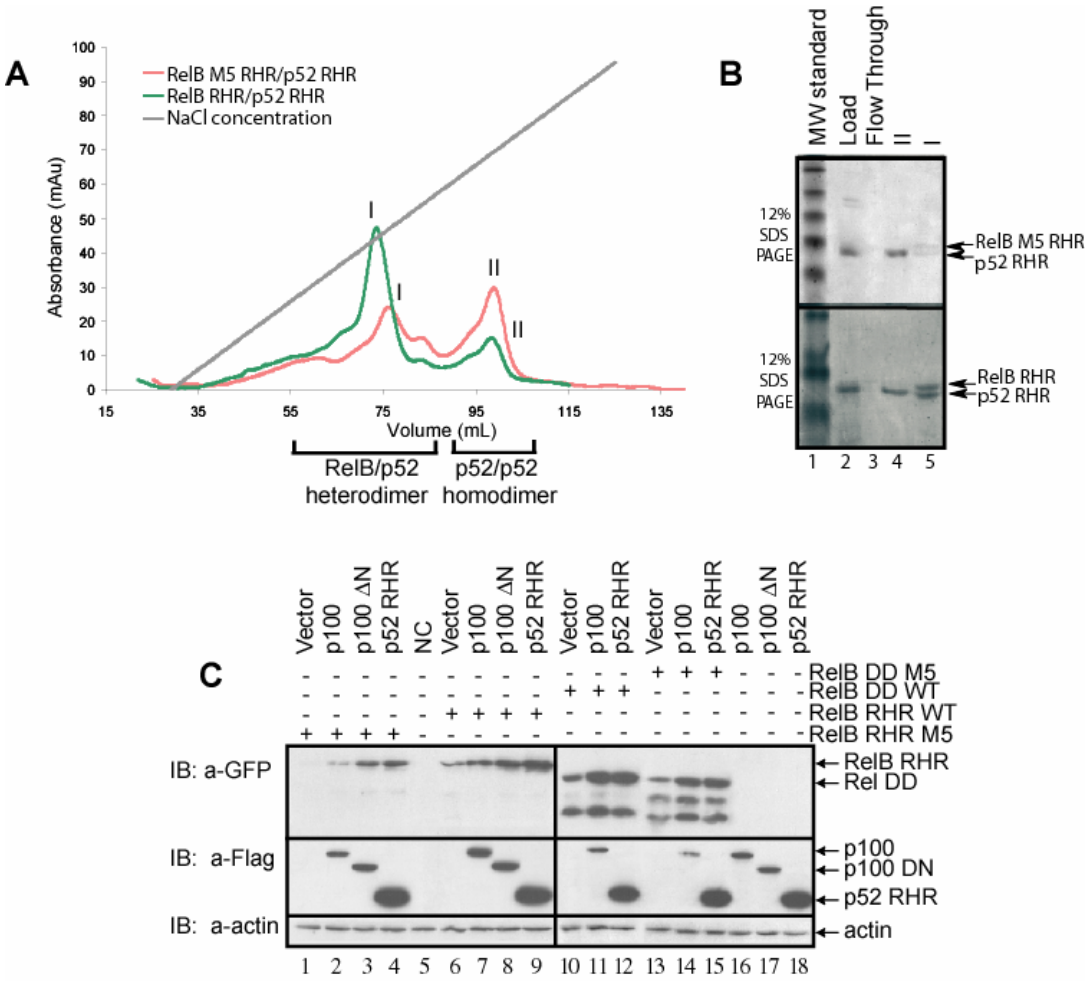

Figure 5-13. *Hydrophobic patch has an effect on RelB stability.* A.) Co-refolded mixtures of RelB RHR and p52 RHR (green), and RelB M5 RHR and p52 RHR (pink) were separated by cation exchange (S-sepharose column) chromatography. The amount of RelB M5/p52 complex formed is much less than wt RelB. B.) Coomassie stained SDS-PAGE of samples from the S-column chromatography of the RelB M5 RHR/p52 RHR (top) and RelB RHR/p52 RHR (bottom). The load appears to contain excess p52, which masks the RelB RHR. C.) Western blot analysis of the steady state levels of RelB wt and M5 RHR and RelB wt and M5 DD proteins in HEK 293 cells transfected with Flag-p100, Flag-p100ΔN, Flag-p52 and GFP-RelB in different combinations. In the presence of p100 and p52, RelB protein levels are enhanced. However, RelB M5 RHR and DD are more susceptible to degradation than wt.

6. RelB inhibits stimulus-dependent p100 degradation/processing

The results described above demonstrate a unique relationship between p100 and RelB, where all structural domains and flexible regions of each molecule play a role in complex formation. Whereas such extensive contacts might be required for RelB stabilization, it is unclear if p100 activity or processing, is affected when it remains bound to RelB. We wished to investigate whether RelB influences the degradation and/or processing of p100 both in resting and stimulated cells. First, we examined p100 processing in *relb*$^{-/-}$ MEF cells. Upon induction with α-LTβR, a significant increase of p52 level is observed over time with concomitant decrease of p100 (Figure 5-14A, top panel, lanes 1-5). The ratio of p52 to p100 in *relb*$^{-/-}$ cells is significantly increased at 24 hours of α-LTβR stimulation compared to that in wt cells (Figure 5-14B). These observations suggest that RelB is not essential for processing. We next tested how exogenous RelB affects p100 processing/degradation. We reconstituted wt *relb* in a *relb*$^{-/-}$ cell line and tested the effect of RelB protein in p100 processing. The most striking feature is that p100 is stabilized significantly in the reconstituted cells. Also, in both reconstituted and wt cells, processing is less efficient, compared to the processing seen in the *relb*$^{-/-}$ cells (Fig. 5-14A). In all, these experiments suggest that RelB inhibits p100 degradation in stimulated cells.

To further understand the dynamic mode of p100 processing we investigated the role of de novo p100 protein synthesis in the processing event. Wild type and *relb*$^{-/-}$ MEF cells were treated with an inhibitor of protein synthesis, cycloheximide, or cycloheximide + α-LTβR. As noted previously (Mordmuller et al., 2003) we also observe that processing is completely inhibited in the presence of cycloheximide with

no or little degradation of p100 (Figure 5-14C). However, in the presence of both cycloheximide and α-LTβR, p100 is degraded without any processing. Degradation of p100 suggests that the signaling pathway stimulated by LTβ remains intact, evident by degradation of p100 upon stimulation, even in the presence of cycloheximide. Therefore the lack of new p100 protein synthesis is responsible for the defect in processing in both wt and *relb*$^{-/-}$ MEF cells. However, the precise role that RelB plays in processing remains unclear.

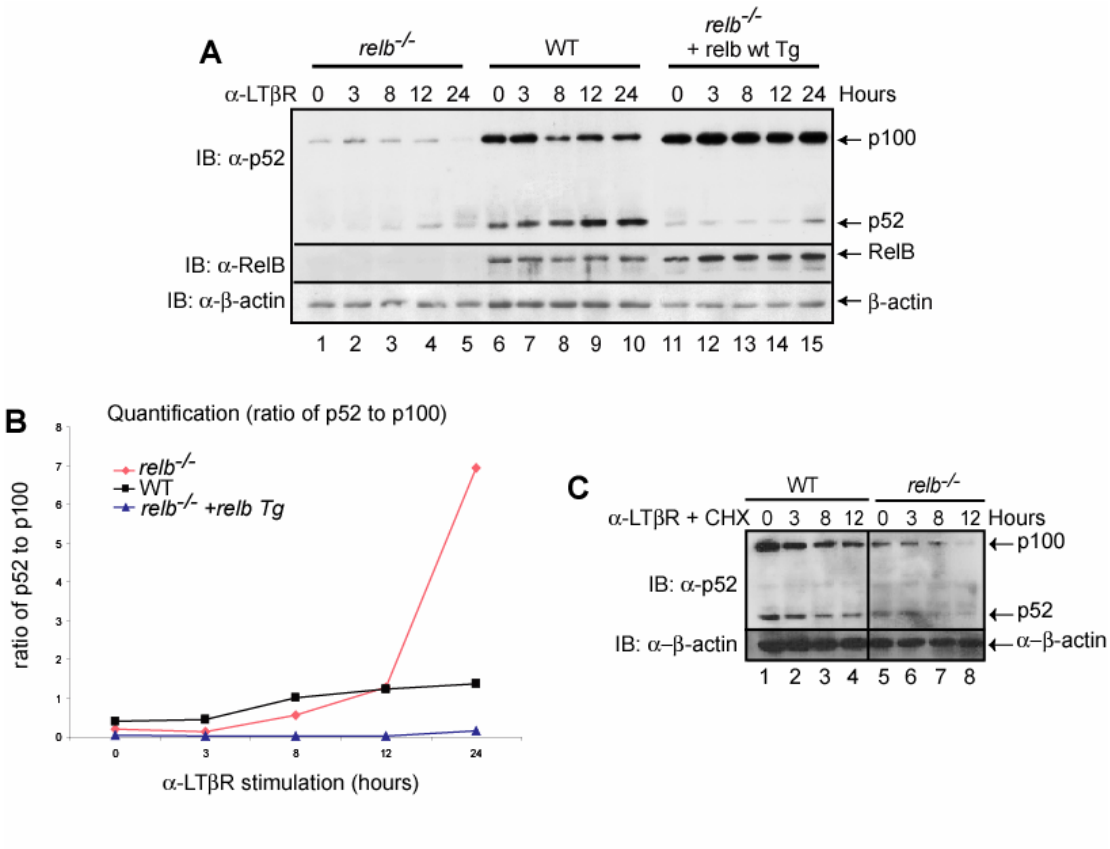

Figure 5-14. *RelB inhibits stimulus dependent p100 degradation*. A.) wt, *relb*$^{-/-}$, and *relb*$^{-/-}$ MEF cells with transgenic wt RelB were stimulated with α-LTβR for up to 24 hours and processing of p100 was observed by IB (top panel). The levels of RelB and β-actin (loading control) were analyzed by IB (middle and bottom panel, respectively). B.) Relative amounts of p52 to p100 in the cells are shown graphically. C.) wt and *relb*$^{-/-}$MEF cells were stimulated with α-LTβR in the presence of CHX for up to 12 hours and degradation with out the accumulation of p52 is observed by IB (top panel). β-actin (loading control) was analyzed by IB (bottom panel).

7. Processing of p100 is dependent on the stability of the p100/RelB and p52/RelB complexes

The two RelB mutants, RelB M5 and RelB Y300A, were then used to test the effect of destabilization of the p100/RelB complex. We generated MEF cell lines expressing these two mutants on *relb*$^{-/-}$ background and tested the processing of p100 through stimulation with α-LTβR. A small but reproducible enhancement of p100 processing was observed in RelB M5 reconstituted cells compared to wt RelB reconstituted cells (Figure 5-15A, top panel, compare lanes 1-5 with 6-10). This enhancement is more clearly seen in the quantification of the ratio between p52 and p100 (Fig. 5-15A, right panel). Little or no induced processing of p100 was observed in RelB Y300A cells compared to wt RelB reconstituted *relb*$^{-/-}$ MEF cells (Figure 5-15A, top panel, compare lanes 1-5 with 6-10). Twenty four hours after induction, we see a decrease in p100 and RelB levels indicating their complete degradation (Figure 5-15A, top and middle panel, lane 15). However, in unstimulated cells treated with CHX the levels of p100 remain constant over 32 hours (Figure 5-15B). This suggests that the significant reduction of p100 observed 24 hours after stimulation is signal induced. We also observe that the disappearance of p100 and p52 coincides with the loss of RelB, as seen in Figure 5-15A lane 15, which reconfirms our earlier conclusion that RelB stabilizes only in the presence of p100 and p52. The lower level of p100 protein in MEF cells devoid of RelB or expressing RelBY300A suggests that RelB may also play a role in p100 transcription. RPA experiments confirmed that notion (Figure 5-15D). To further test the observation of the lack of processing of p100 in the presence of the RelB Y300A mutant, we used transient transfection in HEK 293

cells. The effect of the RelB Y300A mutant was tested by co-transfection of p100 and RelB Y300A with or without NIK. It has been previously shown that over-expression of NIK is sufficient for p100 processing (Xiao et al., 2001b). The lack of p100 processing is also observed in the presence of NIK, from HEK 293 cells cotransfected with p100 and RelB Y300A (Figure 5-15C).

Immunoprecipitation experiments reveal that RelB M5 associates with both p100 and p52 similarly to wt RelB (Figure 5-16A and B). These observations suggest that the hydrophobic patch of RelB plays a small role in the binding interactions with p100/p52. Nevertheless, these observations suggest that even a minor defect in the assembly between p100 and RelB results in the modulation of p100 processing. Unlike the RelB M5 mutant, the RelB Y300A mutant does not bind p52 RHR (Figure 5-16C). This experiment confirms the conserved dimerization role of RelB Y300 (Figure 5-16D). To our surprise, p100 is able to bind to the RelB Y300A mutant. Multiple contacts between various domains in the p100/RelB complex reveal an unusual feature about it; weakening of any contact in the complex does not significantly reduce the affinity of the whole complex. However, the inability of RelB Y300A mutant to associate with p52 RHR following or simultaneous to its processing, the p100/RelB Y300A complex leads to the complete degradation of p100. These results clearly suggest that RelB protects p100 from complete degradation by forming a highly stable complex, and that dimerization of RelB/p52 is important for this protective mechanism. These observations suggest that the dimerization-defective RelB mutant sensitizes p100 to undergo complete degradation. Our results suggest

that RelB plays two roles; a role at the level of transcription and a role in protecting p100 from complete degradation and/or processing in induced cells.

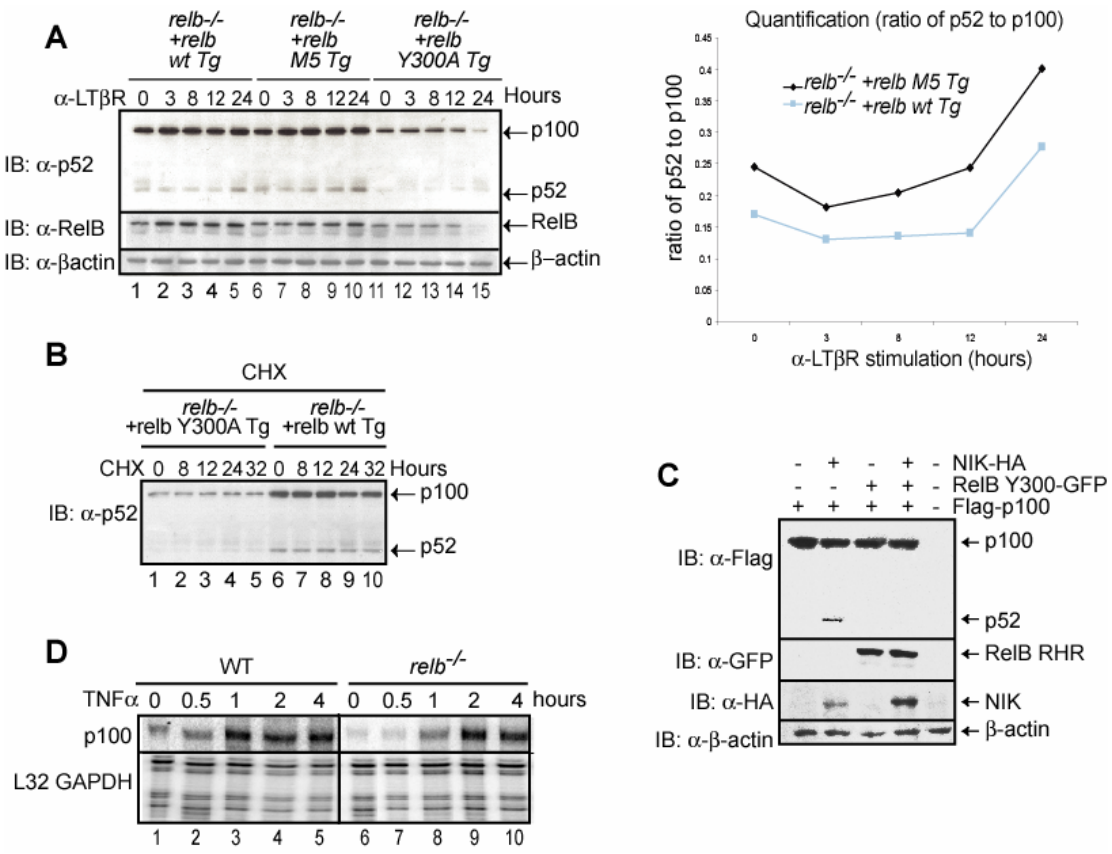

Figure 5-15. *Destabilization of p100 complexes affects its processing/degradation*. A.) Processing of p100 was monitored in MEF cells expressing two different mutants of RelB; RelB M5 and RelB Y300A. relb$^{-/-}$ MEF cells with transgenic wt, M5 and Y300A RelB were stimulated with α-LTβR for up to 24 hours and processing of p100 was observed by IB (top panel). The levels of RelB and β-actin (loading control) were analyzed by IB (middle and bottom panel, respectively). Relative amounts of p52 to p100 in the cells are shown graphically in the right panel. Complete degradation upon stimulation is observed in RelB Y300A MEF cells. B.) Stability of p100 was analyzed for wt and RelB Y300A expressing MEF cells in the presence of CHX for up to 32 hours. The level of p100 remained constant for up to 32 hours. C.) Processing of p100 was monitored in HEK 293 cells expressing p100 in the presence or absence of NIK and RelB Y300A. Processing was analyzed by IB (top panel). The levels of RelB, HA-NIK and β-actin (loading control) were analyzed by IB (middle two panels and bottom panel, respectively). D.) RPA of p100 mRNA in wt and *relb*$^{-/-}$ MEF cells in resting and TNFα induced cells in the top panel and a control mRNA (ribosomal protein L32 and GAPDH) in the bottom panel (Figure 5-15D credit: Jeffery Kearns and Alex Hoffmann).

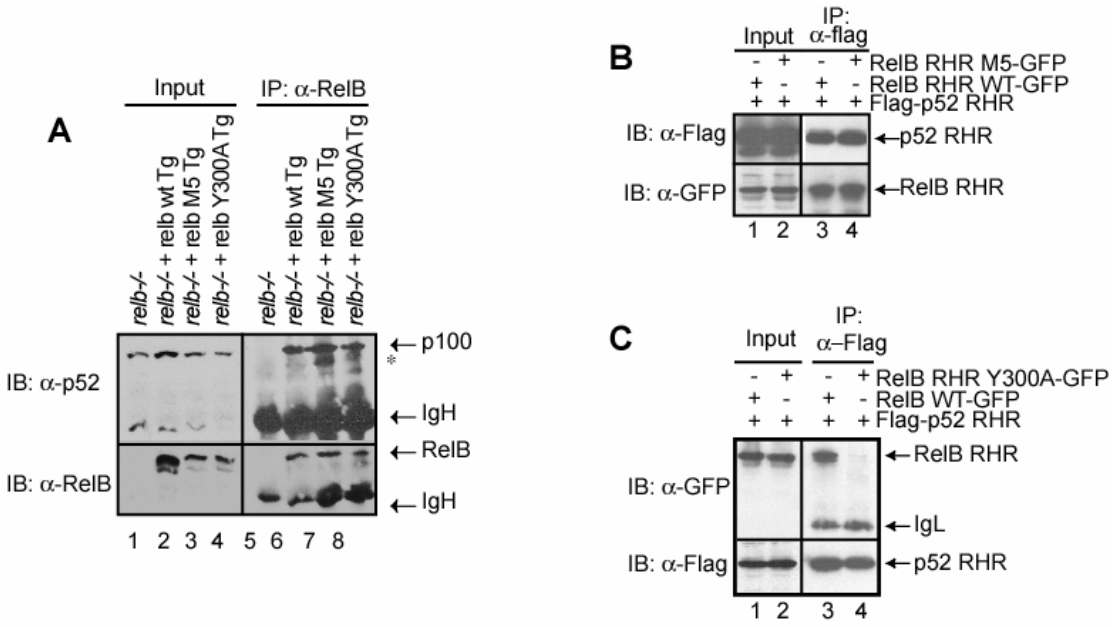

Figure 5-16. *Effect of destabilization of p100 complex on its processing.* A.) The binding interactions between p100 and RelB mutants were tested by Co-IP experiments using α-RelB antibody followed by IB with α-p52 (top panel) and α-RelB (bottom panel) antibodies. B.) Co-IP experiments were done to determine the binding of p52 RHR to RelB RHR wt and RelB M5 mutant using the extracts of HEK 293 cells transfected with Flag-p52 RHR and RelB RHR-GFP or RelB RHR M5-GFP. p52 was isolated by IP, and co-precipitated RelB was analyzed by IB (top panel). The level of p52 was analyzed by IB (bottom panel). C.) Co-IP experiments were done to determine the binding of p52 RHR to RelB RHR wt and RelB Y300A RHR mutant using the extracts of HEK 293 cells transfected with Flag-p52 RHR and RelB RHR-GFP or RelB Y300A RHR-GFP. p52 was isolated by IP, and co-precipitated RelB was analyzed by IB (top panel). The level of p52 was analyzed by IB (bottom panel).

To further elucidate the role of dimer formation by the processed product (p52) in the processing of p100, we reconstituted dimerization-defective p100 mutant in *nfkb2*$^{-/-}$ MEF cells. In this case, we mutated tyrosine at position 247 (homologous to RelB Y300) to an alanine in p100. This p52 mutant is unable to form a dimer with RelB, which may suggest that this mutant is severely defective in association with any NF-κB subunit including p52 (Figure 5-17B). However, like the apparently stable interaction between p100 and RelB Y300A mutant, p100 Y247A mutant is also able to bind to wt RelB (Figure 5-17C). In this case the processing defect is more severe than that observed for the RelBY300A mutant. Both basal and induced processing of p100 into p52 is abolished. In this case, the defect in basal processing is due to its inability to bind to any other NF-κB subunits. Furthermore, as observed previously, both p100 Y247A and RelB undergo complete degradation by 24 hours (Figure 5-17A). Our results demonstrate that that the processed product of p100 must be stabilized by dimerization with other NF-κB subunits, including RelB.

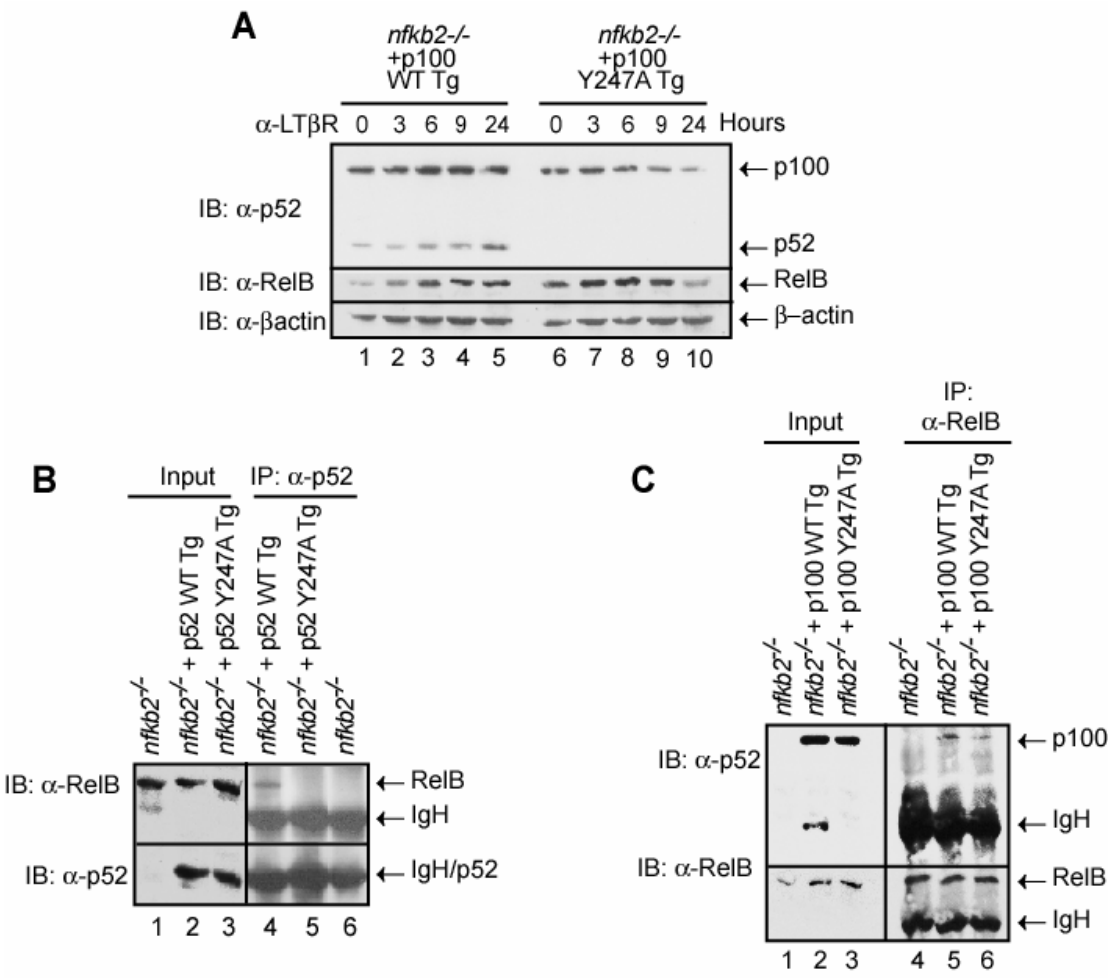

Figure 5-17. *Dimerization of p100 is required for processing.* A.) Effect of a dimerization defective p100 mutant on its processing. Stable MEF cells expressing p100 Y247A mutant in *nfkb2*$^{-/-}$ cells were treated with α-LTβR for up to 24 hours and processing was monitored by IB using α-p52 Ab (top panel). The levels of RelB were analyzed by IB (middle panel) and the loading control, β-actin, was analyzed by IB (bottom panel). B.) IP experiments to show the lack of binding between p52 Y247A and RelB. (G) IP experiments showing binding of p100 Y247A and RelB. IP's were done similarly to the IP described in figure 5-16.

8. RelB/p52 generation is coupled to the processing event

In order to further investigate the mechanism of processing and the role of RelB in processing, we next asked if p52 is generated from free p100 or if p100 must remain bound to non-RelB NF-κB subunits. To this end, we extended our investigation into two different types of MEF cells, one devoid of both RelA and RelB subunits (*rela*$^{-/-}$/*relb*$^{-/-}$) and the other devoid of all three transcription activation competent NF-κB subunits RelA, RelB and c-Rel (*relb*$^{-/-}$/*rela*$^{-/-}$/*c-rel*$^{-/-}$ triple knock out cells). Upon induction, processing is observed without any stabilization of p100 in *rela*$^{-/-}$/*relb*$^{-/-}$ cells (Figure 5-18A). This is consistent with the notion that wt RelB must be present to stabilize p100. In *relb*$^{-/-}$/*rela*$^{-/-}$/*c-rel*$^{-/-}$ cells p100 protein level is extremely low and the small amount that is present is completely degraded when cells are treated with α-LTβR (Figure 5-18C, lanes 6-10). This suggests that continuous synthesis of p100 is essential for processing and when all three transcription competent NF-κB subunits are absent no endogenous p100 is synthesized upon stimulation. We reconstituted p100 in *relb*$^{-/-}$/*rela*$^{-/-}$/*c-rel*$^{-/-}$ MEF cells where a heterologous promoter drives p100 transcription. In these cells, accumulation of only a small amount of p52 is observed in response to α-LTβR stimulation with the majority of p100 being completely degraded (Figure 5-18C, lanes 11-15). This clearly suggests that p52 can be processed solely from p100 in the absence of an interacting NF-κB subunit. We next tested processing in cells reconstituted with both p100 and RelB. Both p100 and p52 are stabilized in induced cells. These results suggest that p52 is generated from p100; however, the nascent p52 must be stabilized by

association through complex formation with other NF-κB subunits such as RelA, RelB and c-Rel (Figure 5-18). Taken together these observations indicate a novel dual function of RelB in both the protection of the precursor (p100) and the processed product (p52).

Observations in our lab by Olga Salvinova and a previous report showed that p100 is able to interact with non-RelB containing NF-κB dimers (Basak et al., 2006). We used *in vitro* GST pulldown experiments to look at the interaction between p100 and p65 in the presence or absence of RelB. GST pulldown experiments, using pure p52/p52 RHR, p52/RelB RHR, p65/p65 and GST-p100 CTDΔGRR, revealed that p65 homodimer has a weak affinity for GST-p100 CTD. However, in the presence of p52 homodimer, p65 is able to interact strongly with p100 CTD. It is likely that the p52 and p65 homodimers form a p52/p65 heterodimer that binds strongly to p100 CTD. In the presence of p52/RelB heterodimer, a weak interaction is observed for p65 with p100 CTD (Figure 5-20A). GST pulldowns with GST-p65 homodimer confirmed the dimerization between p65 and p52 (Figure 5-19B). When p100 CTD is in a complex with p52 homodimer, p65 is able to form a p100 CTD/p52/p65 complex. However when p100 CTD is complexed with p52/RelB heterodimer, p65 is unable to interact with any portion of the complex (Figure 5-19B, compare lanes 6 and 8). Full length p100 is also able to interact with GST-p65 (Figure 5-19B, lane 7). These observations support the previous reports that p100 is able to form a complex with non-RelB NF-κB dimers. Interestingly, when RelB is bound to p100 (or the CTD), p65 is no longer able to interact with p100. This supports our previous observations that the RelB/p100 complex is a highly stable complex that involves all functional domains and regions.

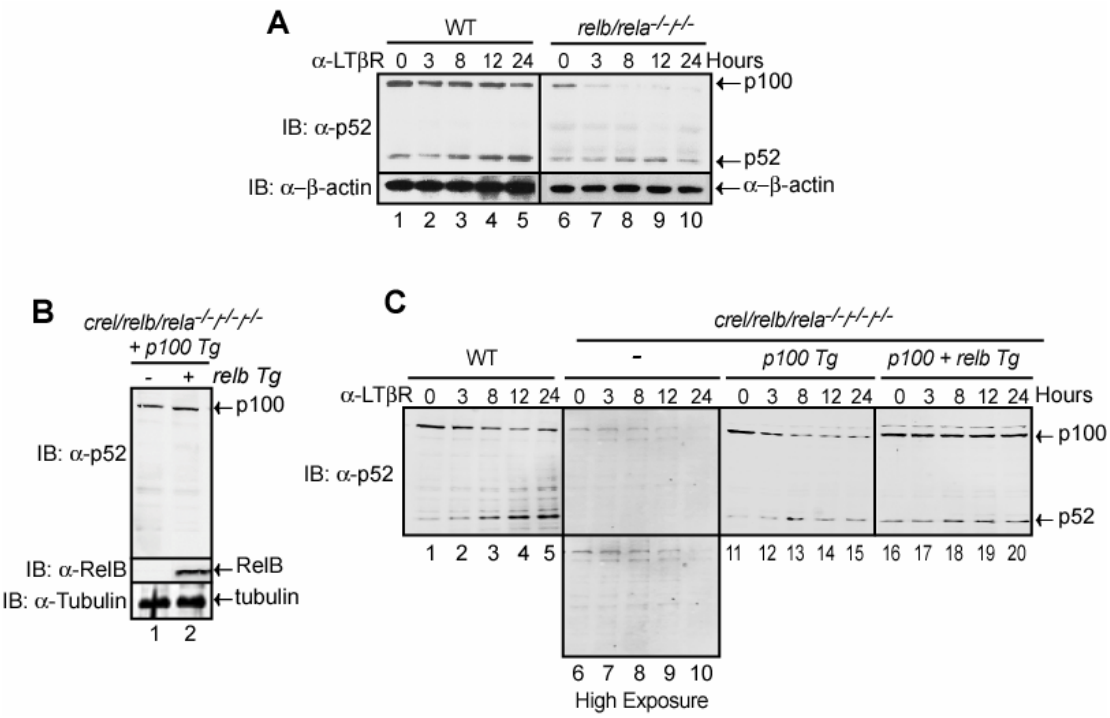

Figure 5-18. *The generation of RelB/p52 is coupled to the processing of p100.* A.) Wild type and *rela/relb*$^{-/-/-/-}$ MEF were stimulated with α-LTβR for up to 24 hours. Processing of p100 was observed by IB. B.) Loading control (α-tubulin) and RelB and p100 expression for Figure 5-18C are observed by IB. C.) *rela/relb/crel*$^{-/-/-/-/-}$ MEF cells and *rela/relb/crel*$^{-/-/-/-/-}$ MEF cells expressing p100 and p100 with RelB were stimulated with α-LTβR for 24 hours and processing of p100 is observed by IB. A higher exposure of *rela/relb/crel*$^{-/-/-/-/-}$ MEF cells upon stimulation is shown (bottom panel) due to the low expression of p100 in these cells. Figure 5-18A and B were done by Soumen Basak.

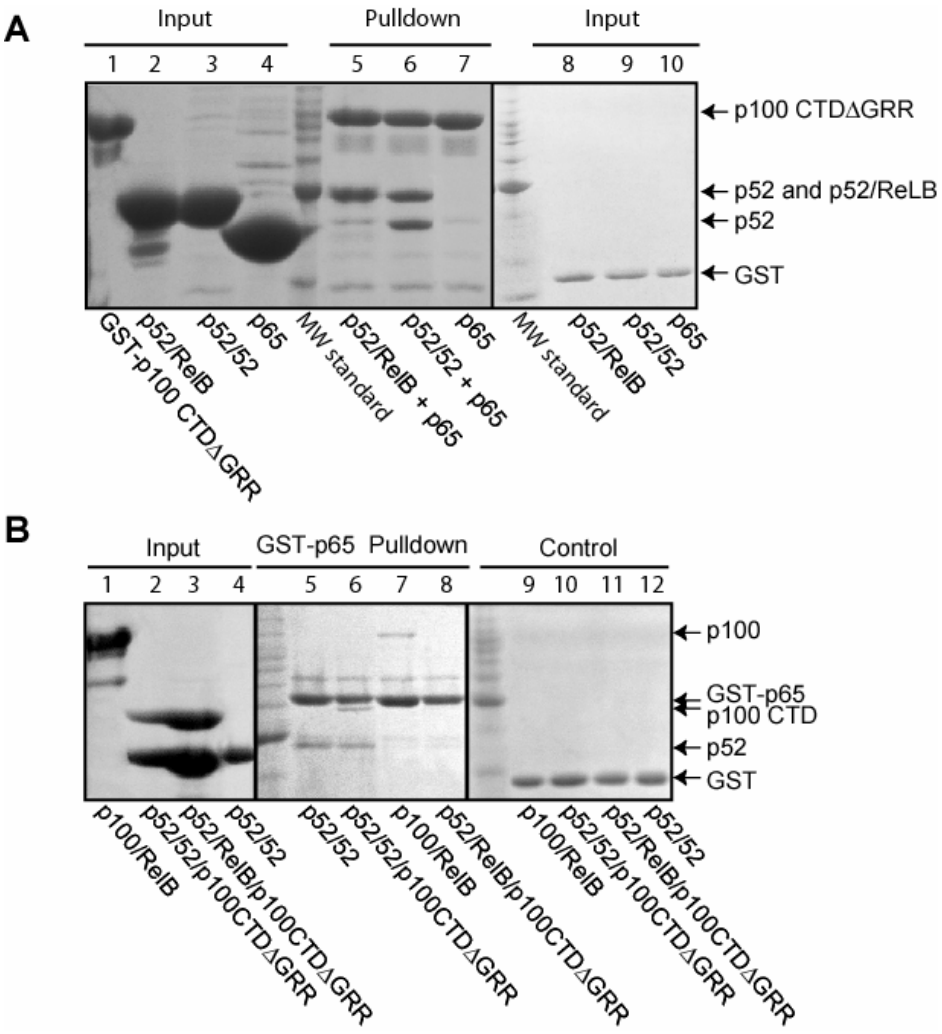

Figure 5-19. *p100 forms a complex with p65.* A.) *In vitro* GST pulldown experiments were done with pure GST tagged p100 CTDΔGRR showing that p65 RHR is able to bind in the presence of p52. GST-p100 CTDΔGRR was mixed with equal amounts of pure p65 in the presence of either p52/p52 RHR or p52/RelB RHR. B.) In *vitro* GST pulldown experiments were done with GST-p65 RHR reconfirming the interactions seen in 'A'.

C. Discussion

1. RelB stabilization by association with p100

Thermodynamic stabilization of proteins through association with their partners is a common regulatory mechanism adopted by eukaryotic cells. Cell cycle inhibitor p21, ornithine decarboxylase (ODC), and p53 have been shown to undergo degradation unless they are self associated or bound to partner proteins (Asher et al., 2005; Asher et al., 2002; Sheaff et al., 2000). An example of partner-mediated protein stabilization can be drawn from the NF-κB-IκB system. In the absence of RelA and c-Rel, levels of IκBα are significantly reduced (Hoffmann et al., 2002). Unfolding studies have demonstrated low folding stability of free IκBα(Croy et al., 2004). This may allow free IκBα to be easily targeted and degraded by cellular proteases. In wt cells, IκBα is primarily bound by RelA and c-Rel dimers, which explains how the steady state levels of IκBα are different in wt and NF-κB-deficient cells.

NF-κB dimers are highly stable with the exception of RelB. Intriguingly, it is not the non-homologous LZ and TAD domains that render RelB unstable. Rather, it is the RHR of RelB that appears to be the primary reason for its lack of stability. The structure of the RelB DD homodimer shows a lack of surface hydrogen bonds in these domains which, at least in part, explains why the molecule might not be able to fold properly and consequently, forms a domain swapped homodimer in the crystal (Huang et al., 2005b). We also observe similar sparse surface hydrogen bonds in the RelB

NTD X-ray crystal structure (Moorthy & Ghosh, unpublished observation). These observations are consistent with previous reports, which showed that the NTD of RelB induces its degradation in cells (Marienfeld et al., 2001). We suggest that the entire RHR of RelB is susceptible to degradation due to its low folding stability. p100 protects RelB from degradation by forming a highly stable complex. Results from our binding experiments suggest a complicated mode of interaction between RelB and p100, where different structural domains and flexible regions participate in the complex formation. Protection of flexible regions in the complex suggests a simple mechanism of how RelB avoids degradation by cellular proteases.

RelB also interacts stabily with p52 and p50. However, the RelB/p52 and RelB/p50 heterodimers are not expected to be as stable as the RelB/p100 complex. The TAD and LZ of RelB become exposed in these complexes. How are these RelB domains stabilized in the RelB/p50 and RelB/p52 heterodimers, and how do they protect RelB form degradation? It is likely that these dimers exist only transiently *in vivo* as free dimers. They localize to the nucleus and associate with DNA and are involved in transcriptional regulation. These transcriptionally active dimers remain mostly in DNA bound states, where the NTD interacts with target DNA and the TAD presumably interacts with other proteins. The apparent lack of RelB's stability is not unusual. It is possible that the unstable regions of RelB can interact with p100 more efficiently, which would not be possible if RelB was a more stable protein. Alternatively, the presence of RelB in the absence of its partners, p100, p52, and p50 could result in unwanted interactions between RelB and other cellular proteins that

could be detrimental to the cell. Future studies are needed to determine the residues involved and the physical-chemical mechanism underlying RelB destabilization.

2. RelB regulates p100 degradation/processing in induced cells

We show here that the RelB/p100 complex is an architecturally different complex from other possible p100 complexes such as the RelA/p100 complex. Three noteworthy interactions observed in the RelB/p100 complex are between i) the NTD of p52 and RelB RHR, ii) the LZ/NTD of RelB and the C-terminus of p100, and iii) the TAD of RelB and the site of processing in p100. Interaction of the NTD of p52 with RelB is unique to RelB complexes and this mode of binding is important for further assembly of the CTD of p100 to the RelB/p52 sub-complex. Interactions between the C-terminal region of p100 and the LZ/NTD of RelB are also intriguing as this region of p100 contains the death domain and the inducible processing sites. Although, the exact site of p100 processing is unknown, it is located at or C-terminal to residue 406 (Heusch et al., 1999). A recent article has shown that constitutive nuclear processing of C-terminally truncated p100 requires Asp 415 (Qing et al., 2007). The interaction of RelB TAD with this region has an impact on processing. This interaction is NFκB subunit specific, since the RelA TAD does not interact with p100.

Involvement of RelB in contacting all functionally critical segments and/or domains of p100 must impinge upon p100 functions, such as its role as a precursor protein (Fong and Sun, 2002; Senftleben et al., 2001; Xiao et al., 2004; Xiao et al., 2001b). This work confirmed that destabilization of this complex can relieve

stabilization of p100 by RelB. The hydrophobic patch mutation of RelB has a marginal effect on destabilizing the RelB/p100 complex but is able to form a stable RelB/p52 complex. The RelB Y300A mutant has little or no affinity for p52 but is able to form a complex with p100. This mutant leads to the complete degradation of p100 with little or no generation of p52 in stimulated cells. This result suggests that one of the conditions of processing is the stable dimerization of the processed product. Consistent with this notion, a p100 mutant defective in dimerization cannot generate a processed product. It is also noteworthy that in RelB Y300A expressing cells, basal processing of p100 is observed whereas in p100 Y247A expressing cells basal processing is absent. This more dramatic effect of the p100 Y247A mutant is due to the inability of the processed p52 Y247A mutant to associate with any NFκB's, including RelB.

3. A model for the RelB/p52 production

One of the critical but unanswered questions in the area of NF-κB biology is the mechanism of activation of the RelB/p52 heterodimer in response to stimulus. A more specific question in this regard is whether or not the p100/RelB complex serves as a precursor for the RelB/p52 complex. We have provided evidence that the preexisting p100/RelB complex is not the source of transcriptionally active RelB/p52 heterodimer. We have further evidence showing that in the absence of all possible p100 and p52 binding partners (*relb*$^{-/-}$/*rela*$^{-/-}$/*c-rel*$^{-/-}$ MEF cells), continuously synthesized p100 is able to undergo processing(Claudio et al., 2002; Mordmuller et al., 2003). This suggests that p52 can be generated from newly synthesized p100.

However, we do not observe a strong 1:1 ratio between the disappearance of p100 and appearance of p52; the protein level of p100 at 0 hours it not equal to the protein level of p52 at 24 hours. The 1:1 ratio of p100 to p52 however is observed in wild type MEF cells. This suggests that processing is inefficient in *relb*$^{-/-}$/*rela*$^{-/-}$/*c-rel*$^{-/-}$ MEF cells and that a significant amount of p100 is completely degraded. We propose that in wt cells generation of RelB/p52 heterodimer is coupled to the processing of p100, where a pool of RelB binds to p52 immediately after the processing event and the other pool binds to p100 to block its processing. The non-RelB subunits (RelA or c-Rel) can also bind p100, which does not involve the p100 processing site and therefore processing could occur from such complexes (Figure 20).

What is the role of the inactive RelB/p100 complex generated during induction? One possibility is that with the termination of signals, a large pool of p100 associates with RelB, thus squelching most of the transcriptionally active RelB and at the same time disabling p100 from being processed. Thus, with the withdrawal of stimulus the basal state is restored; where p100 functions again as a fourth IκB molecule to inhibit not only RelB but also p50/RelA heterodimer (Fig. 9 (Basak et al., 2006)). This is also an important mechanism to prevent generation of excess p52 and to maintain normal cell function, as it is known that unregulated generation of p52 can lead to pathological states(Ciana et al., 1997; Ishikawa et al., 1997; Qing et al., 2005a; Xiao et al., 2001a). It is also noteworthy to mention that constitutive processing of p100 due to truncation of the p100 C-terminus is directly linked to cancer (Ciana et al., 1997; Rayet and Gelinas, 1999; Xiao et al., 2001b).

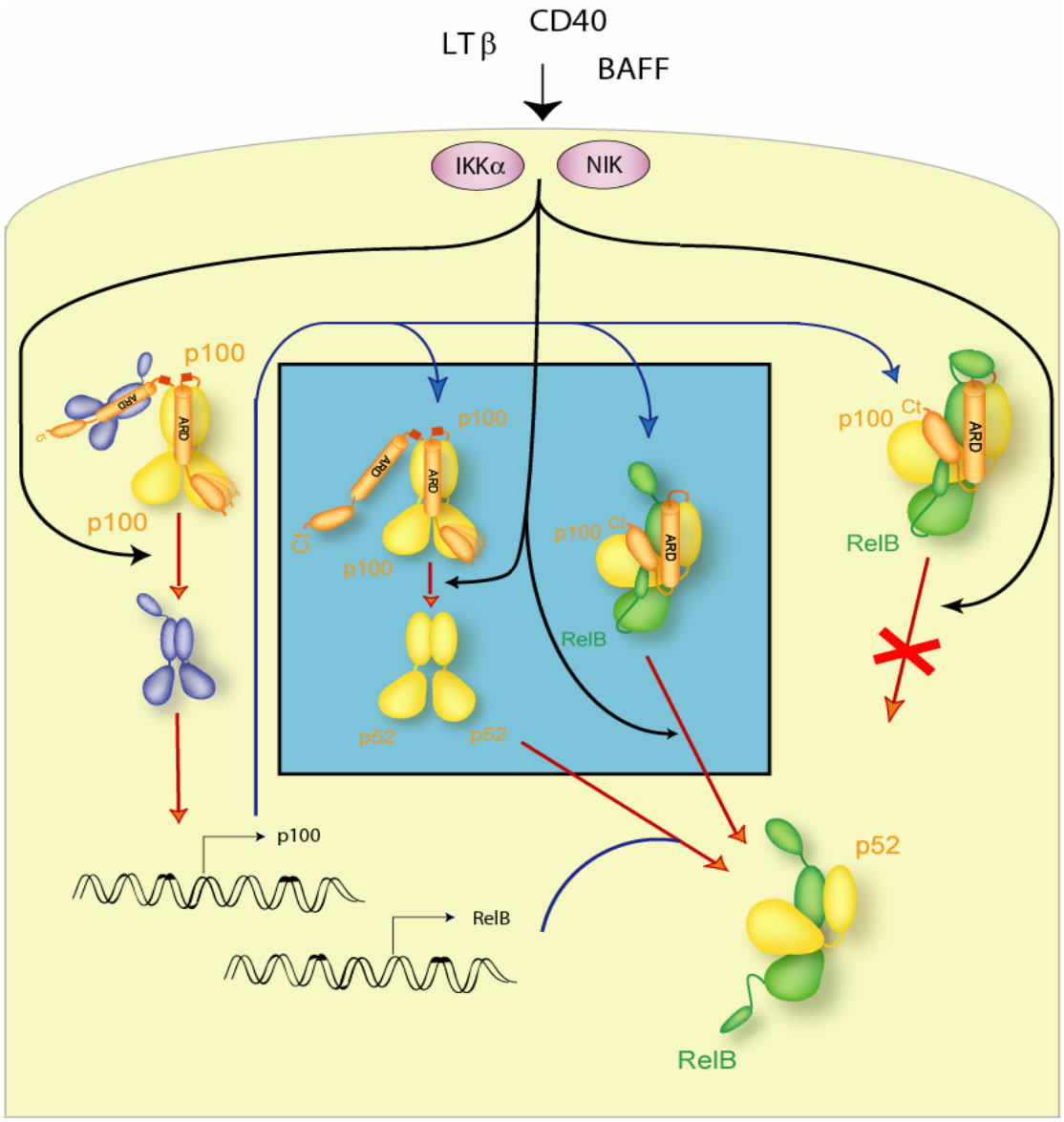

Figure 5-21. *Model of the processing of p100 and generation of the RelB/p52.* Please see the text for description.

Chapter V, in part, is in preparation as Stabilization of RelB requires multi-domain interaction with p100/p52, Amanda J. Fusco, Olga V. Savinova, Rashmi Talwar, Jeffrey D. Kearns, Alexander Hoffmann & Gourisankar Ghosh. The dissertation author was the primary researcher and author of this publication.

VI. Discussion

RelB is the most poorly understood member of the NF-κB family. Initial work on RelB revealed properties that were uncharacteristic of properties demonstrated for other NF-κB family members (Ruben et al., 1992; Ryseck et al., 1992; Ryseck et al., 1995). The most striking feature is the inability to function as a homodimer. RelB has been shown to preferentially heterodimerize with p50, p52 and p100. In resting cells a large fraction of RelB remains associated with p100 and upon cell stimulation RelB/p52 heterodimer is generated. The RelB/p52 heterodimer has been shown to function as an activator of transcription while the RelB/p50 heterodimer has been shown to function as both an inhibitor and activator of transcription. These observations raise several questions. Why does RelB preferentially interact with p50, p52 and p100? Upon stimulation is the RelB/p52 heterodimer generated from the p100/RelB complex? Is the RelB/p50 heterodimer an activator or repressor of transcription? What are the principles underlying the κB DNA recognition by RelB/p52 heterodimer?

The goal of my thesis dissertation was to gain a better understanding of the structure-function relationship of RelB with a hope of addressing some of the questions raised above. Specifically, I analyzed the relationship between RelB and the inhibitor protein, p100, and its activating partner, p52. I used structural and biochemical methods to analyze the nature of the RelB/p100 and RelB/p52 complexes and determine how RelB/p52 is able to bind its DNA response elements in a selective manner.

A. Activation of the RelB/p52 heterodimer

Genetic studies have shown that in the absence of p100/p52 protein, the level of RelB protein is drastically reduced (observations made by Hoffmannm lab). This reinforced the special relationship between RelB and p100. I demonstrated that the introduction of p100 by gene transfer resulted in an enhanced protein level of RelB. Biochemical studies have revealed that RelB is inherently an unstable protein that is stabilized by p100 and p52. RelB interacts with p100 and p52 in a unique manner that involves all functional domains of both proteins. One striking observation is the involvement of the N-terminus of p100 (same as the N-terminus of p52) in the binding interaction with the RelB RHR but not with the RelA RHR. The p50 N-terminus also exhibits similar interaction properties with RelB. This interaction was shown to be important for the stabilization effect of p52. In addition the interaction involving the classical NF-κB dimerization domain is also unique in RelB. The interaction is observed between RelB and p52 or p50. However, RelB cannot make either interaction with itself (to form a homodimer) or with RelA and cRel. In particular, the contact made by the two conserved tyrosine residues across the dimer interfaces in the case of RelB/p50 and RelB/p52 is unique to these heterodimers. These contacts are not made possible in the case of RelB/RelA and RelB/cRel as the tyrosine residue is replaced by a phenylalanine in RelA and cRel. A stable RelB homodimer is unlikely because of several unfavorable contacts. This gives some answers as to why RelB preferentially interact with p50 and p52.

Why does RelB prefer p100? It may be due, in part, to the interaction between the activation domain of RelB and the site of processing of p100, as this interaction is

specific to RelB. Is this highly stable p100/RelB complex the substrate for induced generation of the RelB/p52 heterodimer? No prior studies have shown a precursor-product relationship between the p100/RelB and RelB/p52 complexes. It has also been previously shown that the generation of p52 from p100 requires new protein synthesis (Mordmuller et al., 2003). In this work I show that the multi-domain interactions between RelB and p100 enables RelB to play a dual role in the processing of p100 (Figure 6-1). One role that RelB plays is protecting p100 from processing/degradation. Therefore the pre-existing RelB/p100 complex is not the source of the RelB/p52. We demonstrate that generation of the RelB/p52 heterodimer requires new protein synthesis of both RelB and p100. The second role that RelB plays is stabilization of p52. p52 is able to be processed from p100 itself, however this processing event is not efficient. This indicates that p52 needs a binding partner for stabilization, such as RelB. Although RelA and c-Rel can also stabilize p52, p100 processing signals, such as BAFF, LTβ, CD40, stimulate the synthesis of RelB along with p100. Therefore RelB/p52 is observed in response to these stimuli. We predict if a stimulus induced new synthesis of p100 along with RelA or cRel but not RelB, then the resulting complexes would be p52/RelA or p52/cRel, without the accumulation of an inactive RelB/p100 complex.

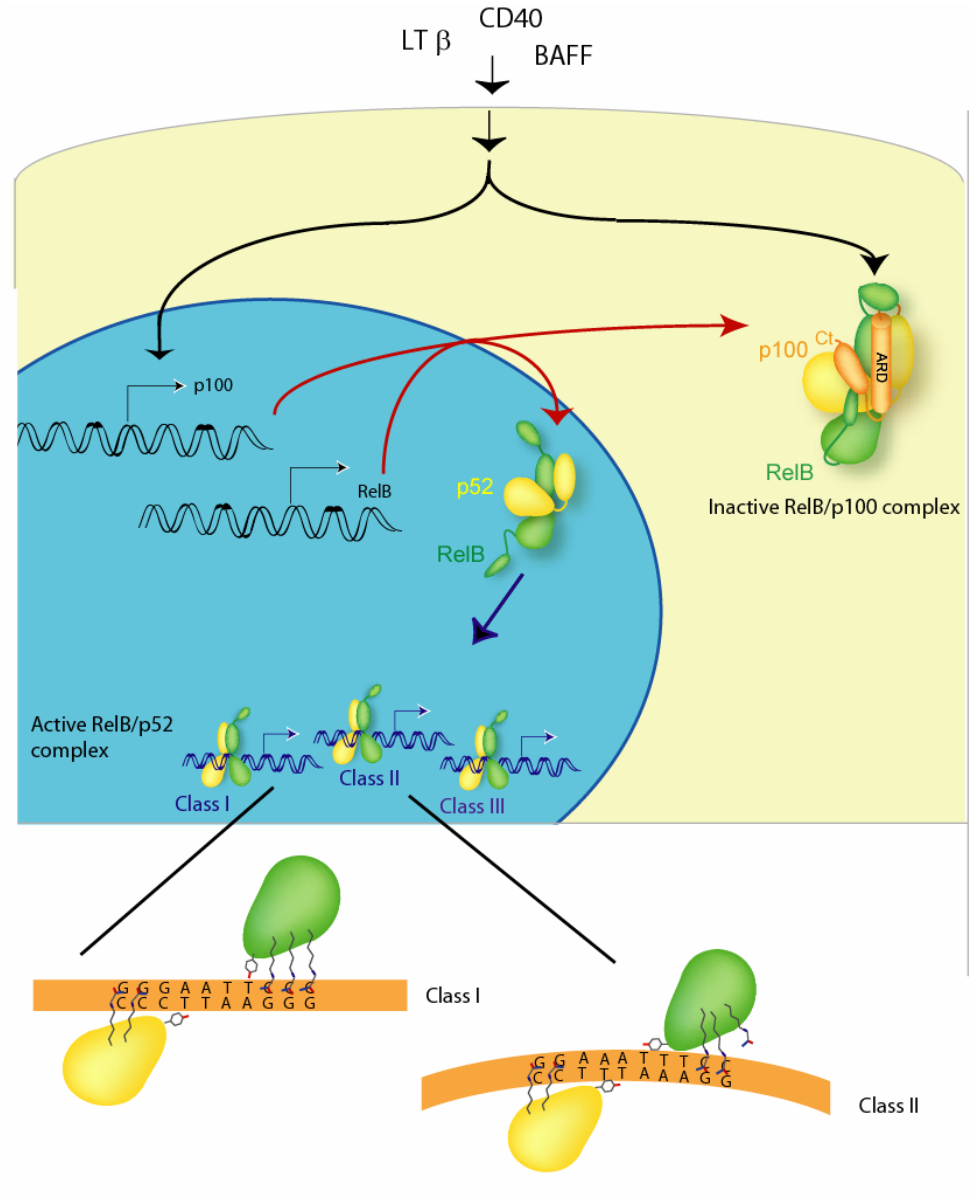

Figure 6-1. *Model of the effects RelB has on p100 processing and κB DNA binding.*. RelB acts as both an inhibitor and activator of processing. The active RelB/p52 heterodimer binds to three classes of κB sites. RelB regulates the differential binding mode of the RelB/p52 heterodimer to the different classes of κB sites. The binding modes of the RelB/p52 heterodimer to class I and class II is depicted.

The processing of p100 into p52 is a dynamic process that is signal dependent in contrast to the constitutive processing of p105. Although the two proteins are highly homologous, the requirement of stimulus dependent new protein synthesis could explain the difference observed between p100 and p105. An additional explanation is the apparent lack of stability of the p52 homodimer compared with the p50 homodimer. DNA binding has only been observed for the p52 homodimer when complexed with Bcl-3 (Ghosh et al., 1998; Nishikori et al., 2005; Nolan et al., 1993), while the p50 homodimer has been observed bound to many κB sites (Guan et al., 2005; Ma et al., 2003). This suggests that unlike p105/p50, p100/p52 must by synthesized in the presence of other NF-κB proteins such as RelB.

B. DNA binding by the RelB/p52 heterodimer

Crystallographic analysis of the RelB/p52 heterodimer bound to a symmetric κB DNA elucidated distinct DNA binding features, the most striking of which is the involvement of a conserved arginine residue of RelB (*Arg125*) in contacting the outermost G:C bp of the DNA half site recognized by RelB. This base-specific contact results in the recognition of an 11 base pair κB site (two 5 base pair half sites plus one base pair spacer) flanked by GGG:CCC base pairs at each end. The RelB/p52:DNA complex structure also predicts that RelB should be able to contact the distal G:C base pair irrespective of the strand specificity of guanine. The flexibility of RelBs *Arg125* side chain should enable it to make hydrogen bonds with a G in either strand. Therefore the optimal sequence of the RelB half site could be either 5'-NNGGG-3' or 5'-NNGGC-3'. Another feature revealed by the structure is the lack of

base-specific interactions observed at the central 'AATT' region. Strikingly, the stacking interaction between the first A:T bp of the RelB half site and *Tyr120* of RelB is absent. These structural observations led to the conclusion that the RelB/p52 heterodimer prefers a sequence containing flaking G:C bp.

However the DNA binding affinity data does not fully explain the structural findings. As shown in chapter III, I have determined the binding affinities of RelB/p52 to different physiological κB sites. This demonstrated that the RelB/p52 heterodimer was more versatile in DNA recognition than observed by the structure. That is, this heterodimer binds to diverse κB sequences with similar affinities. How then is RelB/p52 heterodimer able to bind to a range of κB sequences? Based on their sequences, these κB sites can be divided into two types; one type contains G:C rich flanking sequences with fewer AT bp at the center; exemplified by the one used for structure determination. The other class contains more AT bp at the center with fewer G:C base pairs in the flanking regions. It is possible that RelB/p52 heterodimer has two modes of DNA interaction. The structure captured one mode of interaction, in which DNA binding occurs predominately through the G:C base pair interactions and the role of the central base pairs is insignificant. The heterodimer may bind the second class of κB sequences with a different mode. The other mode could be achieved through a rearrangement of the *Tyr120* residue in RelB, allowing for multiple Van der Waals contacts at the central base pairs. p50 and p52 homodimer and p50/RelA heterodimers display some preference for the first class of κB sequences whereas RelA and cRel homodimers prefer the second class of κB sequences.

Therefore RelB/p52 heterodimer exhibits a much greater degree of adaptability in κB DNA recognition. RelB is primarily responsible for this property.

This broad specificity in κB DNA recognition by the RelB/p52 heterodimer could have an implication in gene activation. RelB/p52 heterodimer has been demonstrated to be essential for the activation of a number of genes involved in lymphoid organogenesis and B cell maturation, such as SLC, BLC, SDF-1 and ELC. κB DNA sequences present in the promoters of these genes show little similarity with κB sequences discussed above, in particular at the RelB half sites. One feature is common in all cases however, the presence of a G:C base pair at the 5^{th} position of the 3' half site. This class of κB sequences may lie between the two classes mentioned above. However, further biochemical analysis of these κB sites is important for their characterization.

In all, the RelB/p52 heterodimer displays a relaxed κB recognition specificity. This heterodimer is activated slower as compared to the p50/RelA heterodimer. RelB/p52 has also been implicated in the prolonged activation of genes that are activated early by other NF-κB dimers (Saccani et al., 2003). A broad DNA binding specificity explains how the RelB/p52 heterodimer can accomplish that feat in addition to the regulation of a specific set of genes.

C. κB binding affinity, cooperativity with other activators and gene activation by NF-κB

Transcription involves an elaborate system involving multiple transcription factors, co-activators, post translational modifications and transcriptional machinery. There is no model that explains all the intricacy seen in gene activation by inducible activators. A simple view of transcription is that an activator protein binds to its response site, often helped by another activator bound to a neighboring site, and recruits a coactiavtor/mediator followed by the recruitment of transcriptional machinery. However, how stable the interaction has to be between an activator and its response DNA element is unknown. It is also unknown if in fact two activators cooperate with each other upon binding to their respective response elements. I do not observe cooperativity between the DNA binding domains of two activators. In fact, if anything, I observe mutual DNA binding, i.e., two activators negatively affect each other's DNA binding activities. However, synergistic transcriptional activation by the same two activators in cell-based experiments is undeniable. Therefore, more biochemical experiments are needed to better understand the role of multiple activators for gene activation. It is possible there is no simple rule in gene activation. Each promoter functions differently by responding to its activators differently. Whereas in some cases activators and coactivators assemble stably on a promoter by forming an enhanceosome complex, the process is more dynamic in other promoters.

In the case of dynamic assembly and disassembly of promoter-sepcific transcription complexes, the kinetics of activator binding might be the determining factor. Therefore, in addition to the equilibrium binding affinity, kinetic

measurements would be necessary. Such measurements, when carried out in the presence of neighboring activators, may reveal a new mode of binding regulation that can explain their transcriptional synergism.

References

Agrawal, A., Cha-Molstad, H., Samols, D. and Kushner, I. (2001) Transactivation of C-reactive protein by IL-6 requires synergistic interaction of CCAAT/enhancer binding protein beta (C/EBP beta) and Rel p50. *J Immunol*, 166, 2378-2384.

Agrawal, A., Samols, D. and Kushner, I. (2003) Transcription factor c-Rel enhances C-reactive protein expression by facilitating the binding of C/EBPbeta to the promoter. *Mol Immunol*, 40, 373-380.

Agre, P., Johnson, P.F. and McKnight, S.L. (1989) Cognate DNA binding specificity retained after leucine zipper exchange between GCN4 and C/EBP. *Science*, 246, 922-926.

Akira, S., Isshiki, H., Sugita, T., Tanabe, O., Kinoshita, S., Nishio, Y., Nakajima, T., Hirano, T. and Kishimoto, T. (1990) A nuclear factor for IL-6 expression (NF-IL6) is a member of a C/EBP family. *Embo J*, 9, 1897-1906.

Arenzana-Seisdedos, F., Thompson, J., Rodriguez, M.S., Bachelerie, F., Thomas, D. and Hay, R.T. (1995) Inducible nuclear expression of newly synthesized I kappa B alpha negatively regulates DNA-binding and transcriptional activities of NF-kappa B. *Mol Cell Biol*, 15, 2689-2696.

Arenzana-Seisdedos, F., Turpin, P., Rodriguez, M., Thomas, D., Hay, R.T., Virelizier, J.L. and Dargemont, C. (1997) Nuclear localization of I kappa B alpha promotes active transport of NF-kappa B from the nucleus to the cytoplasm. *J Cell Sci*, 110 (Pt 3), 369-378.

Asher, G., Bercovich, Z., Tsvetkov, P., Shaul, Y. and Kahana, C. (2005) 20S proteasomal degradation of ornithine decarboxylase is regulated by NQO1. *Mol Cell*, 17, 645-655.

Asher, G., Lotem, J., Sachs, L., Kahana, C. and Shaul, Y. (2002) Mdm-2 and ubiquitin-independent p53 proteasomal degradation regulated by NQO1. *Proc Natl Acad Sci U S A*, 99, 13125-13130.

Baeuerle, P.A. and Baltimore, D. (1996) NF-kappa B: ten years after. *Cell*, 87, 13-20.

Baeuerle, P.A. and Henkel, T. (1994) Function and activation of NF-kappa B in the immune system. *Annu Rev Immunol*, 12, 141-179.

Baldwin, A.S., Jr. (1996) The NF-kappa B and I kappa B proteins: new discoveries and insights. *Annu Rev Immunol*, 14, 649-683.

Baldwin, A.S., Jr. (1996) The NF-kappa B and I kappa B proteins: new discoveries and insights. *Annu Rev Immunol*, 14, 649-683.

Basak, S., Kim, H., Kearns, J., Terganokar, V., Werner, S., Benedict, C., Ware, C., Ghosh, G., Verma, I. and Hoffmann, A. (2006) A fourth IkB protein in the NF-kB signaling module. *Cell*, In press.

Beinke, S. and Ley, S.C. (2004) Functions of NF-kappaB1 and NF-kappaB2 in immune cell biology. *Biochem J*, 382, 393-409.

Berkowitz, B., Huang, D.B., Chen-Park, F.E., Sigler, P.B. and Ghosh, G. (2002) The x-ray crystal structure of the NF-kappa B p50.p65 heterodimer bound to the interferon beta -kappa B site. *J Biol Chem*, 277, 24694-24700.

Betts, J.C., Cheshire, J.K., Akira, S., Kishimoto, T. and Woo, P. (1993) The role of NF-kappa B and NF-IL6 transactivating factors in the synergistic activation of human serum amyloid A gene expression by interleukin-1 and interleukin-6. *J Biol Chem*, 268, 25624-25631.

Bonizzi, G., Bebien, M., Otero, D.C., Johnson-Vroom, K.E., Cao, Y., Vu, D., Jegga, A.G., Aronow, B.J., Ghosh, G., Rickert, R.C. and Karin, M. (2004) Activation of IKKalpha target genes depends on recognition of specific kappaB binding sites by RelB:p52 dimers. *Embo J*, 23, 4202-4210.

Bours, V., Franzoso, G., Azarenko, V., Park, S., Kanno, T., Brown, K. and Siebenlist, U. (1993) The oncoprotein Bcl-3 directly transactivates through kappa B motifs via association with DNA-binding p50B homodimers. *Cell*, 72, 729-739.

Bours, V., Villalobos, J., Burd, P.R., Kelly, K. and Siebenlist, U. (1990) Cloning of a mitogen-inducible gene encoding a kappa B DNA-binding protein with homology to the rel oncogene and to cell-cycle motifs. *Nature*, 348, 76-80.

Brown, K., Park, S., Kanno, T., Franzoso, G. and Siebenlist, U. (1993) Mutual regulation of the transcriptional activator NF-kappa B and its inhibitor, I kappa B-alpha. *Proc Natl Acad Sci U S A*, 90, 2532-2536.

Bryan, R.G., Li, Y., Lai, J.H., Van, M., Rice, N.R., Rich, R.R. and Tan, T.H. (1994) Effect of CD28 signal transduction on c-Rel in human peripheral blood T cells. *Mol Cell Biol*, 14, 7933-7942.

Butscher, W.G., Powers, C., Olive, M., Vinson, C. and Gardner, K. (1998) Coordinate transactivation of the interleukin-2 CD28 response element by c-Rel and ATF-1/CREB2. *J Biol Chem*, 273, 552-560.

Caamano, J.H., Rizzo, C.A., Durham, S.K., Barton, D.S., Raventos-Suarez, C., Snapper, C.M. and Bravo, R. (1998) Nuclear factor (NF)-kappa B2 (p100/p52) is required for normal splenic microarchitecture and B cell-mediated immune responses. *J Exp Med*, 187, 185-196.

Cao, Y., Bonizzi, G., Seagroves, T.N., Greten, F.R., Johnson, R., Schmidt, E.V. and Karin, M. (2001) IKKalpha provides an essential link between RANK signaling and cyclin D1 expression during mammary gland development. *Cell*, 107, 763-775.

Carey, M. (1998) The enhanceosome and transcriptional synergy. *Cell*, 92, 5-8.

Cha-Molstad, H., Agrawal, A., Zhang, D., Samols, D. and Kushner, I. (2000) The Rel family member P50 mediates cytokine-induced C-reactive protein expression by a novel mechanism. *J Immunol*, 165, 4592-4597.

Chandler, N.M., Canete, J.J. and Callery, M.P. (2004) Increased expression of NF-kappa B subunits in human pancreatic cancer cells. *J Surg Res*, 118, 9-14.

Chen, F.E., Huang, D.B., Chen, Y.Q. and Ghosh, G. (1998a) Crystal structure of p50/p65 heterodimer of transcription factor NF-kappaB bound to DNA. *Nature*, 391, 410-413.

Chen, G., Cao, P. and Goeddel, D.V. (2002) TNF-induced recruitment and activation of the IKK complex require Cdc37 and Hsp90. *Mol Cell*, 9, 401-410.

Chen, Y.Q., Ghosh, S. and Ghosh, G. (1998b) A novel DNA recognition mode by the NF-kappa B p65 homodimer. *Nat Struct Biol*, 5, 67-73.

Chen, Y.Q., Sengchanthalangsy, L.L., Hackett, A. and Ghosh, G. (2000) NF-kappaB p65 (RelA) homodimer uses distinct mechanisms to recognize DNA targets. *Structure*, 8, 419-428.

Chiao, P.J., Miyamoto, S. and Verma, I.M. (1994) Autoregulation of I kappa B alpha activity. *Proc Natl Acad Sci U S A*, 91, 28-32.

Ciana, P., Neri, A., Cappellini, C., Cavallo, F., Pomati, M., Chang, C.C., Maiolo, A.T. and Lombardi, L. (1997) Constitutive expression of lymphoma-associated NFKB-2/Lyt-10 proteins is tumorigenic in murine fibroblasts. *Oncogene*, 14, 1805-1810.

Claudio, E., Brown, K., Park, S., Wang, H. and Siebenlist, U. (2002) BAFF-induced NEMO-independent processing of NF-kappa B2 in maturing B cells. *Nat Immunol*, 3, 958-965.

Cogswell, P.C., Guttridge, D.C., Funkhouser, W.K. and Baldwin, A.S., Jr. (2000) Selective activation of NF-kappa B subunits in human breast cancer: potential roles for NF-kappa B2/p52 and for Bcl-3. *Oncogene*, 19, 1123-1131.

Coope, H.J., Atkinson, P.G., Huhse, B., Belich, M., Janzen, J., Holman, M.J., Klaus, G.G., Johnston, L.H. and Ley, S.C. (2002) CD40 regulates the processing of NF-kappaB2 p100 to p52. *Embo J*, 21, 5375-5385.

Cramer, P., Larson, C.J., Verdine, G.L. and Muller, C.W. (1997) Structure of the human NF-kappaB p52 homodimer-DNA complex at 2.1 A resolution. *Embo J*, 16, 7078-7090.

Croy, C.H., Bergqvist, S., Huxford, T., Ghosh, G. and Komives, E.A. (2004) Biophysical characterization of the free IkappaBalpha ankyrin repeat domain in solution. *Protein Sci*, 13, 1767-1777.

Darlington, G.J., Ross, S.E. and MacDougald, O.A. (1998) The role of C/EBP genes in adipocyte differentiation. *J Biol Chem*, 273, 30057-30060.

Dash, P.K., Karl, K.A., Colicos, M.A., Prywes, R. and Kandel, E.R. (1991) cAMP response element-binding protein is activated by Ca2+/calmodulin- as well as cAMP-dependent protein kinase. *Proc Natl Acad Sci U S A*, 88, 5061-5065.

Dejardin, E., Droin, N.M., Delhase, M., Haas, E., Cao, Y., Makris, C., Li, Z.W., Karin, M., Ware, C.F. and Green, D.R. (2002) The lymphotoxin-beta receptor induces different patterns of gene expression via two NF-kappaB pathways. *Immunity*, 17, 525-535.

Descombes, P. and Schibler, U. (1991) A liver-enriched transcriptional activator protein, LAP, and a transcriptional inhibitory protein, LIP, are translated from the same mRNA. *Cell*, 67, 569-579.

Diehl, A.M. (1998) Roles of CCAAT/enhancer-binding proteins in regulation of liver regenerative growth. *J Biol Chem*, 273, 30843-30846.

Dobrzanski, P., Ryseck, R.P. and Bravo, R. (1995) Specific inhibition of RelB/p52 transcriptional activity by the C-terminal domain of p100. *Oncogene*, 10, 1003-1007.

Elewaut, D., Shaikh, R.B., Hammond, K.J., De Winter, H., Leishman, A.J., Sidobre, S., Turovskaya, O., Prigozy, T.I., Ma, L., Banks, T.A., Lo, D., Ware, C.F., Cheroutre, H. and Kronenberg, M. (2003) NIK-dependent RelB activation defines a unique signaling pathway for the development of V alpha 14i NKT cells. *J Exp Med*, 197, 1623-1633.

Fong, A. and Sun, S.C. (2002) Genetic evidence for the essential role of beta-transducin repeat-containing protein in the inducible processing of NF-kappa B2/p100. *J Biol Chem*, 277, 22111-22114.

Franzoso, G., Bours, V., Park, S., Tomita-Yamaguchi, M., Kelly, K. and Siebenlist, U. (1992) The candidate oncoprotein Bcl-3 is an antagonist of p50/NF-kappa B-mediated inhibition. *Nature*, 359, 339-342.

Franzoso, G., Carlson, L., Poljak, L., Shores, E.W., Epstein, S., Leonardi, A., Grinberg, A., Tran, T., Scharton-Kersten, T., Anver, M., Love, P., Brown, K. and Siebenlist, U. (1998) Mice deficient in nuclear factor (NF)-kappa B/p52 present with defects in humoral responses, germinal center reactions, and splenic microarchitecture. *J Exp Med*, 187, 147-159.

Fraser, J.D., Irving, B.A., Crabtree, G.R. and Weiss, A. (1991) Regulation of interleukin-2 gene enhancer activity by the T cell accessory molecule CD28. *Science*, 251, 313-316.

Fu, Y.X. and Chaplin, D.D. (1999) Development and maturation of secondary lymphoid tissues. *Annu Rev Immunol*, 17, 399-433.

Gerondakis, S., Grossmann, M., Nakamura, Y., Pohl, T. and Grumont, R. (1999) Genetic approaches in mice to understand Rel/NF-kappaB and IkappaB function: transgenics and knockouts. *Oncogene*, 18, 6888-6895.

Gerondakis, S., Grumont, R., Gugasyan, R., Wong, L., Isomura, I., Ho, W. and Banerjee, A. (2006) Unravelling the complexities of the NF-kappaB signalling pathway using mouse knockout and transgenic models. *Oncogene*, 25, 6781-6799.

Ghosh, G., van Duyne, G., Ghosh, S. and Sigler, P.B. (1995) Structure of NF-kappa B p50 homodimer bound to a kappa B site. *Nature*, 373, 303-310.

Ghosh, P., Tan, T.H., Rice, N.R., Sica, A. and Young, H.A. (1993) The interleukin 2 CD28-responsive complex contains at least three members of the NF kappa B family: c-Rel, p50, and p65. *Proc Natl Acad Sci U S A*, 90, 1696-1700.

Ghosh, S. and Baltimore, D. (1990) Activation in vitro of NF-kappa B by phosphorylation of its inhibitor I kappa B. *Nature*, 344, 678-682.

Ghosh, S. and Karin, M. (2002) Missing pieces in the NF-kappaB puzzle. *Cell*, 109 Suppl, S81-96.

Ghosh, S., May, M.J. and Kopp, E.B. (1998) NF-kappa B and Rel proteins: evolutionarily conserved mediators of immune responses. *Annu Rev Immunol*, 16, 225-260.

Giese, K., Kingsley, C., Kirshner, J.R. and Grosschedl, R. (1995) Assembly and function of a TCR alpha enhancer complex is dependent on LEF-1-induced DNA bending and multiple protein-protein interactions. *Genes Dev*, 9, 995-1008.

Gloire, G., Dejardin, E. and Piette, J. (2006) Extending the nuclear roles of IkappaB kinase subunits. *Biochem Pharmacol*, 72, 1081-1089.

Gonzalez, G.A., Menzel, P., Leonard, J., Fischer, W.H. and Montminy, M.R. (1991) Characterization of motifs which are critical for activity of the cyclic AMP-responsive transcription factor CREB. *Mol Cell Biol*, 11, 1306-1312.

Gross, J.A., Dillon, S.R., Mudri, S., Johnston, J., Littau, A., Roque, R., Rixon, M., Schou, O., Foley, K.P., Haugen, H., McMillen, S., Waggie, K., Schreckhise, R.W., Shoemaker, K., Vu, T., Moore, M., Grossman, A. and Clegg, C.H. (2001) TACI-Ig neutralizes molecules critical for B cell development and autoimmune disease. impaired B cell maturation in mice lacking BLyS. *Immunity*, 15, 289-302.

Grosschedl, R. (1995) Higher-order nucleoprotein complexes in transcription: analogies with site-specific recombination. *Curr Opin Cell Biol*, 7, 362-370.

Guan, H., Hou, S. and Ricciardi, R.P. (2005) DNA binding of repressor nuclear factor-kappaB p50/p50 depends on phosphorylation of Ser337 by the protein kinase A catalytic subunit. *J Biol Chem*, 280, 9957-9962.

He, J.Q., Saha, S.K., Kang, J.R., Zarnegar, B. and Cheng, G. (2007) Specificity of TRAF3 in its negative regulation of the noncanonical NF-kappa B pathway. *J Biol Chem*, 282, 3688-3694.

Heusch, M., Lin, L., Geleziunas, R. and Greene, W.C. (1999) The generation of nfkb2 p52: mechanism and efficiency. *Oncogene*, 18, 6201-6208.

Hoffmann, A., Levchenko, A., Scott, M.L. and Baltimore, D. (2002) The IkappaB-NF-kappaB signaling module: temporal control and selective gene activation. *Science*, 298, 1241-1245.

Huang, D.B., Chen, Y.Q., Ruetsche, M., Phelps, C.B. and Ghosh, G. (2001) X-ray crystal structure of proto-oncogene product c-Rel bound to the CD28 response element of IL-2. *Structure*, 9, 669-678.

Huang, D.B., Phelps, C.B., Fusco, A.J. and Ghosh, G. (2005a) Crystal structure of a free kappaB DNA: insights into DNA recognition by transcription factor NF-kappaB. *J Mol Biol*, 346, 147-160.

Huang, D.B., Vu, D., Cassiday, L.A., Zimmerman, J.M., Maher, L.J., 3rd and Ghosh, G. (2003) Crystal structure of NF-kappaB (p50)2 complexed to a high-affinity RNA aptamer. *Proc Natl Acad Sci U S A*, 100, 9268-9273.

Huang, D.B., Vu, D. and Ghosh, G. (2005b) NF-kappaB RelB forms an intertwined homodimer. *Structure (Camb)*, 13, 1365-1373.

Huxford, T., Huang, D.B., Malek, S. and Ghosh, G. (1998) The crystal structure of the IkappaBalpha/NF-kappaB complex reveals mechanisms of NF-kappaB inactivation. *Cell*, 95, 759-770.

Ishikawa, H., Carrasco, D., Claudio, E., Ryseck, R.P. and Bravo, R. (1997) Gastric hyperplasia and increased proliferative responses of lymphocytes in mice lacking the COOH-terminal ankyrin domain of NF-kappaB2. *J Exp Med*, 186, 999-1014.

Jacobs, M.D. and Harrison, S.C. (1998) Structure of an IkappaBalpha/NF-kappaB complex. *Cell*, 95, 749-758.

Jeang, K.T. (2001) Functional activities of the human T-cell leukemia virus type I Tax oncoprotein: cellular signaling through NF-kappa B. *Cytokine Growth Factor Rev*, 12, 207-217.

Karin, M. and Ben-Neriah, Y. (2000) Phosphorylation meets ubiquitination: the control of NF-[kappa]B activity. *Annu Rev Immunol*, 18, 621-663.

Kerppola, T. and Curran, T. (1995) Transcription. Zen and the art of Fos and Jun. *Nature*, 373, 199-200.

Khare, S.D., Sarosi, I., Xia, X.Z., McCabe, S., Miner, K., Solovyev, I., Hawkins, N., Kelley, M., Chang, D., Van, G., Ross, L., Delaney, J., Wang, L., Lacey, D., Boyle, W.J. and Hsu, H. (2000) Severe B cell hyperplasia and autoimmune disease in TALL-1 transgenic mice. *Proc Natl Acad Sci U S A*, 97, 3370-3375.

Kieran, M., Blank, V., Logeat, F., Vandekerckhove, J., Lottspeich, F., Le Bail, O., Urban, M.B., Kourilsky, P., Baeuerle, P.A. and Israel, A. (1990) The DNA binding subunit of NF-kappa B is identical to factor KBF1 and homologous to the rel oncogene product. *Cell*, 62, 1007-1018.

Kleemann, R., Gervois, P.P., Verschuren, L., Staels, B., Princen, H.M. and Kooistra, T. (2003) Fibrates down-regulate IL-1-stimulated C-reactive protein gene expression in hepatocytes by reducing nuclear p50-NFkappa B-C/EBP-beta complex formation. *Blood*, 101, 545-551.

Lai, J.H., Horvath, G., Subleski, J., Bruder, J., Ghosh, P. and Tan, T.H. (1995) RelA is a potent transcriptional activator of the CD28 response element within the interleukin 2 promoter. *Mol Cell Biol*, 15, 4260-4271.

Landschulz, W.H., Johnson, P.F. and McKnight, S.L. (1988) The leucine zipper: a hypothetical structure common to a new class of DNA binding proteins. *Science*, 240, 1759-1764.

Landschulz, W.H., Johnson, P.F. and McKnight, S.L. (1989) The DNA binding domain of the rat liver nuclear protein C/EBP is bipartite. *Science*, 243, 1681-1688.

LeClair, K.P., Blanar, M.A. and Sharp, P.A. (1992) The p50 subunit of NF-kappa B associates with the NF-IL6 transcription factor. *Proc Natl Acad Sci U S A*, 89, 8145-8149.

Lee, K.A. and Masson, N. (1993) Transcriptional regulation by CREB and its relatives. *Biochim Biophys Acta*, 1174, 221-233.

Lee, K.H., Bowen-Pope, D.F. and Reed, R.R. (1990) Isolation and characterization of the alpha platelet-derived growth factor receptor from rat olfactory epithelium. *Mol Cell Biol*, 10, 2237-2246.

Lekstrom-Himes, J. and Xanthopoulos, K.G. (1998) Biological role of the CCAAT/enhancer-binding protein family of transcription factors. *J Biol Chem*, 273, 28545-28548.

Lernbecher, T., Kistler, B. and Wirth, T. (1994) Two distinct mechanisms contribute to the constitutive activation of RelB in lymphoid cells. *Embo J*, 13, 4060-4069.

Liang, C., Zhang, M. and Sun, S.C. (2006) beta-TrCP binding and processing of NF-kappaB2/p100 involve its phosphorylation at serines 866 and 870. *Cell Signal*, 18, 1309-1317.

Liao, G., Zhang, M., Harhaj, E.W. and Sun, S.C. (2004) Regulation of the NF-kappaB-inducing kinase by tumor necrosis factor receptor-associated factor 3-induced degradation. *J Biol Chem*, 279, 26243-26250.

Liou, H.C., Nolan, G.P., Ghosh, S., Fujita, T. and Baltimore, D. (1992) The NF-kappa B p50 precursor, p105, contains an internal I kappa B-like inhibitor that preferentially inhibits p50. *Embo J*, 11, 3003-3009.

Lu, Q., Hutchins, A.E., Doyle, C.M., Lundblad, J.R. and Kwok, R.P. (2003) Acetylation of cAMP-responsive element-binding protein (CREB) by CREB-binding protein enhances CREB-dependent transcription. *J Biol Chem*, 278, 15727-15734.

Ma, X.Y., Wang, H., Ding, B., Zhong, H., Ghosh, S. and Lengyel, P. (2003) The interferon-inducible p202a protein modulates NF-kappaB activity by inhibiting the binding to DNA of p50/p65 heterodimers and p65 homodimers while enhancing the binding of p50 homodimers. *J Biol Chem*, 278, 23008-23019.

Mackay, F., Woodcock, S.A., Lawton, P., Ambrose, C., Baetscher, M., Schneider, P., Tschopp, J. and Browning, J.L. (1999) Mice transgenic for BAFF develop lymphocytic disorders along with autoimmune manifestations. *J Exp Med*, 190, 1697-1710.

Malek, S., Huxford, T. and Ghosh, G. (1998) Ikappa Balpha functions through direct contacts with the nuclear localization signals and the DNA binding sequences of NF-kappaB. *J Biol Chem*, 273, 25427-25435.

Malinin, N.L., Boldin, M.P., Kovalenko, A.V. and Wallach, D. (1997) MAP3K-related kinase involved in NF-kappaB induction by TNF, CD95 and IL-1. *Nature*, 385, 540-544.

Marienfeld, R., Berberich-Siebelt, F., Berberich, I., Denk, A., Serfling, E. and Neumann, M. (2001) Signal-specific and phosphorylation-dependent RelB degradation: a potential mechanism of NF-kappaB control. *Oncogene*, 20, 8142-8147.

May, M.J., Marienfeld, R.B. and Ghosh, S. (2002) Characterization of the Ikappa B-kinase NEMO binding domain. ***J Biol Chem*****, 277, 45992-46000.**

Mayr, B. and Montminy, M. (2001) Transcriptional regulation by the phosphorylation-dependent factor CREB. ***Nat Rev Mol Cell Biol*****, 2, 599-609.**

McRee, D.E. (1999) XtalView/Xfit--A versatile program for manipulating atomic coordinates and electron density. ***J Struct Biol*****, 125, 156-165.**

Meyer, T.E. and Habener, J.F. (1993) Cyclic adenosine 3',5'-monophosphate response element binding protein (CREB) and related transcription-activating deoxyribonucleic acid-binding proteins. ***Endocr Rev*****, 14, 269-290.**

Montminy, M.R., Sevarino, K.A., Wagner, J.A., Mandel, G. and Goodman, R.H. (1986) Identification of a cyclic-AMP-responsive element within the rat somatostatin gene. ***Proc Natl Acad Sci U S A*****, 83, 6682-6686.**

Mordmuller, B., Krappmann, D., Esen, M., Wegener, E. and Scheidereit, C. (2003) Lymphotoxin and lipopolysaccharide induce NF-kappaB-p52 generation by a co-translational mechanism. ***EMBO Rep*****, 4, 82-87.**

Muller, C.W., Rey, F.A., Sodeoka, M., Verdine, G.L. and Harrison, S.C. (1995) Structure of the NF-kappa B p50 homodimer bound to DNA. ***Nature*****, 373, 311-317.**

Navaza, J. (2001) Implementation of molecular replacement in AMoRe. ***Acta Crystallogr D Biol Crystallogr*****, 57, 1367-1372.**

Neri, A., Chang, C.C., Lombardi, L., Salina, M., Corradini, P., Maiolo, A.T., Chaganti, R.S. and Dalla-Favera, R. (1991) B cell lymphoma-associated chromosomal translocation involves candidate oncogene lyt-10, homologous to NF-kappa B p50. ***Cell*****, 67, 1075-1087.**

Nishikori, M., Ohno, H., Haga, H. and Uchiyama, T. (2005) Stimulation of CD30 in anaplastic large cell lymphoma leads to production of nuclear factor-kappaB p52, which is associated with hyperphosphorylated Bcl-3. ***Cancer Sci*****, 96, 487-497.**

Nolan, G.P., Fujita, T., Bhatia, K., Huppi, C., Liou, H.C., Scott, M.L. and Baltimore, D. (1993) The bcl-3 proto-oncogene encodes a nuclear I kappa B-like molecule that preferentially interacts with NF-kappa B p50 and p52 in a phosphorylation-dependent manner. ***Mol Cell Biol*****, 13, 3557-3566.**

Novack, D.V., Yin, L., Hagen-Stapleton, A., Schreiber, R.D., Goeddel, D.V., Ross, F.P. and Teitelbaum, S.L. (2003) The IkappaB function of NF-kappaB2 p100 controls stimulated osteoclastogenesis. *J Exp Med*, 198, 771-781.

Otwinowski, Z. and Minor, W. (1997) Processing of x-ray diffraction data collected in oscillation mode. In Sweet, R.M. and Carter, C.W. (eds.), *Methods in Enzymology*. Academic Press, New York, pp. 307-326.

Pahl, H.L. (1999) Activators and target genes of Rel/NF-kappaB transcription factors. *Oncogene*, 18, 6853-6866.

Perkins, N.D. (1997) Achieving transcriptional specificity with NF-kappa B. *Int J Biochem Cell Biol*, 29, 1433-1448.

Poli, V., Mancini, F.P. and Cortese, R. (1990) IL-6DBP, a nuclear protein involved in interleukin-6 signal transduction, defines a new family of leucine zipper proteins related to C/EBP. *Cell*, 63, 643-653.

Qing, G., Qu, Z. and Xiao, G. (2005a) Regulation of NF-kappa B2 p100 processing by its cis-acting domain. *J Biol Chem*, 280, 18-27.

Qing, G., Qu, Z. and Xiao, G. (2005b) Stabilization of basally translated NF-kappaB-inducing kinase (NIK) protein functions as a molecular switch of processing of NF-kappaB2 p100. *J Biol Chem*, 280, 40578-40582.

Qing, G., Qu, Z. and Xiao, G. (2007) Endoproteolytic processing of C-terminally truncated NF-kappaB2 precursors at kappaB-containing promoters. *Proc Natl Acad Sci U S A*, 104, 5324-5329.

Ran, R., Lu, A., Zhang, L., Tang, Y., Zhu, H., Xu, H., Feng, Y., Han, C., Zhou, G., Rigby, A.C. and Sharp, F.R. (2004) Hsp70 promotes TNF-mediated apoptosis by binding IKK gamma and impairing NF-kappa B survival signaling. *Genes Dev*, 18, 1466-1481.

Rayet, B. and Gelinas, C. (1999) Aberrant rel/nfkb genes and activity in human cancer. *Oncogene*, 18, 6938-6947.

Rothwarf, D.M. and Karin, M. (1999) The NF-kappa B activation pathway: a paradigm in information transfer from membrane to nucleus. *Sci STKE*, 1999, RE1.

Ruben, S.M., Klement, J.F., Coleman, T.A., Maher, M., Chen, C.H. and Rosen, C.A. (1992) I-Rel: a novel rel-related protein that inhibits NF-kappa B transcriptional activity. *Genes Dev*, 6, 745-760.

Ryseck, R.P., Bull, P., Takamiya, M., Bours, V., Siebenlist, U., Dobrzanski, P. and Bravo, R. (1992) RelB, a new Rel family transcription activator that can interact with p50-NF-kappa B. ***Mol Cell Biol*****, 12, 674-684.**

Ryseck, R.P., Novotny, J. and Bravo, R. (1995) Characterization of elements determining the dimerization properties of RelB and p50. ***Mol Cell Biol*****, 15, 3100-3109.**

Saccani, S., Pantano, S. and Natoli, G. (2003) Modulation of NF-kappaB activity by exchange of dimers. ***Mol Cell*****, 11, 1563-1574.**

Sanjabi, S., Hoffmann, A., Liou, H.C., Baltimore, D. and Smale, S.T. (2000) Selective requirement for c-Rel during IL-12 P40 gene induction in macrophages. ***Proc Natl Acad Sci U S A*****, 97, 12705-12710.**

Sen, R. and Baltimore, D. (1986) Multiple nuclear factors interact with the immunoglobulin enhancer sequences. ***Cell*****, 46, 705-716.**

Senftleben, U., Cao, Y., Xiao, G., Greten, F.R., Krahn, G., Bonizzi, G., Chen, Y., Hu, Y., Fong, A., Sun, S.C. and Karin, M. (2001) Activation by IKKalpha of a second, evolutionary conserved, NF-kappa B signaling pathway. ***Science*****, 293, 1495-1499.**

Sengchanthalangsy, L.L., Datta, S., Huang, D.B., Anderson, E., Braswell, E.H. and Ghosh, G. (1999) Characterization of the dimer interface of transcription factor NFkappaB p50 homodimer. ***J Mol Biol*****, 289, 1029-1040.**

Sheaff, R.J., Singer, J.D., Swanger, J., Smitherman, M., Roberts, J.M. and Clurman, B.E. (2000) Proteasomal turnover of p21Cip1 does not require p21Cip1 ubiquitination. ***Mol Cell*****, 5, 403-410.**

Sheng, M., McFadden, G. and Greenberg, M.E. (1990) Membrane depolarization and calcium induce c-fos transcription via phosphorylation of transcription factor CREB. ***Neuron*****, 4, 571-582.**

Sheng, M., Thompson, M.A. and Greenberg, M.E. (1991) CREB: a Ca(2+)-regulated transcription factor phosphorylated by calmodulin-dependent kinases. ***Science*****, 252, 1427-1430.**

Siebenlist, U., Franzoso, G. and Brown, K. (1994) Structure, regulation and function of NF-kappa B. ***Annu Rev Cell Biol*****, 10, 405-455.**

Silverman, N. and Maniatis, T. (2001) NF-kappaB signaling pathways in mammalian and insect innate immunity. ***Genes Dev*****, 15, 2321-2342.**

Sivakumar, V., Hammond, K.J., Howells, N., Pfeffer, K. and Weih, F. (2003) Differential requirement for Rel/nuclear factor kappa B family members in natural killer T cell development. *J Exp Med*, 197, 1613-1621.

Solan, N.J., Miyoshi, H., Carmona, E.M., Bren, G.D. and Paya, C.V. (2002) RelB cellular regulation and transcriptional activity are regulated by p100. *J Biol Chem*, 277, 1405-1418.

Sun, S.C., Ganchi, P.A., Ballard, D.W. and Greene, W.C. (1993) NF-kappa B controls expression of inhibitor I kappa B alpha: evidence for an inducible autoregulatory pathway. *Science*, 259, 1912-1915.

Sun, S.C. and Xiao, G. (2003) Deregulation of NF-kappaB and its upstream kinases in cancer. *Cancer Metastasis Rev*, 22, 405-422.

Thanos, D. and Maniatis, T. (1995) Virus induction of human IFN beta gene expression requires the assembly of an enhanceosome. *Cell*, 83, 1091-1100.

Thomas, R. (2005) The TRAF6-NF kappa B signaling pathway in autoimmunity: not just inflammation. *Arthritis Res Ther*, 7, 170-173.

Vales, L.D. and Friedl, E.M. (2002) Binding of C/EBP and RBP (CBF1) to overlapping sites regulates interleukin-6 gene expression. *J Biol Chem*, 277, 42438-42446.

Van Nguyen, T., Kobierski, L., Comb, M. and Hyman, S.E. (1990) The effect of depolarization on expression of the human proenkephalin gene is synergistic with cAMP and dependent upon a cAMP-inducible enhancer. *J Neurosci*, 10, 2825-2833.

Verma, I.M., Stevenson, J.K., Schwarz, E.M., Van Antwerp, D. and Miyamoto, S. (1995) Rel/NF-kappa B/I kappa B family: intimate tales of association and dissociation. *Genes Dev*, 9, 2723-2735.

Verweij, C.L., Geerts, M. and Aarden, L.A. (1991) Activation of interleukin-2 gene transcription via the T-cell surface molecule CD28 is mediated through an NF-kB-like response element. *J Biol Chem*, 266, 14179-14182.

Vinson, C.R., Hai, T. and Boyd, S.M. (1993) Dimerization specificity of the leucine zipper-containing bZIP motif on DNA binding: prediction and rational design. *Genes Dev*, 7, 1047-1058.

Weih, D.S., Yilmaz, Z.B. and Weih, F. (2001) Essential role of RelB in germinal center and marginal zone formation and proper expression of homing chemokines. *J Immunol*, 167, 1909-1919.

Weih, F. and Caamano, J. (2003) Regulation of secondary lymphoid organ development by the nuclear factor-kappaB signal transduction pathway. *Immunol Rev*, 195, 91-105.

Wulczyn, F.G., Naumann, M. and Scheidereit, C. (1992) Candidate proto-oncogene bcl-3 encodes a subunit-specific inhibitor of transcription factor NF-kappa B. *Nature*, 358, 597-599.

Xiao, G., Cvijic, M.E., Fong, A., Harhaj, E.W., Uhlik, M.T., Waterfield, M. and Sun, S.C. (2001a) Retroviral oncoprotein Tax induces processing of NF-kappaB2/p100 in T cells: evidence for the involvement of IKKalpha. *Embo J*, 20, 6805-6815.

Xiao, G., Fong, A. and Sun, S.C. (2004) Induction of p100 processing by NF-kappaB-inducing kinase involves docking IkappaB kinase alpha (IKKalpha) to p100 and IKKalpha-mediated phosphorylation. *J Biol Chem*, 279, 30099-30105.

Xiao, G., Harhaj, E.W. and Sun, S.C. (2001b) NF-kappaB-inducing kinase regulates the processing of NF-kappaB2 p100. *Mol Cell*, 7, 401-409.

Yilmaz, Z.B., Weih, D.S., Sivakumar, V. and Weih, F. (2003) RelB is required for Peyer's patch development: differential regulation of p52-RelB by lymphotoxin and TNF. *Embo J*, 22, 121-130.

Yin, L., Wu, L., Wesche, H., Arthur, C.D., White, J.M., Goeddel, D.V. and Schreiber, R.D. (2001) Defective lymphotoxin-beta receptor-induced NF-kappaB transcriptional activity in NIK-deficient mice. *Science*, 291, 2162-2165.

Zandi, E., Rothwarf, D.M., Delhase, M., Hayakawa, M. and Karin, M. (1997) The IkappaB kinase complex (IKK) contains two kinase subunits, IKKalpha and IKKbeta, necessary for IkappaB phosphorylation and NF-kappaB activation. *Cell*, 91, 243-252.